Anatomical correlates of driving and modulatory glutamatergic projections in the mammalian visual system

By

Pooja Balaram

Dissertation

Submitted to the Faculty of the
Graduate School of Vanderbilt University
in partial fulfillment of the requirements
for the degree of
DOCTOR OF PHILOSOPHY
in
Psychology

December 2014

Nashville, Tennessee

Approved:

Jon H. Kaas, Ph.D.

Troy A. Hackett, Ph.D.

Vivien A. Casagrande, Ph.D.

Ramnarayan Ramachandran, Ph.D.

For my first mentor,

Dr. Samuel D. Crish,

who showed me that science, in its purest form, will always be amazing

and that feeling, of being amazed by scientific discovery, will never go away

Acknowledgements

I owe a great deal to the people on the following pages. They have been unwavering sources of support for my life and my career thus far; I would not be who I am without them.

Jon Kaas has been my graduate advisor and scientific mentor for the past six years. I first met Jon at the Mellow Mushroom in the spring of 2008, where a mutual interest in visual neuroscience, Vanderbilt football, and Yazoo pale ales kept us in conversation for most of the following year. In the fall of 2009, I joined Jon's lab as a graduate student and the rest, as they say, is history. Over the years, Jon has allowed me to pursue just about any research topic that caught my interest and his constant endorsement has been the key to my success. Jon understands that his students are most productive when they love what they're working on, and permitting me to choose my own projects ensured that I was always interested in and happy with my work. He's refined my thinking and writing skills over many drafts of manuscripts, supported me through the highs and lows of graduate school, and taught me to choose wisely – in science and in life. Joining Jon's lab was the best decision I've made in my academic career.

Troy Hackett has been my secondary advisor and the voice of reason in all of my graduate school work. He taught me to think twice through every experiment, find every flaw in my data and determine all the alternative hypotheses that could explain my results. The quality of my science has increased dramatically because of his attention to detail and for that, I cannot thank him enough. Troy has also given me unrestricted access to all of his lab resources for several years and his lab has been the primary location for most of my experiments and data

analysis. My projects would, quite literally, not exist without his support. Troy and I have been collaborating on research for several years now, and with any luck, will continue to do so in the future. Without ever being required to do so in an official capacity (you're the best!), Troy has been an exceptional mentor to me throughout my graduate school years.

Ram Ramachandran is a recent addition to the Vanderbilt faculty, but he's been expanding my skill set ever since he set foot in Wilson hall. He taught me to trust a drill instead of a scalpel and the virtue of sutures over staples, along with many other priceless pieces of advice regarding my academic career. I look forward to bothering him with many more questions about auditory physiology over the next few years. Vivien Casagrande has been a member of my thesis committee since my first year of graduate school and has been my role model for a successful female academic. She is a brilliant scientist and a wonderful teacher to all of her advisees. Anna Roe has also been a great role model for me; both she and Vivien are living proof that women can be extraordinary scientists without sacrificing the rest of their lives. Isabel Gauthier showed me how to teach undergraduate courses in a way that allows students to learn the material while still having fun in class, and Tom Palmeri, René Marois, and Andrew Tomarken have all been great sources of advice and support throughout graduate school.

Current and former members of the Kaas lab know that our relationships with each other extend well beyond our years in Wilson hall, and there are many people in the extended Kaas lab family who have helped me through this phase of my life. First and foremost, our lab manager Laura Trice has seen me through every aspect of graduate school and without her I would not have survived. She's helped me process mountains of brain sections from a dozen different

species, test out new protocols regardless of how weird they were, transform lab spaces multiple times over, build surgical equipment from scratch, and kept my science organized despite my astonishing ability to mislabel (or never label) anything I touch. My science would have been derailed a long time ago if it wasn't for her. Mary Baldwin took me under her wing when I first joined Jon's lab and taught me everything she knew about visual neuroscience and comparative neuroanatomy; we've been friends and collaborators ever since. Christina Cerkevich taught me how to interpret Jon's handwriting and how to put bacon in everything. Nicole Young listened to me complain about my undergrads (only the terrible ones) for hours on end and taught me to drink, steal, and swear like a Canadian (no relationship between the two, of course). Reuben Fan taught me not to panic under any circumstances, and Omar Gharbawie is the definition of patience as a virtue. Lisa de la Mothe and Corrie Camalier have been wonderful big sisters to me in research and in life; I'm glad I'm joining the 'dark side' with people like them around. Jamie Reed has guided me through multiple grad school decisions and her proficiency with SPSS has allowed me to avoid statistics entirely for the past six years. Toru Takahata taught me everything I know about in situ hybridization and has been a great technical resource for all of my projects in grad school. Huixin Qi and Iwona Stepniewska have helped me with a whole host of research projects and animal protocols, and constantly supplied me with histological material for all of my work. Eva Sawyer, Emily Rockoff, and Dan Miller have all been great fun to work with and I'm glad they'll be continuing the Kaas lab legacy once I'm gone. Ken Catania has allowed me to work in his lab whenever needed, nerd out over every single creature he's brought into the building, and supported and encouraged me as a member of the J. B. Johnston Club. Finally, Mary Feurtado and Dr. Troy Apple have worked tirelessly to ensure that all of my experiments went as smoothly as possible. I am forever indebted to all of these people for making my time in

graduate school a truly rewarding experience, and am proud to be a permanent member of the Kaas lab family.

I've also had the opportunity to train several outstanding undergraduate students during my time in Jon's lab. Their proficiency with lab techniques was a key component of my overall productivity and their work has appeared in several of my manuscripts. I thank Hannah McCloskey, Mir Isaamullah, Emily Brignola and James Baker-McKee, and look forward to seeing them grow and develop in their own professional careers.

Outside of graduate school, I thank my parents Ranjit and Yamuna Balaram, for all of the love and support they've given me my entire life. They raised me to be an exceptional person, no matter what the circumstances of life may be, and I think I've lived up to that goal. I cannot thank them enough for their unwavering support of my scientific career. My brother, Prithvi Balaram, is one of my best friends as well as my sibling, and that relationship has promoted us both through extraordinary careers.

The last person on this list is my husband, JT Brogan. JT has been a part of every moment and every decision I've made over the past five years, and my life is far better for it. We've made it through graduate school together and I can't wait to see what we'll do next.

TABLE OF CONTENTS

Page

LIST OF TABLES AND FIGURES

the stratum griseum super_ciale or super_cial gray layer (SGS) that is divided into upper and lower sublayers (uSGS and lSGS respectively); the stratum opticum or optic layer (SO) lies below the SGS and separates the super_cial layers from the intermediate layers; below the SGS lies the stratum griseum intermediale or intermediate gray layer (SGI), which is divided into three sublayers (SGIa, SGIb, and SGIc from dorsal to ventral); the stratum album intermediale or intermediate white layer (SAI) lies below the SGI and separates the intermediate layers from the deep layers; below the SAI lies the stratum griseum profundum or deep gray layer (SGP) and lastly; ventral to the SGP lies the stratum album profundum or deep white layer (SAP), which borders the periaqueductal gray. Scale bar is 0.5mm for panels A-D, 100um for panels E-F

5.4.2.1 Figure 4. Low magnification images of coronal sections through V1 and V2. Dorsal surface of cortex is up, ventral surface is down, hemispheric midline is to the left. Scale bar is 2mm.

5.4.2.2 Figure 5. High magnification images of the laminar organization of V1 (Area 17). Scale bar is 250um.

5.4.2.3 Figure 6. High magnification images of the laminar organization of V2. Scale bar is 250um.

5.4.2.4 Figure 7. Low magnification images of coronal sections through the middle temporal area (MT). Scale bar is 1mm.

5.4.2.5 Figure 8. High magnification images of the laminar organization of MT. Scale bar is 250um.

adapted from May, 2006. Midline is to the right, scale bar is 500um. Abbreviations: SZ – zonal layer, uSGSd – dorsal division of the upper superficial gray layer, uSGSv – ventral division of the upper superficial gray layer, LSGS – lower superficial gray layer, SO – optic layer.

6.4.2.2 Figure 4: High magnification images of panels C-F in figure 3 show variations in VGLUT1 and VGLUT2 protein (A, B) and mRNA (C, D) distributions between layers of the SC. Layer conventions as in figure 3. Scale bar is 50um. Abbreviations: SZ – zonal layer, uSGSd – dorsal division of the upper superficial gray layer, uSGSv – ventral division of the upper superficial gray layer, LSGS – lower superficial gray layer, SO – optic layer.

6.4.3.2 Figure 6: High magnification images of individual pulvinar divisions from panels C-F in figure 5 reveal differences in VGLUT1 and VGLUT2 protein (A, B) and mRNA (C, D) labeling across these nuclei. Scale bar is 50μm. Abbreviations: Pd – dorsal pulvinar, Pc – central pulvinar, Pv- ventral pulvinar.

6.4.4.1 Figure 7: Coronal sections through primary visual cortex (V1) in tree shrews stained for (A) cytochrome oxidase, (B) neuronal nuclear antigen, (C) VGLUT1 protein, (D) VGLUT2 protein, (E) VGLUT1 mRNA, and (F) VGLUT2 mRNA. Individual V1 layers are named following the convention of Hässler (1967) and are shown on the left of each section. Solid lines are boundaries between V1 layers, dotted lines are sublaminar divisions. Hemispheric midline is to the right, scale bar is 500um.

CHAPTER 1

Introduction to vesicular glutamate transporters and their role in excitatory neurotransmission

Excitatory neurotransmission in the mammalian central nervous system (CNS) is primarily mediated by the release of glutamate, a small amino acid utilized as a metabolic substrate in most living cells and as a signaling molecule in excitatory neurons (Reimer et al., 2001). The presynaptic sequestration and release of glutamate from small synaptic vesicles in the axon terminals of glutamatergic neurons is regulated by a family of transmembrane transport proteins known as vesicular glutamate transporters (VGLUTs), which are either expressed alone or in combination with other transmitter transporters, in every glutamatergic neuron across the CNS (Fremeau et al., 2004b; Takamori, 2006). Three VGLUT isoforms are known to exist to date – VGLUT1, VGLUT2, and VGLUT3. All three VGLUTs are genetically (Aihara et al., 2000; Fremeau et al., 2001; Gras et al., 2002) and functionally (Danbolt et al., 1994; Fremeau et al., 2002; Reimer and Edwards, 2004; Blakely and Edwards, 2012) similar to one another; however, subtle differences in their distribution and function have allowed researchers to discern how VGLUTs contribute to variations in glutamatergic signaling across a range of excitatory neuronal populations. It is now apparent that each VGLUT protein may mediate distinct forms of glutamatergic neurotransmission in the CNS via its interaction with a wide range of proteins and small molecules in the synaptic terminals of host neurons (Fremeau et al., 2001; Herzog et al., 2001; Kaneko and Fujiyama, 2002; Fremeau et al., 2004b; Takamori, 2006; Blakely and Edwards, 2012; Rovó et al., 2012). The following sections outline the similarities and differences in function and distribution of all three VGLUT isoforms in the mammalian CNS, to highlight

the slight changes in transporter function that give each VGLUT their unique characteristics in glutamatergic neurotransmission.

1.1 Mechanisms of VGLUT-mediated glutamate transport into presynaptic vesicles

The primary function of VGLUT proteins is the transport of cytosolic glutamate into presynaptic vesicles in the axon terminals of glutamatergic neurons. All three VGLUT isoforms use similar intracellular mechanisms to package glutamate into presynaptic vesicles (Bellocchio et al., 2000; Takamori et al., 2000; Fremeau et al., 2001; Hayashi et al., 2001; Herzog et al., 2001; Reimer et al., 2001; Fremeau et al., 2002; Schäfer et al., 2002). The driving force behind VGLUT-mediated glutamate uptake is a proton-dependent electrochemical gradient driven by a vacuolar H^+ATPase, also located on the vesicle membrane, which converts individual adenosine diphosphate (ADP) molecules into adenosine triphosphate (ATP) molecules along its cytosolic region (Bellocchio et al., 2000; Takamori et al., 2000; Fremeau et al., 2001; Hayashi et al., 2001). For every molecule of ADP converted to ATP, a single hydrogen (H^+) proton is transported into the vesicle lumen. The steady rise of H^+ cations within the vesicle electrically charges its interior and drives the accumulation of glutamate anions into the vesicle to neutralize the increased charge. VGLUTs pump individual glutamate molecules into the vesicle in exchange for individual H+ ions. Thus, larger electrochemical gradients across the vesicle membrane drive faster VGLUT-mediated glutamate uptake into presynaptic vesicles (Danbolt et al., 1994; Blakely and Edwards, 2012; Anne and Gasnier, 2014), unlike vesicular monoamine (VMAT) or vesicular GABA (VGAT) transporters, whose efficacy depends on the pH differential across the vesicle membrane (Anne and Gasnier, 2014). All three VGLUT proteins have a relatively low affinity for glutamate under neutral conditions (Disbrow et al., 1982; Naito

and Ueda, 1983; Bellocchio et al., 2000; Fremeau et al., 2001; Schäfer et al., 2002; Reimer and Edwards, 2004), thus large differences in the electrochemical gradient across vesicle membranes *in vivo* are required to produce physiologically relevant rates of glutamate uptake in neurons (Takamori et al., 2000; Takamori, 2006; Edwards, 2007).

Other ions that diffuse through the presynaptic cytosol influence this electrochemical gradient, and the functions of all three VGLUTs depend these small molecules as well. Chloride (Cl^-) ions diffuse through vesicles via transmembrane chloride channels and their negative charge also neutralizes the H^+ gradient driven by the vacuolar H^+ATPase. Thus, all three VGLUT isoforms exhibit a biphasic dependency on chloride concentrations; high levels of chloride conductance inhibit glutamate uptake into vesicles by reducing the electrochemical gradient across the vesicle membrane, while lower levels between 2-10 mM Cl^- concentrations drive glutamate uptake (Fremeau et al., 2004a; Takamori, 2006). Interestingly, much lower levels of Cl^- conductance interferes with glutamate uptake and the loss of chloride channels in glutamatergic neurons induces widespread neuronal degeneration due to excessive glutamate vesicle filling and excitotoxicity, providing further evidence that chloride levels directly influence how much glutamate is sequestered into individual glutamatergic vesicles. Chloride ions may also bind directly to VGLUT proteins via an allosteric binding site and directly alter the rate of glutamate transport into synaptic vesicles (Hartinger and Jahn, 1993). Both VGLUT1 and VGLUT2 are also known to transport inorganic phosphate (Pi) in exchange for sodium ions once they are present on the presynaptic plasma membrane following vesicle fusion, and an increase in Pi within the presynaptic terminal triggers phosphate-activated glutaminase (PAG) to convert glutamine into glutamate in the cytosol. PAG activity also produces ammonia as a byproduct, which diffuses into the vesicle lumen and gets trapped, increasing the lumenal charge and further

driving glutamate uptake into the vesicle (Bellocchio et al., 1998; Schäfer et al., 2002; Varoqui et al., 2002). Thus, intracellular chloride and phosphate levels both directly influence VGLUT-mediated glutamate uptake into presynaptic vesicles.

The number of VGLUT proteins present on individual vesicles appears to determine the volume of glutamate stored within each vesicle, as determined by the presence of absence of presynaptic VGLUT1 on postsynaptic responses *in vitro* and *in vivo*. Overexpression of VGLUT1 (Wilson et al., 2005) or similar VGLUT homologs (Daniels et al., 2004) at individual glutamatergic synapses causes a drastic increase in the amplitude of excitatory postsynaptic currents (EPSCs), which suggests that the expression of VGLUTs directly influences the amount of glutamate released from individual glutamatergic synapses. Similarly, hippocampal neuronal cultures from VGLUT1 knockout mice (Wojcik et al., 2004) showed a large reduction in EPSC amplitude compared to wild type neurons, indicating that the presence of VGLUT1 on presynaptic vesicles is coupled to the quantal size of the postsynaptic response. Interestingly, heterozygous mice with only one VGLUT1 allele in the same study showed an exact 50% reduction in EPSC amplitude compared to wild type mice, further suggesting that the number of VGLUT1 proteins present in a synapse directly relates to the quantal size of the excitatory postsynaptic response. Overexpressing VGLUT1 on native synaptic vesicles causes an increase in the amount of glutamate stored within a single vesicle as opposed to an increase in the number of vesicles available for release (Wojcik et al., 2004; De Gois et al., 2005; Wilson et al., 2005; Erickson et al., 2006), possibly by increasing the overall diameter of individual glutamatergic vesicles (Daniels et al., 2004), which would allow for more glutamate per vesicle without a drastic change in the concentrations of glutamate inside or outside of the vesicle membrane. The effect of VGLUT2 expression on quantal vesicle content has yet to be fully determined

(Edwards, 2007), but VGLUT3 also appears to regulate the amount of neurotransmitter stored in individual vesicles of serotonergic and dopaminergic neurons in a similar manner (Amilhon et al., 2010). Thus, the number of VGLUT proteins present on a single synaptic vesicle is directly coupled to the amount of glutamate stored in that vesicle, which determines the quantal size of the postsynaptic response following the release of glutamate from the axon terminal. Since single glutamatergic vesicles are not usually filled to maximal capacity and postsynaptic receptors don't saturate in response to individual quanta of vesicular glutamate release (Yamashita et al., 2003; Wojcik et al., 2004; Edwards, 2007), variations in glutamate content per vesicle- as regulated by the number and type of VGLUTs present on each vesicle- may be responsible for the range of excitatory potentials produced by individual glutamatergic neurons in the CNS.

In traditional glutamatergic synapses, which express VGLUT1 or VGLUT2 and not VGLUT3, the interaction of VGLUT1 and VGLUT2 with other presynaptic proteins suggests that each isoform is targeted to separate pathways of vesicle exo- and endocytosis (Voglmaier et al., 2006; Weston et al., 2011; Foss et al., 2013). The tail ends of each protein, known as the N-terminus and the C-terminus, remain unbound in the terminal cytoplasm and vesicle lumen, instead of bound within the vesicle membrane, and are free to interact with other proteins to guide vesicle trafficking mechanisms. A highly conserved C-terminal domain on all three VGLUTs is known to interact with endophilin A1, a synaptic protein that is essential to the reformation and internalization of synaptic vesicles. Endophilin A1 binds to sections of the presynaptic terminal membrane where vesicle endocytosis has been initiated and recruits other proteins that mold and separate individual vesicles from the plasma membrane. The C-terminus of VGLUT1 has the highest affinity for endophilin A1, but acts in a negative allosteric manner, where binding of VGLUT1 to endophilin A1 reduces the probability of vesicle endocytosis and

subsequent glutamate release. The C-terminus of VGLUT2 has a lower affinity for endophilin A1 and thus, neurons expressing VGLUT2 are able to maintain a comparably faster rate of vesicle endocytosis (Weston et al., 2011). However, endophilin A1 binding to the C-terminus of VGLUT1 is required for normal endocytosis (Voglmaier et al., 2006), suggesting that this interaction may influence other components of vesicle formation such as vesicle biogenesis or trafficking to separate vesicle pools. Vesicles formed with endophilin A1 are also sorted to a faster vesicle recycling pathway mediated by the binding of endophilin A1 to adaptor protein 2 (AP2), and fast recycling of synaptic vesicles allows for response facilitation during repetitive activation, which is a common feature of VGLUT1-positive neurons. VGLUT2's lower affinity for endophilin A1 may underlie the trafficking of VGLUT2-positive vesicles to a slower recycling pathway mediated by adaptor protein 3 instead (Voglmaier et al., 2006). The N-terminus of VGLUT1 contains two additional domains that are absent in VGLUT2 (Foss et al., 2013). One of these domains also interacts with endophilin A1 and recruits VGLUT1-positive vesicles to the Ap2-mediated endocytotic pathway, thus giving VGLUT1 two points of access to the same recycling pathway. VGLUT2, which lacks this domain entirely, relies only on the C-terminus domain for its transport to the AP2-mediated recycling pathway, which may contribute to its reduced probability of vesicle recycling and release. The second N-terminal domain on VGLUT1 recruits VGLUT-positive vesicles to a third adaptor protein 3 (AP3)-mediated endocytotic pathway with a different rate of vesicle internalization than the AP2-mediated pathway, which gives VGLUT1-positive vesicles a greater temporal range of vesicle endocytosis compared to VGLUT2. Thus, VGLUT1 and VGLUT2 appear to be trafficked through separate vesicle recycling pathways following their fusion with the presynaptic terminal membrane, which may give rise to temporal variations in their properties of glutamate release.

The relative levels of VGLUT1 and VGLUT2 in individual terminals affect mechanisms of homeostatic plasticity across those synapses. Further experiments with VGLUT1 deficient hippocampal cultures showed that many neurons lacking VGLUT1 did not entirely lose their ability to produce EPSCs (Wojcik et al., 2004). In these cells, small EPSCs with low frequencies were still present and examination at the electron microscopic level showed that these neurons expressed low levels of VGLUT2 instead. Similar studies in differentiated neocortical cultures show that VGLUT2 expression levels increase and VGLUT1 levels decrease in response to bicuculine treatment, which increases the overall firing activity of neurons. Conversely, VGLUT1 levels increase and VGLUT2 levels decrease in response to tetrodotoxin treatment, which decreases the overall firing activity in neurons (De Gois et al., 2005). Thus, fluctuations in the activity patterns of glutamatergic neurons causes a corresponding shift in the distribution of VGLUT1 and VGLUT2 proteins in their terminals, which allows them to maintain constant levels of glutamate release despite such large shifts in neural activity. During development, cerebellar granule cells express VGLUT2 during early differentiation, which requires high levels of excitatory neural activity, but switch to expressing VGLUT1 during synaptic maturation (Miyazaki et al., 2003), which requires comparatively lower levels of activity, indicating that VGLUT expression in these synapses is dependent on the level of excitatory transmission in these cells. Directly manipulating spiking activity via calcium flux also causes shifts in vesicular transporter expression and specifies neurotransmitter choice in most neurons (Spitzer et al., 2004). Similar developmental coexpression and bidirectional regulation of VGLUT1 and VGLUT2 has been observed in neocortical cultures (Boulland et al., 2004; De Gois et al., 2005) and intact neocortical sections (Nakamura et al., 2005; Liguz-Lecznar and Skangiel-Kramska, 2007). Altering the expression levels of either VGLUT1 or VGLUT2 in a synapse

correspondingly changes the amount of glutamate released from that synapse, as well as the time course of glutamate release from individual vesicles. Thus, by regulating VGLUT expression within terminals, glutamatergic neurons can maintain constant levels of glutamate release and excitatory activity in response to fluctuations in the strength of action potentials coursing through them (Erickson et al., 2006). During development, this facilitates the formation and maturation of functional glutamatergic synapses (Boulland et al., 2004). In adulthood, VGLUT subtype switching prevents excitotoxicity and maintains normal synapse function in response to drastic changes in neural activity within glutamatergic circuits (Hnasko and Edwards, 2012).

1.2 VGLUT expression patterns in the developing and adult brain

In addition to differences in membrane trafficking, quantal content and size, and homeostatic response properties, the expression patterns of each VGLUT isoform differs significantly across the CNS, with limited overlap between VGLUTs in any region (Fremeau et al., 2001; Herzog et al., 2001; 2004). The presence of individual VGLUTs within a given projection is determined in two ways; first, the proteins themselves are identifiable in axon terminals (Gras et al., 2002; Kaneko et al., 2002), or in dendrodendritic contacts in the case of VGLUT3 (Fremeau et al., 2002), via immunohistochemistry with antibodies specific to each VGLUT protein. Second, the mRNA transcripts of each isoform are identifiable in the cell bodies of neurons that utilize VGLUTs in their terminations (Ni et al., 1995; Aihara et al., 2000; Gras et al., 2002), via in situ hybridization with complementary mRNA sequences to each VGLUT transcript. Thus, the origin and termination of individual VGLUT-positive projections can be identified using a combination of these two techniques. Most studies show that VGLUT1 and VGLUT2 are distributed in traditional glutamatergic terminals that form asymmetric

synapses on the dendrites of their postsynaptic targets and generate excitatory postsynaptic responses, while VGLUT3 is distributed in nontraditional glutamatergic terminals that form symmetric and asymmetric axodendritic or dendrodenritic synapses, and generate excitatory or inhibitory postsynaptic responses (Bellocchio et al., 1998; Fremeau et al., 2001; 2002). Since VGLUT1 and VGLUT2 predominate in the majority of glutamatergic circuits across the mammalian CNS (Fremeau et al., 2001; Herzog et al., 2001; Kaneko and Fujiyama, 2002), the remainder of this chapter will focus on differences in expression and function between VGLUT1 and VGLUT2.

In rodents, VGLUT1 protein is abundantly distributed in small terminals throughout the cerebellum, hippocampus, and in all layers of the neocortex, with only slightly less dense distributions in layers 4 and 6 of some neocortical areas (Fujiyama et al., 2001; Kaneko and Fujiyama, 2002; Kaneko et al., 2002). In contrast, VGLUT2 protein is densely distributed in layers 4 and 6 of the neocortex but more moderately distributed in other neocortical layers and in restricted regions of the hippocampus and cerebellum. In subcortical regions (Fujiyama et al., 2001; 2003), VGLUT2 is densely distributed across the thalamus, midbrain, and brainstem nuclei, while VGLUT1 is more moderately distributed in the same regions. During development, both VGLUT1 and VGLUT2 mRNA are transiently coexpressed in the same neurons and glutamatergic terminals either switch between the two protein isoforms at different developmental time points or express both isoforms for a limited period of time (Herzog et al., 2001; Boulland et al., 2004; Fremeau et al., 2004a; Nakamura et al., 2005; Liguz-Lecznar and Skangiel-Kramska, 2007; Nakamura et al., 2007). In adulthood, VGLUT1 and VGLUT2 mRNA are coexpressed in subsets of neurons within specific brain regions, such as thalamic sensory relay nuclei (Herzog et al., 2001; Barroso-Chinea et al., 2007), but the two proteins don't appear

to colocalize in individual terminals (Herzog et al., 2001; Altschuler et al., 2008; Graziano et al., 2008; Zeng et al., 2011; Rovó et al., 2012). Glutamatergic neurons in adult mammals either possess the ability to transcribe both VGLUT isoforms in their cell bodies but only utilize a single isoform in their terminals, or both isoforms are transcribed and instead trafficked to separate terminals (Herzog et al., 2001; Fremeau et al., 2004a). Since the N- and C-termini of both VGLUTs contain distinct sequences of amino acids that facilitate the trafficking of each protein to different portions of the vesicular and terminal membranes (Santos et al., 2009; Weston et al., 2011; Foss et al., 2013), it is possible that the differential distribution of VGLUT1 and VGLUT2 between individual terminals of glutamatergic neurons gives rise to the temporal and spatial dynamics of glutamate release seen in excitatory neurotransmission across the CNS (Erickson et al., 2006; Edwards, 2007; Davanger et al., 2009).

1.3 VGLUT expression correlates with distinct classes of glutamatergic projections

The largely segregated distribution patterns of VGLUT1 and VGLUT2 in the mammalian CNS strongly suggests that each VGLUT isoform may be restricted to a functionally distinct category of excitatory projections (Herzog et al., 2001; Fremeau et al., 2004a; b; Takamori, 2006; Blakely and Edwards, 2012). VGLUT1-positive synapses from the cerebellum (parallel fibers), hippocampus, and neocortex are associated with a lower probability of glutamate release compared to VGLUT2-positive synapses from the cerebellum (climbing fibers), brainstem, and thalamus (Fremeau et al., 2001). VGLUT1-positive synapses also exhibit paired-pulse facilitation in response to repetitive stimulation while VGLUT2-positive synapses exhibit paired pulse depression instead (Varoqui et al., 2002). VGLUT1-positive terminals are also typically much smaller than VGLUT2-positive terminals (Fujiyama et al., 2001), and make synaptic

contacts along distal dendritic regions while VGLUT2-positive terminals make contacts closer to the cell soma instead (Altschuler et al., 2008; Masterson et al., 2009). Glutamatergic neurons in the few brain regions that coexpress VGLUT1 and VGLUT2 mRNA (Herzog et al., 2001) often send branched projections to multiple targets and, since the two proteins aren't found in the same terminals, it is possible that individual neurons utilize separate VGLUT isoforms in different terminal locations. If VGLUT1 and VGLUT2 do segregate to functionally distinct types of glutamatergic synapses (Herzog et al., 2001; Fremeau et al., 2004a; b; Santos et al., 2009; Blakely and Edwards, 2012), then these isoforms could serve as anatomical markers for each type of glutamatergic projection and potentially give rise to some of their functional characteristics.

Since VGLUT1 and VGLUT2 appear to distinguish between functionally classes of glutamatergic projections in the mammalian CNS, a further examination of their distribution patterns across a larger range of species may aid in the identification of homologous glutamatergic projections in mammalian brains. Additionally, the presence of VGLUT1 or VGLUT2 within a given projection may reveal novel features, or confirm prior findings, of functional properties of that projection within its larger neural network. In the mammalian visual system, the presence of VGLUT1 and VGLUT2 in segregated projections may distinguish between thalamocortical and corticothalamic connections (Kaneko and Fujiyama, 2002; Fremeau et al., 2004b; Takamori, 2006), feedforward and feedback projections (Rockland and Pandya, 1979; Felleman and Van Essen, 1991), driving and modulatory projections (Crick and Koch, 1998; Sherman and Guillery, 1998; Sherman, 2005), or other undefined categories of glutamatergic connections between visual structures.

The primary goals of the following chapters are to (1) document the distribution of VGLUT1 and VGLUT2 across visual glutamatergic projections of Old World macaque monkeys, New World squirrel and owl monkeys, prosimian galagos, and tree shrews, and (2) determine whether each VGLUT isoform characterizes a distinct projection type between visual structures. Each of these species represents a closely related but phylogenetically distinct member of the mammalian lineage (figure 1), thus allowing for comparisons of VGLUT distributions in homologous visual projections between related mammals. Additionally, the anatomical and functional characteristics of visual projections in these species have been well documented, which facilitates the correlation of VGLUT1 and VGLUT2 distributions with distinct classes of glutamatergic visual projections in the mammalian CNS.

1.3.1.1 Figure 1. The phylogeny of living mammals. Stars indicate lineages examined for VGLUT1 and VGLUT2 distributions in visual projections (Chapters 2-6). Adapted from Kaas, 2004

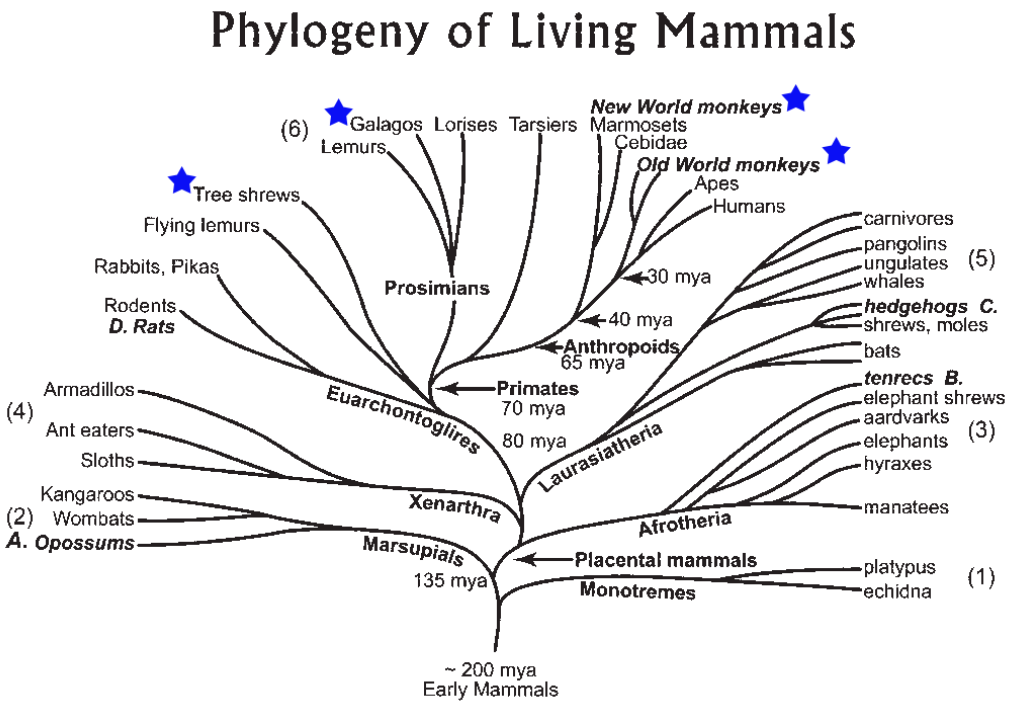

CHAPTER 2

Differential expression of vesicular glutamate transporters 1 and 2 may identify distinct modes of glutamatergic transmission in the macaque visual system

The following chapter was published under the same title in the Journal of Chemical Neuroanatomy by Pooja Balaram, Troy Hackett, and Jon Kaas; May 2013.

2.1 Abstract

Glutamate is the primary neurotransmitter utilized by the mammalian visual system for excitatory neurotransmission. The sequestration of glutamate into synaptic vesicles, and the subsequent transport of filled vesicles to the presynaptic terminal membrane, is regulated by a family of proteins known as vesicular glutamate transporters (VGLUTs). Two VGLUT proteins, VGLUT1 and VGLUT2, characterize distinct sets of glutamatergic projections between visual structures in rodents and prosimian primates, yet little is known about their distributions in the visual system of anthropoid primates. We have examined the mRNA and protein expression patterns of VGLUT1 and VGLUT2 in the visual system of macaque monkeys, an Old World anthropoid primate, in order to determine their relative distributions in the superior colliculus, lateral geniculate nucleus, pulvinar complex, V1 and V2. Distinct expression patterns for both VGLUT1 and VGLUT2 clearly identify regions of glutamatergic input in visual structures, and may identify common architectonic features of visual areas and nuclei across the primate radiation. Additionally, we find that VGLUT1 and VGLUT2 characterize distinct subsets of glutamatergic projections in the macaque visual system; VGLUT2 predominates in driving or

feedforward projections from lower order to higher order visual structures while VGLUT1 predominates in modulatory or feedback projections from higher order to lower order visual structures. The distribution of these two proteins suggests that VGLUT1 and VGLUT2 may identify class 1 and class 2 type glutamatergic projections within the primate visual system (Sherman and Guillery, 2006).

2.2 Introduction

The primate visual system consists of an intricate network of brain structures that process visual information (Valverde, 1985; Van Essen, 1985; Krubitzer and Kaas, 1989; Felleman and Van Essen, 1991; Casagrande and Kaas, 1994; Salin and Bullier, 1995; Van Essen, 2005). The dense connections that interlink individual visual structures have been examined through tracer studies that define projections to and from given areas and nuclei. However, the neuronal populations that give rise to individual projections in the visual system are often morphologically indistinct from each other, making it difficult to characterize the types of neurons that comprise a single projection (Lund et al., 1975; Lund, 1988; Levitt et al., 1996). The use of cellular and genetic markers to identify discrete populations of cells now allows us to isolate neurons that express a unique marker and correlate their connections and functional attributes within sensory systems (Lein et al., 2006; Hevner, 2007; Baldwin et al., 2011; Bernard et al., 2012). Thus, groups of neurons that give rise to distinct visual projections can now be classified based on their genetic and molecular characteristics. Since these molecular markers are also intrinsically tied to cellular processes, their expression patterns may identify neuronal properties that give rise to specific functions within a neuronal circuit as well (Kubota and Kawaguchi, 1994; Hevner et al., 2003; Fremeau et al., 2004a; b; Yamamori, 2011). Thus, the diversity of genetic and molecular

markers within neurons of the primate visual system could contribute to the range of neuronal responses within visual circuits. The molecular characterization of excitatory neurons and neuronal circuits in the primate visual system depends, in large part, on the use of glutamate as an excitatory neurotransmitter. However, the identification of glutamate within a neuron is not enough to classify it as glutamatergic, since glutamate is a ubiquitous amino acid in most cells of the nervous system. The classification of glutamate as a signaling molecule within a neuron requires the identification of a glutamate transporter, a protein responsible for containing glutamate within secretory vesicles that are released upon signal transmission (Danbolt et al., 1994; Reimer et al., 2001; Davanger et al., 2009). A family of such transport proteins, the vesicular glutamate transporters (VGLUTs), have been identified in the mammalian central nervous system (Aihara et al., 2000; Bellocchio et al., 2000; Herzog et al., 2001; Gras et al., 2002; Kaneko et al., 2002; Fyk-Kolodziej et al., 2004; Hackett and la Mothe, 2009; Hackett, 2011; Bryant et al., 2012) and are known to contribute to glutamatergic signaling within neuronal circuits (Fremeau et al., 2001; Varoqui et al., 2002; Fremeau et al., 2004a; b; Santos et al., 2009). Thus, VGLUT expression characterizes a glutamatergic phenotype in neuronal populations.

Two VGLUT isoforms, VGLUT1 and VGLUT2, are widely distributed across the mammalian brain, and appear to distinguish separate types of projections between and within parts of the visual system. A third isoform, VGLUT3, is distributed in subsets of neurons across the cortex, hippocampus, and striatum, but appears to have a more complex role in glutamatergic transport and synaptic activity (Fremeau et al., 2002; Gras et al., 2002; Schäfer et al., 2002; Herzog et al., 2004; Seal and Edwards, 2006). In order to further elucidate the role of VGLUTs in visual projections and the relative distributions of VGLUT isoforms in visual areas, we

examined the mRNA and protein distributions of VGLUT1 and VGLUT2 in select subcortical nuclei and cortical visual areas of macaque monkeys. We find that VGLUT1 and VGLUT2 characterize distinct types of visual projections; VGLUT2 predominates in relay or feedforward projections from hierarchical lower order to higher order levels of the visual system, while VGLUT1 appears in modulatory connections between and within visual areas, as well as feedback connections from higher order to lower order structures. Since VGLUT1 and VGLUT2 are known to characterize distinct types of glutamatergic synapses in the central nervous system and regulate differential rates of glutamate release in neurons (Fremeau et al., 2004a; b), we can conclude that these isoforms also define separate glutamatergic projections at the level of neuronal circuits as well. Thus, VGLUT1 and VGLUT2 may define distinct types of excitatory projections within the primate visual system.

2.3 Materials and Methods

Tissue acquisition

One monkey was transcardially perfused with sterile 0.1M phosphate-buffered saline (PBS) followed by sterile 1% paraformaldehyde (PFA) in PBS at the University of Washington. The intact brain was removed and shipped overnight to Vanderbilt University, where the cortical hemispheres were bisected and separated from the thalamus and brainstem. One cortical hemisphere, as well as the thalamus and brainstem, were postfixed in sterile 4% PFA for 6 hours. The unfixed cortical hemisphere was used in an unrelated study. Following postfixation, pia was removed from the exterior surfaces, all pieces were blocked, and all blocks were cryoprotected in 30% sucrose for at least 24 hours prior to histology. The other three monkeys were overdosed with sodium pentobarbital (120mg/kg) and transcardially perfused with PBS followed by 4%

PFA in PBS. The brains were removed and the cortical hemispheres were separated from the thalamus and brainstem. Two of the six cortical hemispheres were used in unrelated studies. The remaining hemispheres, as well as the thalamus and brainstem from all three animals, were blocked and cryoprotected in 30% sucrose for 24 hours prior to histology.

Histology

Cryoprotected blocks from each cortical hemisphere were cut on a sliding microtome into 40-50μm coronal sections and separated into alternating series for further study. Each series contained 50-70 sections distanced ~240μm apart in the brain. One series from each block was processed for cytochrome oxidase (Wong-Riley, 1979) and another series was processed for Nissl substance with thionin; both were used as references for architectonic boundaries of visual areas. Remaining series were cryoprotected (30% glycerol, 30% ethylene glycol, 0.1M PBS) and stored at -20°C for further use.

Immunohistochemistry (IHC)

Immunolabeling for VGLUT1 and VGLUT2 used commercial antibodies against each transporter (see Table 1 for details). Briefly, sections were postfixed for 30min in 4% PFA and rinsed in 0.01% Triton X-100 (Fisher, Pittsburgh PA) in 0.01M PBS. Endogenous peroxidase reactivity was quenched using 0.01% hydrogen peroxide in 0.01M PBS. Sections were rinsed again in 0.01% Triton/PBS, blocked in 5% normal serum (Vector Labs, Burlingame CA) and 0.05% Triton in 0.01M PBS for two hours, and then incubated overnight in the desired concentration of primary antibody (Table 1) with 5% serum and 0.05% Triton in 0.01M PBS. Two antibodies were used for VGLUT1 labeling to confirm the diffuse and variable staining pattern of VGLUT1 in all areas. Following primary incubation, sections were rinsed three times in 0.01% Triton/PBS, and then incubated in the desired secondary antibody with 5% serum and

0.05% Triton in PBS for two hours. Sections were rinsed three times in 0.01% Triton/PBS again, and then incubated in an avidin/biotinyl-peroxidase complex solution (ABC kit, Vector Labs) overnight. Sections were then rinsed three times in 0.01% Triton/PBS to remove nonspecific binding, and then incubated in 0.0002% 3'3' diaminobenzidine with 0.02% nickel in 0.1M PBS to visualize the stain. Sections were mounted on gelatin-subbed slides, dehydrated, and coverslipped with Permount (Fisher). Two series for each area were processed separately for VGLUT1 and VGLUT2 IHC.

Western Blotting (WB)

The specificity of each antibody used in VGLUT1 and VGLUT2 IHC was confirmed using standard western blotting techniques. Prior to perfusion, macaque cerebellar tissue was collected and placed in lysis buffer (0.32M sucrose, 2mM EDTA, 1% sodium dodecyl sulfate, 1mg/ml leupeptin, 50um phenylmethylsulfonyl fluoride, Roche Complete protease inhibitors; Roche) on ice for 10 minutes. Tissue was homogenized using a Kontes pellet pestle (VWR, Radnor PA) and centrifμged at 1700g for 10 minutes. Supernatant was collected from each sample, total protein concentration was determined using a bicinchoninic acid assay kit (Pierce, Rockford IL), and all samples were normalized to 1μg/μl. Roughly 20-40μg of total protein was separated using SDS-PAGE and transferred to PVDF blotting membranes (Roche) overnight. Membranes were rinsed in 0.1M Tris-buffered saline (pH 8.0; Sigma) with 0.01% Triton, blocked in 5% bovine serum albumin (BSA, Roche) with 0.01% Triton for one hour, and then incubated overnight in the desired primary antibody (see Table 1 for details) with 5% BSA and 0.01% Triton, at 4°C with gentle agitation. Following primary incubation, membranes were rinsed in TBS/Triton and incubated in the desired horseradish peroxidase (HRP)-conjugated secondary antibody with 5% BSA and 0.01% Triton for one hour. Membranes were rinsed

several times in TBS/Triton to remove background reactivity and labeled protein on each membrane was visualized using chemiluminescence and exposure to film. Film exposures for each western blot were scanned using a digital scanner and converted to digital images.

2.3.1.1 Table 1. Commercial antibodies and relative concentrations used for western blotting and immunohistochemistry of VGLUT1 and VGLUT2.

	Primary antibody (IHC, WB)	Secondary Antibody (IHC)	Normal Serum (IHC)	Secondary Antibody (WB)
VGLUT1 (cortex)	Rabbit anti-VGLUT1 (MAb Technologies) 1:3000 IHC 1:1000 WB	Biotinylated goat anti-rabbit IgG (Vector Labs) 1:500	Goat serum (Vector Labs)	HRP-conjugated goat anti-rabbit IgG (Jackson Labs) 1:30,000
VGLUT1 (thalamus, midbrain)	Mouse anti-VGLUT1 (Synaptic Systems) 1:3000 IHC 1:1000 WB	Biotinylated goat anti-mouse IgG (Vector Labs) 1:500	Goat serum (Vector Labs)	HRP-conjugated goat anti-mouse IgG (Jackson Labs) 1:20,000
VGLUT2 (thalamus, midbrain, cortex)	Mouse anti-VGLUT2 (Millipore) 1:5000 IHC 1:2000 WB	Biotinylated horse anti-mouse IgG (Vector Labs) 1:500	Horse serum (Vector Labs)	HRP-conjugated goat anti-mouse IgG (Jackson Labs) 1:30,000

In situ hybridization (ISH)

Digoxigenin-labeled riboprobes for *VGLUT1* and *VGLUT2* mRNA were prepared from macaque cDNA libraries under previously described conditions (Tochitani et al., 2001) and labeled using a conventional DIG-dUTP labeling kit (Roche). ISH was performed with slight modifications of previously described techniques. All sections were postfixed overnight in 4% PFA, incubated in 0.75% glycine for 15 minutes to remove background reactivity due to formaldehyde fixation, and then incubated in 0.3% Triton for 15 minutes to increase

permeability. Sections were treated with 0.1% Proteinase K (Sigma) for 30 minutes at 37°C, excess Proteinase K was acetylated using 0.25% acetic anhydride in 0.9% triethanolamine and 0.12% hydrochloric acid for 10 minutes, and all sections were preincubated in hybridization buffer (pH 7.5) containing 5% saline sodium citrate (SSC; 150 mM sodium chloride, 15 mM sodium citrate, pH 7.0), 50% formamide (FA), 2% blocking reagent (Roche), 0.1% N-lauroylsarcosine (NLS), 0.1% sodium dodecyl sulphate (SDS), and 20 mM maleic acid for one hour at 60°C. Sections were then hybridized overnight at 60°C in the same buffer, along with 1μg/ml of the desired probe. Hybridized sections were treated with 20 μg/mL RNase A (Sigma) in RNase A buffer (10 mM Tris-HCl, 10 mM ethylenediamine-N,N,N′,N′ -tetraacetic acid (EDTA), 500 mM NaCl; pH 8.0) for 15 minutes at 37°C to remove nonspecific mRNA. Finally, sections were thoroughly rinsed in Tris-buffered saline (pH 7.5; Sigma) for 15 minutes, blocked in 0.5% blocking reagent (Roche) for 30 minutes, and incubated with an alkaline phosphatase labeled anti-DIG antibody (1:1000, Roche) in 0.5% blocking reagent for four hours. Sections were then visualized overnight with 1:50 NBT/BCIP (Roche) in Tris 9.5, mounted on gelatin-subbed slides, dehydrated in ethanol and cleared in xylene, and coverslipped with Permount. Two series for each area were processed separately for *VGLUT1* and *VGLUT2* ISH.

Imaging and analysis

Digital photomicrographs and montages were captured using an MBF CX9000 camera mounted on a Nikon E80i microscope with Neurolucida software (MBF Bioscience, Williston, VT). All images were cropped and adjusted for brightness and contrast, but were otherwise unaltered.

2.4 Results

Protein and mRNA distributions of VGLUT1 and VGLUT2 varied significantly between and within visual structures, but remained largely consistent with known VGLUT distributions in other primate species (Hackett and la Mothe, 2009; Balaram et al., 2011a; b; Garcia-Marin et al., 2013). We find that VGLUT1 and VGLUT2 appear to characterize distinct types of glutamatergic projections within the macaque visual system. *VGLUT1* mRNA was moderately expressed in the lateral geniculate nucleus and pulvinar complex but strongly expressed in V1 (area 17) and V2 (area 18). *VGLUT2* mRNA, in contrast, was strongly expressed in the lateral geniculate nucleus, discrete layers of the superior colliculus, and the pulvinar complex, but only moderately expressed in certain layers of V1 and V2. VGLUT1 and VGLUT2 protein labeling was restricted to axon terminals in all areas examined, with the exception of a few cells in the pulvinar complex. VGLUT1 protein was diffusely expressed in all visual structures, and the intensity of labeling varied between and within regions of interest. VGLUT2 protein, however, was localized to retinorecipient regions of the lateral geniculate nucleus and superior colliculus and tectorecipient regions of the pulvinar complex, as well as specific layers of V1 and V2. The detailed distributions of VGLUT1 and VGLUT2 are discussed below.

2.4.1 Specificity controls for VGLUT1 and VGLUT2

In situ hybridization using sense and antisense probe strands against *VGLUT1* and *VGLUT2* mRNA confirmed the specificity of both probes to their respective RNA targets, with no crossreactivity between sequences and no detectable background reactivity, in macaque brain tissue (Figs. 1A and B). Western blots for all antibodies against VGLUT1 and VGLUT2 protein also showed strong specificity with no detectable background immunoreactivity in macaque

cerebellar tissue (Fig. 1C). VGLUT1 was localized at 73kDa and VGLUT2 was localized at 56kDa, consistent with known molecular weights of both proteins. The rabbit polyclonal antibody against VGLUT1 labeled a portion of the full VGLUT1 protein (65kDa), as noted by the manufacturer, but comparisons of staining distributions confirm that both VGLUT1 antibodies label the correct protein (data not shown). Additionally, no differences in staining intensity were noted between sections from animals perfused with 1% PFA or 4% PFA. These findings demonstrate the specificity of the antibodies to VGLUT1 and VGLUT2, and eliminate concerns about nonspecific selectivity of the chosen probes and antibodies in macaque tissue.

2.4.1.1 Figure 1. (A and B) Sense and antisense staining of *VGLUT1* and *VGLUT2* mRNA in macaque thalamus sections confirms probe specificity. (C) Western blotting for VGLUT1 and VGLUT2 protein in macaque cerebellum lysate confirms antibody specificity for both proteins.

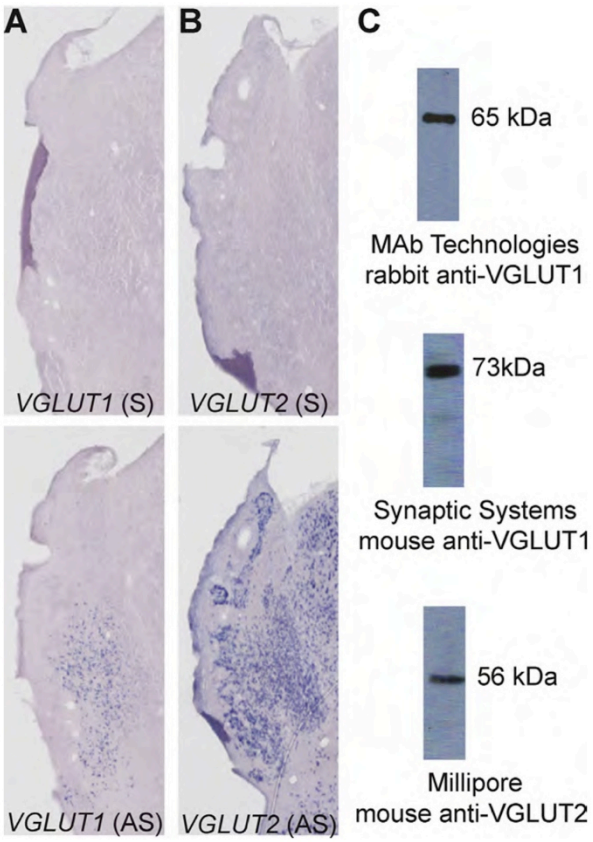

2.4.2 Subcortical distributions of VGLUT1 and VGLUT2

VGLUT1 protein was densely and evenly distributed across the lateral geniculate nucleus, superior colliculus, and pulvinar complex while VGLUT2 protein was confined to more discrete distributions such as the retinorecipient layers of the lateral geniculate nucleus and superior colliculus, and tectorecipient regions of the inferior pulvinar. In all three subcortical areas, *VGLUT1* mRNA was expressed at low levels while *VGLUT2* mRNA was expressed at high levels, and both mRNA distributions correlated with known projections from these structures. Differences in VGLUT distributions in subcortical visual areas appear to identify distinct afferent and efferent projections from each area, as detailed below.

Superior colliculus (SC)

The superior colliculus in macaques is a large, well-laminated midbrain structure that is traditionally divided into superficial, intermediate, and deep sets of layers, each of which mediates different functions within the SC (May, 2006). The majority of visual processing in the SC occurs in the superficial layers, while the deep layers regulate multisensory integration and brainstem motor functions. For the purposes of this study, only the superficial layers are considered. The most superficial layer of the SC is the stratum zonale or zonal layer (SZ), a narrow band of axon fibers that covers the dorsal surface of the colliculus. Just ventral to the SZ lies the stratum griseum superficiale or superficial gray layer (SGS), an intermediately sized, cell dense layer that can be divided into upper and lower subdivisions (uSGS and lSGS, respectively) in most primates. Ventral to the SGS lies the stratum opticum or optic layer (SO), similar in size to the SGS but largely cell free and instead filled with fiber tracts that run lateral to medial through the layer. Laminar divisions of the superior colliculus are indicated in figure 2.

2.4.2.1 Figure 2. Low magnification images through the macaque superior colliculus. Scale bar is 1mm, thalamic midline is to the left.

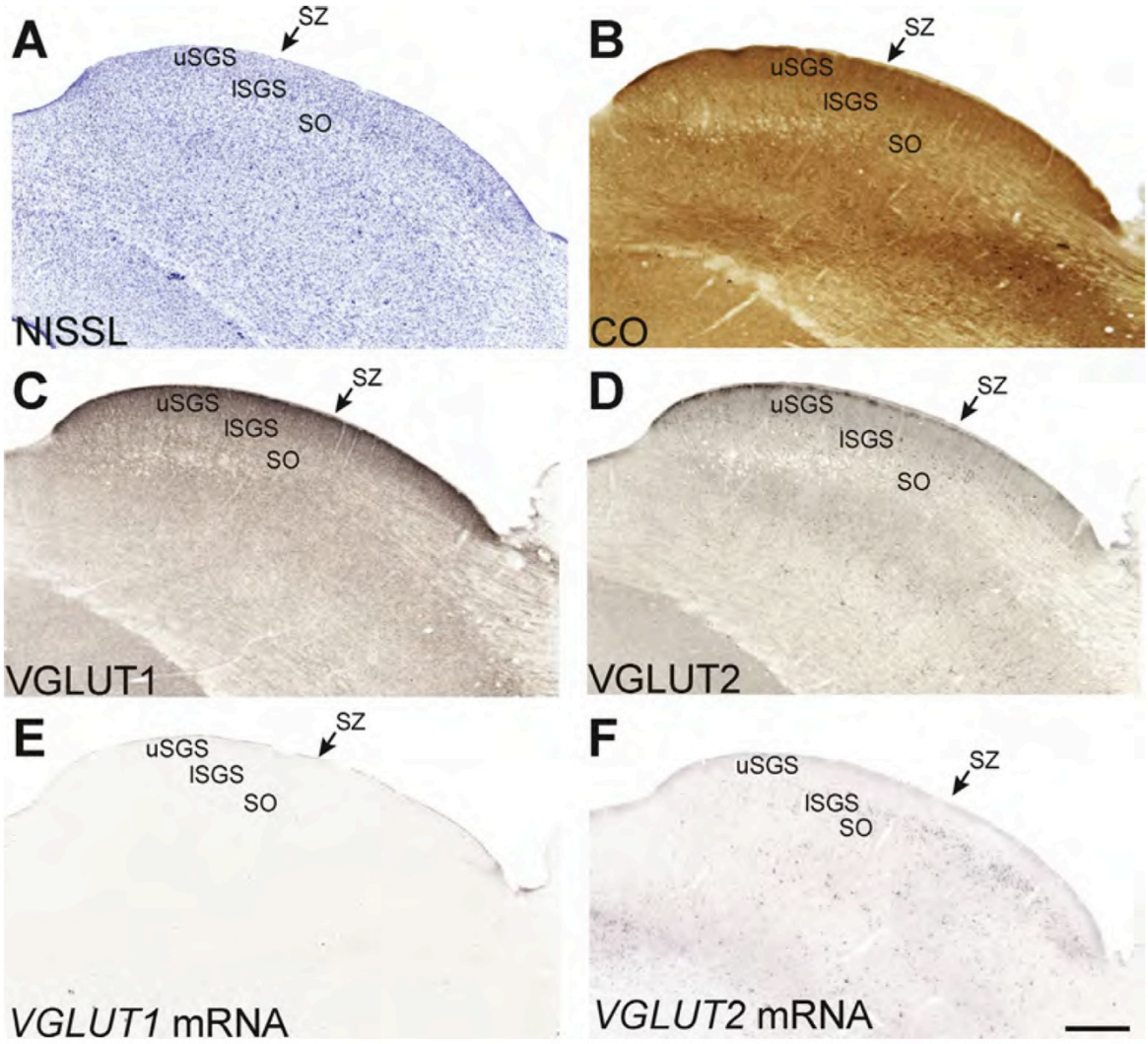

In Nissl preparations of the superior colliculus (Fig. 2A), the SZ was distinguishable as two layers across the dorsal surface of the colliculus, the upper layer consisting of a thin row of cells of mostly astrocytes (Lund, 1972), and a lower layer of fibers that cross the extent of the SC. The SGS was also visible below the SZ, and could be separated into upper and lower subdivisions based on cell density. The SO showed much sparser cell distributions than the overlying layers of the SC. In CO preparations (Fig. 2B), the upper SZ stained weakly for CO

and appeared as a light band across the surface of the colliculus, while the lower SZ stained strongly for CO and appeared as a thin, dark band. The SGS could also be differentiated into its respective subdivisions, the upper SGS showed dense CO staining while the lower SGS showed more moderate CO reactivity. The SO stained lightly for CO, mostly between the fiber tracts running through this layer, appearing as a light, medium-sized band that originated from the optic tract on the lateral edge and continued to the medial aspect of the SC. From rostral to caudal sections in the colliculus, the SZ remained a uniform size while the SGS and SO appeared to decrease in relative thickness. No cells were visible in CO-stained sections of the SC. With the exception of upper and lower subdivisions of the SZ in CO preparations, both Nissl and CO distributions in the macaque SC are consistent with previous descriptions of lamination in the primate colliculus (May, 2006).

2.4.2.2 Figure 3. High magnification images of VGLUT distributions in the superior colliculus. Laminar divisions are listed on the left, scale bar is 25um.

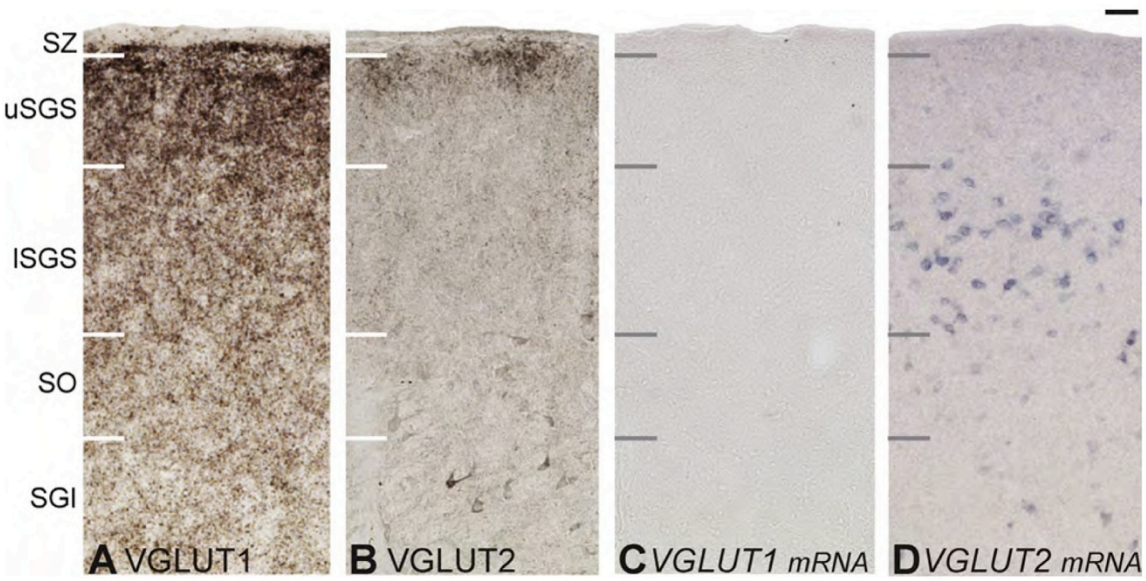

The labeling of VGLUT1 and VGLUT2 protein in the superficial layers of the SC likely reflects retinotectal and corticotectal terminal projections (Tigges and Tigges, 1970; Symonds and Kaas, 1978) (Figs. 2C, D and 3A, B). VGLUT1 was densely distributed across all the superficial layers of the SC, indicating its considerable use in retinal or cortical projections (Figs. 2C and 3A). The SZ was discernible as two bands; the upper astrocytic layer was devoid of VGLUT1 and the lower fiber layer was densely labeled with VGLUT1. The SGS was also clearly split into two divisions; the upper SGS stained darkly for VGLUT1 and the lower SGS stained more moderately for VGLUT1. The SO showed even, diffuse labeling of VGLUT1 throughout the SC, mostly apparent as punctate labeling around the fibers running through this layer. No differences in VGLUT1 labeling were seen between rostral and caudal extents of the SC. In contrast, VGLUT2 labeling in the SC was concentrated in the lower SZ and dorsal parts of the upper SGS, appearing as dense, regular patches of label through the rostrocaudal extent of the colliculus (Figs. 2D and 3B). VGLUT2 labeling in the lower SZ/upper SGS was consistently denser along the medial aspect compared to the lateral aspect of the SC. Moderate VGLUT2 terminal labeling was observed through the rest of the SGS and SO, but remained at reduced levels through the colliculus. The discrete, patchy labeling of VGLUT2 terminals seen in the superficial layers of the SC closely resembles previous descriptions of retinotectal terminations in macaques (Wilson and Toyne, 1970; Hubel et al., 1975; Pollack and Hickey, 1979) while the diffuse, even labeling of VGLUT1 terminals more resembles patterns of corticotectal terminations (Wilson and Toyne, 1970). Thus, VGLUT1 and VGLUT2 likely characterize the terminations of distinct visual projections to the macaque SC.

Tectopulvinar and tectogeniculate projection neurons were examined using *VGLUT1* mRNA expression, which identified *VGLUT1* or *VGLUT2* mRNA-positive cells in the SC that

utilize the respective protein in their axon terminals (Figs. 2E, F and 3C, D). *VGLUT1* mRNA was notably absent from all superficial layers of the SC (Figs. 2E and 3C). A few large *VGLUT1*-positive neurons were found in the intermediate layers and along the edge of the periacqueductal gray, confirming the reaction technique, but similarly stained cells were not found in the SZ, SGS, or SO, indicating that efferent projections from the SC do not appear to utilize *VGLUT1* for excitatory transmission. *VGLUT2* mRNA however, was differentially distributed throughout the superficial layers of the SC (Figs. 2F and 3D). Both layers of the SZ and the upper SGS were devoid of *VGLUT2* mRNA, but the lower SGS contained numerous medium-sized cells that stained strongly for *VGLUT2* mRNA. In caudal sections of the SC, *VGLUT2*-positive cells in the lower SGS were evenly distributed from the medial to lateral edge, but in more rostral sections they were concentrated along the lateral aspect of the SC. The SO contained a scattered distribution of smaller and more moderately stained *VGLUT2*-positive cells. Cells in the lower SGS of the colliculus project to specific divisions of the inferior pulvinar in macaques (Stepniewska et al., 2000; Lyon et al., 2010) and strong *VGLUT2* mRNA expression in this layer corresponds to strong VGLUT2 terminal labeling in those divisions of the pulvinar complex (discussed below).

Pulvinar

The primate pulvinar is a large complex of several nuclei within the thalamus that are well connected to a number of visual and nonvisual cortical areas, with some nuclei also receiving inputs from the SC (Stepniewska, 2004). The pulvinar of macaques has been traditionally subdivided into four major regions; the anterior pulvinar (PA), the medial pulvinar (PM), lateral pulvinar (PL), and inferior pulvinar (PI). PI in macaques has been subdivided into four areas, posterior inferior pulvinar (PIp), medial inferior pulvinar (PIm), and central inferior

pulvinar (PIc), which was further subdivided into medial and lateral divisions, PIcm and PIcl respectively (Stepniewska and Kaas, 1997). While the traditional boundary between PI and PL and PM has been the brachium of the superior colliculus, all subdivisions of PI continue into the ventral portions of PM and PL. PA is not connected to occipital and other visual areas that contribute to early stages of visual processing, and thus, is not discussed here. PM, PL, and PI, however, are connected with various cortical visual areas and likely serve a crucial role in processing and integrating visual information. Subdivisions of the pulvinar complex in macaques are shown in figure 4.

Nissl preparations through the pulvinar complex (fig. 4A) clearly distinguished the three major pulvinar subdivisions as previously described (Olszewski, 1952). Nissl stained cells in PM were densely packed and evenly distributed, while cells in PL were irregularly distributed between fiber bundles running lateral to medial through the nucleus. PI could be separated into three divisions based on cell density; PIm showed dense cell distributions, clearly distinguishing it from the more diffuse cell distributions of PIp and PIc. CO-stained sections through the pulvinar better delineated the subdivisions of this area (fig. 4B); PM showed moderate CO reactivity with multiple darker patches along the ventrolateral aspect that were continuous with subdivisions of PI, while PL showed more irregular CO reactivity with light and dark areas dispersed between fiber bundles. PI could be divided into four regions; PIm stained strongly for CO, distinguishing it from PIp and PIcm, both of which stained weakly for CO. PIcl showed slightly stronger CO reactivity than PIcm in rostral and middle sections through the pulvinar complex. Previous CO descriptions of the macaque pulvinar identified similar patterns as those described above (Stepniewska and Kaas, 1997; Stepniewska et al., 2000; Stepniewska, 2004), providing us with consistent definitions of boundaries between pulvinar divisions.

2.4.2.3 Figure 4. Low magnification images through the pulvinar complex. Scale bar is 1mm, thalamic midline is to the left.

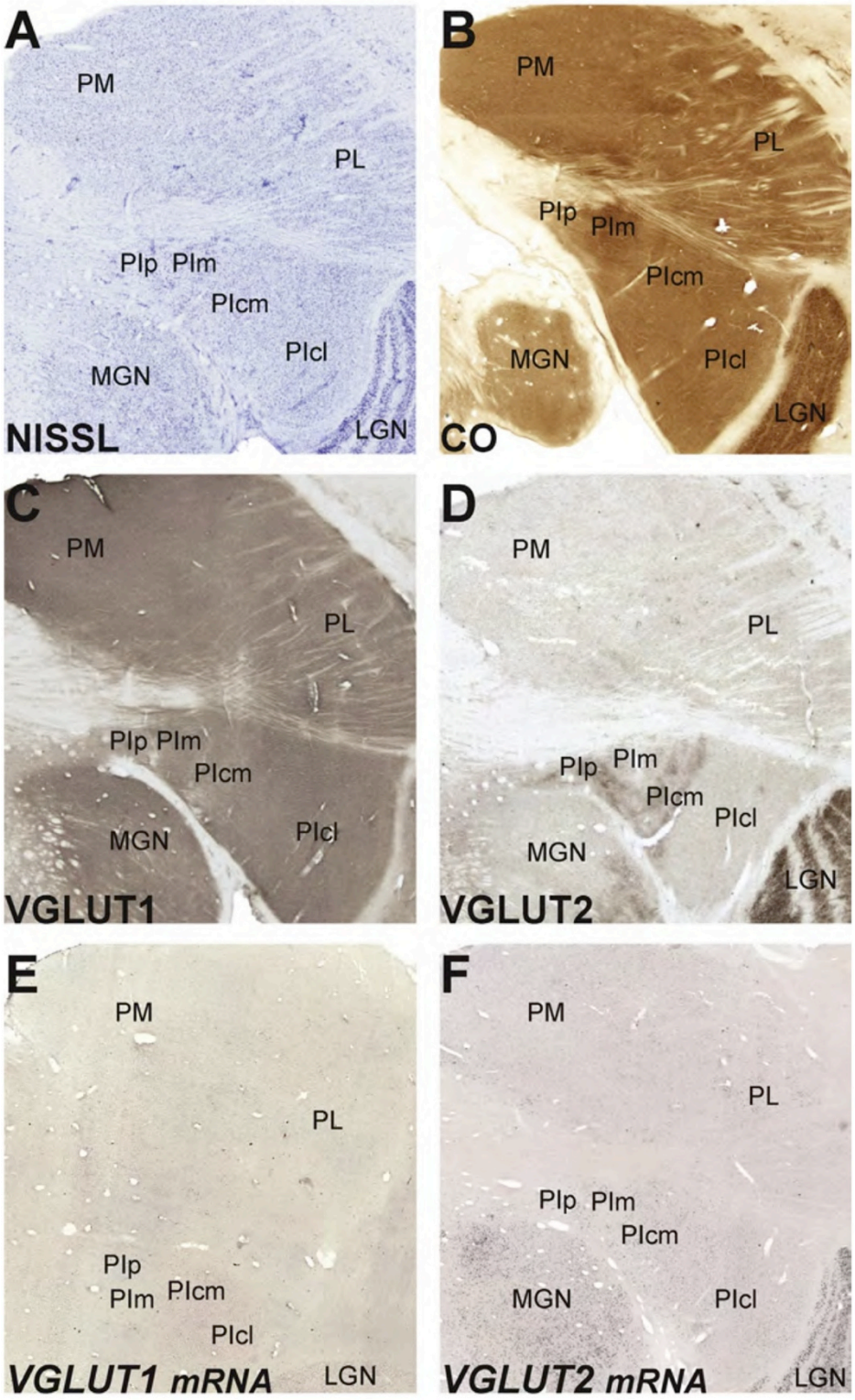

2.4.2.4 Figure 5. High magnification images of VGLUT1 protein (A-F), VGLUT2 protein (G-L), *VGLUT1* mRNA (M-R), and *VGLUT2* mRNA (S-X) distributions in each division of the pulvinar complex. VGLUT1 and VGLUT2 distributions vary distinctly between each nucleus but the varied labeling patterns of each isoform highlight the heterogeneity of afferent and efferent projections through this nucleus.

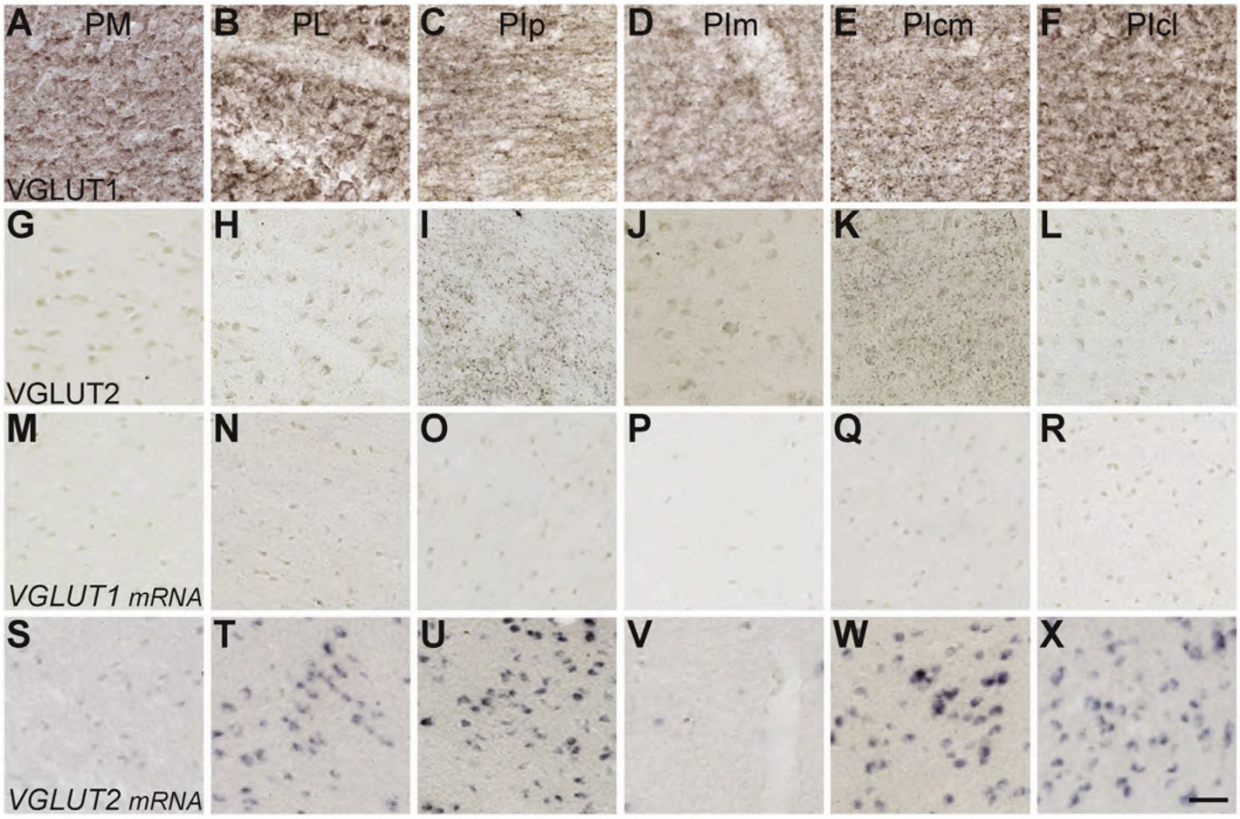

Afferent terminations in the pulvinar complex were largely characterized by dense, even distributions of VGLUT1 and not VGLUT2 (figs. 4C, D and 5A, L). PM showed dark, punctate staining of VGLUT1 across its extent (figs. 4C and 5A-F), with slightly darker labeling along the dorsomedial boundary of PM (best seen in fig. 4C). PL showed more diffuse VGLUT1 reactivity dispersed between the brachial fiber bundles (fig. 5B). PI could be separated into four divisions; PIp and PIcm stained less darkly for VGLUT1, with small punctate terminals distributed throughout both structures (figs. 5C, E), and appeared as lighter bands around PIm (best seen in fig. 4C). Labeled terminals in PIm appeared much smaller than those seen in PIp and PIcm, and

diffuse neuropil labeling of VGLUT1 was also apparent in this region (fig. 5D). Lastly, VGLUT1 staining in PIcl closely resembled that of PL (fig. 5F), with diffuse terminal labeling distributed throughout the region. In contrast to VGLUT1, strong VGLUT2 reactivity was only found in two subdivisions of the pulvinar complex, PIp and PIcm (figs. 4D and 5G-L). Both regions showed dense, patchy distributions of VGLUT2 positive terminals (fig. 5I and K), while all other pulvinar divisions showed weak cellular labeling of VGLUT2. Strong labeling of VGLUT2 positive terminals in PIcm and PIp also continued dorsal and ventral to PIm in most sections (fig. 4D), suggesting that these two regions of dense VGLUT2 labeling are parts of the same nucleus. Diffuse cellular labeling of VGLUT2 clearly distinguished PIm from the surrounding pulvinar, and differentiated PIcl from PIcm, but did not distinguish PM from PL. The diffuse labeling of VGLUT1 in all divisions of the pulvinar likely correspond to multiple cortical projections that terminate within this structure, while the discrete labeling of VGLUT2 terminals in PIp and PIcm correspond to subcortical projections from the lower SGS of the colliculus. Thus, VGLUT1 and VGLUT2 likely typify the synaptic terminations of distinct afferent projections within the pulvinar complex (Masterson et al., 2009).

Neurons within the pulvinar, which project to a variety of visual cortical areas, were disparately characterized by both *VGLUT1* and *VGLUT2* mRNA (figs. 4E, F and 5M-R). VGLUT1 was only weakly expressed in scattered cells throughout the pulvinar complex, making it difficult to detect changes in *VGLUT1* expression between pulvinar divisions (figs. 4E and 5M-R). *VGLUT2* mRNA was more strongly expressed in all divisions of the pulvinar, but expression patterns were often heterogeneous within each division (figs. 4F and 5T, X). In general, PIp and PIcm showed similarly strong *VGLUT2* expression, with dense clusters of large and medium sized *VGLUT2* positive cells (figs. 5U, W). PL and PIcl also showed strong

VGLUT2 expression, in smaller cells that were closely packed (figs. 5T, X). Lastly, PM and PIm showed weak levels of *VGLUT2* expression in a small percentage of cells within each division (figs. 5S, V). The distinct patterns of *VGLUT1* and *VGLUT2* mRNA highlight the heterogeneity of glutamatergic projection neurons within the pulvinar complex.

Lateral geniculate nucleus (LGN)

The dorsal lateral geniculate nucleus in macaques is composed of cell-dense layers, interleaved by cell-sparse interlaminar zones (fig. 6). LGN layers are traditionally defined by their cell type and relative location within the nucleus; from ventral to dorsal, they are classified as external magnocellular (ME), internal magnocellular (MI), internal parvocellular (PI), and external parvocellular (PE). In macaques, both parvocellular layers split into alternating leaflets and appear as four layers instead of two (Kaas et al., 1978). Boundaries between LGN layers and interlaminar zones were easily distinguishable in CO and Nissl stained sections (fig. 6A, B) and were consistent with previous descriptions of this nucleus (Kaas et al., 1978).

Major afferent terminations in the LGN from the retina, superior colliculus, and primary visual cortex were labeled by staining for VGLUT1 and VGLUT2 protein. Sections stained for VGLUT1 showed dense but diffuse labeling of axon terminations through the M and P layers, as well as the interlaminar zones of the LGN (figs. 6C, 7A-C). The dorsal leaflet of PE appeared to stain darker for VGLUT1 compared to the other layers, across all sections of the LGN (best seen in Fig 6C), but no other differences were noted in staining intensity between the layers. The interlaminar zones stained more diffusely for VGLUT1 and could be distinguished from neighboring LGN layers based on their reduced staining intensity. In comparison to VGLUT1, VGLUT2 distributions in the LGN were remarkably different; punctate terminal labeling of VGLUT2 was densely packed in the M and P layers but largely absent from the interlaminar

zones (figs. 6D and 7D-F). Stronger and denser VGLUT2 labeling was seen in the M layers in comparison to the P layers in all sections of the LGN (figs. 6D. 7D). The discrete labeling of VGLUT2 terminals within the LGN layers matches patterns of retinogeniculate terminations in macaques (Kaas et al., 1978; Conley and Fitzpatrick, 1989) while the diffuse labeling of VGLUT1 terminals resemble cortical projections to this nucleus (Lund et al., 1975). Thus, VGLUT1 and VGLUT2 appear to resemble distinct projections within the macaque LGN.

LGN projection neurons were examined for *VGLUT* mRNA expression (figs. 6E, F and 7G-L). *VGLUT1* mRNA was weakly expressed in cells of all LGN layers and interlaminar zones (figs. 6E and 7G-I). In sections stained for *VGLUT2* mRNA, most cells in the M and P layers strongly expressed *VGLUT2*, while cells in the interlaminar zones did not (figs. 6F and 7J-L). VGLUT2 positive cells in the P layers were more densely packed than those in the M layers, but no other laminar differences were found. Lastly, no rostrocaudal differences in *VGLUT1* and *VGLUT2* expression were seen in the LGN. Cells in the LGN primarily project to V1 (Hendrickson et al., 1978) and the dual expression of both *VGLUT1* and *VGLUT2* mRNA within the magnocellular and parvocellular LGN layers suggests that these cells use both isoforms in their cortical projections. Isolated *VGLUT1* expression in the koniocellular layers suggests that these cells use a single isoform in glutamatergic transmission instead.

2.4.2.5 Figure 6. Low magnification images through the lateral geniculate nucleus (LGN). Scale bar is 1mm, thalamic midline is to the left.

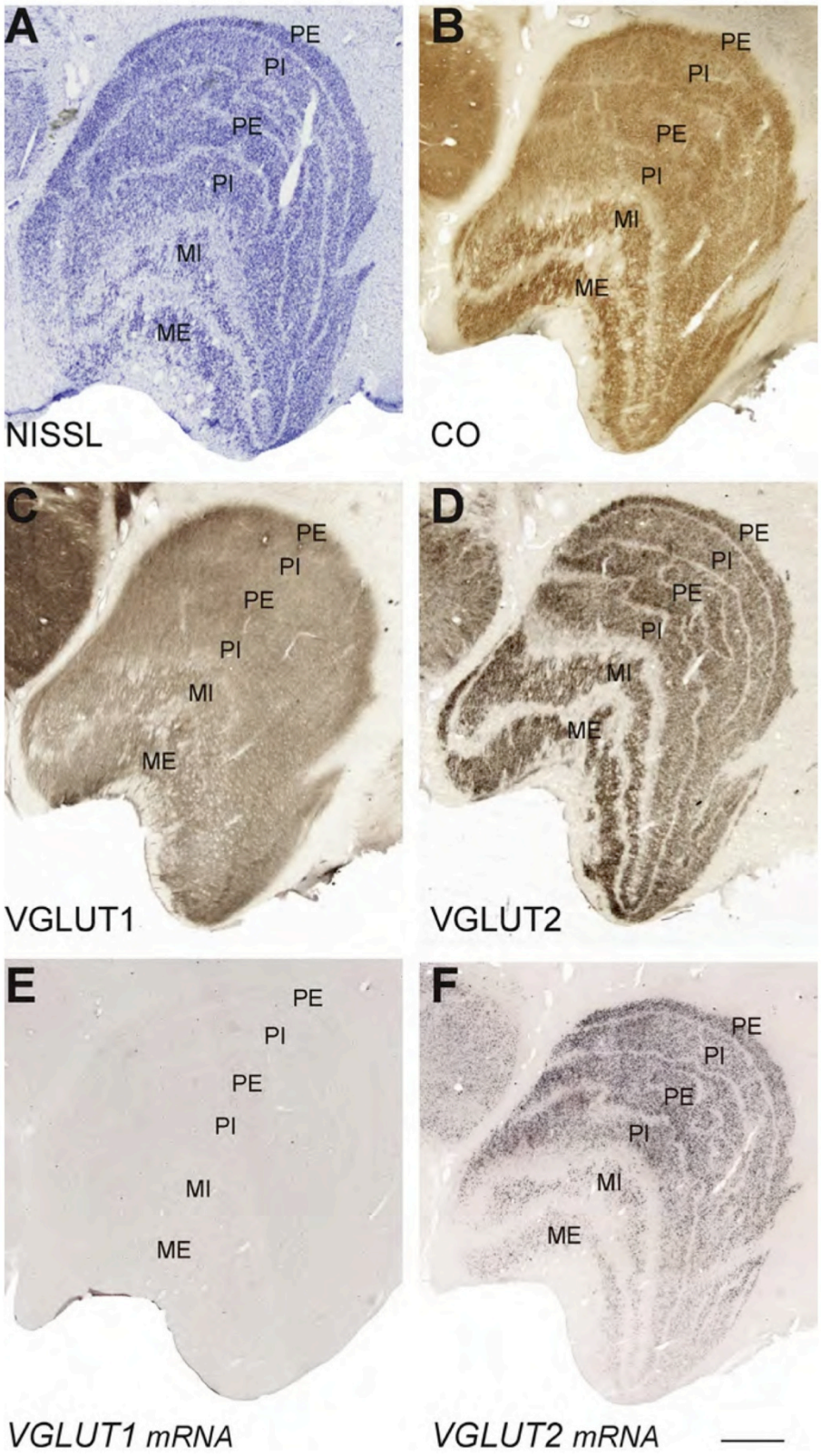

2.4.2.6 Figure 7. High magnification images of VGLUT distributions in the LGN stained for (A-C) VGLUT1 protein, (D-F) VGLUT2 protein, (G-I) *VGLUT1* mRNA, and (J-L) *VGLUT2* mRNA. Scale bar is 100um.

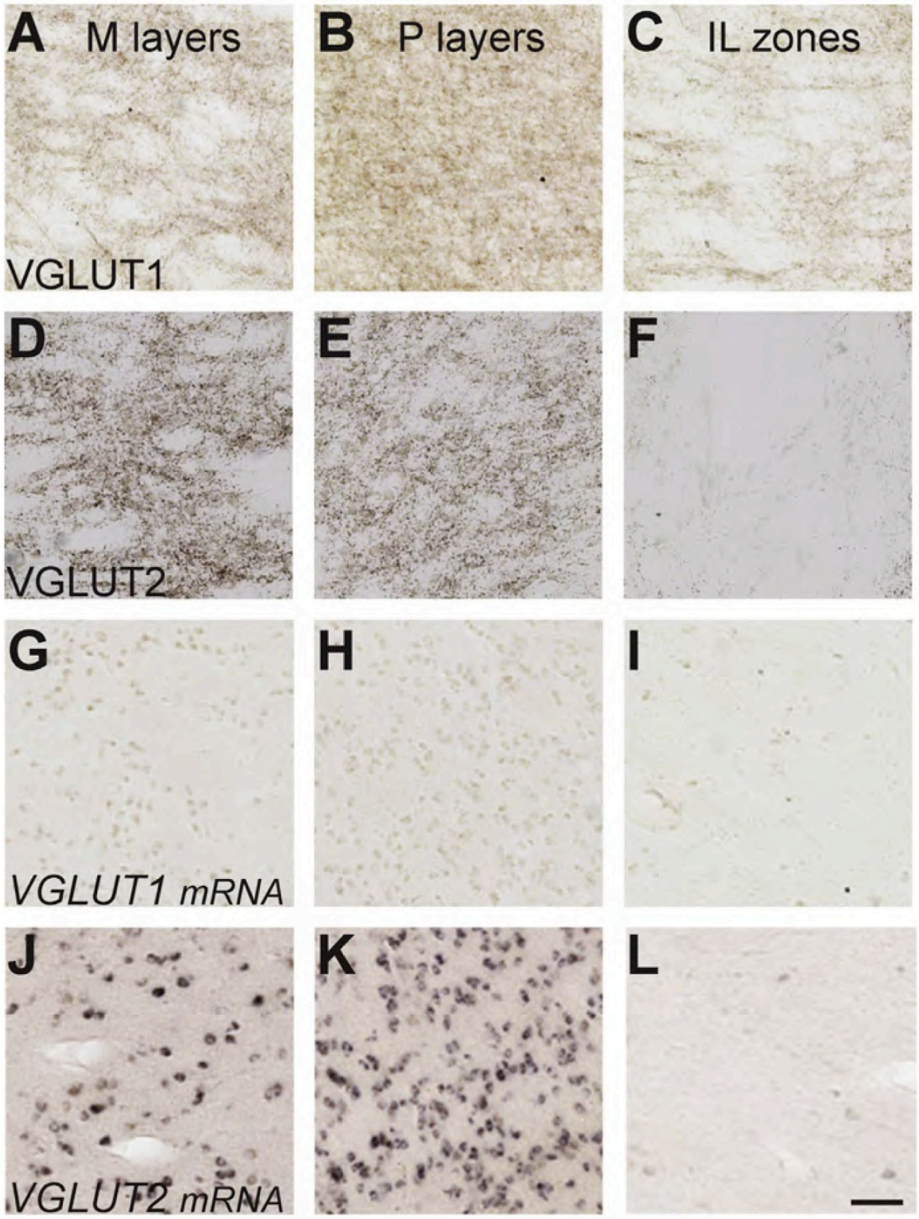

2.4.3 Cortical distributions of VGLUT1 and VGLUT2

Large-scale differences were seen in VGLUT distributions between V1 and V2. Overall, *VGLUT1* mRNA predominated in cortical neurons while *VGLUT2* mRNA only identified a subset of neurons from these areas. Additionally, VGLUT1 protein was diffusely distributed in V1 and V2 while VGLUT2 was restricted to discrete terminations. The differential distribution of VGLUT isoforms in cortical areas again suggests that these proteins characterize separate glutamatergic projections in the macaque visual system.

Area V1

V1 in macaques is easily identifiable by its extensive lamination and distinct architectonic characteristics. Here, V1 layers and sublayers are numbered according to Hässler's (1967) scheme (fig 8B), rather than the more common scheme of Brodmann (1909), as evidence from numerous comparative and other studies support this classification (Brodmann, 1909; Hässler, 1967; Casagrande and Kaas, 1994; Garey, 2006). The primary difference between these schemes is their delineation of layer 4 in V1; Brodmann's scheme includes 3 sublayers of layer 4, 4A, 4B, and 4C, while Hässler's scheme labels Brodmann's 4A and 4B as sublayers of layer 3, 3B and 3C respectively, and Brodmann's layer 4C as a single layer 4. Subdivisions of all V1 layers in macaques are distinctly visible in Nissl stains that demarcate cell size and density in this area (figs. 8C and 9A). The abrupt change in lamination between V1 and V2 also clearly marks the boundary between both areas (fig. 8). CO stained sections through V1 revealed distinct patterns of lamination based on staining intensity (figs. 8D and 9B). Layer 1 showed no reactivity, and layers 2, 3, and 5 stained lightly for CO. Layers 3Bb and 4 stained darkly for CO and appeared as distinct bands that terminated at the border between V1 and V2. Patches of strong CO reactivity were visible at regular intervals in layer 3, identifying the blob and interblob

compartments of V1 (Wong-Riley, 1979). Lastly, layer 6 stained moderately for CO and appeared as another distinct band ventral to layer 5. CO and Nissl stains through V1 were consistent with previous reports, and provided a reliable basis of laminar and areal definitions in the macaque visual cortex (Casagrande and Kaas, 1994).

VGLUT protein distributions varied distinctly between the layers of V1 (figs. 8E, F and 9C, D). Layers 1 and 3A stained densely for VGLUT1 but not VGLUT2. Layer 2 showed scattered populations of VGLUT2 positive terminals clustered toward to dorsal boundary of the layer (best seen in 8D), which resembled pulvinar terminations in V1 (Ogren and Hendrickson, 1977), and dense VGLUT1 reactivity throughout. Layers 3B and 3C stained weakly for both VGLUT proteins and appeared as lighter bands within the superficial layers of V1. Layer 3Bb, however, showed unique staining patterns of both VGLUT isoforms; a thin band of strong VGLUT1 labeling and a thin band of strong VGLUT2 labeling were present, with the VGLUT1 band consistently dorsal to the VGLUT2 band throughout V1. When aligned with CO sections, both bands fell within the strong belt of CO reactivity seen in layer 3Bb. Thus, two different types of VGLUT inputs are segregated within layer 3Bb. Layer 4 also showed unique expression patterns of VGLUT1 and VGLUT2. Both 4A and 4B had dense distributions of VGLUT1 and VGLUT2 compared to the other layers of V1, but the densest labeling of VGLUT1 appeared at the border between 4A and 4B while the densest labeling of VGLUT2 appeared in 4B proper. Alignment with CO sections confirmed that both dense VGLUT bands were within layer 4. Layer 5 labeled weakly for VGLUT1 and VGLUT2, while layer 6 exhibited more moderate labeling of both proteins. With the exception of 6A, which had slightly stronger VGLUT1 staining than 6B, neither layer 5 nor layer 6 presented any sublaminar differences in VGLUT

reactivity. The distinctive laminar distributions of VGLUT1 and VGLUT2 proteins ended at the border between V1 and V2 (figs. 8E, F), indicating that these patterns are unique to V1.

2.4.3.1 Figure 8. Low magnification images of V1 and V2. (A) Coronal section of cytochrome oxidase (CO) reactivity in V1 and V2, showing region of interest for panels B-H. (B) Areal and laminar divisions of V1 and V2 in reference to panels C-H, adapted from Casagrande and Kaas, 1994. Scale bars in are 1mm.

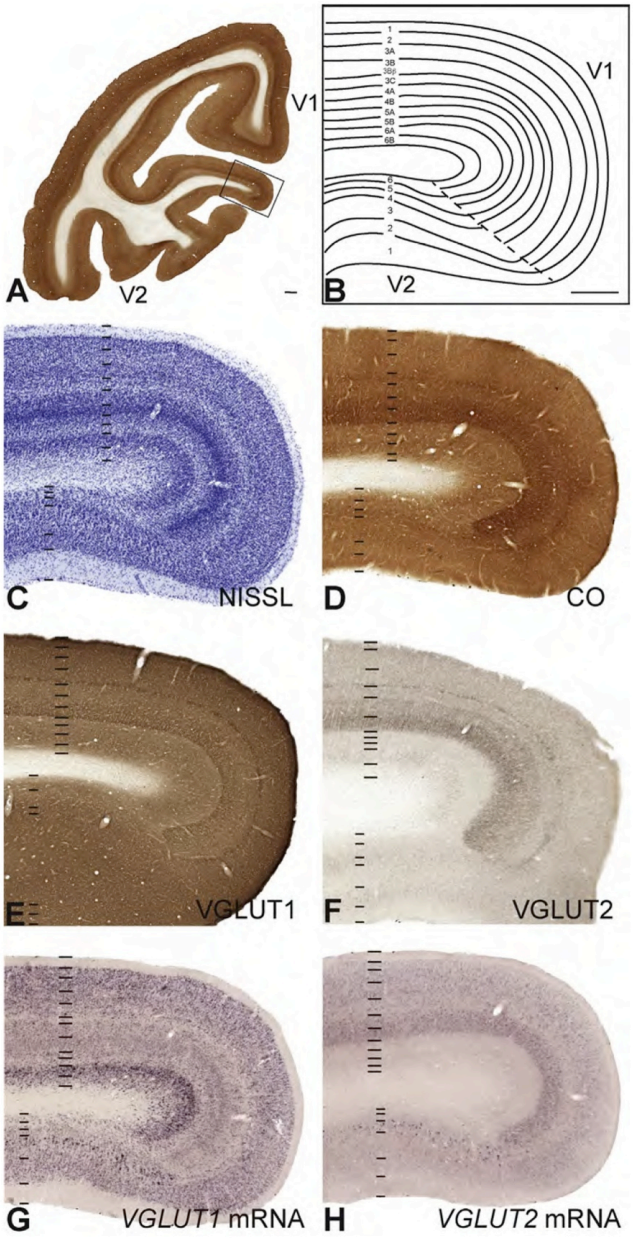

Dense VGLUT2 labeling in layers 4A, 4B, and 3Bb likely reflects magnocellular and parvocellular geniculostriate input to V1 (Hendrickson et al., 1978; Blasdel and Lund, 1983), as evidenced by strong *VGLUT2* mRNA expression in those layers of the LGN. The dorsal band of VGLUT1 labeling in layer 3Bb, as well as dense VGLUT1 labeling at the 4A/4B border, likely reflects a distinct subset of parvocellular geniculate inputs to V1 (Hendrickson et al., 1978) and corresponds to the expression of *VGLUT1* mRNA in those LGN layers as well. Alternatively, but less likely given the weak levels of *VGLUT1* mRNA seen in the cell bodies of these projections, the bands of VGLUT1 labeling in V1 could correspond to koniocellular geniculate terminations in layer 3Bb (Lund et al., 1988).

2.4.3.2 Figure 9. High magnification images through V1. Laminar divisions indicated on the left, adapted from Casagrande and Kaas, 1994. Scale bar is 100um.

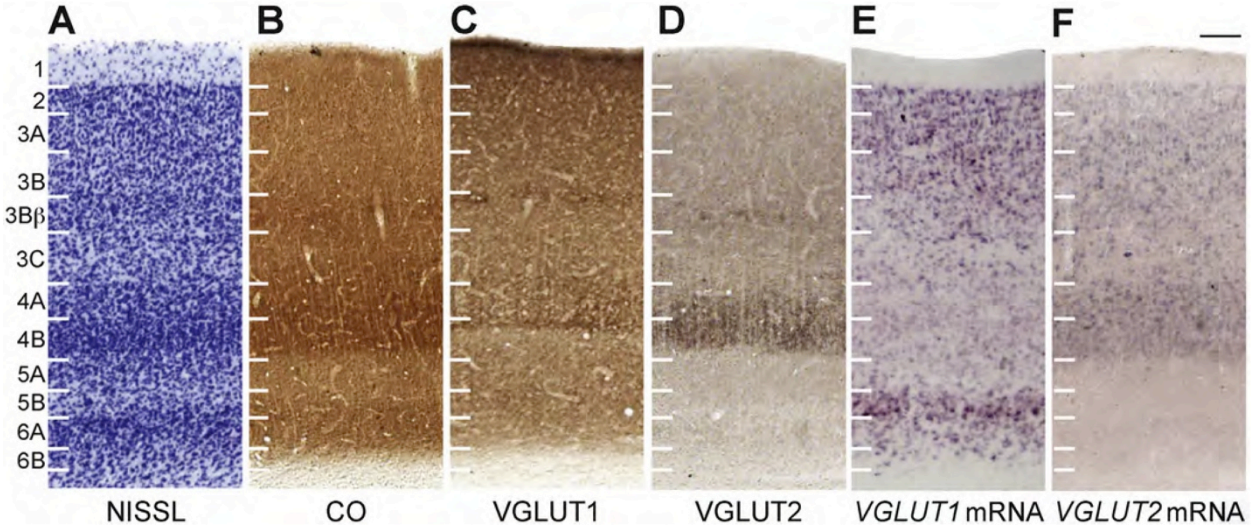

Neurons that expressed *VGLUT1* and *VGLUT2* mRNA were found in discrete layers of V1 (figs. 8G, H and 9E, F). Layer 1 did not express either *VGLUT* isoform, consistent with its

very sparse distributions of neurons. Layers 2 and 3A showed dense expression of *VGLUT1* and weak expression of *VGLUT2*. In both layers, labeled cells were small and densely packed. Sublayers 3B and 3Bb were slightly more heterogeneous in expression patterns and cellular distributions; both layers contained small, medium and large cells interspersed with each other, some cells with strong *VGLUT1* or *VGLUT2* expression and others with more moderate labeling, making it difficult to determine consistent expression patterns within these layers. In general, it appeared that larger cells stained darkly for *VGLUT2* while smaller cells stained darkly for *VGLUT1*, although further quantification would be needed to support this conclusion. Layer 3C exhibited distinct differences in *VGLUT* distributions; while neither *VGLUT* isoform was particularly predominant in 3C, *VGLUT1*-positive cells tended to cluster toward the dorsal and ventral edges of layer 3C while *VGLUT2*-positive cells were evenly distributed through the center of the layer. No differences in labeled cell size or density were observed in 3C. In layer 4, medium-sized cells throughout 4A and 4B moderately expressed *VGLUT2*, while much smaller cells in both layers weakly expressed *VGLUT1*. On average, *VGLUT2*-positive cells in 4A were larger, darkly stained, and more frequently distributed that *VGLUT2* positive cells in 4B, which were lightly stained but densely packed. *VGLUT1*-positive cells in 4B were again crowded together compared to 4A. Layer 5 of V1 contained weak *VGLUT1* expression in small cells but now *VGLUT2* expression; in general *VGLUT1* positive cells in 5A were clustered together compared to *VGLUT1* positive cells in 5B. In contrast, layer 6A showed strong *VGLUT1* expression while 6B showed weaker *VGLUT1* expression, clearly distinguishing them through the extent of V1. Some cells in layer 6 stained weakly for *VGLUT2* but could not be reliably identified through the area. Overall, *VGLUT1* and *VGLUT2* mRNA expression overlapped significantly in the superficial layers, but varied distinctly in layer 4 and the deep layers of V1.

Area V2

V2 in macaques covers a thin strip of the cortical surface along the full extent of the anterior border of V1 (DeYoe and Van Essen, 1985; Kaas, 2005). Like V1, it contains a topographic map of the contralateral visual field across its surface. In coronal sections through the occipital cortex, V2 is identified by its distinct border with V1. Nissl stains in coronal sections of V2 reveal its laminar characteristics, most notably a thin, cell dense layer 4 and a broad layer 3 that can be subdivided into three layers based on relative cell density (figs. 8C, 10A). CO staining in coronal sections of V2 reveals fewer distinct characteristics; ventral parts of layer 3 and dorsal parts of layer 4 showed slightly stronger CO reactivity, but the remaining layers show uniform CO staining across V2 (figs. 8D and 10B). Since the rostral border of V2 is relatively ambiguous in coronal sections stained for Nissl and CO, VGLUT distributions aligned to these stains were largely analyzed from caudal regions in V2, near the border of V1.

Overall, VGLUT protein distributions in V2 were remarkably homogeneous, making it difficult to identify distinct laminar patterns in this area. However, general differences in staining intensity were observed (figs. 8E, F and 10C, D). Layers 1, 2, and 3 stained strongly for VGLUT1 and weakly for VGLUT2, appearing almost continuous through the extent of V2. Layer 4 contained strong VGLUT2 reactivity, which resembled patterns of pulvinar terminations in V2 (Ogren and Hendrickson, 1977; Levitt et al., 1995; Marion et al., 2013) but relatively weak VGLUT1 staining throughout V2. Layer 5 showed slightly weaker VGLUT1 labeling than layer 4, and diffuse labeling of VGLUT2. Numerous darkly staining cell bodies were seen throughout layers 5 and 6 in VGLUT2 preparations (best seen in fig. 8F). Layer 6 also stained moderately for VGLUT1, identifying it as a distinct band along the ventral edge of V2 (fig. 10C). Just as in

V1, VGLUT1 and VGLUT2 distributions largely overlap in the superficial layers but become more distinct in the middle and deep layers of V2.

2.4.3.3 Figure 10. High magnification images through V2. Laminar divisions indicated on the left, adapted from Casagrande and Kaas, 1994. Scale bar is 100um.

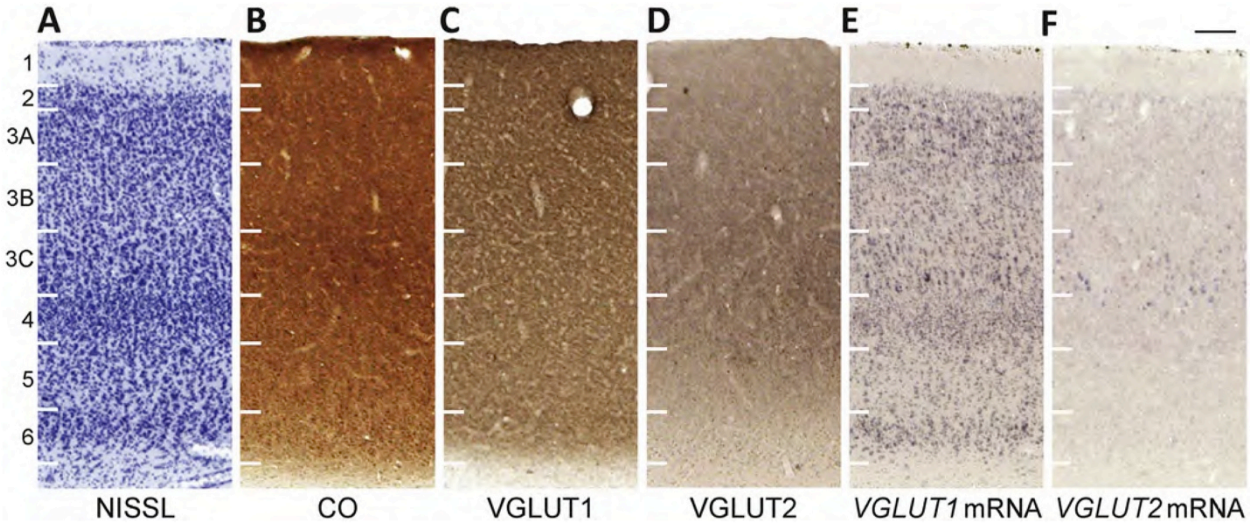

Neurons expressing *VGLUT1* or *VGLUT2* mRNA revealed laminar patterns in V2 (figs. 8G, H and 10E, F). Layer 1 again did not express either isoform, and layer 2 weakly expressed both *VGLUT1* and *VGLUT2* in small, densely packed cells. Layer 3 could be differentiated into three sublaminae based on VGLUT expression. The dorsal sublayer, 3A, strongly expressed *VGLUT1* and moderately expressed *VGLUT2*; *VGLUT1*-positive cells were both medium or small in size and evenly interspersed within 3A, while *VGLUT2*-positive cells were small and diffusely spread through the layer. The middle sublayer, 3B, showed moderate *VGLUT1* expression and sparse *VGLUT2* expression; *VGLUT1* positive cells were smaller compared to cells in the other sublayers, but more densely packed. The ventral sublayer, 3C, strongly expressed both *VGLUT1* and *VGLUT2*; *VGLUT1*-positive cells ranged in size but were evenly distributed in 3C, while *VGLUT2* positive cells were large but scattered unevenly through the layer. Layers 4, 5 and 6 all strongly expressed *VGLUT1* but did not express *VGLUT2*. *VGLUT1*-

positive cells were small and densely packed in layer 4, large and diffusely spread in layer 5, and large or medium in size but more condensed in layer 6. Similar to patterns seen in V1, *VGLUT1* and *VGLUT2* expression overlapped to some extent in the superficial layers of V2, but varied distinctly in the middle and deep layers of V2.

2.5 Discussion

The present study examined the distribution patterns of VGLUT1 and VGLUT2 mRNA and protein in cortical and subcortical structures of the macaque visual system. The specific distributions of VGLUT1 and VGLUT2 were informative in two ways; first, discrete patterns of VGLUT mRNA and protein allowed us to identify subdivisions of visual cortical areas and subcortical nuclei; second, the distributions of VGLUT1 and VGLUT2 in visual pathways correlate with cortical and subcortical circuits that have been defined as driving or modulatory connections between visual areas and nuclei. Thus, VGLUT1 and VGLUT2 usefully define subdivisions of visual structures, and they appear to characterize driving and modulatory inputs at different levels of the macaque visual system. A detailed analysis of our results with respect to these two conclusions follows below.

2.5.1 VGLUT1 and VGLUT2 identify functional subdivisions of subcortical and cortical visual structures in macaque monkeys.

Architectonic boundaries between and within visual cortical areas and subcortical nuclei were clearly visible in VGLUT1 and VGLUT2 preparations. Distinct patterns of VGLUT1 and VGLUT2 terminal labeling distinguished previously defined layers of the superior colliculus, lateral geniculate nucleus, V1 and V2, as well as subdivisions of the inferior pulvinar, while

distributions of cells expressing *VGLUT1* or *VGLUT2* mRNA also identified the laminar or regional origins of glutamatergic projections from each structure.

Laminar divisions of the superior colliculus were clearly demarcated in VGLUT preparations. Dense, patchy VGLUT2 terminal labeling identified the superficial gray layers where retinal projections terminate (Hubel et al., 1975; Pollack and Hickey, 1979), while diffuse VGLUT1 terminal labeling identified the laminar extent of corticotectal projections through the superficial gray layers that largely terminate at the boundary of the optic layer (Lund, 1972; Maunsell and Van Essen, 1983; Fries, 1984; Lock et al., 2003; May, 2006). The distribution of cells expressing *VGLUT2* mRNA also distinguished the extent of the lower superficial gray layer, and these cells project to the posterior and central medial divisions of the inferior pulvinar (Benevento and Fallon, 1975; Trojanowski and Jacobson, 1975; Harting et al., 1980; Benevento and Standage, 1983; Stepniewska et al., 2000) and their terminations were identified by dense VGLUT2 labeling in both inferior pulvinar divisions.

VGLUT distributions in the lateral and inferior pulvinar highlighted the heterogeneity of afferent and efferent projections in these nuclei, but were still instrumental in defining subdivisions in the inferior pulvinar. Diffuse VGLUT1 terminal labeling across the lateral and inferior pulvinar that resembled patterns of corticopulvinar terminations in macaques (Campos-Ortega and Hayhow, 1972; Ogren and Hendrickson, 1979; Maunsell and Van Essen, 1983) supports the conclusion that these structures are dominated by inputs from visual cortical areas and not subcortical structures (Bender, 1983; Adams et al., 2000; Shipp, 2001; Van Essen, 2005). Clear exceptions to this inference are the posterior and central medial nuclei of the inferior pulvinar, which primarily receive inputs from the superior colliculus (see above) and showed dense distributions of VGLUT2-positive terminals instead. Significant differences in the extent

and localization of architectonic divisions within the inferior pulvinar have been reported in previous studies of Old World and New World primates (Stepniewska et al., 2000 for discussion), but four subdivisions of PI have been consistently identified across primates (Lin and kaas, 1979; Cusick et al., 1993; Gutierrez et al., 1995; Stepniewska et al., 2000); the posterior inferior pulvinar (PIp), medial inferior pulvinar (PIm), central medial inferior pulvinar (PIcm) and central lateral inferior pulvinar (PIcl). PIcm and PIcl were originally considered a single nucleus until histological preparations identified them as distinct subdivisions (Stepniewska and Kaas, 1997), and some studies suggest that PIp and PIcm were originally a single nucleus that was later divided by the evolution and intrusion of PIm into this area. Thus, PIp and PIcm often appear "bridged" or adjoined dorsally and ventrally around PIm in coronal histological preparations through the inferior pulvinar (for example, figs 12-14 in Stepniewska et al., 2000). VGLUT1 and VGLUT2 distributions clearly identified three subdivisions of the inferior pulvinar that are spatially organized to form four regions within this structure (fig. 4). The remarkable similarity in size, density, and and VGLUT mRNA expression of cells in PIp and PIcm suggest that these two regions are functionally related but separated parts of the same nucleus, as previously proposed (Symonds and Kaas, 1978; Stepniewska et al., 2000; Baldwin et al., 2013b). The continuation of VGLUT2 terminal labeling both dorsal and ventral to PIm also resembles the bridged pattern seen in previous histological preparations (Stepniewska and Kaas, 1997) and supports the conclusion that PIp and PIcm were originally a single nucleus that have since separated and evolved distinct functions and connections (Cusick et al., 1993; Baldwin et al., 2013b). PIm, which did not express VGLUT1 or VGLUT2 mRNA, and only showed dense labeling of VGLUT1 protein, could also be identified as a distinct subdivision between PIp and PIcm. PIcl, along the lateral most edge of the inferior pulvinar, could not be distinctly divided

from PIcm, but general differences in cell size, density, and levels of VGLUT mRNA suggest that these regions are indeed distinct subdivisions of the inferior pulvinar. Thus, three anatomically distinct regions, PIcl, PIm, and PIcm-PIp, could be identified in VGLUT preparations and coincided with the spatial arrangement of four divisions seen in previous reports of the inferior pulvinar. Further studies of VGLUT expression in the inferior pulvinar of other mammals will undoubtedly help identify homologous subdivisions, leading to more consistent descriptions of the inferior pulvinar across species.

VGLUT distributions identified laminar divisions and the extent of visual projections within the lateral geniculate nucleus (Casagrande et al., 2006 for review). Strong *VGLUT2* expression in geniculostriate projection neurons clearly delineated the boundaries of magnocellular and parvocellular layers within the LGN while weak *VGLUT1* expression also identified koniocellular cells in the interlaminar zones. Discrete VGLUT2-positive terminal labeling also identified the extent of retinogeniculate projections while diffuse VGLUT1-positive labeling identified the extent of corticogeniculate projections in this nucleus.

VGLUT preparations were also instrumental in defining laminar boundaries within cortical visual areas V1 and V2. Differences in cell size, density, and levels of *VGLUT* mRNA expression distinguished laminar boundaries in both visual areas, while distinct patterns of VGLUT1 and VGLUT2 terminal labeling identified afferent and efferent projections to these areas (DeYoe and Van Essen, 1985; Lund et al., 1988; Levitt et al., 1995; Callaway, 1998; Bullier, 2004; Sincich et al., 2010). Most notably, two different depths of terminations were noted for parvocellular geniculate projections to V1: a dorsal band of dense, VGLUT1-positive terminals along the 4A/4B border and a ventral band of equally dense, VGLUT2-positive terminals within layer 4B, neither of which overlap with the zone of magnocellular geniculate

terminations in layer 4A of V1 (Lund, 1988). The significance of these distinct terminations is underscored by the expression of both *VGLUT1* and *VGLUT2* mRNAs in parvocellular cells of the LGN; it suggests that the dual use of VGLUT isoforms in geniculate projections can give rise to distinct terminations and perhaps separate functions in visual processing. Since cells in the LGN do project to several areas of visual cortex (Benevento and Yoshida, 1981; Yukie and Iwai, 1981; Bullier and Kennedy, 1983; Sincich et al., 2004), it is possible that geniculate projections differentially utilize VGLUT1 and VGLUT2 in their terminations across cortical areas. Since VGLUT1 and VGLUT2 regulate different probabilities of glutamatergic transmission (Fremeau et al., 2004a,b, for review), these distinct terminations may contribute to different valences of glutamatergic input to cortical areas in the macaque visual system.

2.5.2 VGLUT1 and VGLUT2 distinguish between driving and modulating visual projections

The distinct distributions of VGLUT1 and VGLUT2 in connections between visual structures suggest that these isoforms characterize separate types of glutamatergic projections. Previous studies have proposed that VGLUT1 characterizes corticothalamic projections while VGLUT2 characterizes thalamocortical projections (Fremeau et al., 2001; Herzog et al., 2001; Fremeau et al., 2004a; b; Barroso-Chinea et al., 2007; Graziano et al., 2008), but recent work has shown more heterogeneous distributions of these isoforms in both cortical and subcortical projections (Masterson et al., 2009; Hackett et al., 2011; Ito et al., 2011; Balaram et al., 2011a; b; Storace et al., 2012). With further examination of these distributions, and their correlation with previously reported functional properties of each projection (Felleman and Van Essen, 1991; Sherman and Guillery, 1996; Crick and Koch, 1998; Sherman and Guillery, 2002; Sherman, 2005; Van Essen, 2005; Sherman and Guillery, 2006; 2011), we propose that VGLUT1 and

VGLUT2 do characterize distinct types of glutamatergic projections; VGLUT2 predominates in feedforward or driving connections while VGLUT1 predominates in feedback or modulatory connections between visual structures. The visual projections evaluated in this study are outlined in Fig. 11.

The first major glutamatergic projection in the macaque visual system consists of retinal projections to all layers of the LGN as well as the SC. These projections are considered driving or feedforward connections from sensory afferents (Sherman and Guillery, 1996), and were characterized by dense VGLUT2 terminal labeling in the retinorecipient layers of both structures. The next major visual projection, the geniculostriate pathway, arises from cells in all layers of the LGN and terminates in layers 3Bb and 4 of V1 (Casagrande and Kaas, 1994 for review). Projections from the magnocellular and parvocellular geniculate layers are functionally considered driving or feedforward afferents (Sherman and Guillery, 1996; 1998; Sherman, 2005) and both projections are dominated by VGLUT2. While both geniculate cell types expressed low levels of *VGLUT1* mRNA as well, a characteristic of sensory relay nuclei (Fremeau et al., 2001; Herzog et al., 2001; Barroso-Chinea et al., 2007; Ito and Oliver, 2010; Balaram et al., 2011a; b; Storace et al., 2012), these cells send branched afferents to multiple layers in V1 and the use of both VGLUT isoforms in their terminals may give rise to different valences of driving and modulatory visual inputs to this area, as described above. Koniocellular cells in the LGN exclusively expressed VGLUT1 mRNA, and these cells project to several visual cortical areas (Stepniewska et al., 1999; Sincich and Horton, 2003; Sincich et al., 2004; Casagrande et al., 2006) as well as several layers of V1 (Casagrande et al., 2007) and have more of a modulatory role in geniculostriate visual processing (Kaas and Huerta, 1988; Casagrande and Norton, 1991; Casagrande, 1994).

2.5.2.1 Figure 11. Summary of major feedforward and feedback projections in the macaque visual system, adapted from Casagrande and Kaas, 1994. Circles indicate origins of projection, arrowheads indicate termination of projection. Black lines indicate glutamatergic projections that do not appear to utlize VGLUT1 or VGLUT2.

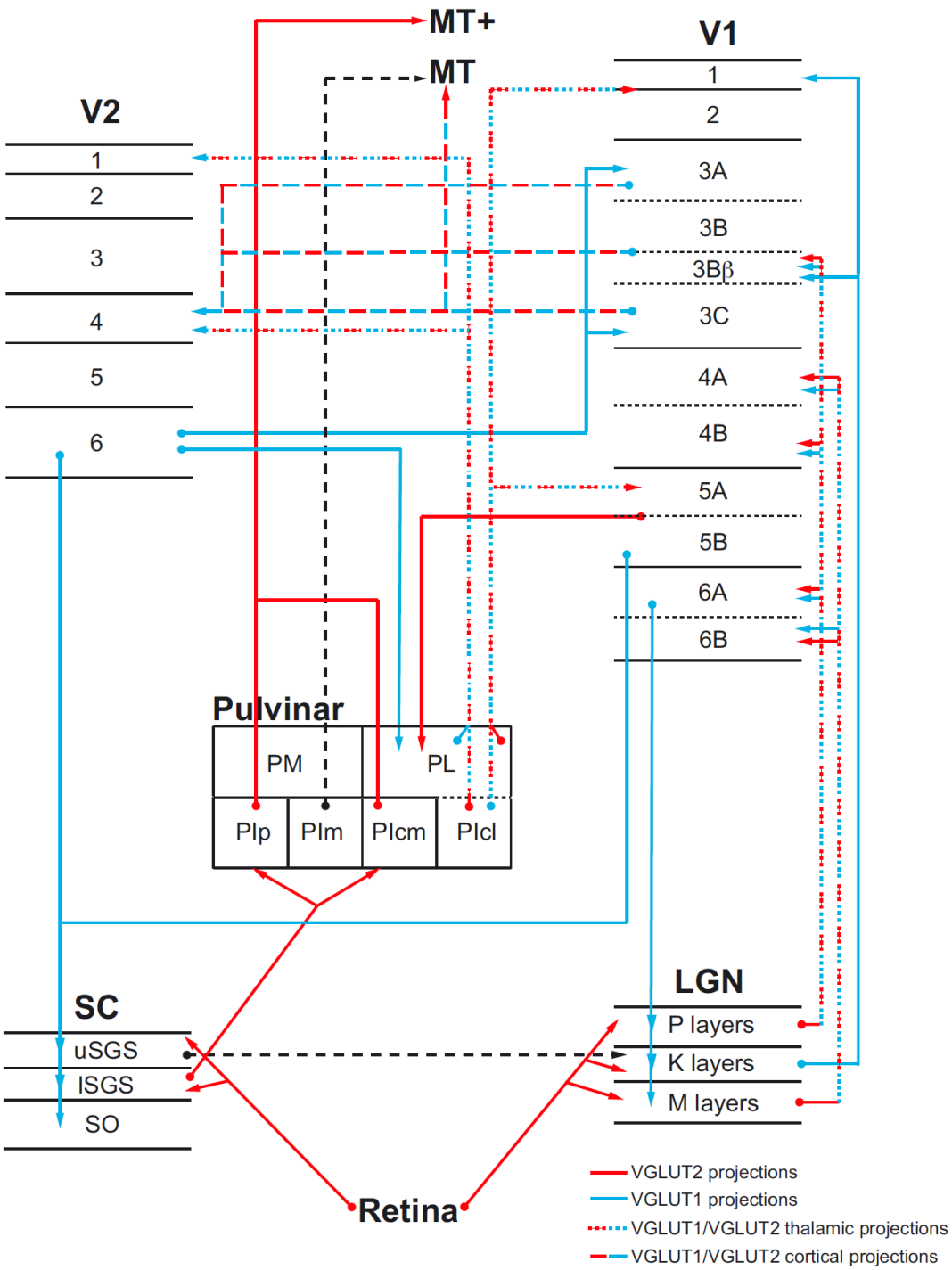

Feedback projections from V1 to the LGN, which primarily modulate visual signals passing through this nucleus (Sherman and Guillery, 1998; 2006), arise in layer 6 of V1 and terminate diffusely across all layers of the LGN (Graham et al., 1979; Graham, 1982; Fitzpatrick et al., 1994). Cells in layer 6 of V1 exclusively expressed VGLUT1 mRNA, which corresponded to the diffuse VGLUT1 terminal labeling resembling corticogeniculate projections that was seen throughout the LGN. Thus, VGLUT1 and VGLUT2 appear to characterize modulatory and driving connections throughout the geniculostriate pathway of the macaque visual system.

Another glutamatergic projection, from the lower superficial gray layer of the superior colliculus to the posterior and central medial divisions of the pulvinar, exhibits several characteristics of a driving or feedforward projection (Partlow et al., 1977; Marrocco et al., 1981; Berman and Wurtz, 2010). Strong *VGLUT2* expression in tectal neurons of the lower SGS corresponding to VGLUT2 terminal labeling in the lateral and central medial divisions of PI indicates that this projection also preferentially utilizes VGLUT2 for glutamatergic transmission. Cells in the tectorecipient regions of the pulvinar project to visual areas of temporal cortex that may play a role in blindsight (Poppel et al., 1973; Stoerig and Cowey, 2007; Tamietto et al., 2010) and predominant *VGLUT2* expression in these cells suggests that this driving projection preferentially utilizes VGLUT2 as well. While the upper superficial gray layer in the colliculus does have excitatory connections with the interlaminar zones of the LGN (Harting et al., 1991), the specific neurotransmitter used in these projections has yet to be identified in any species (Bickford et al., 2000) and tectogeniculate projections may have more of a modulatory role in visual processing given their specific terminations on koniocellular cells of the LGN (Harting et al., 1978; Casagrande, 1994). Feedback projections to the superior colliculus in layers 5 and 6 of V1 and layer 6 of V2, in addition to projections from other cortical areas (Fries, 1984), and the

dense expression of *VGLUT1* mRNA in these cortical layers corresponded to diffuse VGLUT1 terminal labeling seen across the superficial layers of the SC.

Feedforward or driving projections from V1 in layer 3, which projects to V2 and MT, and in layer 5, which projects to the lateral and inferior pulvinar (Rockland and Pandya, 1979; Livingstone and Hubel, 1983; Felleman and Van Essen, 1991; Casagrande and Kaas, 1994; Sherman and Guillery, 1998; Sincich and Horton, 2002; Sherman, 2005; Anderson and Martin, 2009; Sherman, 2012). The majority of smaller cells in the superficial layers of V1 express both *VGLUT1* and *VGLUT2* mRNA and likely give rise to both driving and modulatory connections depending on their intrinsic or extrinsic projections, as well as the context of transmitted information (Sherman, 2005). However, large pyramidal neurons that only expressed *VGLUT2* were largely confined to layers 3C and 5A, which primarily project to MT and the pulvinar, respectively. Layer 4 of MT, where V1 projections terminate, showed dense distributions of VGLUT2-positive terminals as well. Layer 4 of V2, which is the primary recipient of feedforward projections from the lateral and inferior pulvinar, as well as V1, also showed dense VGLUT2 terminal labeling as well (Marion et al., 2013). Feedback or modulatory projections from V1 primarily arise in layers 5 and 6 and terminate diffusely in the LGN and superior colliculus, as described above, and these projections are dominated by VGLUT1. Future studies will help to elucidate the distinctions between efferent projections from cortical visual areas and their respective VGLUT isoforms, but both VGLUT1 and VGLUT2 do appear to characterize specific types of glutamatergic projections from V1 and V2.

The pulvinar nucleus of primates consists of several subnuclei with distinct afferent and efferent projections to multiple cortical areas (Kaas and Lyon, 2007, for review). The majority of its visually related driving and modulatory inputs arises from projection neurons in the deep

layers of cortical areas (Lund and Boothe, 1975; Levitt et al., 1995; Sherman and Guillery, 2002; Van Horn and Sherman, 2004; Sherman, 2007), which terminate primarily in the lateral and inferior pulvinar. Projections from layer 5 of V1 to the pulvinar are classified as driving projections while projections from layer 6 of V2 to the pulvinar are largely feedback or modulatory in nature. Large VGLUT2-positive neurons in layer 5 of V1 are the likely source of the driving pulvinar input (Lund et al., 1975) while smaller VGLUT1-positive neurons in layer 6 of V2 are the source of modulatory input to these two pulvinar divisions. Efferent projections from the pulvinar to V2 are feedforward or driving connections, while projections from the pulvinar to V1 are modulatory projections instead. Dense VGLUT2 terminal labeling in layer 4 of V2 closely resembles the pattern of pulvinar terminations in this area, while VGLUT1 terminal labeling in layers 1, 3 and 5 of V1 resembles pulvinar projections to V1 instead. Although further studies are necessary to isolate individual afferent and efferent projections of the visual pulvinar, it appears that driving and modulatory projections from this nucleus are also characterized by VGLUT1 and VGLUT2.

There are several anatomical and functional characteristics of driving and modulating projections, independent of the source of the projection, that also match the physiological properties of VGLUT1 and VGLUT2 within a synapse (Fremeau et al., 2004a; b; Blakely and Edwards, 2012; Hnasko and Edwards, 2012). For example, driving inputs tend to have large excitatory post-synaptic potentials (EPSPs) with a high probability of neurotransmitter release and paired-pulse depression (Sherman and Guillery, 2006; Covic and Sherman, 2011; Sherman and Guillery, 2011; Viaene et al., 2011a; b), and VGLUT2 is exclusively expressed at synapses with a high probability of glutamate release (Fremeau et al., 2001). Conversely, modulatory inputs tend to have smaller EPSPs with a lower probability of neurotransmitter release, and

VGLUT1 is localized to synapses with the same properties. Driving inputs also exhibit paired-pulse depression (Sherman and Guillery, 2006), as do VGLUT2-positive synapses (Graziano et al., 2008), while modulatory inputs exhibit paired-pulse facilitation, which is found in VGLUT1-positive synapses (Santos et al., 2009; Sherman and Guillery, 2011). Many of these characteristics now define class 1 and class 2 type projections in sensory systems (Sherman and Guillery, 2011) and VGLUT1 and VGLUT2 may be unique markers for each type. Thus, VGLUT1 and VGLUT2 may differentiate between class 1 and class 2 projections, and could give rise to some of the physiological properties seen in these driving and modulatory connections as well.

2.6 Conclusion

The discrete distributions of VGLUT1 and VGLUT2 clearly identify individual structures in the macaque visual system, as well as subdivisions within each area of nucleus. Additionally, VGLUT1 and VGLUT2 appear to characterize modulatory and driving connections respectively, in glutamatergic projections between visual cortical areas and subcortical nuclei.

CHAPTER 3

Normal and activity-dependent expression of VGLUT1 and VGLUT2 in the visual system of New World monkeys

Pooja Balaram, Toru Takahata, Troy Hackett, and Jon Kaas

3.1 Abstract

The dynamic range of neural responses from glutamatergic neurons in the central nervous system is regulated, in part, by the quantal sequestration and release of glutamate from presynaptic vesicles in excitatory neurons. Vesicular glutamate transporters (VGLUTs) mediate this process by trafficking glutamate into synaptic vesicles and aiding in vesicle recycling via their interactions with other synaptic proteins, and temporal differences in these two actions give rise to a wide range of excitatory postsynaptic potentials in glutamatergic neurons. The expression of VGLUT proteins within synaptic terminals is conversely regulated by levels of neural activity moving through the individual circuit, and two VGLUT isoforms, VGLUT1 and VGLUT2, appear to be bidirectionally regulated in response to changes in excitatory neural activity. We examined the distributions of VGLUT1 and VGLUT2 in central visual projections of New World monkeys under normal conditions, and then induced short periods of peripheral visual deprivation to determine changes in VGLUT distributions following fluctuations in neural activity within visual circuits. Under normal conditions, VGLUT1 and VGLUT2 are largely segregated to nonoverlapping visual projections, with the exception of thalamic nuclei where both isoforms may be coexpressed. Under deprived conditions, VGLUT1 expression increases

and VGLUT2 expression decreases in a central visual projection, the geniculostriate pathway, although other factors relating to the strength and type of geniucate projection may contribute the regulation of these two proteins as well. These results provide further support for the segregation of VGLUT1 and VGLUT2 to functionally distinct classes of glutamatergic projections, as well as the bidirectional regulation of these two proteins in response to changing neural activity within a sensory circuit.

3.2 Introduction

Vesicular glutamate transporters (VGLUTs) mediate the storage and release of glutamate from the presynaptic vesicles of excitatory neurons in the central nervous system (CNS) (Bellocchio et al., 2000; Takamori et al., 2000; Herzog et al., 2001; Reimer et al., 2001; Fremeau et al., 2004a; b; Takamori, 2006; Blakely and Edwards, 2012). Three VGLUT isoforms have been documented to date - VGLUT1, VGLUT2, and VGLUT3 – and two of these three isoforms, VGLUT1 and VGLUT2, are distributed in the majority of glutamatergic neurons across the mammalian CNS (Ni et al., 1995; Bellocchio et al., 1998; Aihara et al., 2000; Kaneko and Fujiyama, 2002; Varoqui et al., 2002; Wang et al., 2002; Gong et al., 2006; Liguz-Lecznar and Skangiel-Kramska, 2007; Graziano et al., 2008; Hackett and la Mothe, 2009; Hackett et al., 2011; Ito et al., 2011; Balaram et al., 2011a; b; 2013) with largely complementary patterns of expression (Herzog et al., 2001; Fremeau et al., 2004a). In general, VGLUT1 is restricted to feedback or modulatory glutamatergic synapses, which produce slight, fluctuating postsynaptic responses in their target cells, while VGLUT2 is restricted to feedforward or driving glutamatergic synapses, which significantly shape or ‘drive’ excitatory activity in postsynaptic neurons. Most individual glutamatergic terminals appear to contain only one VGLUT isoform at

any time (Herzog et al., 2001; but see Persson et al., 2006; Altschuler et al., 2008; Ito and Oliver, 2010; Rovó et al., 2012), but the mRNA transcripts for both VGLUT1 and VGLUT2 are frequently expressed in the same neurons within specific regions, particularly sensory relay nuclei of the thalamus (Herzog et al., 2001; Fremeau et al., 2004a; Ito et al., 2011; Balaram et al., 2013). Thus, three populations of glutamatergic neurons can be identified based on *VGLUT1* and *VGLUT2* mRNA expression; those containing only *VGLUT1*, those containing only *VGLUT2*, and those containing both *VGLUT1* and *VGLUT2*.

The dual expression of VGLUT1 and VGLUT2 mRNA in the cell bodies of glutamatergic neurons contrasts with the segregated distribution of VGLUT1 and VGLUT2 protein in glutamatergic axon terminals, and two possible hypotheses for this discrepancy have been previously discussed. First, since VGLUT1 and VGLUT2 move through distinct membrane trafficking pathways, it is possible that each pathway segregates VGLUT isoforms to separate populations of glutamatergic terminals from the same neuron (Herzog et al., 2001 for discussion). Thus, neurons that send branched projections to discrete or overlapping targets could use VGLUT1 and VGLUT2 in separate terminations to conduct different valences of excitatory postsynaptic activity. Alternatively, since VGLUT1 and VGLUT2 directly influence glutamate release probability, the two isoforms could be paired in the same synapses and work together to maintain constant levels of glutamate release in response to large variations in presynaptic excitation (De Gois et al., 2005; Erickson et al., 2006). Thus, for thalamic relay nuclei in particular, the dual use of VGLUT1 and VGLUT2 in individual neurons could protect against overstimulation or excitotoxicity from a wide range of peripheral stimuli. Coexpression of both VGLUT isoforms could also provide a mechanism for altering the quantal size of postsynaptic responses at individual synapses, which would give rise to a wider range of excitatory activity

and perhaps mediate synaptic plasticity in those terminations (Wojcik et al., 2004; De Gois et al., 2005; Erickson et al., 2006; Seal and Edwards, 2006; Edwards, 2007).

Previous studies of fluctuations in *VGLUT1* and *VGLUT2* mRNA expression in response to variations in presynaptic activity are limited to *in vitro* preparations of hippocampal and neocortical cultures (Wojcik et al., 2004; De Gois et al., 2005; Wilson et al., 2005; Erickson et al., 2006), which demonstrate an inverse relationship between *VGLUT1* and *VGLUT2* expression over a range of excitatory synaptic activity. Under high levels of stimulation or hyperexcitation, glutamatergic neurons downregulate the expression of *VGLUT1* mRNA and upregulate the expression of *VGLUT2* mRNA. The opposite effect occurs under low levels of stimulation, glutamatergic neurons downregulate *VGLUT2* expression and upregulate *VGLUT1* expression instead. Bidirectional regulation of *VGLUT1* and *VGLUT2* expression occurs during the development and maturation of glutamatergic synapses in the neocortex (De Gois et al., 2005) as well, suggesting that the balanced expression of both VGLUT isoforms in individual synapses plays a key role in the homeostatic maintenance of excitatory neurotransmission.

In order to explore possible changes in *VGLUT1* and *VGLUT2* mRNA expression *in vivo*, we performed monocular intravitreal injections of tetrodotoxin (TTX) in New World owl and squirrel monkeys, and analyzed the expression patterns of *VGLUT1* and *VGLUT2* mRNA using in situ hybridization. TTX is a sodium channel antagonist that blocks neural activity in affected cells by preventing sodium influx during membrane depolarization; when injected into the eye, TTX mimics total vision loss without structural damage to the eye or optic nerve by preventing retinal ganglion cells (RGCs) from responding to light. The primary pathway for the transmission of peripheral visual stimuli to the cerebral cortex in primates is the retinogeniculate pathway, where RGC axons from the retina terminate in the ipsilateral and contralateral lateral

geniculate nuclei (LGNs) and LGN neurons subsequently send projections to the ipsilateral primary visual cortex (V1). Following TTX-induced sensory loss, neurons in both the ipsilateral and contralateral LGN showed bidirectional fluctuations in *VGLUT* mRNA expression; *VGLUT2* mRNA expression decreased while VGLUT1 mRNA expression increased in response to TTX-induced sensory loss. However, no significant changes in VGLUT protein expression were detected in the ipsilateral or contralateral LGN. These results are the first demonstration of *in* vivo changes in *VGLUT* mRNA expression in primate sensory systems, and provide further evidence for the bidirectional regulation of VGLUT1 and VGLUT2 mRNA expression in glutamatergic neurons following sensory loss.

3.3 Materials and Methods

Three adult squirrel monkeys *(Saimiri sciureus; 1-2kg, either sex)* and four adult owl monkeys *(Aotus trivirgatus; 1-2kg, either sex)* were used to examine VGLUT1 and VGLUT2 expression in New World primates. All experimental procedures were approved by the Vanderbilt Institutional Animal Care and Use Committee and followed the guidelines established by the National Institutes of Health.

Surgical procedures

Animals undergoing TTX-induced monocular deprivation were sedated with an intramuscular dose of ketamine (10-20mg/kg) and maintained under isofluorane anesthesia (1-2%) for the duration of the intraocular injection. Once anesthetized, the left eye of each case was rotated and 5ul of tetrodotoxin (TTX: 1mM) was slowly injected into the vitreal cavity using a Hamilton syringe fitted with a glass pipette tip. The syringe was kept in place for 5 min to allow full diffusion of the TTX through the vitreal chamber and then slowly removed. The eye was

rotated back to normal orientation and the animal was allowed to recover normally. Once alert, animals were returned to their home cage for the remainder of the deprivation period. TTX-injected animals were allowed to recover for 1, 3, or 24 hours prior to perfusion. Normal animals were maintained in their home cage until perfusion as well.

For transcardial perfusion, all animals were intramuscularly sedated with ketamine (10-20mg/kg) and lethally dosed with sodium pentobarbital (80mg/kg). Once areflexive, animals were perfused with 0.9% phosphate-buffered saline (PBS: 0.1M, pH 7.6) followed by 2-4% paraformaldehyde in 0.1M PBS. The brains were extracted and cryoprotected in 30% sucrose for 24-48 hours prior to histology.

Staining procedures

Cryoprotected brain blocks were cut into 40-50um coronal sections through the visual cortical and subcortical structures, and separated into 6 or 8 alternating series for further study. In some cases, one series of sections was processed immediately for cytochrome oxidase (CO: Wong-Riley, 1979) to identify areal boundaries of visual structures. The remaining series were stored at -20°C until labeled for VGLUT1 or VGLUT2 mRNA and protein. VGLUT1 or VGLUT2 protein was detected in visual structures using standard immunohistochemistry with commercially available antibodies, while *VGLUT1* or *VGLUT2* mRNA was detected using in situ hybridization with custom probes derived from primate cDNA libraries. A few sections from each case were also labeled for *c*-fos mRNA using in situ hybridization to confirm sensory deprivation following TTX injections (Takahata et al., 2008). Details of all staining techniques have been previously described (Balaram et al., 2013).

Imaging and analysis

All sections were imaged at 20X magnification using a Leica SCN400 slide scanner and VGLUT mRNA and protein densities were analyzed using Leica Ariol software (Leica Microsystems, Buffalo Grove IL, USA). Images of individual structures were exported using Ariol and figure panels were generated in Adobe Illustrator (Adobe Systems, San Jose CA). All images were adjusted for brightness and contrast, but were otherwise unaltered for the purposes of this study. Relative density and intensity of *VGLUT1* and *VGLUT2* mRNA were automatically quantified using Ariol as well. Changes in VGLUT mRNA intensity were analyzed by comparing the intensity of labeled cells in TTX-affected regions against the intensity of labeled cells in unaffected regions; while changes in VGLUT mRNA density were analyzed by comparing the ratio of labeled area to unlabeled area within TTX- affected and unaffected regions and then comparing ratios between TTX-affected and unaffected regions in each visual structure.

3.4 Results

VGLUT1 and VGLUT2 mRNA and protein distributions were characterized in the superior colliculus, lateral geniculate nucleus, pulvinar complex, and primary visual cortex in two species of New World monkeys, diurnal squirrel monkeys and nocturnal owl monkeys. Some owl monkeys underwent monocular TTX injections, in order to explore fluctuations in *VGLUT* mRNA expression following induced sensory loss. Overall, distributions of VGLUT1 and VGLUT2 mRNA and protein in each visual structure are highly similar to those described in other primate species (Balaram et al., 2011a; b; 2013). VGLUT2 predominates in hierarchical feedforward or driving projections while VGLUT1 predominates in hierarchical feedback or modulatory projections, and both VGLUT1 and VGLUT2 may be coexpressed in thalamic visual

structures. Complete deprivation of neural activity in TTX-injected cases were confirmed by labeling for *c-fos*, an immediate early gene that is rapidly downregulated in response to sensory loss (Tochitani et al., 2001; Takahata et al., 2008; Nakadate et al., 2012). In all cases, TTX completely blocked RGC activity in the injected eye. Following TTX-induced sensory loss, *VGLUT2* mRNA expression decreased and *VGLUT1* mRNA expression increased in the retinorecipient lateral geniculate nuclei, while protein distributions for both isoforms remained unchanged in this structure. Detailed observations of normal VGLUT1 and VGLUT2 distributions in each visual structure, as well as altered distributions in the LGN following TTX-induced sensory deprivation, are discussed below.

3.4.1 Normal distributions of VGLUT1 and VGLUT2 mRNA and protein in the visual system of New World monkeys

Lateral geniculate nucleus

The lateral geniculate nucleus of New World monkeys consists of four discrete layers divided by a series of interlaminar zones (Doty et al., 1966; Kaas et al., 1978; Fitzpatrick et al., 1983). The two ventral most layers closest to the optic tract, termed the external and internal magnocellular (M) layers, receive inputs from motion-sensitive RGCs and contain large diameter neurons that project to the upper half of layer 4 and lower half of layer 6 in V1. The two dorsal most layers, termed the external and internal parvocellular (P) layers, receive inputs from contrast-sensitive RGCs and contain medium diameter neurons that project to the lower half of layer 4 and upper half of layer 6 in V1. In squirrel monkeys, the parvocellular layers often interdigitate to form alternating leaflets that resemble multiple distinct layers, whereas in owl monkeys, both P layers remain largely intact (Kaas et al., 1978; Kaas and Huerta, 1988). Four

distinct interlaminar zones exist in the LGN of New World monkeys; the first lies below the ventral most M layer, the second between the internal and external M layers, the third between the M layer pairs and P layer pairs, and the fourth between the internal and external P layers. All four interlaminar zones contain numerous small diameter neurons that receive inputs from color-opponent RGCs, specifically blue ON/yellow OFF RGCs (Hendry and Reid, 2000), and thus are often referred to as koniocellular (K) layers despite their lack of clear cut laminar boundaries. All four interlaminar zones project to layer 1 and the 'blob' regions of layer 3B in V1 (Fitzpatrick et al., 1983). Laminar locations and nomenclature for the LGN of squirrel monkeys and owl monkeys are displayed in Figure 1.

CO stained sections through the LGN in owl monkeys and squirrel monkeys (figs 1A, C) revealed two darkly stained M layers separated by a thin, lightly stained interlaminar zone. Another pale interlaminar zone was visible between the M layer pair and P layer pair, but both P layers labeled as a single mass with intermediate levels of CO. However, Nissl stained sections through the LGN in both species (figs 1B, D) revealed two distinct parvocellular layers with densely distributed medium diameter neurons, separated by a thin layer of small cells. This division was more apparent in rostral sections through the LGN (fig. 1D) compared to caudal sections (fig. 1B), where both P layers resembled a continuous mass of medium sized neurons. Both the internal and external M layers were visible as dense regions of large diameter cell bodies, and were separated from the optic tract, each other, and the P layers, by wide bands of small, lightly labeled cells. Laminar patterns revealed by CO and Nissl staining in the LGN of squirrel and owl monkeys are in agreement with previous descriptions of CO and Nissl staining in both species (Wong-Riley, 1972a; b; Kaas et al., 1978; Norden and Kaas, 1978; Fitzpatrick et al., 1983; Kaas and Huerta, 1988).

3.4.1.1 Figure 1. Coronal sections through the lateral geniculate nucleus (LGN) of New World squirrel monkeys and owl monkeys stained for (A, C) cytochrome oxidase (CO), (B, D) Nissl, (E, G) VGLUT1 protein, (F, H) VGLUT2 protein, (I, K) *VGLUT1* mRNA, and (J, L) *VGLUT2* mRNA. Squirrel monkey panels depict caudal regions of the LGN in New World monkeys and owl monkey panels depict more rostral regions of the LGN in this lineage. Laminar locations and nomenclature for individual LGN layers are depicted in each panel. Scale bar is 500 um.

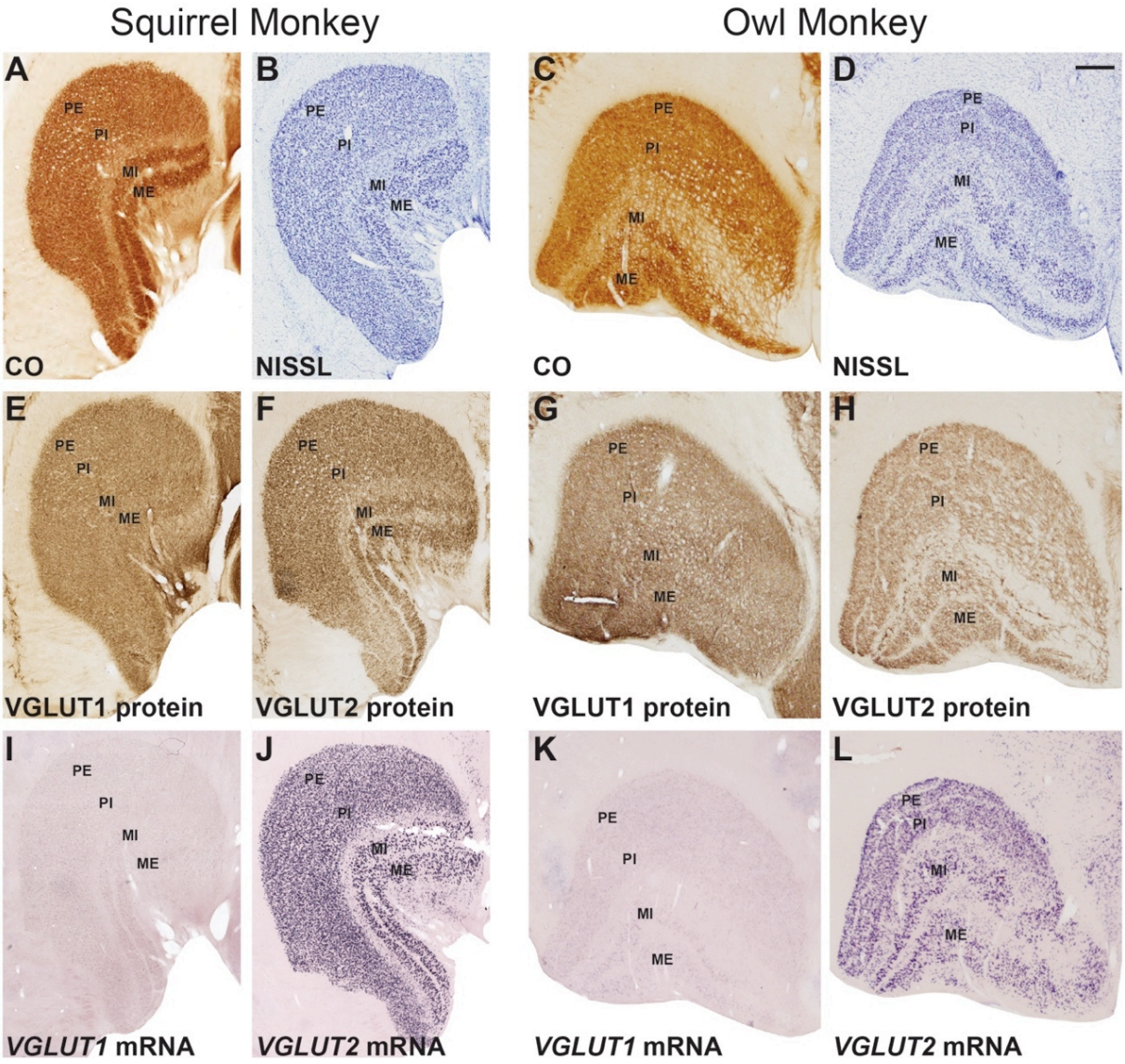

VGLUT1 protein was densely and evenly distributed throughout the LGN of squirrel monkeys and owl monkeys (figs 1E, 1G, 2A), closely resembling corticogeniculate projections in these species (Wong-Riley, 1972a; Lin and kaas, 1977; Casagrande and Kaas, 1994). Slightly denser distributions of VGLUT1-positive terminals were present in all four interlaminar zones, which allowed the faint detection of two M layers and two P layers by alternating bands of light and dark VGLUT1 terminal label. No changes in VGLUT1 protein distributions were detected across the rostrocaudal extent of the LGN in either species. VGLUT2 protein label was almost entirely restricted to the two pairs of M and P layers where dense distributions of large caliber terminals, much like retinogeniculate terminals, labeled strongly for VGLUT2 (figs 1F, 1H, 2B). An additional thin layer of darkly labeled VGLUT2-positive terminals was visible in the interlaminar zone between the M layer pairs and P layer pairs in rostral sections through the LGN (fig. 1H) but similarly punctate labeling was not distinguishable in more caudal LGN sections (fig. 1F). The other three interlaminar zones contained more diffuse populations of VGLUT2-labeled terminals in both species.

LGN sections labeled for *VGLUT1* mRNA in squirrel monkeys and owl monkeys showed weak levels of *VGLUT1* expression in cells throughout the M and P layers, and almost no expression in cells within the interlaminar zones (figs 1I, 1K, 2C). No differences in labeling density were visible between the M layer pairs or P layer pairs, or between layers in each pair. *VGLUT1*-expressing cells in the M layers appeared slightly larger than *VGLUT1*-expressing cells in the P layers, similar to known differences in neuron diameter between M and P LGN cells (Casagrande et al., 2006), but both populations had similarly even distributions within the LGN. *VGLUT2* mRNA, in contrast, was densely expressed by neurons across all LGN layers and interlaminar zones (figs. 1J, 1L, 2D). Cells expressing *VGLUT2* mRNA in the M and P layers

were larger and more densely labeled compared to *VGLUT2*-positive cells in the interlaminar zones, which were small and expressed more moderate levels of *VGLUT2* mRNA. In both squirrel monkeys and owl monkeys, the region between the external M layer and the optic tract contained two populations of *VGLUT2*-expressing cells; the first population displayed relatively large cell bodies and densely expressed *VGLUT2* mRNA, similar to *VGLUT2*-positive cells in the M layers, while the other population displayed smaller cell bodies and more moderate *VGLUT2* expression, similar to cells in the interlaminar zones. The first population likely coincides with a displaced portion of the external magnocellular layer while the second population likely coincides with the koniocellular cells typical of interlaminar zones in New World monkeys (Kaas et al., 1978; Fitzpatrick et al., 1983).

3.4.1.2 Figure 2. High magnification images of coronal sections through the LGN of New World monkeys stained for (A) VGLUT1 protein, (B) VGLUT2 protein, (C) *VGLUT1* mRNA, and (D) *VGLUT2* mRNA. Scale bar is 50um.

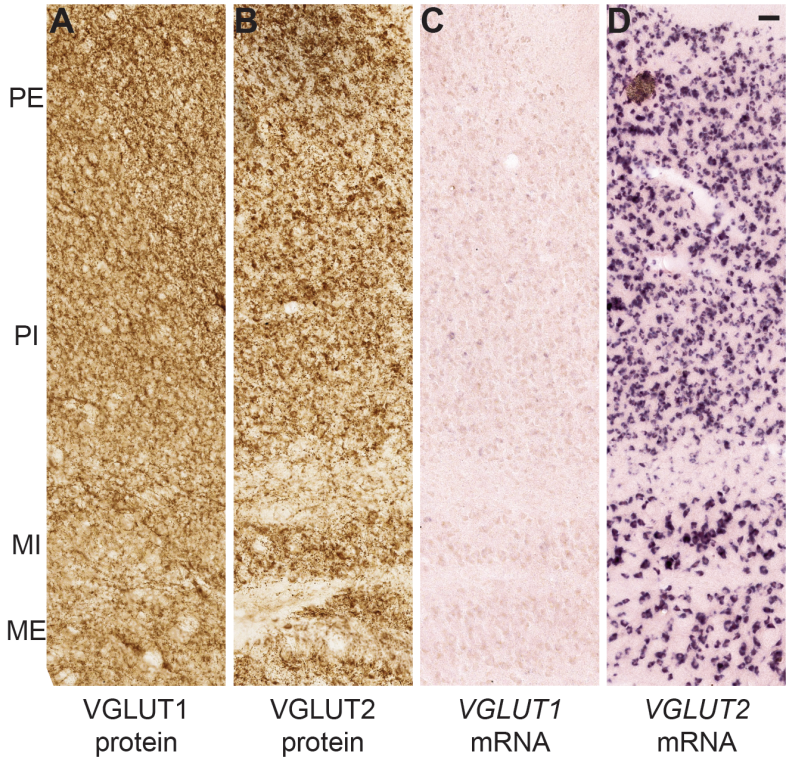

Superior Colliculus

The superior colliculus (SC) in New World monkeys is a large, well-laminated midbrain structure that receives visual and multisensory inputs from several brain regions. The three most dorsal layers of the monkey SC – the upper superficial gray layer (uSGS), the lower superficial gray layer (lSGS), and the optic layer (SO) – primarily receive and relay visual inputs, while the deeper layers of the SC process multisensory information (May, 2006). Ipsilateral and contralateral retinal projections to the SC terminate in alternating patches across the upper SGS in both squirrel monkeys (Tigges and Tigges, 1981; Huerta and Harting, 1983) and owl monkeys (Kaas and Huerta, 1988), while cortical projections to the SC terminate diffusely across the lower SGS and SO (Spatz et al., 1970; Graham et al., 1979). Efferent projections from the upper and lower SGS respectively terminate within the interlaminar zones of the LGN and the posterior and central medial divisions of the inferior pulvinar (PIp and PIcm) (Harting et al., 1978; Lin and kaas, 1979; Harting et al., 1991). Laminar boundaries for the SC in squirrel and owl monkeys are demonstrated in figure 3.

CO staining through the superficial SC in both species clearly identified the boundary between the SGS and SO, based on dark CO staining in the SGS and light CO staining in the SO (figs 3A, C). However, no difference in CO staining density was noted between the upper and lower SGS. Nissl sections through the SC (figs 3B, D) could differentiate the upper and lower SGS divisions, based on small lightly stained cells in the upper SGS and darker, slightly larger cells in the lower SGS. The SO was also distinguishable by sparsely distributed large cells interspersed with smaller cells between parallel fiber tracts that ran through the layer, as well as weaker distributions of CO in both species.

3.4.1.3 Figure 3. Coronal sections through the superior colliculus (SC) of New World squirrel and owl monkeys stained for (A, C) CO, (B, D) Nissl, (E, G) VGLUT1 protein, (F, H) VGLUT2 protein, (I, K) *VGLUT1* mRNA, and (J, L) *VGLUT2* mRNA. Laminar divisions for the superficial layers of the SC are listed on each panel. Midline is to the right, scale bar is 1mm. Abbreviations: uSGS – upper superficial gray layer, lSGS – lower superficial gray layer, SO – optic layer.

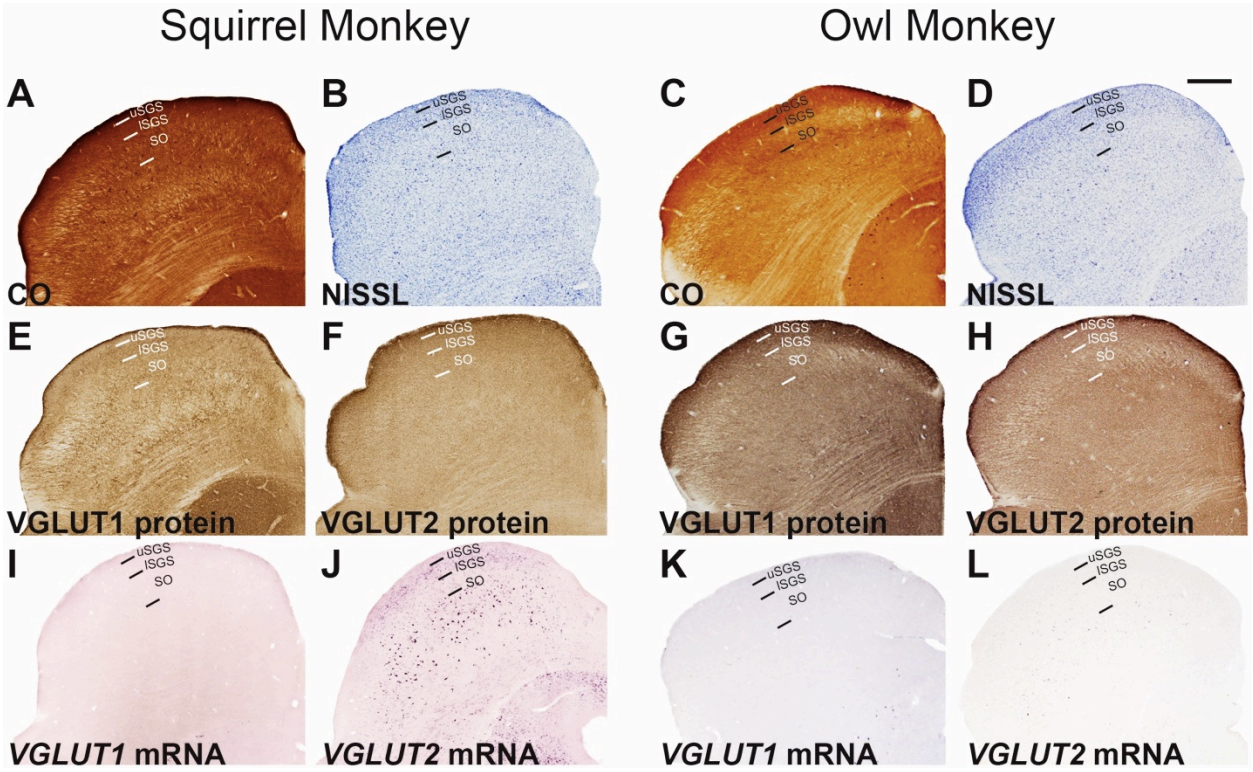

VGLUT1 protein was diffusely distributed across all superficial layers of the SC (figs (3E, 3G, 4A), similar to the distribution of corticotectal terminals in monkeys (Graham et al., 1979; Tigges and Tigges, 1981), with only slightly denser concentrations in the lower SGS compared to the upper SGS and SO in both species (figs. 2E, G). VGLUT2 protein was most densely distributed in the upper SGS (figs 3F, 3H, 4B), which appeared as a thin, dark band of VGLUT2-positive terminals and closely resembled retinotectal projections in these species (Tigges and Tigges, 1981; Kaas and Huerta, 1988). Some VGLUT2-positive terminals were also

present in the lower SGS and SO, but these were more diffusely distributed compared to VGLUT2-positive terminals in the upper SGS.

3.4.1.4 Figure 4. High magnification images through the superficial layers of the SC in New World monkeys stained for (A) VGLUT1 protein, (B) VGLUT2 protein, (C) *VGLUT1* mRNA, and (D) *VGLUT2* mRNA. Scale bar is 10um.

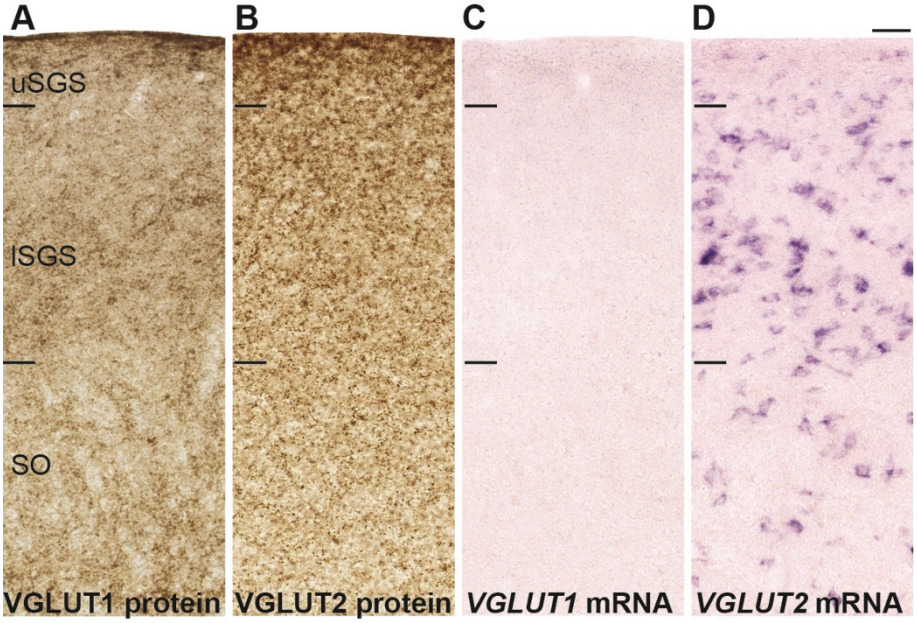

VGLUT1 mRNA was entirely absent from the superficial SC in both squirrel and owl monkeys (figs 3I, 3K, 4C). A few large *VGLUT1*-expressing neurons were found along the boundary of the periaqueductal gray in the deep SC, but no other SC cells expressed *VGLUT1*. In contrast, *VGLUT2* mRNA was widely expressed in the superficial SC layers (figs 3J, 3L, 4D). The upper SGS contained scattered distributions of small cells that moderately expressed *VGLUT2* mRNA. The lower SGS contained larger cells that strongly expressed *VGLUT2* mRNA and the SO also contained sparse populations of *VGLUT2*-expressing neurons that were more variable in size compared to those of the upper or lower SGS. Thus, most tectal glutamatergic

neurons in New World monkeys appear to use VGLUT2 in efferent projections to the LGN and inferior pulvinar.

Pulvinar complex

The pulvinar complex in anthropoid monkeys is generally divided into three major nuclei – the lateral pulvinar (PL), medial pulvinar (PM), and inferior pulvinar (PI) (Stepniewska, 2004). The inferior pulvinar is further divided into four distinct subdivisions: the central lateral inferior pulvinar (PIcl), the central medial inferior pulvinar (PIcm), the medial inferior pulvinar (PIm), and the posterior inferior pulvinar (PIp) (Stepniewska, 2004; Kaas and Lyon, 2007), although growing evidence suggests that PIp and PIcm are divided parts of the same nucleus (Cusick et al., 1993; Stepniewska et al., 2000; Balaram et al., 2013; Baldwin et al., 2013a). The lateral pulvinar and all four divisions of the inferior pulvinar are involved in processing visual information, while the medial pulvinar appears to be more involved in multisensory processing and higher order cortical functions (Kaas and Lyon, 2007). In both owl monkeys and squirrel monkeys, the pulvinar complex is similarly sized, and individual pulvinar nuclei appear to maintain the same spatial locations within the overall structure. Areal boundaries of each pulvinar nucleus in both species are shown in figure 5.

CO-stained sections through the pulvinar complex in both species showed largely uniform distributions of moderate CO label through its rostrocaudal extent (figs 5A, C). PL could be separated from PM and PI by the presence of fiber tracts running tangentially through the nucleus, and slightly darker CO labeling was present in PIp and PIcm, but no other nuclei differentially labeled for CO in either species. Nissl-stained sections through the pulvinar complex were also largely ineffective in revealing divisions between individual pulvinar nuclei

(figs 5B, D). Fiber tracts once again separated PL from PM and PI, but significant qualitative differences in cell density could not be distinguished using Nissl stains in either species.

3.4.1.5 Figure 5. Coronal sections through the pulvinar complex of New World squirrel monkeys and owl monkeys stained for (A, C) CO, (B, D) Nissl, (E, G) VGLUT1 protein, (F, H) VGLUT2 protein, (I, K) *VGLUT1* mRNA, and (J, L) *VGLUT2* mRNA.

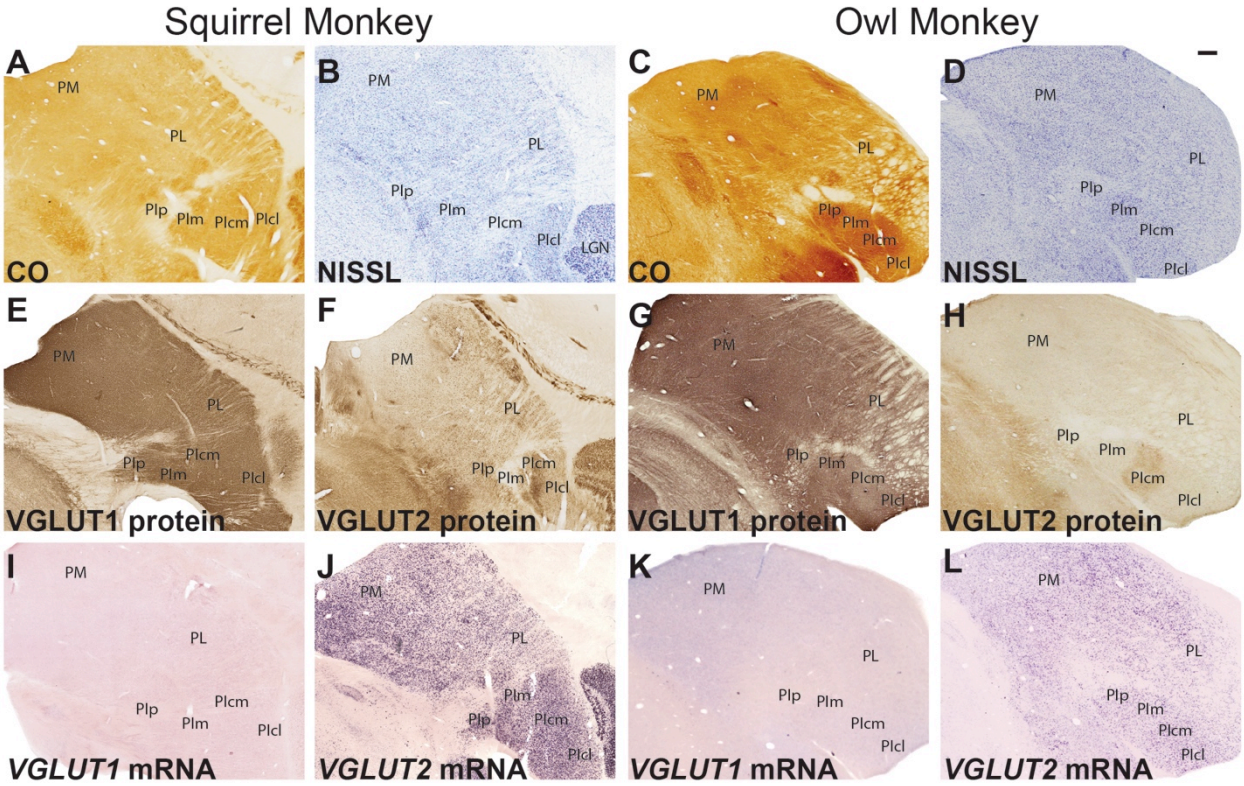

VGLUT1 protein was also densely and uniformly expressed by PM, PL and all four divisions of PI (figs. 5E, 5G, 6A-F). Both PIp and PIcm contained slightly less dense distributions of VGLUT1 protein compared to their surrounding pulvinar divisions, and appeared as lighter patches of VGLUT1 label in PI (best seen in fig 5G, also 6C-F). In sections labeled for VGLUT2 protein however, both PIp and PIcm contained the densest distributions of VGLUT2 protein and appeared as dark patches of label throughout PI in both species (figs. 5F, 5H, 6J, 6L).

PM, PL, and the remaining PI divisions all stained less densely for VGLUT2 protein (figs. 6G-I, 6K), with the exception of scattered patches of dense VGLUT2-positive terminals along the dorsal boundary of PL (best seen in fig. 5F). Interestingly, a large population of cell bodies stained moderately for VGLUT2 protein in all six pulvinar divisions (figs. 6G-L), which is unusual given the normal distribution of VGLUT2 protein in synaptic terminals of glutamatergic neurons. Similar labeling patterns have been previously documented in prosimian galagos (Balaram et al., 2011b), but have not been documented in nonprimate species to date (Kaneko and Fujiyama, 2002; Masterson et al., 2010; Wei et al., 2011).

3.4.1.6 Figure 6. High magnification images through each division of the pulvinar complex in New World monkeys show regional differences in (A-F) VGLUT1 protein (G-L) VGLUT2 protein, (M-R) *VGLUT1* mRNA, and (S-X) *VGLUT2* mRNA distributions. Scale bar is 10um.

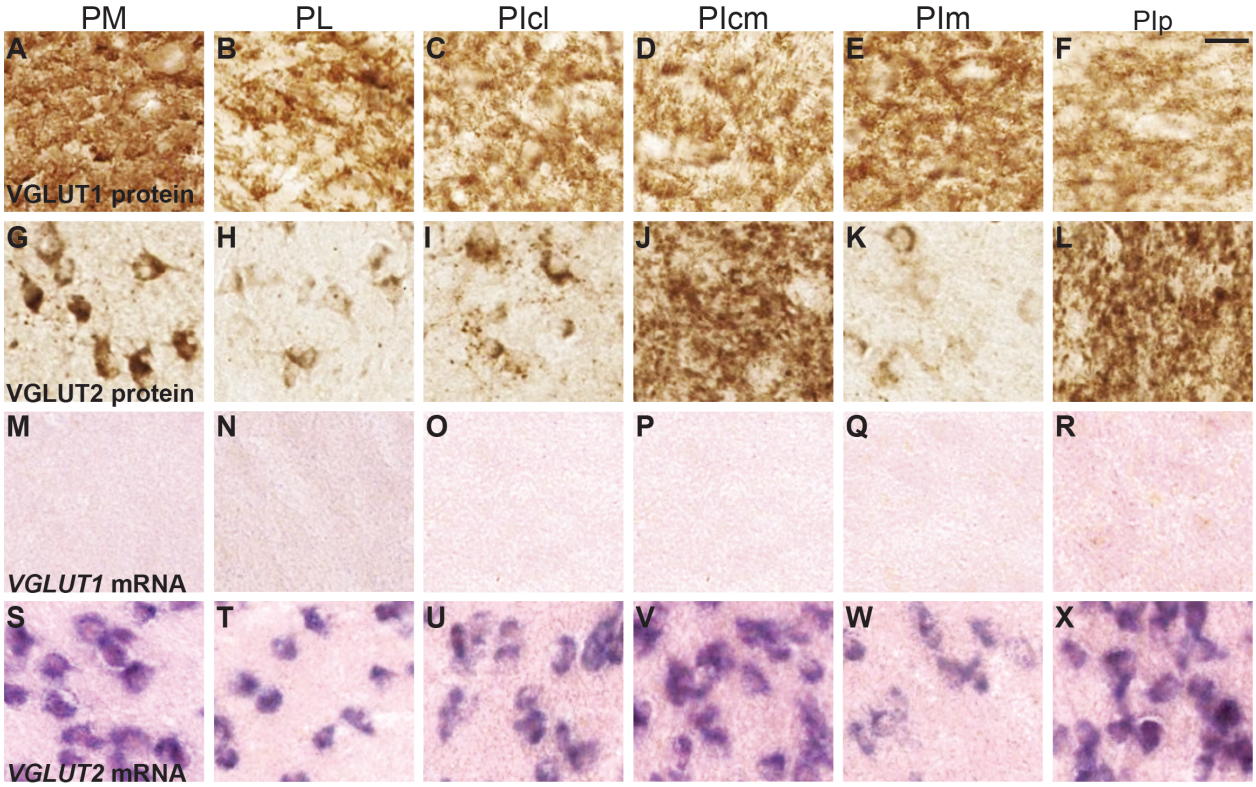

Sections stained for *VGLUT1* and *VGLUT2* mRNA through the pulvinar complex in squirrel and owl monkeys highlighted the fact that most projections neurons in the pulvinar utilize VGLUT2. All five pulvinar divisions appeared to faintly express *VGLUT1* mRNA compared to surrounding thalamic nuclei (figs 5I, 5K), with some differences in staining density between pulvinar regions, but individual labeled cells were difficult to detect at higher magnifications (figs 6M-R). However, all six pulvinar divisions densely expressed VGLUT2 mRNA (figs. 5J, 5L, 6S-X) and showed differences in labeling intensity and cell density between individual nuclei. Both PM and PL contained heterogeneous populations of VGLUT2-positive neurons that expressed moderate to high levels of VGLUT2 mRNA (figs. 6S, T). VGLUT2-positive cells in PM were more densely distributed compared to cells in PL but this may be due to the presence of fiber tracts in PL that occupy a significant volume within the nucleus. In the inferior pulvinar, PIp and PIcm contained neurons that densely expressed *VGLUT2* mRNA (figs. 6V, X) while PIm and PIcl contained neurons that more moderately expressed *VGLUT2* mRNA (figs. 6U, W). The same differences in *VGLUT2* mRNA expression were consistently present throughout the rostrocaudal extent of the pulvinar in both species.

Primary visual cortex (V1)

Primary visual cortex, or V1, in anthropoid monkeys is a large, anatomically distinct area of the cerebral cortex that is characterized by dense myelination and a clear stratification of individual cortical layers (Spatz et al., 1970; Allman and Kaas, 1971; Allman and McGuinness, 1988; Casagrande and Kaas, 1994; Kaas, 2012). In both squirrel monkeys and owl monkeys, eleven distinct cortical layers and sublayers could be identified based on CO and Nissl staining in V1 (figs 7 and 8). For the purposes of this study, laminar divisions in V1 follow Hässler's (1967) naming scheme for V1 layers since this scheme allows for comparisons of V1 layers

across a greater range of mammalian species (Hässler, 1967; Billings-Gagliardi et al., 1974; Balaram and Kaas, 2014) as well as laminar-specific designations for feedforward and feedback projections from V1 (Rockland and Pandya, 1979). Layer 1 stained moderately for CO and was largely devoid of cell bodies, consistent with prior descriptions of this layer across primates (Casagrande and Kaas, 1994). Layer 2 was thin, stained lightly for CO and contained small neurons that were densely packed within the layer. Layer 3 in V1 of primates is often subdivided into three distinct divisions – 3A, 3B, and 3C – on the basis of varying cell density through the cortical depth. Layer 3A contained mixed populations of small and medium sized neurons that were more evenly distributed compared to cells in layer 2 or 3B, thus appearing as a lightly labeled superficial layer in Nissl stained sections through V1. Layer 3B contained dense distributions of small neurons that were more crowded towards the dorsal and ventral edges of the layer compared to the middle, making its boundaries more distinct in Nissl stained sections. Layer 3C in contrast, contained distributions of medium and large sized neurons that were variably scattered throughout the layer, thus distinguishing it from the closely packed neurons of 3B and 4A. All three divisions of layer 3 stained moderately for CO, with the exception of patchy regions of denser CO label throughout 3B that correspond to the well-known blob structures of V1 (Horton, 1984). Layer 4 of V1 in New World monkeys consists of two subdivisions, 4A and 4B; both divisions label darkly for CO and contain dense distributions of small neurons, but 4B consistently shows darker CO label and neuron density compared to 4A. Layer 5 can also be divided into two sublayers 5A and 5B. 5A is a thin layer immediately ventral to 4B that contains moderate CO levels and an even distribution of small neurons, thus appearing as a lightly labeled layer below layer 4 in both CO and Nissl stained sections. Layer 5B in contrast, is wide and contains scattered populations of medium and large neurons with moderate

CO expression throughout. Similarly, layer 6 can be divided into two subdivisions, 6A and 6B; layer 6A contains dense distributions of medium sized neurons that label strongly for CO while 6B contains scattered distributions of small neurons that label weakly for CO. Similar descriptions of laminar divisions in V1 of squirrel monkeys and owl monkeys, as well as other primate species, have been previously documented (Casagrande and Kaas, 1994 for review).

VGLUT1 protein was densely and uniformly expressed across all layers of V1 in both species, with only slight variations in labeling density between select layers (figs 7E, 7G, 8A). Layers 1 and 2 of V1 showed the densest distributions of VGLUT1 protein and stained darkly along the dorsal cortical surface, while layers 3A through 3C showed decreasing distributions of VGLUT1 protein from dorsal to ventral, such that 3A showed the darkest labeling for VGLUT1 and 3C showed the lightest labeling for VGLUT1 within layer 3. Layer 4 in contrast, showed slightly less dense VGLUT1 protein in both species, and was faintly visible as a light band in the middle of V1 (figs. 7E, G). Layers 5 and 6 labeled darkly for VGLUT1 protein, but in both species, layer 5 showed slightly denser distributions of VGLUT1 compared to layer 6 (best seen in fig. 7G).

VGLUT2 protein was variably expressed in each cortical layer as well (figs. 7F, 7H, 8B). The ventral edge of layer 1 contained a thin line of VGLUT2-positive terminals, but the remainder of layer 1 and layer 2 did not contain significant amounts of VGLUT2. Layers 3A, 3B, and 3C all contained even distributions of moderate VGLUT2 label, but layer 3B also contained a thin, dense band of VGLUT2-positive terminals along its ventral edge as well as patches of darker VGLUT2 label that appeared to coincide with the CO-dark blobs. These VGLUT2-positive terminals likely derive from LGN projections from the P layers and.

3.4.1.7 Figure 7. Low magnification images of coronal sections through primary visual cortex (V1) of New World squirrel and owl monkeys stained for (A, C) CO, (B, D) Nissl, (E, G) VGLUT1 protein, (F, H) and VGLUT2 protein. Laminar divisions in V1 are listed on each panel and follow Hässler's (1967) nomenclature for V1 layers, since this scheme allows for comparisons of V1 layers across a greater range of mammalian species (Hässler, 1967; Billings-Gagliardi et al., 1974; Balaram and Kaas, 2014). Scale bar is 1mm.

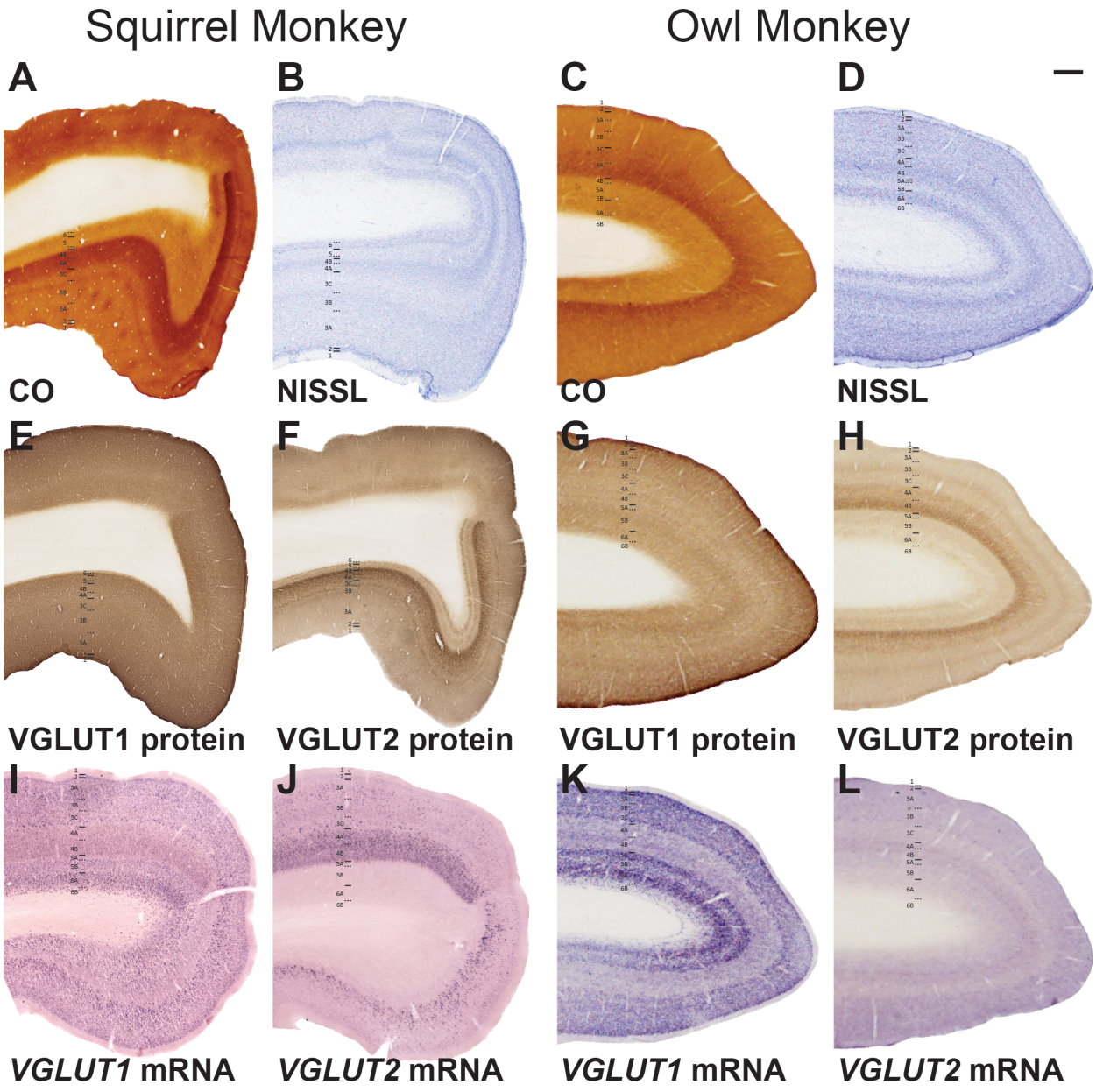

interlaminar zones to V1 and occupy a distinct V1 sublayer known as 3Bβ (Casagrande and Kaas, 1994; Casagrande et al., 2006), which is almost exclusive to anthropoid monkeys (Balaram and Kaas, 2014)At the boundary of V1 and V2 (fig. 7F) Layer 4 of V1 contained the densest distributions of VGLUT2 protein, likely deriving from M and P LGN projections to these layers (Kaas et al., 1976; Fitzpatrick et al., 1983), and 4B consistently showed denser distributions of VGLUT2 compared to 4A in both species. Layer 5A weakly labeled for VGLUT2 while 5B labeled more moderately for VGLUT2. In both squirrel and owl monkeys, a thin region at the boundary of layer 5 and layer 6 showed less dense VGLUT2 distributions and appeared as a light band between the two layers (best seen in fig. 7H). Ventral to this band, layer 6A stained darkly for VGLUT2 protein while layer 6B stained weakly for VGLUT2. Thus, each laminar division of V1 in squirrel monkeys and owl monkeys revealed distinct distributions of VGLUT1 and VGLUT2 positive terminals.

VGLUT1 mRNA also showed distinct laminar differences in expression in V1 of squirrel monkeys and owl monkeys (figs. 7I, 7K, 8C). Neurons in layer 1 did not express *VGLUT1* mRNA but neurons in layer 2 moderately expressed *VGLUT1*, appearing as a thin band of densely packed cells below layer 1. Layers 3A, 3B, and 3C all contained dense distributions of cells that expressed VGLUT1 mRNA. In 3A and 3B, VGLUT1-postive cells were small to medium in size and evenly distributed, whereas in layer 3C, VGLUT1-expressing neurons were larger and darkly labeled, but more diffusely spread through the layer. Layer 4 neurons in both divisions moderately expressed *VGLUT1* mRNA, and again, cells in 4B were more closely packed compared to cells in 4A. Neurons in layer 5A weakly expressed *VGLUT1* mRNA, appearing as a pale band immediately below layer 4, while neurons in layer 5B showed higher levels of *VGLUT1* mRNA.

3.4.1.8 Figure 8. High magnification images through the cortical depth of V1 in sections stained for (A) VGLUT1 protein, (B) VGLUT2 protein, (C) *VGLUT1* mRNA, and (D) *VGLUT2* mRNA. Scale bar is 100um.

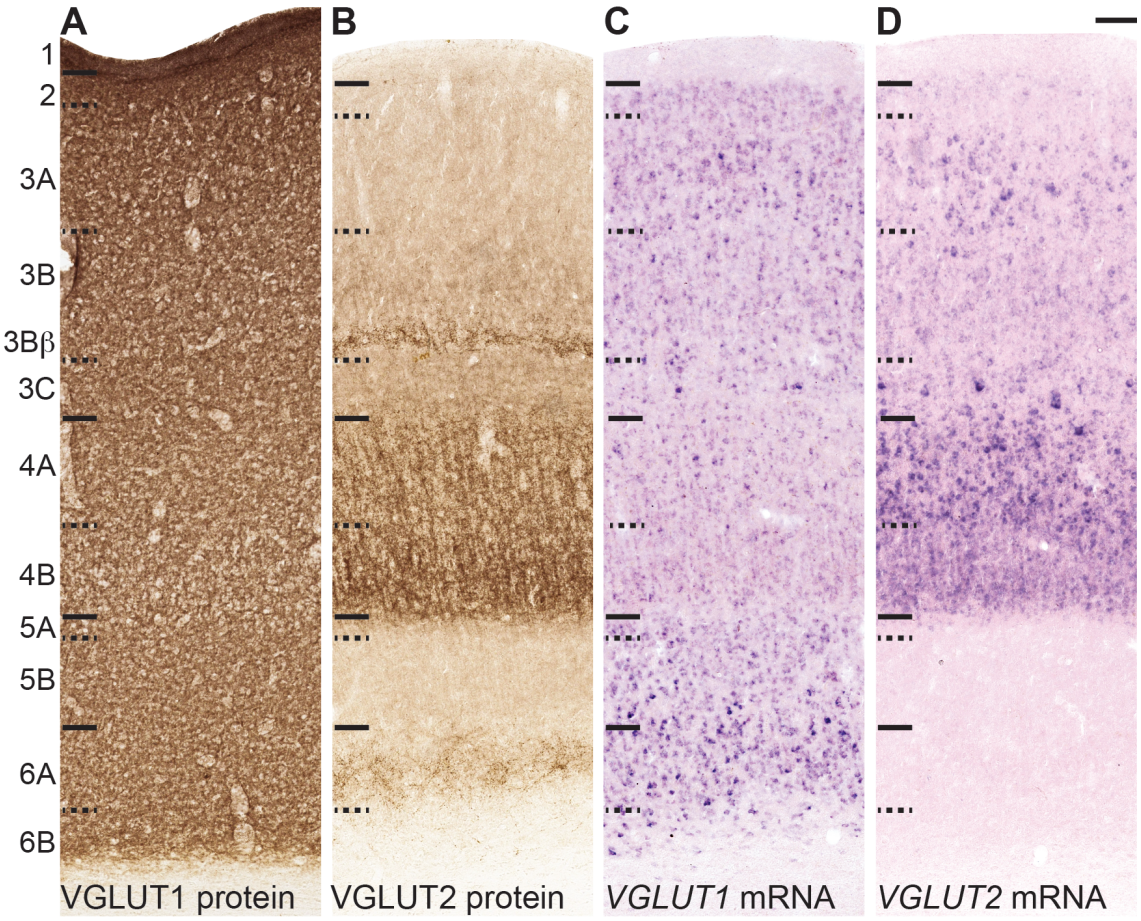

The region between layers 5 and 6 showed more moderate levels of *VGLUT1* mRNA and appeared as a light band between 5B and 6A (best seen in figs. 7I, 7K). Neurons in layers 6A and 6B both densely expressed *VGLUT1* mRNA, similar to neurons in 5B, but neurons in 6B were more diffusely spread compared to those in 6A. *VGLUT2* mRNA was only expressed in the superficial and middle layers of V1 in both species. Layers 1, 5, and 6 contained no *VGLUT2* mRNA. Layer 2 contained a thin band of small cells moderately expressing *VGLUT2* mRNA, just ventral to layer 1. Layer 3A contained a scattered distribution of large neurons with strong *VGLUT2* expression interspersed with a more even distribution of small cells that weakly

expressed *VGLUT2* mRNA. Layer 3B contained a denser distribution of small cells that moderately expressed VGLUT2, while layer 3C contained variable populations of small cells with weak VGLUT2 expression alongside large cells with much stronger VGLUT2 expression. Interestingly, both divisions of layer 4 in squirrel monkeys showed the densest distribution of *VGLUT2*-expressing cells. Cells in layer 4A showed stronger expression levels for *VGLUT2* mRNA compared to cells in 4B, but 4B cells were more densely packed throughout the layer compared to those in 4A.

3.4.2 Activity-dependent changes in VGLUT1 and VGLUT2 distributions in the lateral geniculate nucleus of New World monkeys following TTX-induced sensory loss

Three adult owl monkeys received monocular intravitreal injections of TTX in the left eye and maintained for 1, 3, and 24 hours post-injection to allow for varying rates of TTX-induced visual deprivation. Ipsilateral and contralateral retinal projections terminate in alternating LGN layers; the external M and P layers receive contralateral retinal input while the internal M and P layers receive ipsilateral retinal input. Thus, LGN layers receiving input from the unaffected eye served as an internal comparison against LGN layers receiving input from the deprived eye, and the relative magnitude of deficit in ipsilateral and contralateral retinal projections from the deprived eye could be compared across LGNs in each case. No changes in VGLUT1 or VGLUT2 mRNA and protein levels were seen following 1 hour of TTX-induced deprivation (data not shown), but slight changes were visible following 3 hours of deprivation and significant changes were present following 24 hours of sensory loss.

In the 3 hour condition, both VGLUT1 (fig. 9A, B) and VGLUT2 (fig. 9C, D) protein levels remained unchanged across the LGN layers, suggesting that retinogeniculate and

corticogeniculate terminals were still largely intact despite the marked reduction in visual activity within the retina. In the LGN ipsilateral to the injected eye (figs. 9F, 10A), *VGLUT1* mRNA expression increased in the layers receiving deprived eye input and remained largely constant across layers receiving normal eye input. However, in the contralateral LGN (figs. 9E, 10B), LGN layers receiving deprived eye input remained relatively constant while LGN layers receiving normal eye input showed elevated levels of *VGLUT1* mRNA.

VGLUT2 mRNA showed slightly different changes in expression; in the ipsilateral LGN (fig. 9H, 10C) *VGLUT2* mRNA levels didn't differ significantly between layers receiving normal or deprived input. In the contralateral LGN (fig. 10D), both M layers showed similar levels of *VGLUT2* mRNA, but the P layer receiving input from the deprived eye showed a marked reduction in *VGLUT2* mRNA when compared to the P layer receiving normal eye input. The interlaminar zone in the contralateral LGN, which also received deprived eye input, showed reduced *VGLUT2* mRNA levels compared to the interlaminar zone in the ipsilateral LGN, which received normal eye inputs instead. Thus, *VGLUT1* mRNA levels appeared to increase and *VGLUT2* mRNA levels appeared to decrease in the LGN following short periods of sensory deprivation, although some differences between ipsilateral and contralateral projections, as well as magnocellular and parvocellular projections, may exist. Following 24 hours of TTX-induced sensory deprivation, overall levels of *VGLUT1* and *VGLUT2* mRNA decreased in both the ipsilateral and contralateral LGN (~35% max label in figure 11 compared to ~90% max label in figure 10, except for 10D). In the ipsilateral LGN (figs. 9N, 11A) the M layer receiving normal eye input showed higher levels of *VGLUT1* mRNA compared to the M layer receiving deprived eye input, but conversely, the P layer receiving deprived eye input showed higher levels of *VGLUT1* compared to the P layer receiving input from the normal eye.

3.4.2.1 Figure 9. VGLUT1 and VGLUT2 protein levels in the lateral geniculate nucleus following three hours and 24 hours of TTX-induced sensory deprivation. Right (R) LGN is contralateral to the injected eye while left (L) LGN is ipsilateral to the injected eye. Laminar designations are listed within each panel. Scale bar is 1mm. Abbreviations: ME – external magnocellular layer, MI – internal magnocellular layer, ILZ – interlaminar zone, PI – internal parvocellular layer, PE – external parvocellular layer.

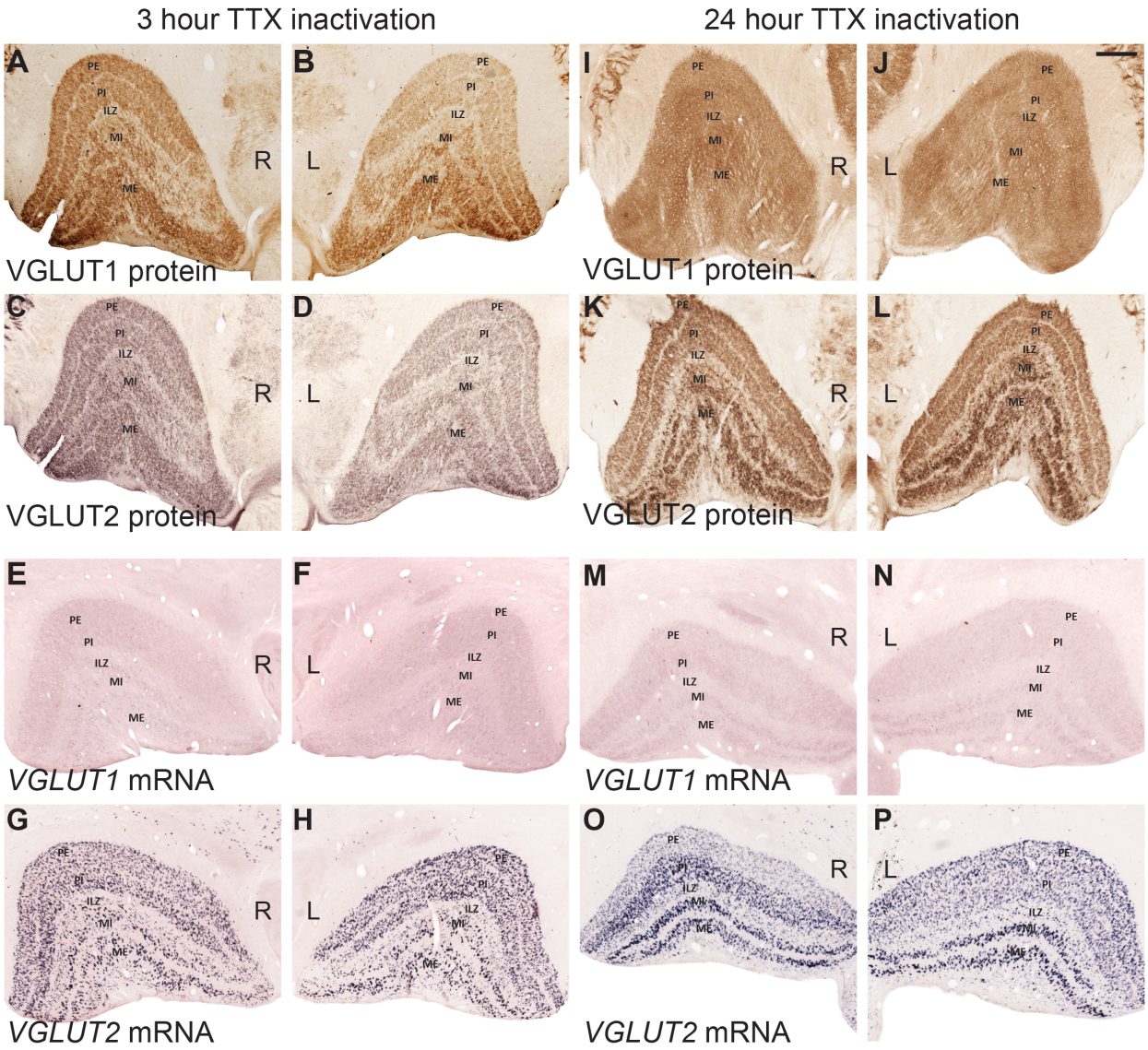

In the contralateral LGN (figs. 9M, 11B), the opposite occurred; the M layer receiving deprived eye input contained more *VGLUT1* mRNA than the M layer receiving normal eye input, while the P layer receiving normal eye input contained more *VGLUT1* mRNA than the P

layer receiving deprived eye input. The interlaminar zone in the contralateral LGN, which received deprived eye input, also contained less *VGLUT1* mRNA than the interlaminar zone in the ipsilateral LGN that received normal eye input. Differences between the two M layers in both the ipsilateral and contralateral LGN were minor compared to differences between the two P layers in both LGNs, suggesting that the P layers are more sensitive to sensory deprivation. However, the bidirectional change in *VGLUT1* mRNA expression between ipsilateral and contralateral inputs to each LGN suggests a greater level of complexity in the activity-dependent regulation of geniculocortical activity.

Expression levels of *VGLUT2* mRNA were less variable than *VGLUT1* mRNA expression levels following 24 hours of TTX-induced sensory deprivation. In the ipsilateral LGN (figs. 9P, 11C), *VGLUT2* mRNA levels were almost equal in both the normal and deprived M layers, and only slightly decreased in the deprived P layer compared to the normal P layer. In the contralateral LGN (figs. 9O, 11D), *VGLUT2* mRNA levels were slightly decreased in the deprived M layer compared to the normal M layer, and significantly decreased in the deprived P layer compared to the normal P layer. The contralateral interlaminar zone also showed decreased *VGLUT2* mRNA levels compared to the ipsilateral interlaminar zone, consistent with its reception of inputs from the deprived eye. Thus, overall, *VGLUT2* mRNA levels decreased in response to a loss of sensory input, while *VGLUT1* mRNA levels variably increased or decreased depending on the ipsilateral or contralateral source of input as well as the M or P layer type. Further experiments with additional time points around 24 hours will help elucidate upward or downward trends in *VGLUT* mRNA expression levels in response to sensory loss.

3.4.2.2 Figure 10. Comparative estimates of *VGLUT1* mRNA and *VGLUT2* mRNA expression in normal and deprived LGN layers following 3 hours of TTX-induced sensory loss. Ipsilateral and contralateral designations are in relation to the injected eye. Y axes reflect the ratio of labeled area to unlabeled area in each LGN layer as percent label. Abbreviations: ME – external magnocellular layer, MI – internal magnocellular layer, IL – interlaminar zone between M layers and P layers, PI – internal parvocellular layer, PE – external parvocellular layer.

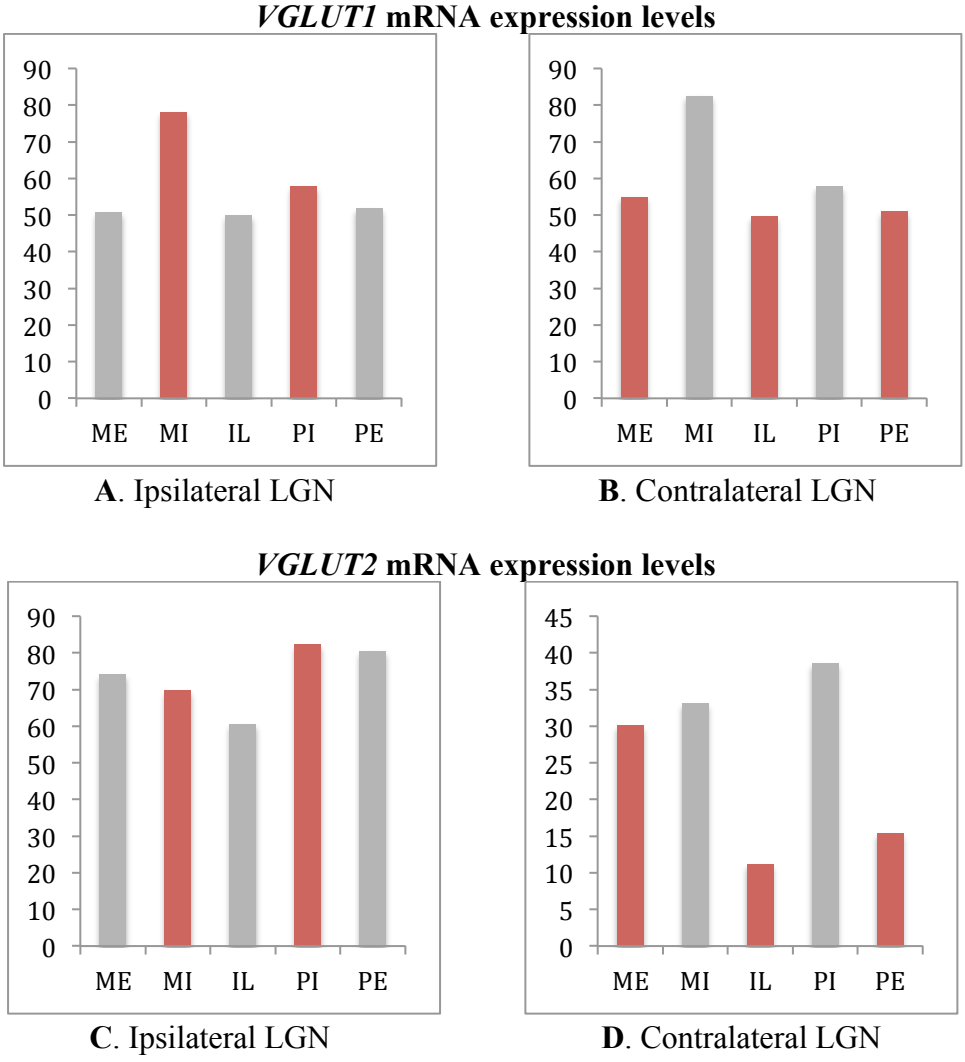

3.4.2.3 Figure 11. Comparative estimates of *VGLUT1* mRNA and *VGLUT2* mRNA expression in normal and deprived LGN layers following 24 hours of TTX-induced sensory loss. Ipsilateral and contralateral designations are in relation to the injected eye. Y axes reflect the ratio of labeled area to unlabeled area in each LGN layer as percent label. Abbreviations: ME – external magnocellular layer, MI – internal magnocellular layer, IL – interlaminar zone between M layers and P layers, PI – internal parvocellular layer, PE – external parvocellular layer.

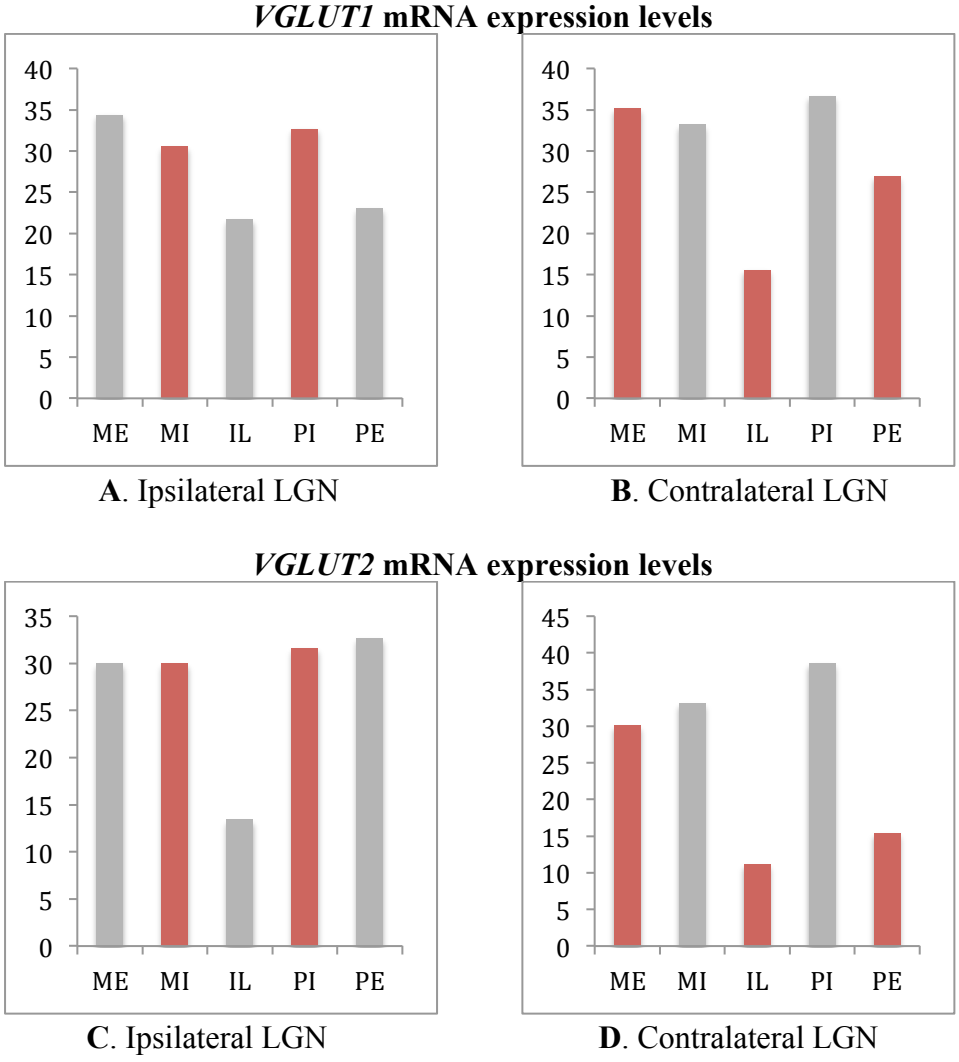

3.5 Discussion

The primary goals of this study were to (1) identify and characterize the distribution of VGLUT1 and VGLUT2 across visual projections in the central nervous system of New World squirrel monkeys and owl monkeys, and (2) to explore whether mRNA or protein levels of VGLUT1 and VGLUT2 in a single projection were dynamically regulated in response to changes in sensory input. We find that VGLUT1 and VGLUT2 distributions in New World monkeys are consistent with previous reports of VGLUT distributions in Old World monkeys (Balaram et al., 2013), and relatively similar to VGLUT distributions in prosimian primates (Balaram et al., 2011a; b) and nonprimate mammals (Bellocchio et al., 1998; Aihara et al., 2000; Kaneko and Fujiyama, 2002; Kaneko et al., 2002; Fujiyama et al., 2003). In general, VGLUT1 predominates in feedback or modulatory glutamatergic projections while VGLUT2 predominates in feedforward or driving projections (Fremeau et al., 2004b; Rovó et al., 2012; Balaram et al., 2013). Both *VGLUT1* and *VGLUT2* mRNA levels appear to be differentially regulated in the LGN following short-term sensory deprivation, although normal levels of VGLUT1 and VGLUT2 protein in the same pathway reveals temporal differences in the transcription and translation of these proteins following fluctuations in sensory inputs. Further insights on these two findings are discussed below.

3.5.1 Normal distributions of VGLUT1 and VGLUT2 across central visual projections in New World monkeys.

Across the majority of central visual projections in New World monkeys, VGLUT1 and VGLUT2 appear to be segregated to nonoverlapping neural populations. Patterns of VGLUT2-positive terminations in the SC and LGN suggest that retinal projections to both structures (Doty

et al., 1966; Wong-Riley, 1972a; Kaas et al., 1978; Tigges and Tigges, 1981; Kaas and Huerta, 1988) utilize VGLUT2 and not VGLUT1. Similarly, dense *VGLUT2* mRNA expression in neurons across the lower superficial gray layer of the SC, along with correspondingly dense VGLUT2 protein labeling in tectorecipient regions of the inferior pulvinar, PIp and PIcm, indicate that tectopulvinar projections (Stepniewska et al., 2000) preferentially utilize VGLUT2. Moderate expression of *VGLUT2* mRNA by tectal neurons in the upper superficial gray layer may also correspond to diffuse VGLUT2 protein labeling in the interlaminar zones of the LGN (Harting et al., 1991). However, neurons in the upper SGS of macaque monkeys lacked *VGLUT2* mRNA (Balaram et al., 2013) and diffuse VGLUT2-positive terminals in the interlaminar zones of the LGN may also arise from retinal projections to koniocellular cells in these layers (Kaas et al., 1978; Fitzpatrick et al., 1983; Diamond et al., 1985; Kaas and Huerta, 1988; Casagrande, 1994), so further experiments colocalizing *VGLUT2* mRNA with tracer-labeled tectogeniculate projections may be necessary to justify this conclusion. However, the complete lack of *VGLUT1* mRNA in the superficial SC layers does confirm that efferent projections from this structure solely utilize VGLUT2 and not VGLUT1. Conversely, the abundant and exclusive expression of *VGLUT1* mRNA by the deep layers of V1, alongside similarly dense VGLUT1 protein labeling across the LGN, SC, and visual pulvinar nuclei, suggests that most cortical projections to subcortical visual structures utilize VGLUT1 instead of VGLUT2. Thus, VGLUT2 is most abundant in feedforward projections from lower order visual structures to higher order visual structures while VGLUT1 is most abundant in feedback projections from higher order to lower order structures.

Some central visual projections in New World monkeys appear to utilize both VGLUT1 and VGLUT2. Both thalamic visual regions, the LGN and pulvinar complex, contained large

populations of neurons that expressed *VGLUT1* mRNA and *VGLUT2* mRNA. Dense VGLUT1 and VGLUT2 protein labeling in the geniculorecipient and pulvinorecipient layers of V1 did not allow the differentiation of individual projections from each thalamic structure, thus two conclusions are possible. First, separate populations of neurons in the LGN and pulvinar that express either *VGLUT1* or *VGLUT2* may project to and terminate in the same regions of V1. Second, individual LGN and pulvinar neurons may express both *VGLUT1* and *VGLUT2* and utilize each isoform to different extents in their terminations within V1 and other geniculorecipient structures. Prior studies in nonprimates have demonstrated the dual expression of *VGLUT1* and *VGLUT2* mRNA within individual thalamic neurons (Herzog et al., 2001; Fremeau et al., 2004b; Barroso-Chinea et al., 2008) and varying reports on the colocalization of both proteins in sensory structures do exist (Li et al., 2003; Todd et al., 2003; Graziano et al., 2008; Ito and Oliver, 2010). Thus, it is possible that primate thalamic neurons also coexpress both *VGLUT* mRNA isoforms, and their terminations in V1 could utilize both proteins (Balaram et al., 2013), but the functional consequences of this coexpression are still unknown. The dense expression of *VGLUT1* and *VGLUT2* mRNA in the superficial layers of V1 also suggests that neurons in these layers may use both isoforms in their terminations, although direct evidence of colocalization within the same cortical neurons does not exist to date. Neurons in these layers send efferent projections to other visual cortical areas and intrinsic projections to other layers within V1 (Casagrande and Kaas, 1994 for review), and may differentially utilize VGLUT1 and VGLUT2 in these projections to produce different valences of excitatory neural activity.

Neurons in most divisions of the pulvinar complex showed strong labeling for VGLUT2 protein within cell bodies, which is unusual since VGLUT2 is found on vesicles in synaptic terminations across the CNS (Fremeau et al., 2001 for review; 2004a). Similar accounts of

cellular VGLUT2 labeling has been reported in the prosimian pulvinar complex (Balaram et al., 2011b) but not in nonprimate species (Fremeau et al., 2001; Kaneko et al., 2002; Masterson et al., 2009), although a closely related isoform, VGLUT3, is often found in dendrites and cell bodies as well as synaptic terminals (Fremeau et al., 2002; Gras et al., 2002; Herzog et al., 2004), Thus, it is possible that pulvinar neurons utilize VGLUT2 in distinct types of signaling mechanisms compared to other glutamatergic cells in the visual pathway.

3.5.2 Activity-dependent changes in *VGLUT1* and *VGLUT2* mRNA expression following short-term visual deprivation

Prior accounts of dynamic changes in *VGLUT* mRNA expression in cultured preparations have demonstrated bidirectional shifts in *VGLUT1* and *VGLUT2* levels following changes in neural activity (Wojcik et al., 2004; De Gois et al., 2005; Erickson et al., 2006). Briefly, *VGLUT1* mRNA levels increase in response to a loss of activity while *VGLUT2* mRNA levels decrease under the same conditions. Under hyperstimulated conditions the opposite occurs, *VGLUT1* mRNA levels decrease while *VGLUT2* mRNA levels increase instead. Our efforts to reveal bidirectional modulation of *VGLUT1* and *VGLUT2 in vivo* showed similar trends in *VGLUT* mRNA regulation following a loss of peripheral neural activity, but also highlighted several other contributing factors in *VGLUT* mRNA regulation following sensory loss.

The use of tetrotoxin (TTX) *in vivo* to abolish neural activity in retinal ganglion cells and disrupt visual processing has been previously documented (Tochitani et al., 2001; Takahata et al., 2008; Trusk et al., 2009; Takahata et al., 2012), but the technical limitations of this application should be considered. First, TTX abolishes RGC activity, presumably by inactivating sodium channels expressed by these cells, but at least two variants of TTX-resistant sodium

channels exist in the mammalian retina (Tate et al., 1998; O'Brien et al., 2008) and in other species, TTX does not entirely abolish light-evoked responses in retinal cells (Djamgoz and Stell, 1984). Different classes of retinal cells also show variable responses to TTX, as demonstrated via changes in CO histochemistry (Wong-Riley et al., 1998), and in the squirrel monkey retina, short periods of TTX exposure have a greater effect on the large ganglion cells of the retina compared to the medium and small ganglion cells (Wong-Riley and Carroll, 1984). Thus, the results presented here may reflect changes in *VGLUT* mRNA expression following an equal loss of neural activity across RGCs of the affected eye, or they may reflect the differential responses of parasol and midget ganglion cells to TTX exposure. Second, in most studies of TTX exposure, the loss of a pupillary eye reflex serves as a control for the efficacy of TTX treatment (Thompson and Holt, 1989; Wong-Riley et al., 1998) since the deficit in retinal activity prevents intrinsic photoreceptive ganglion cells from triggering the pupillary reflex (Gamlin et al., 2007; Schmidt et al., 2011). However, changes in pupillary light reflex were not documented in the monkeys presented in this study; instead, the presence or absence of *c-fos* mRNA in the retinorecipient LGN layers indicated the efficacy of TTX treatment. Since *c-fos* is highly sensitive to a wide variety of changes in intracellular and extracellular activity (Dai and Sun, 2005; Soares et al., 2005; Nakadate et al., 2012; Takahata et al., 2014), not just the presence of TTX, variability in the present results may reflect incomplete deprivation in the injected eye of each case.

Despite the technical limitations of this study, some evidence for the differential regulation of *VGLUT1* and *VGLUT2* mRNA was present. In both the 3 hour and 24 hour conditions, increased expression of *VGLUT1* mRNA alongside decreased expression of *VGLUT2* mRNA was observed in some LGN layers receiving input from the deprived eye, consistent with

previous reports of upregulated *VGLUT1* and downregulated *VGLUT2* following a loss of neural activity (De Gois et al., 2005). The larger difference in *VGLUT2* mRNA expression in normal and deprived P layers compared to normal and deprived M layers suggests that the parvocellular pathway is more sensitive to changes in peripheral inputs compared to the magnocellular pathway. However, this could stem from a differential TTX sensitivity of midget ganglion cells, which project to the P layers, compared to parasol ganglion cells, which project to the M layers instead. Larger studies of gene expression changes in response to visual deprivation have identified several transcripts that are differentially regulated between the M and P pathways (Cheng et al., 2008), thus it is possible that *VGLUT1* and *VGLUT2* have distinct sequences of activity-dependent modulation in response to visual activity in each pathway.

The variable levels of *VGLUT1* mRNA in the M and P layers following 3 hours of TTX-deprivation suggests a difference in the strength of ipsilateral and contralateral projections. In the LGN on both sides, *VGLUT1* mRNA levels were higher in the layers receiving ipsilateral input and lower in the layers receiving contralateral input, regardless of whether the input came from the deprived or normal eye. If horizontal interactions between ipsilateral and contralateral retinal inputs in each M and P layer pair were mediated via *VGLUT1*-positive synapses, then the effect of monocular TTX deprivation could induce a similar bidirectional effect on *VGLUT1* mRNA levels between layers in each M and P layer pair. Similar effects on *VGLUT1* mRNA expression between the LGN layers receiving ipsilateral and contralateral retinal input were present in the 24 hour deprivation case, providing further evidence for differences in *VGLUT1* mRNA regulation within layers in each LGN pair. However, additional cases to determine baseline differences in *VGLUT1* mRNA levels between layers under normal conditions, as well as experimental cases that compare monocular and binocular deprivation effects, would be needed

to further this conclusion. In addition to the difference between ipsilateral and contralateral inputs, possible differences in the temporal regulation of *VGLUT1* mRNA between the M and P layers may exist. In the 3 hour condition, greater differences in *VGLUT1* mRNA levels were visible in the P layers compared to the M layers, whereas in the 24 hour condition, greater differences in *VGLUT1* mRNA were observed in the M layers compared to the P layers instead. Pathway-specific differences in *VGLUT1* mRNA as well as *VGLUT2* mRNA are likely, but additional cases with time points between these two extremes would aid in documenting this trend. Lastly, the interlaminar zone between the M layer pairs and P layer pairs, which receives contralateral retinal input, showed decreased levels of both *VGLUT1* and *VGLUT2* mRNA when receiving input from a deprived eye compared to input from a normal eye, although this was less apparent in *VGLUT1* mRNA levels following 3 hours of deprivation. The unidirectional shift in *VGLUT1* and *VGLUT2* mRNA in this layer suggests distinct mechanisms for their regulation in response to sensory loss, but again, further experiments that also include the other interlaminar zones of the LGN are needed to justify this conclusion. Overall, *VGLUT1* and *VGLUT2* appear to be distinctly modulated *in vivo* following a loss of peripheral neural activity, but the magnitude and temporal sequence of their modulation may depend on larger network factors such as the strength of the individual projection and the behavioral relevance of that projection within the larger sensory circuit. Our results provide further evidence for the segregation of VGLUT1 and VGLUT2 to functionally distinct visual projections in the primate brain and suggest that these two proteins are involved in the dynamic presynaptic control of excitatory neural transmission.

CHAPTER 4

VGLUT2 mRNA and protein expression in the visual thalamus and midbrain of prosimian galagos *(Otolemur Garnetti)*

This chapter was published under the same title in Eye and Brain by Pooja Balaram, Toru Takahata and Jon Kaas; March 2011.

4.1 Abstract

Vesicular glutamate transporters (VGLUTs) control the storage and presynaptic release of glutamate in the central nervous system, and are involved in the majority of glutamatergic transmission in the brain. Two VGLUT isoforms, VGLUT1 and VGLUT2, are known to characterize complementary distributions of glutamatergic neurons in the rodent brain, which suggests that they are each responsible for unique circuits of excitatory transmission. In rodents, VGLUT2 is primarily utilized in thalamocortical circuits, and is strongly expressed in the primary sensory nuclei, including all areas of the visual thalamus. The distribution of VGLUT2 in the visual thalamus and midbrain has yet to be characterized in primate species. Thus, the present study describes the expression of *VGLUT2* mRNA and protein across the visual thalamus and superior colliculus of prosimian galagos to provide a better understanding of glutamatergic transmission in the primate brain. VGLUT2 is strongly expressed in all six layers of the dorsal lateral geniculate nucleus, and much less so in the intralaminar zones, which correspond to retinal and superior collicular inputs, respectively. The parvocellular and magnocellular layers expressed *VGLUT2* mRNA more densely than the koniocellular layers. A patchy distribution of

VGLUT2 positive terminals in the pulvinar complex possibly reflects inputs from the superior colliculus. The upper superficial granular layers of the superior colliculus, with inputs from the retina, most densely expressed VGLUT2 protein, while the lower superficial granular layers, with projections to the pulvinar, most densely expressed *VGLUT2* mRNA. The results are consistent with the conclusion that retinal and superior colliculus projections to the thalamus depend highly on the VGLUT2 transporter, as do cortical projections from the magnocellular and parvocellular layers of the lateral geniculate nucleus and neurons of the pulvinar complex.

4.2 Introduction

The primary mode of excitatory neurotransmission in the central nervous system is performed through the release of glutamate from presynaptic vesicles and its postsynaptic uptake through ionotropic or metabotropic glutamate receptors. The presynaptic release of glutamate is controlled by a family of vesicular glutamate transporters (VGLUTs) that modulate the packaging and transport of glutamate into synaptic vesicles (Fremeau et al., 2001). Three isoforms, VGLUT1, VGLUT2, and VGLUT3, have been previously identified, each classifying a unique subset of glutamatergic projections. VGLUT1 is primarily utilized by projections from the cerebral cortex, cerebellum and hippocampus, while VGLUT2 is primarily employed by projections from the midbrain, thalamus, brainstem, and spinal cord. VGLUT3 differs from VGLUT1 and VGLUT2 in that it does not appear in glutamatergic neurons, it is mainly found in a subpopulation of cholinergic neurons of the caudate-putamen and serotonergic neurons of the raphe nuclei (Fremeau et al., 2004b). The unique distributions of each VGLUT isoform may indicate specialized modes of glutamatergic transport and transmission that are modulated by these transporters.

In previous studies in rodents, *VGLUT2* mRNA is expressed in the thalamus, brainstem, and deep cerebellar nuclei, and VGLUT2 protein is primarily confined to the expected subthalamic and thalamocortical projections (Fremeau et al., 2004b). In the visual subcortical nuclei, *VGLUT2* mRNA is strongly expressed in the dorsal lateral geniculate nucleu (dLGN), the superior colliculus (SC), and the lateral posterior nucleus (LP) or visual pulvinar (Barroso-Chinea et al., 2007). VGLUT2 protein is also strongly expressed in those three nuclei (Kaneko et al., 2002). VGLUT2 has also been associated with a higher probability of synaptic release and functionally distinct synaptic release sites in the brains of adult rodents when compared to the other two VGLUT isoforms (Fremeau et al., 2004a; b). The discrete distribution of *VGLUT2* mRNA and protein in the central nervous system of rodents suggests this isoform plays a unique role in glutamate release and excitatory neurotransmission.

Little work has been done on the distribution of VGLUT2 in primate species. The few studies that discuss VGLUT distributions in primates focus on their immunoreactivity in cortex and do not discuss their expression in thalamic nuclei (Bai et al., 2001; Wong et al., 2009; Wong and Kaas, 2010). Moreover, only one study to date considers the gene expression of VGLUTs in primate sensory pathways (Hackett et al., 2011). In order to expand on the knowledge of VGLUT2 distributions in primate species, we investigated the expression of *VGLUT2* mRNA and protein across the major visual subcortical areas in prosimian galagos *(Otolemur garnetti)*. Galagos are highly visual nocturnal primates with a visual thalamus (Wong et al., 2009) and a distribution of cortical areas that are organized much as they are in anthropoid primates (Kaas, 2006; Wong and Kaas, 2010). Galagos also represent the prosimian branch of the primate radiation, the branch that appears to be the most evolutionarily conserved and most similar to the early ancestors of all primates (Martin, 2003). Previous work on the neocortex of galagos shows

that VGLUT2 protein is abundant in layer 4 of striate cortex and, to a lesser extent, in higher order visual areas, suggesting that VGLUT2 is primarily located in thalamocortical projections (Wong and Kaas, 2010). This interpretation is consistent with rodent studies of VGLUT2 protein expression in cortical areas (Kaneko and Fujiyama, 2002; Kaneko et al., 2002). Our examination of *VGLUT2* mRNA and protein expression in thalamic visual regions similarly supports rodent findings; *VGLUT2* mRNA and protein are strongly expressed in visual relay nuclei in the thalamus, and are consistent with known afferent and efferent projections to cortical and thalamic areas. Moreover, differences in VGLUT2 gene expression and immunoreactivity occur across layers of the dorsal lateral geniculate nucleus and superior colliculus, and within parts of the pulvinar complex, providing additional insights into the functional organization of visual structures in primates.

4.3 Materials and Methods

VGLUT2 mRNA and protein expression were studied in three adult prosimian galagos *(Otolemur garnetti)*. All experimental procedures were approved by the Vanderbilt Institutional Animal Care and Use Committee and followed the guidelines published by the National Institutes of Health.

Tissue preparation

Each animal was given a lethal dose of sodium pentobarbital (80mg.kg) and transcardially perfused with 0.1M phosphate-buffered saline (PBS), followed by 4% paraformaldehyde in sterile PBS. The brain was removed from the skill, postfixed for 2-4 hours in 4% paraformaldehyde in sterile PBS, and then cryoprotected in 30% sucrose in sterile PBS overnight. The subcortical region was separated from the two cortical hemispheres and cut into

40um coronal sections on a sliding microtome. The subcortical sections were then separated into six series for further study.

Histochemistry

One series of sections from each animal was processed for Nissl substance with thionin to determine the cellular architecture and laminar organization of subcortical structures. Another series was processed for cytochrome oxidase (CO) as an additional aid in identifying the subcortical structures (Wong-Riley, 1979).

In situ hybridization

VGLUT2 mRNA distribution was examined in one series of brain sections from each animal using in situ hybridization (ISH). A digoxigenin (DIG)-labeled riboprobe for VGLUT2 was prepared using galago liver cDNA libraries with reverse transcriptase-polymerase chain reaction (RT-PCR) and conventional TA cloning techniques, and labeled using a DIG-dUTP labeling kit (Roche Diagnostics, Indianapolis, IN). The forward and reverse primers used for VGLUT2 were *gccatcgtggacatggtcaa* and *ataactccaccatagtggac* respectively, which targeted position 693-1888 of human VGLUT2 (NM020346). BLAST assessments of this region of galago VGLUT2 (JF290396) to those of macaque VGLUT2 (XM002799604) and human VGLUT2 revealed 99% homology for both comparisons.

Similar assessments of other members of the VGLUT family showed 72% homology between human VGLUT1 (AB032436) and VGLUT2, and 75% homology between human VGLUT3 (AJ459241) and VGLUT2, indicating that although VGLUT2 shows significant homology between species, the protein is genetically distinct from other VGLUT isoforms. Additionally, the VGLUT2 probe used in this study exhibited distinct signals from those of VGLUT1, as previously shown (Hackett et al., 2011).

ISH was carried out as described previously described (Tochitani et al., 2001). Briefly, freefloating sections were soaked in 4% paraformaldehyde/0.1M phosphate buffer (pH 7.4) overnight at 4° C and treated with 10 mg/mL proteinase K for 30 minutes at 37° C. After acetylation with 0.25% acetic anhydride in 0.9% triethanolamine and 0.12% hydrochloric acid, the sections were incubated in hybridization buffer (pH 7.5) containing 5X saline sodium citrate (SSC; 150 mM sodium chloride, 15 mM sodium citrate, pH 7.0), 50% formamide (FA), 2% blocking reagent (Roche Diagnostics), 0.1% N-lauroylsarcosine (NLS), 0.1% sodium dodecyl sulphate (SDS), 20 mM maleic acid buffer, and 1 mg/mL of the appropriate DIG-labeled riboprobe. Sections were hybridized with the probe overnight at 60° C and washed by successive immersion in 2X SSC, 50% FA, 0.1% NLS for 20 minutes at 60° C. Nonspecific mRNA was removed with 20 mg/ml RNase A in RNase A buffer (10 mM Tris-HCl, 10 mM ethylenediamine-N,N,N′,N′-tetraacetic acid (EDTA), 500 mM NaCl; pH 8.0) for 15 minutes at 37° C and sections were washed twice in 2X SSC, 50% FA, 0.1% NLS, followed by two more washes in 0.2X SSC, 50% FA, 0.1% NLS, for 20 minutes each. Hybridized mRNA signals were visualized by alkaline phosphatase (AP) immunohistochemical staining using a DIG detection kit (Roche Diagnostics). Sections were mounted onto gelatin-subbed glass slides and dehydrated through a graded ethanol series (70% for 5 minutes, 95% for 10 minutes, 100% for 10 minutes), cleared in xylene (5 minutes), and then coverslipped with Permount.

Immunohistochemistry

One series of brain sections from each animal was processed for immunohistochemical localization of VGLUT2 protein. Sections were rinsed in 0.1 M PBS and quenched in 0.3% hydrogen peroxide, rinsed again in 0.1 M PBS, and incubated for 2 hours at room temperature in blocking solution (5% normal horse serum, 0.5% Triton X-100 in 0.1 M PBS). Sections were

then incubated overnight in a primary antibody solution of 1:5000 goat anti-mouse VGLUT2 (Millipore, Billerica, MA) in blocking solution, rinsed in PBS, and incubated for 2 hours at room temperature in 1:200 peroxidase anti-goat IgG in blocking solution. Sections were rinsed in PBS and then incubated for 1 hour at room temperature in ABC reaction (ABC kits; Vector, Burlingame, CA). Immunoreactivity was then visualized by developing sections in diaminidobenzidine (DAB) solution (0.2 mg/ml DAB, 0.1% hydrogen peroxide, 1% nickel ammonium sulfate). Sections were rinsed in water to stop the DAB reaction, mounted on gelatin-subbed glass slides, dehydrated though a graded ethanol series (70% for 3 minutes, 95% for 6 minutes, 100% for 6 minutes) followed by xylene (5 minutes), and coverslipped with Permount.

Light microscopy

Digital photomicrographs of relevant thalamic and midbrain structures were captured using a Nikon DXM2200 camera (Nikon, Melville, NY) mounted on a Nikon E800 microscope. The images were adjusted for brightness and contrast using Adobe Photoshop (Adobe Systems, San Jose, CA), but were not otherwise altered.

4.4 Results

The present study characterizes the distribution of VGLUT2 mRNA and protein within the visual thalamus and superior colliculus of prosimian galagos. Overall, VGLUT2 mRNA and protein are strongly expressed in the lateral geniculate nucleus, superior colliculus and pulvinar complex, but further analysis reveals a unique expression pattern for each layer or subdivision of the three regions. Additionally, sense and antisense labeling confirmed probe specificity to *VGLUT2* mRNA (fig. 1). The detailed expression patterns of each subcortical area are discussed below.

4.4.1.1 Figure 1. Specificity controls for ISH probes against *VGLUT2* mRNA in galagos. Sense and anti-sense probes for *VGLUT2* confirm staining specificity for *VGLUT2* mRNA and lack of secondary reactivity due to staining techniques. (A) Anti-sense *VGLUT2* probe stains *VGLUT2* mRNA in the thalamus. (B) Sense *VGLUT2* probe does not stain *VGLUT2* mRNA and does not show any secondary signal in the thalamus. Scale bar is 1mm. The thalamic midline is to the right.

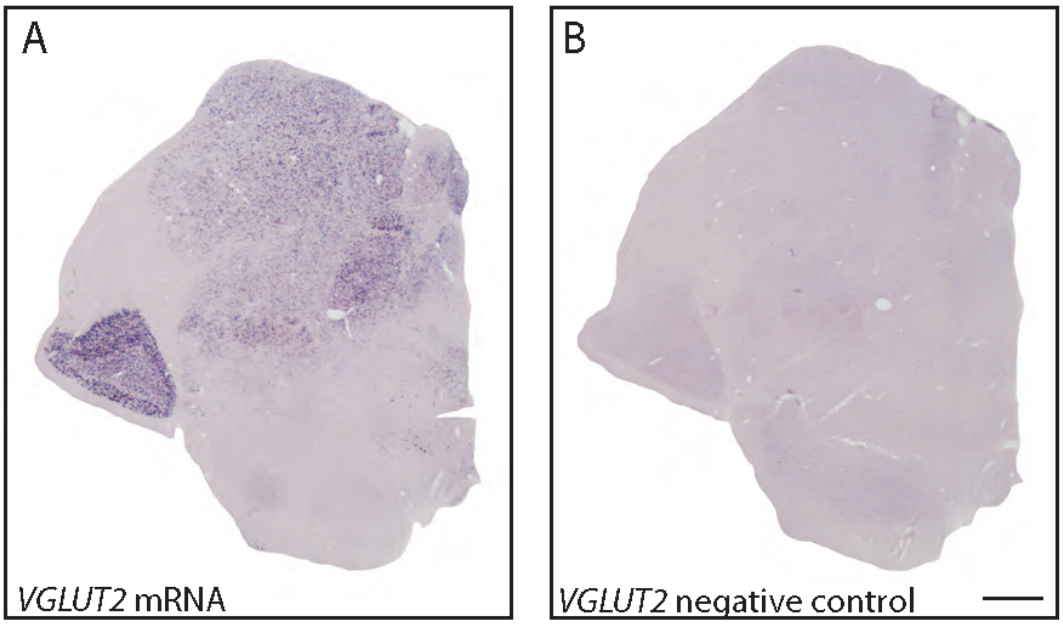

Lateral geniculate nucleus

The dorsal lateral geniculate nucleus (LGN) of galagos is characterized by six layers, each of this receives monocular input from the contralateral or ipsilateral eye and projects to layer IV of the primary visual cortex (Casagrande and Kaas, 1994). As described previously (Kaas et al., 1978), the layers of the LGN are organized from ventral to dorsal as follows: external magnocellular (ME), internal magnocellular (MI), internal parvocellular (PI), internal koniocellular (KI), external koniocellular (KE), and external parvocellular (PE). Low magnification images of coronal sections through the LGN show its laminar organization (figs. 2 and 3). In rostral sections, LGN layers are wide medially where central vision is represented and narrow laterally where peripheral vision is represented (fig. 2). In caudal sections of the LGN,

layers remain the same size from the medial edge to the lateral edge and are easily distinguishable from each other (fig. 3). A sublayer or leaflet of MI, which lies ventral to ME is visible in caudal sections of the LGN, especially in the VGLUT2 preparations (figs. 3A-3D). This sublayer of MI appears medially where MI proper thins to a narrow band.

CO distribution in the galago LGN has been characterized previously (McDonald et al., 1993; Johnson and Casagrande, 1995). Our results also defined a series of darkly stained layers separated by lightly stained interlaminar zones (figs. 2A and 3A). The CO-rich M and P layers were easily distinguishable from their CO-poor surroundings and appeared as four distinct bands in all sections. The K layers, however, were much lighter in CO sections and were barely distinguishable from their surrounding interlaminar zones. In Nissl preparations, the LGN layers were densely packed with darkly stained cell bodies, while the interlaminar zones were lighter in color and diffusely populated with smaller, lightly stained cell bodies (figs. 2B and 3B).

The cell bodies in the parvocellular and magnocellular layers of the LGN stained for *VGLUT2* mRNA (figs. 2D and 3D) suggesting that VGLUT2 is the primary glutamate transporter utilized by LGN projections to layer IV of V1. The magnocellular layers were characterized by large cells that stained densely for *VGLUT2* mRNA and tended to group together in short strings (fig. 4E). This clustered organization appeared to be unique to the magnocellular layers of the LGN (fig. 4). In the parvocellular layers, cells stained for *VGLUT2* mRNA were smaller and evenly distributed, but showed an intensity of staining nearly equal to those of cells in the magnocellular layers (figs. 4A and 4C). In the K layers, cells stained for *VGLUT2* mRNA were widespread and evenly distributed, but individual cells were weakly stained in comparison to individual cells from the M and P layers (fig. 4B). Some of the small cells of the sparsely populated interlaminar zones of the LGN stained weakly for *VGLUT2*

mRNA (figs. 4A-4E). Neurons in both the K layers and the interlaminar zones project to layers I, II, and III of V1 (Casagrande and Kaas, 1994), so their sparse *VGLUT2* mRNA distribution is consistent with the weak VGLUT2-ir previously described in those neocortex layers (Wong and Kaas, 2010).

4.4.1.2 Figure 2. Serial sections through part of the rostral lateral geniculate nucleus (LGN) stained for (A) cytochrome oxidase (CO), (B) Nissl, (C) VGLUT2 protein and (D) VGLUT2 mRNA. Scale bar is 0.5mm. Coronal sections, lateral is right.

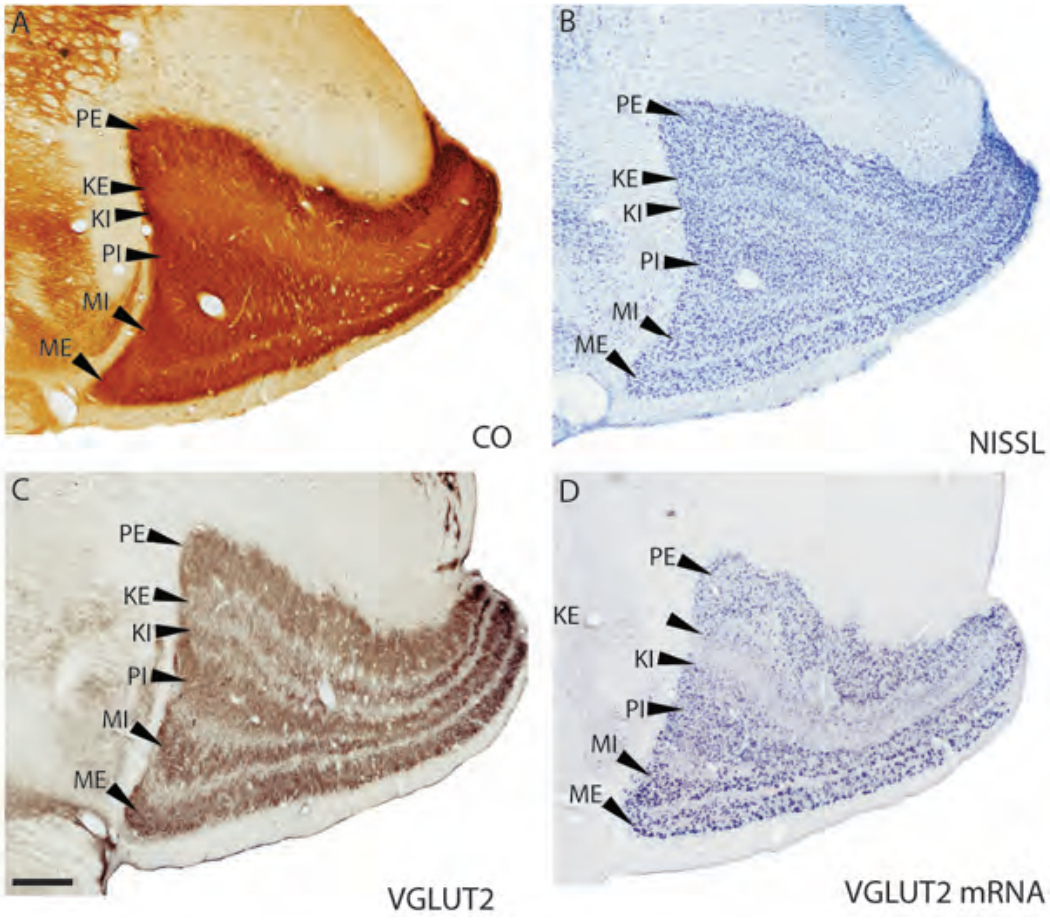

4.4.1.3 Figure 3. Serial sections through the caudal lateral geniculate nucleus (LGN) stained for (A) cytochrome oxidase (CO), (B) Nissl, (C) VGLUT2 protein and (D) VGLUT2 mRNA. Scale bar is 0.5mm. Coronal sections, lateral is left.

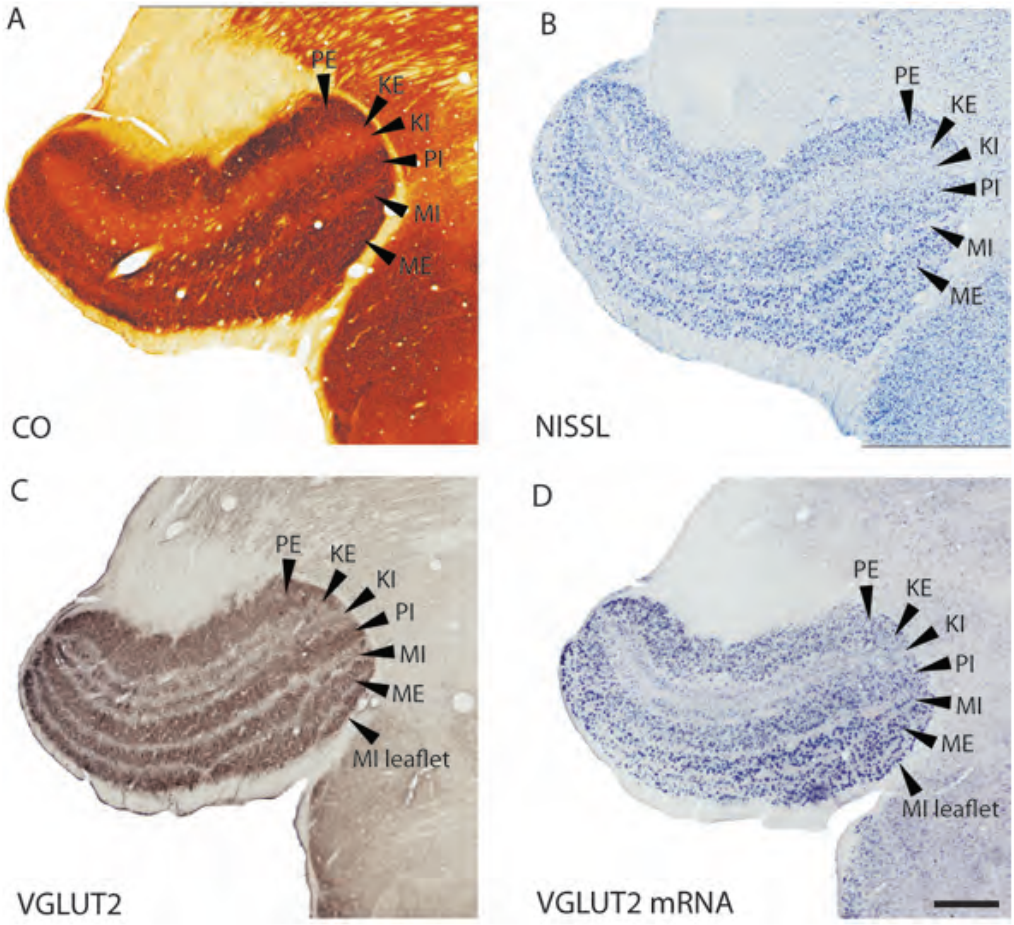

The differences in cell sizes between M, P, and K layers were clearly visible in sections stained for *VGLUT2* mRNA (fig. 5A). M cells were the largest in area and diameter, and their cytoplasm stained darkly for *VGLUT2* mRNA (fig. 5A). P cells were medium in size and stained less intensely (fig. 5B), while K cells were the smallest in size and stained weakly for *VGLUT2* mRNA (fig. 5C). This is consistent with the differences in sizes of M, P, and K cells in the LGN of galagos (Casagrande and Joseph, 1980) and other primates described previously (Norden and Kaas, 1978).

When stained for VGLUT2 protein, all layers of the LGN were easily distinguishable by their strong VGLUT2 immunoreactivity (figs. 2C and 3C). The M layers of the LGN were characterized by large cell bodies surrounded by dense puncta of VGLUT2-stained terminals (figs. 4I, 4J, and 6C), and had the largest proportion of VGLUT2-stained terminals compared to the other layers (figs. 4F-4J). The P layers of the LGN were less densely stained for VGLUT2 protein, but still showed intense staining of glutamatergic terminals and diffuse staining of cell bodies across both layers (figs. 4F, 4H). The K layers of the LGN were less densely stained for VGLUT2 protein (figs. 2C and 3C). At a higher magnification, it was apparent that staining is confined to sparse terminals within the layers and does not appear to be in cell bodies (fig. 4I). In contrast to the layers of the LGN, the interlaminar zones showed sparse immunoreactivity for VGLUT2 protein (fig. 6A). However, when viewed at higher magnification, VGLUT2 terminals were visible throughout the interlaminar zones (fig. 6C).

Pulvinar

The pulvinar complex in galagos is traditionally divided into three regions, the medial pulvinar (PM), lateral pulvinar (PL), and the inferior pulvinar (PI) (Stepniewska and Kaas, 1997; Stepniewska et al., 1999; Kaas and Lyon, 2007). The architecture of these three regions in CO- and Nissl-stained sections has been described previously by Wong et al. (2009). Our results were consistent with those findings (Figs. 7A and 7B) and we could not further subdivide the pulvinar with these two preparations.

4.4.1.4 Figure 4. VGLUT2 mRNA (A-E) and protein (F-J) expression in each layer of the LGN. Scale bar is 100um.

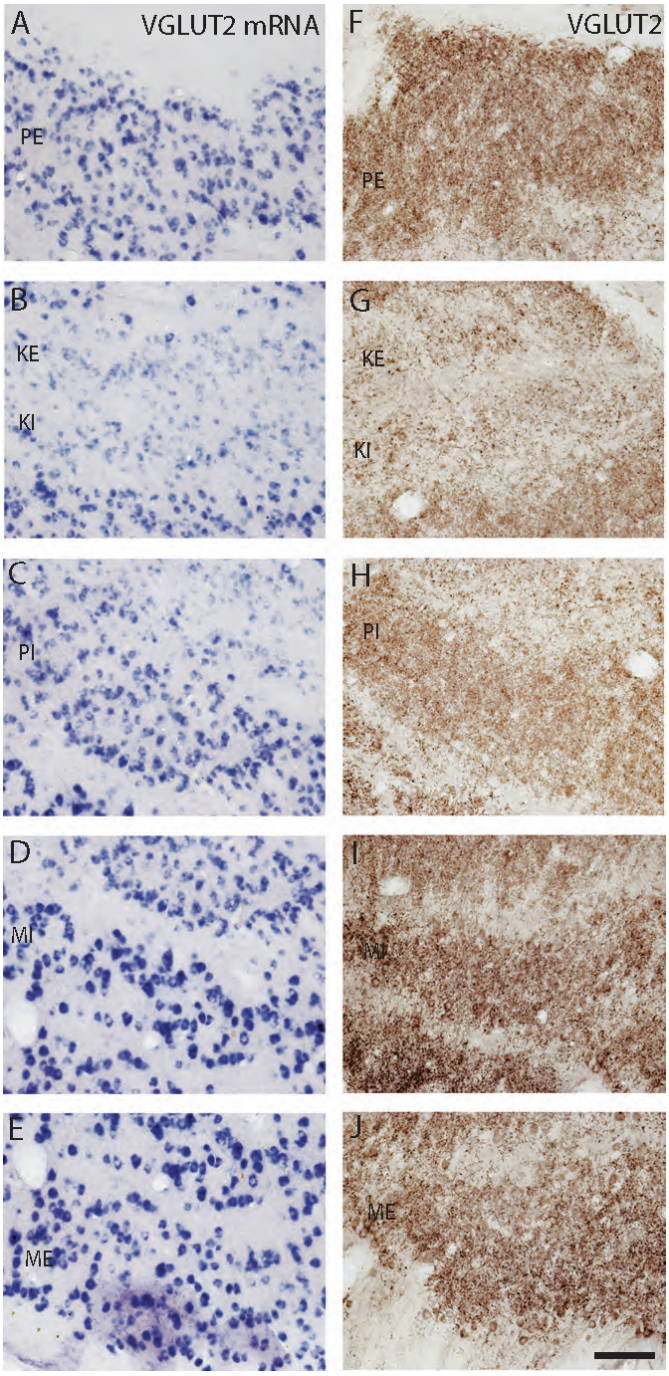

4.4.1.5 Figure 5. LGN cell types can be differentiated according to pattern of staining for VGLUT2 mRNA. (A) M cells are large and exhibit strong nuclear staining for VGLUT2 mRNA. (B) P cells are slightly smaller but also show intense staining for VGLUT2. (C) K cells are the smallest of all three and show weak, diffuse staining for VGLUT2. Scale bar is 50um.

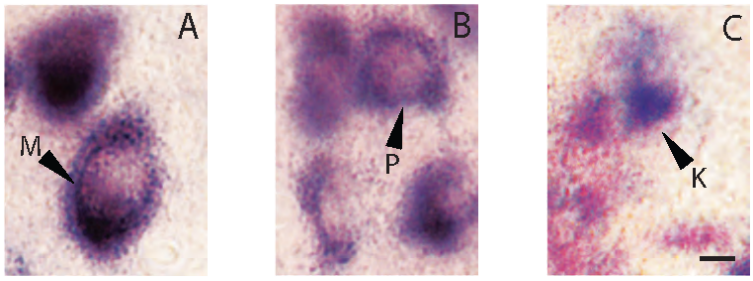

4.4.1.6 Figure 6. Laminar pattern of VGLUT2 immunoreactivity across the LGN. (A) VGLUT2 is strongly expressed in each layer of the LGN but less so in the interlaminar zones. However, high magnification (B) shows VGLUT2-positive terminals throughout the interlaminar zones. Scale bar is (A) 250um and (B-C) 100um.

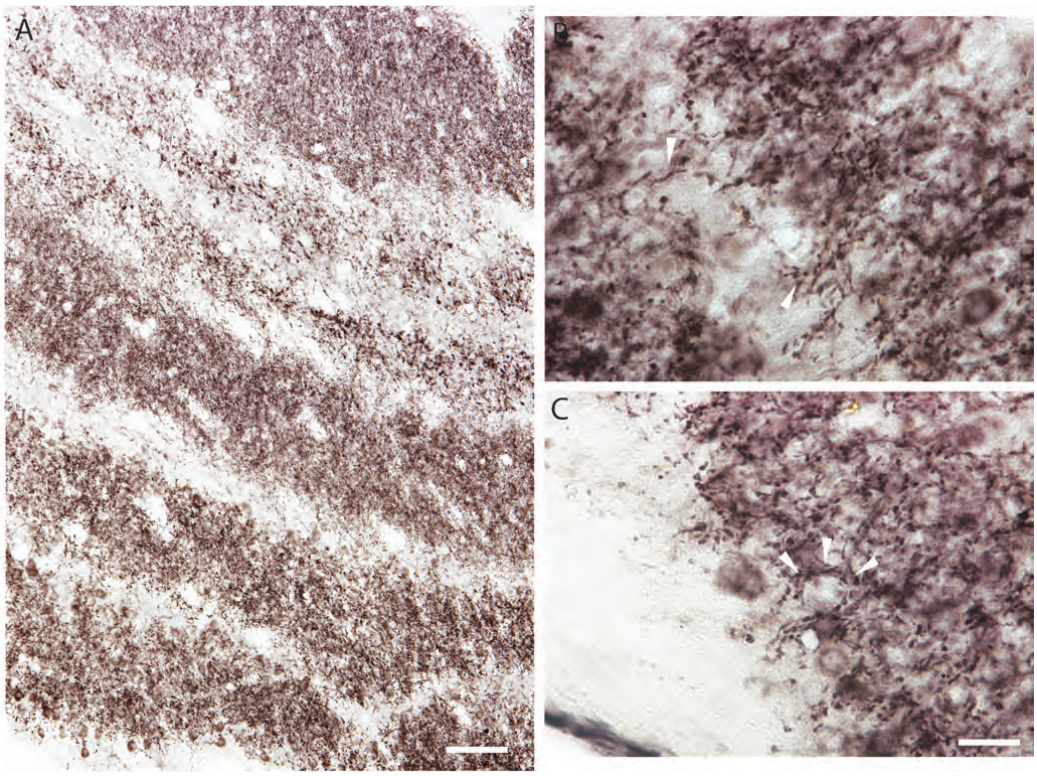

4.4.1.7 Figure 7. Serial sections through the pulvinar complex stained for (A) Nissl, (B) CO, (C) *VGLUT2* mRNA and (D) VGLUT2 protein. Scale bar is 1mm. Coronal sections, medial is left. PM, PL, PI: medial, lateral, and inferior divisions of the pulvinar complex.

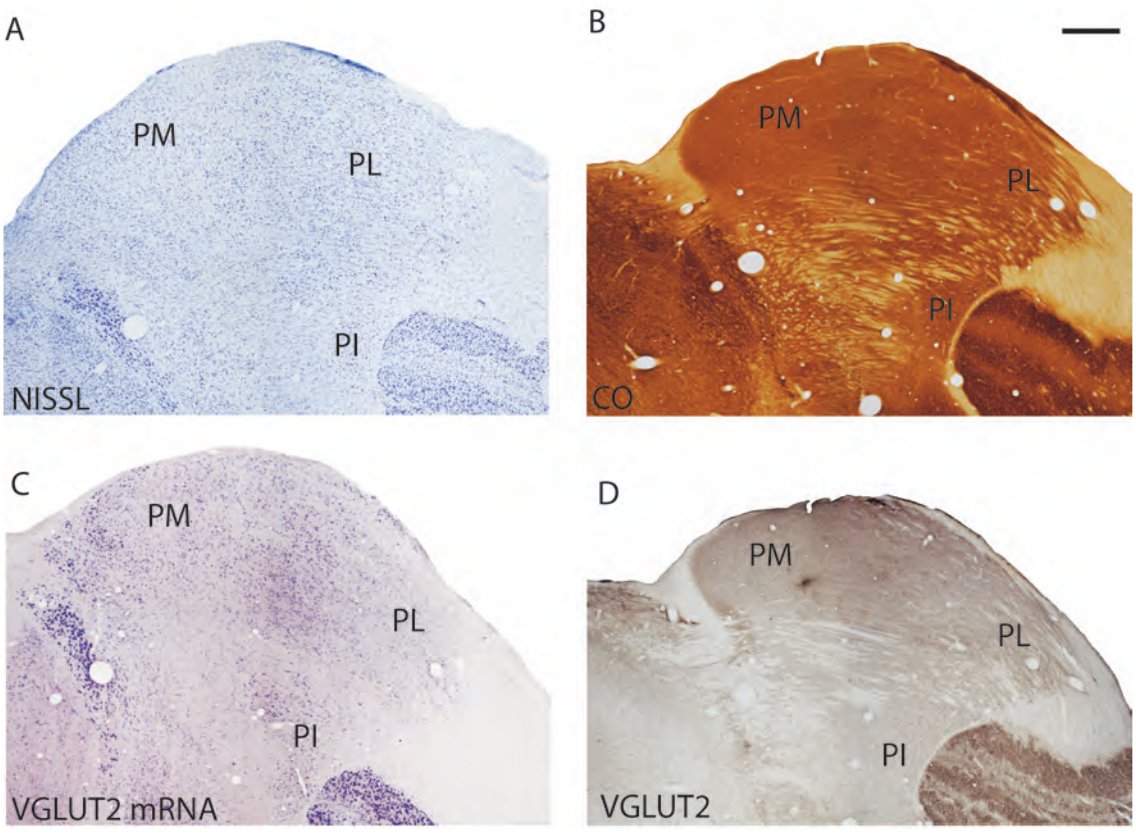

When stained for *VGLUT2* mRNA, PM and PL both showed a uniform distribution of stained ells, and were barely distinguishable from each other by staining intensity (fig. 7C). Higher magnification images show that PL cells stained slightly darker than PM cells (fig. 8A), but quantitative measures would be needed to justify this conclusion. Although the staining density of *VGLUT2* mRNA-positive cells was greater in PL compared to PM, this could be due to the higher cell density characteristic of this region (figs. 7A, 7C, 8A, 8B). PI is separated from PM and PL by the brachium of the SC, which was relatively free of cells positive for *VGLUT2*

mRNA. PI could also be distinguished from surrounding thalamic nuclei by its distribution of strongly stained *VGLUT2* mRNA-positive cells. Further divisions of PI were unclear in this preparation, but varying densities of stained cells (fig. 8C) suggest that PI is not homogeneous in its organization.

4.4.1.8 Figure 8. High magnification images of *VGLUT2* mRNA expression in each division of the pulvinar complex. (A) PM and PL both show intense staining for *VGLUT2* mRNA but (B) PL shows a denser distribution of VGLUT2-positive cells than PM. (C) PI stains variably in density and intensity for *VGLUT2* mRNA, indicating multiple populations of glutamatergic cells in this region. Scale bar is 250um.

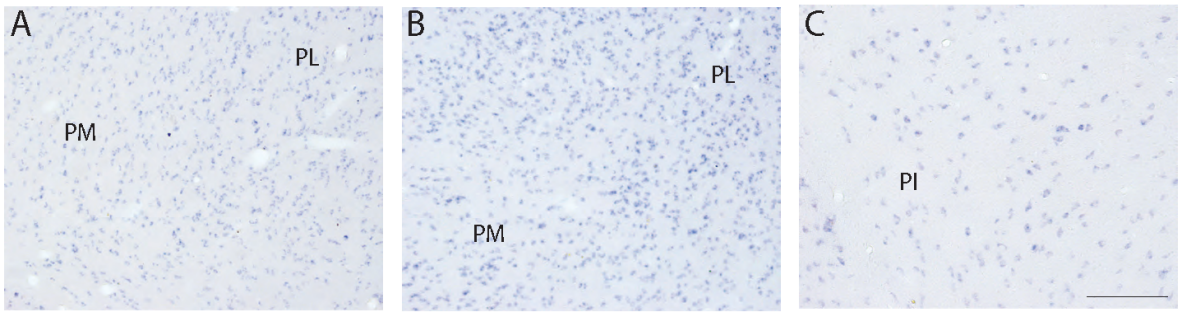

All three divisions of the pulvinar complex exhibited strong immunoreactivity when stained for VGLUT2 protein (fig. 7D). PM, PL, and PI all showed even distributions of punctate VGLUT2-ir and darker background staining in comparison to surrounding fiber tracts and neighboring nuclei (with the exception of the LGN). VGLUT2-ir in each region was primarily confined to cell bodies and axons instead of terminals (fig. 9), suggesting that VGLUT2-ir in the pulvinar is more representative of VGLUT2 protein within projection neurons and their axons in the pulvinar rather than efferent projections from other cortical or thalamic regions. However, in parts of the pulvinar, dense patches of VGLUT2-ir were observed (fig. 10). At higher magnification, these patches were identified as clusters of VGLUT2-positive terminals (fig. 11). These patches were most obvious in medial PL. However, similar patches appeared occasionally

along the lateral edge of PL or in PI, but this was not consistent across all sections. Other than this patchy distribution, no further architectonic subdivisions of the pulvinar complex were identified from either of the VGLUT2 preparations.

4.4.1.9 Figure 9. VGLUT2 protein expression in the pulvinar is largely confined to cell bodies and process instead of terminals. Scale bar is 25um.

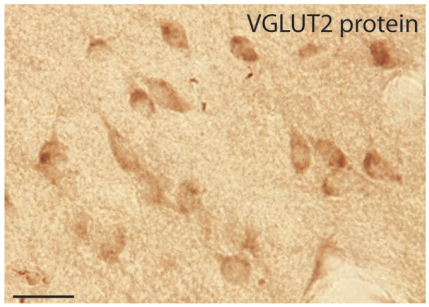

4.4.1.10 Figure 10. Patchy distribution of VGLUT2 positive terminals in the pulvinar complex. Serial sections of the pulvinar complex in low magnification (A-C) and higher magnification (D-F) stained for CO (A, D), Nissl (B, E), and VGLUT2 protein (C, F). VGLUT2 staining shows a region between PM and PL with patches of glutamatergic terminals. These could be projections from the lSGS of the SC to the pulvinar. Scale bar is 1mm (A-C) and 0.5mm (D-F).

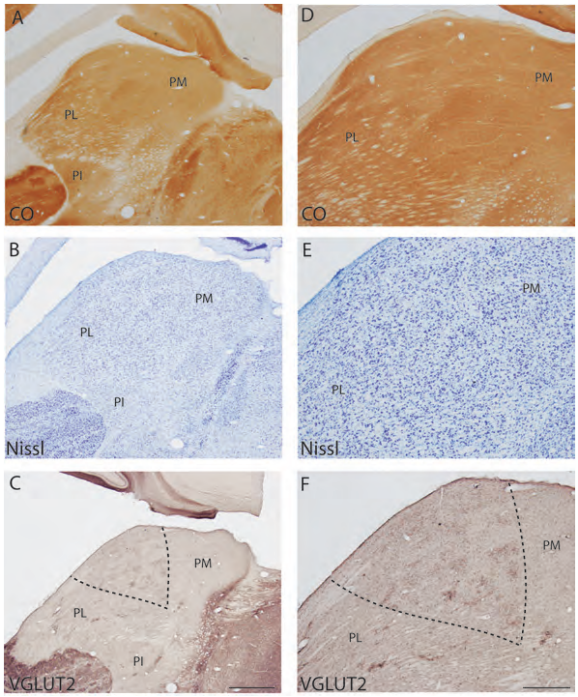

Superior colliculus

The superior colliculus in the galago has been previously subdivided into seven distinct layers in CO and Nissl preparations (Kaas and Huerta, 1988; May, 2006) and our results are largely consistent with these previous findings (fig. 12). However, in CO-stained sections, the stratum griseum intermediale (SGI) could be further subdivided according to staining intensity into three sublayers. The dorsal and ventral outer sublayers were darkly stained while the middle sublayer was weakly stained for CO (fig. 12A). These sublayers were, however, indistinguishable in Nissl preparations (fig. 12B).

4.4.1.11 Figure 11. Differential expression of VGLUT2 protein in each subdivision of the pulvinar complex. (A) PM shows dense staining of VGLUT2-positive cell bodies. (B) The medial region of PL shows dense patches of VGLUT2 positive terminals, which could be SC projections to pulvinar. (C) Lateral PL shows dense VGLUT2 staining of cell bodies and sparse staining of terminals. (D) Most of PI shows diffuse staining of VGLUT2 cell bodies but lacks VGLUT2 positive terminals. Scale bar is 100um.

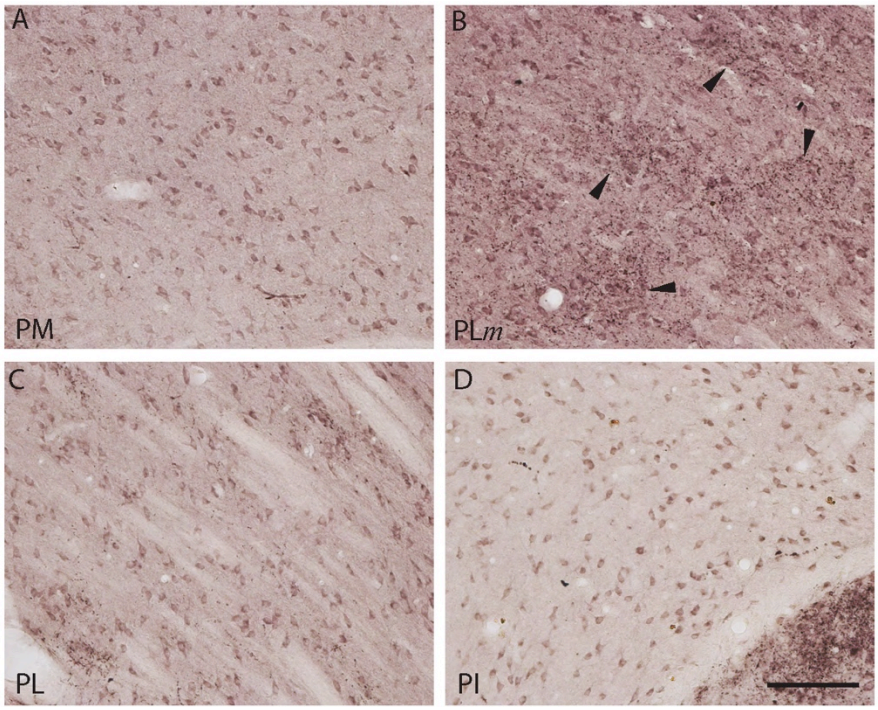

The stratum griseum superficiale (SGS) could be clearly divided into upper and lower sublayers according to the staining intensity of cells for *VGLUT2* mRNA (fig. 12C). The upper sublayer (uSGS) was characterized by weakly stained *VGLUT2* mRNA-positive cells while the lower sublayer (lSGS) was characterized by strongly stained *VGLUT2* mRNA-positive cells. These deeper, strongly stained cells likely project to the pulvinar (Raczkowski and Diamond, 1978). The stratum opticum (SO) exhibited weak staining for *VGLUT2* mRNA and a more diffuse distribution of *VGLUT2* mRNA-positive cells. Each sublayer of the SGI showed a different staining distribution for *VGLUT2* mRNA-positive cells; the dorsal and ventral sublayers had slightly denser distributions of small, weakly-stained *VGLUT2* mRNA-positive cells while the middle sublayer had a sparse distribution of very large, strongly stained *VGLUT2* mRNA-positive cells. This suggests that multiple subsets of cells in the SGI utilize VGLUT2, but additional markers would be required to fully differentiate their projections. Ventral to the SGI rests the stratum album intermediale (SAI) and the stratum griseum profundum (SGP), which were indistinguishable from each other in sections stained for *VGLUT2* mRNA. Both layers showed a diffuse distribution of small, weakly-stained cells. The stratum album profundum (SAP) below the SGP was free of cells stained for *VGLUT2* mRNA, which is consistent with its role as a white matter tract in the SC. The deepest layer of the SC, the periacqueductal gray (PAG), stained strongly for *VGLUT2* mRNA and could be separated into two zones according to staining density. The outer zone of the PAG (oPAG) showed a dense distribution of *VGLUT2* mRNA-positive cells while the thin inner zone (iPAG) was relatively free of cells positive for *VGLUT2* mRNA.

When stained for VGLUT2 protein, the layers of the SC could be similarly subdivided based on staining intensity (fig. 12D). The SZ was characterized by a thin, darkly stained band of VGLUT2-ir across the dorsal SC, which is consistent with its likely role as a recipient layer of retinotectal projections (Schönitzer and Holländer, 1984; Ortega et al., 1995). The SGS also stained strongly for VGLUT2 and could be clearly seprated into two sublayers; uSGS appeared as a dark band across the dorsal SC while lSGS below it appeared as a slightly lighter band. In some sections, a darker layer of VGLUT2-ir appeared between the uSGS and lSGS but this was not consistent across the SC. In galagos, retinal projections from the contralateral eye terminate in the superficial half of the uSGS, while retinal projections from the ipsilateral eye terminate less densely and in the deeper half of the uSGS (May, 2006). The SO showed diffuse projections that weakly stain for VGLUT2 protein. Ventral to the SO, the three layers of the SGI could be separated by their immunoreactivity; the outer sublayers appeared as darker bands of VGLUT2-ir while the middle sublayer appeared as a lighter band of VGLUT2-ir. Finally, the PAG showed strong, uniform VGLUT2-ir, but could not be subdivided into two zones in this preparation.

4.5 Discussion

The present study aimed to characterize the distribution of VGLUT2 mRNA and protein in the visual thalamus and superior colliculus of prosimian galagos. We find that, similar to rodent studies, both VGLUT2 mRNA and protein are widely expressed in the LGN, SC, and pulvinar. Additionally, the differential distribution of VGLUT2 in the SC and pulvinar allowed us to identify novel subdivisions of each region. Overall, we can conclude that VGLUT2 is the primary glutamate transporter utilized by visual subcortical areas in galagos given its widespread distribution in the afferent and efferent projections of these regions

4.5.1.1 Figure 12. Serial sections through the superior colliculus (SC) stained for (A) CO, (B) Nissl, (C) *VGLUT2* mRNA and (D) VGLUT2 protein. Scale bar is 0.5mm. Coronal sections; medial is right.

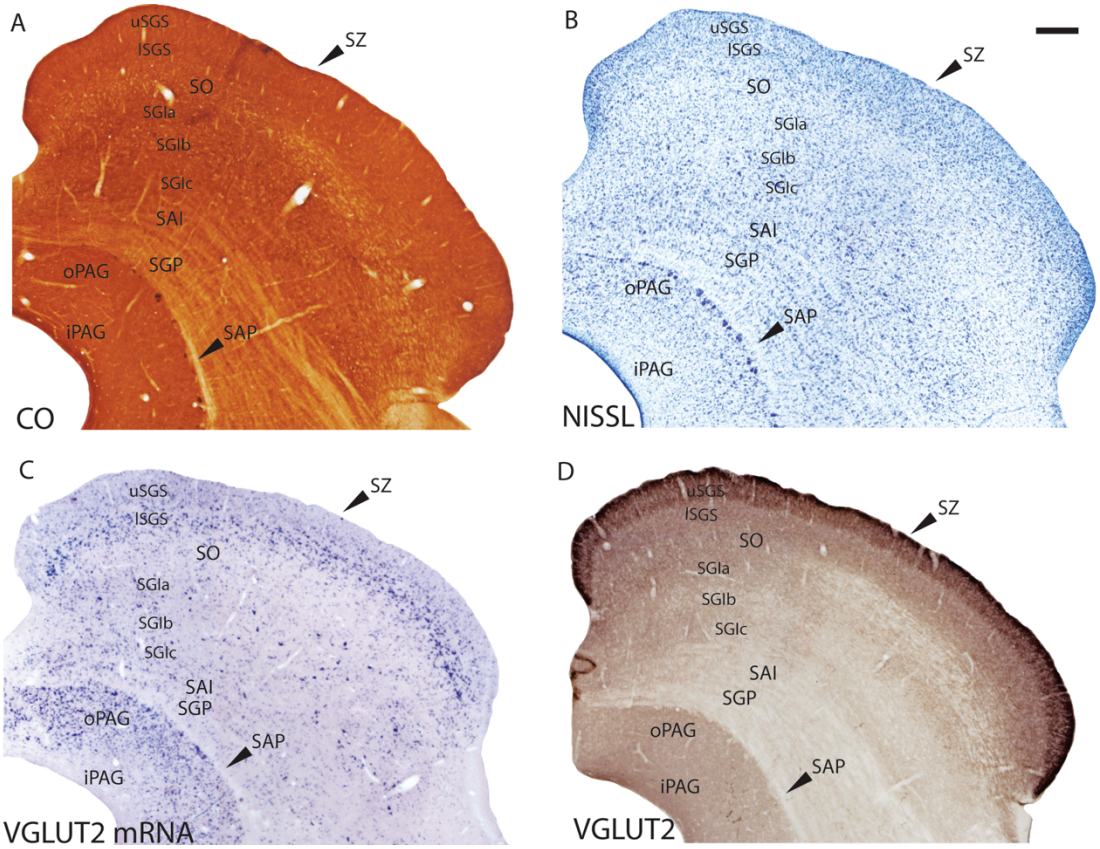

Lateral geniculate nucleus

The lateral geniculate nucleus of galagos receives retinal input from both eyes and projects directly to V1. The strong expression of *VGLUT2* mRNA and protein in all layers of the LGN indicates that both the retinogeniculate and geniculocortical pathways primarily utilize VGLUT2 to modulate glutamatergic transmission. This is consistent with studies in rodents that showed strong expression of both the protein and the mRNA in both pathways. Although the distribution of VGLUT2 has not been previously characterized in the galago retina, VGLUT2-ir was seen in the ganglion cells of both rat and human retinas (Gong et al., 2006), which indicates

that retinal projections to the SC and LGN likely utilize VGLUT2 for excitatory transmission. Thus, the strong expression of VGLUT2 protein in the galago LGN likely arises from retinal projections to each layer, which is consistent with the idea that retinogeniculate projections utilize VGLUT2 as their primary glutamate transporter. The LGN of galagos projects to layers IV, VI, III, and I of striate cortex (Glendenning et al., 1976; Casagrande and DeBruyn, 1982; Florence et al., 1983; Diamond et al., 1985; Florence and Casagrande, 1987; Lachica and Casagrande, 1992). Specifically, M cells project to layer IVa and somewhat to layer IIIC, P cells project to layer IVb and K cells project to the CO blobs in layer III and layer I. The expression of *VGLUT2* mRNA by M and P cells in the LGN suggests that these geniculostriate projections all use VGLUT2 as their primary glutamate transporter. Previous descriptions of VGLUT2-ir in the neocortex of galagos (Wong and Kaas, 2010) showed strong, dense labeling of VGLUT2 protein in layer IV of V1. VGLUT2-ir of layer III was weak in V1, but moderate staining was present in a patchy pattern possibly corresponding to the blobs where the cells in the K layers project. Overall, we found weak *VGLUT2* mRNA expression in the K layers of the LGN.

Pulvinar

The pulvinar complex of galagos is traditionally organized into three regions, the medial pulvinar, lateral pulvinar, and inferior pulvinar (Stepniewska and Kaas, 1997; Kaas and Lyon, 2007), although recent studies have been able to further subdivide each of these nuclei in other primates into separate regions based on histochemical and connectional studies (Stepniewska et al., 1999). Since we were unable to subdivide the pulvinar past the three traditional regions from our results, we limit our discussion to those divisions. The pulvinar complex of galagos is densely connected with multiple areas of visual and nonvisual cortex (Stepniewska, 2004). In galagos, the medial pulvinar has reciprocal connections with frontal and parietal cortex, the

lateral pulvinar is well connected with early visual areas such as V1, V2, and possibly V3, and the inferior pulvinar is linked to V1 and V2, as well as the middle temporal area (MT) and possibly other higher order visual areas. The subcortical connections of the pulvinar nucleus of galagos include afferent projections from the lower stratum griseum superficiale of the superior colliculus to the inferior pulvinar (Wong and Kaas, 2009a). Since VGLUT2 has been described previously as within subcortical projections to the thalamus and thalamocortical projections to rodents, it is not surprising that our results show few VGLUT2-positive terminals in the three subdivisions of the pulvinar complex. The localization of VGLUT2-ir to cell bodies and axons instead of terminals is consistent with the evidence that most of the input to the pulvinar is from cortex, and not from subcortical structures such as the superior colliculus. VGLUT2 immunoreactivity in the pulvinar may also arise from intrinsic connections within the nucleus; collateral branches from thalamocortical projections from relay neurons could terminate on nearby inhibitory neurons and have modulatory connections within that subdivision (25). These intrinsic connections could also be responsible for VGLUT2-ir within this nucleus.

It is surprising that concentrations of VGLUT2-positive terminals did not appear in the inferior pulvinar given its strong connection with the superior colliculus, but these projections might utilize a different form of glutamate transport or a different isoform of the VGLUT family. Additionally, we did find dense patches of VGLUT2-positive terminals in the medial part of the lateral pulvinar, which could be input from the superior colliculus; however, further studies would be required to determine the origin of these dense terminal projections. The strong expression of *VGLUT2* mRNA in all divisions of the pulvinar is consistent with their excitatory projections to cortical areas and corresponds well with the strong VGLUT2 immunoreactivity seen in those cortical areas (7). Thus, we can conclude that the pulvinar complex utilizes

VGLUT2 as its primary glutamate transporter for afferent projections to cortex, but inputs from cortex likely use a different VGLUT isoform in their terminations.

Superior colliculus

The superior colliculus in primates is a complex multisensory structure that receives diverse inputs from cortical and subcortical regions and projects to multiple structures in the central nervous system as well (Kaas and Huerta, 1988). Visual processing in the superior colliculus is largely restricted to the superficial layers, while the deep layers are responsible for sensorimotor integration and motor functions. In galagos, the primary target of retinal projections in the superior colliculus is the stratum griseum superficiale (superficial gray); the upper sublayer of the superficial gray (uSGS) receives a dense superficial projection of retinal afferents from the contralateral eye, and a deeper projection from the ipsilateral eye, while the lower sublayer (lSGS) receives more diffuse retinal input (Casagrande and Joseph, 1980). As discussed above, retinal ganglion cells likely use VGLUT2 as their primary glutamate transporter, so their terminal distribution in the superior colliculus should also exhibit strong VGLUT2-ir. This is consistent with our findings of dense VGLUT2-ir in the stratum zonale and upper superficial gray and less dense, yet still intense, VGLUT2-ir in the lower superficial gray. The upper and lower superficial gray layers in galagos project to the LGN and the pulvinar respectively (Harting et al., 1991; May, 2006). Upper superficial gray projections to the LGN primarily terminate on the K layers of the LGN (Glendenning et al., 1976) and lower superficial gray projections to the pulvinar mainly target the inferior division (Wong et al., 2009). Diffuse staining of *VGLUT2* mRNA in the upper superficial gray corresponds with the sparse VGLUT2-ir seen in the K layers of the LGN, indicating that colliculogeniculate projections do use VGLUT2 for excitatory transmission but at lover levels compared to other projections. The

dense staining of *VGLUT2* mRNA in the lower superficial gray, however, seems incongruent with the lack of densely-labeled VGLUT2-positive terminals in the inferior pulvinar described here. The lack of dense staining for VGLUT2-positive terminals in the inferior pulvinar suggests that projections from the lower superficial gray target different regions of the pulvinar complex. As discussed above, the patchy distribution of VGLUT2-positive terminals in the medial part of the lateral pulvinar could reflect the terminations of colliculus projections. The intermediate and deep layers of the superior colliculus are involved in sensory integration and brainstem-related motor functions, which are outside the scope of this discussion, but the laminar distribution of VGLUT2 mRNA and protein is largely consistent with previous findings in rodents (Kaneko et al., 2002). The three subdivisions of the stratum griseum intermediale (intermediate gray) that we see in cytochrome oxidase, *VGLUT2* mRNA and VGLUT2 protein staining is a novel finding in galagos, but has been previously reported in rodents (Helms et al., 2004), squirrels (Baldwin et al., 2011), which are rodents with well developed visual systems similar to that of primates, and tree shrews (Harting et al., 1973a), which are highly visual mammals that are a close relative of the primate lineage. Thus, our identification of three sublamina in the intermediate gray layer is consistent with architectonic divisions of the superior colliculus in closely related species. The division of the periacqueductal gray into inner and outer layers according to *VGLUT2* mRNA expression is also novel in galagos.

Overall, our conclusions on the distributions of *VGLUT2* mRNA and protein expression, and the subsequent visualization of sublamina in the superior colliculus and pulvinar complex of galagos are largely consistent with related studies in rodent and primate species.

CHAPTER 5

VGLUT1 mRNA and protein expression in the visual system of prosimian galagos

The following chapter was published under the same title in Eye and Brain by Pooja Balaram, Troy Hackett, and Jon Kaas; December 2011.

5.1 Abstract

The presynaptic storage and release of glutamate, an excitatory neurotransmitter, is modulated by a family of transport proteins known as vesicular glutamate transporters. Vesicular glutamate transporter 1 (VGLUT1) is widely distributed in the central nervous system of most mammalian and nonmammalian species, and regulates the uptake of glutamate into synaptic vesicles as well as the transport of filled glutamatergic vesicles to the terminal membrane during excitatory transmission. In rodents, *VGLUT1* mRNA is primarily found in the neocortex, cerebellum, and hippocampus, and the VGLUT1 transport protein is involved in intercortical and corticothalamic projections that remain distinct from projections involving other VGLUT isoforms. With the exception of a few thalamic sensory nuclei, *VGLUT1* mRNA is absent from subcortical areas and does not colocalize with other *VGLUT* mRNAs. VGLUT1 protein is similarly restricted to a few thalamic association nuclei and does not colocalize with other VGLUT proteins. However, recent work in primates has shown that *VGLUT1* mRNA is also found in several subcortical nuclei as well as cortical areas, and that VGLUT1 may overlap with other VGLUT isoforms in glutamatergic projections. In order to expand current knowledge of VGLUT1 distributions in primates and gain insight on glutamatergic transmission in the visual

system of primate species, we examined VGLUT1 mRNA and protein distributions in the lateral geniculate nucleus, pulvinar complex, superior colliculus, V1, V2, and the middle temporal area (MT) of prosimian galagos. We found that, similar to other studies in primates, VGLUT1 mRNA and protein are widely distributed in both subcortical and cortical areas. However, glutamatergic projections involving VGLUT1 are largely limited to intrinsic connections within subcortical and cortical areas, as well as the expected intercortical and corticothalamic projections. Additionally, VGLUT1 expression in galagos allowed us to identify laminar subdivisions of the superior colliculus, V1, V2, and MT.

5.2 Introduction

Glutamatergic transmission in the central nervous system is presynaptically regulated by a family of proteins known as vesicular glutamate transporters (VGLUTs) (Bellocchio et al., 1998; Aihara et al., 2000; Fremeau et al., 2001; 2004a). VGLUT proteins package glutamate into presynaptic vesicles and transport these vesicles to the synaptic membrane prior to excitatory transmission. Two main VGLUT isoforms, VGLUT1 and VGLUT2, are widely distributed in the brain and are responsible for the majority of glutamatergic transmission in the central nervous system (Takamori et al., 2000; Herzog et al., 2001; Fremeau et al., 2002; Varoqui et al., 2002). These two isoforms typically occupy separate circuits, where VGLUT2 is primarily restricted to projections between and within subcortical areas, as well as thalamocortical projections, while VGLUT1 is reserved for intercortical and corticothalamic projections (Kaneko and Fujiyama, 2002; Kaneko et al., 2002; Barroso-Chinea et al., 2007). Previous studies in rodents have shown that VGLUT1 is strongly expressed in the cerebral cortex, cerebellum and hippocampus and largely absent from the thalamus and brainstem (Herzog et al., 2001; Kaneko and Fujiyama,

2002; Kaneko et al., 2002; Fremeau et al., 2004b; Barroso-Chinea et al., 2007). In the cortex, *VGLUT1* mRNA is densely expressed in each of the cortical layers, with varying distributions in each functional area, while VGLUT1 protein is diffusely expressed across all the cortical layers with slight laminar differences in each area. In the thalamus, VGLUT1 mRNA and protein are moderately expressed in primary relay nuclei and weakly expressed in some association nuclei.

Although little work has been done in primates to characterize the distributions of VGLUT proteins in the central nervous system, recent studies show that VGLUT mRNA and protein expression in the brains of primates are quite similar to that of rodent brains, suggesting that the roles of VGLUTs in excitatory neurotransmission are highly conserved across mammalian species (Hackett and la Mothe, 2009; Wong and Kaas, 2010; Hackett et al., 2011; Balaram et al., 2011b). In order to expand on the knowledge of VGLUT distributions in primates and gain insight into the functional organization of the primate visual system, we examined VGLUT1 mRNA and protein distributions within the visual system of prosimian galagos. Galagos are small, nocturnal primates that represent the prosimian brain of the primate order (Kaas, 2006). Prosimians more closely resemble ancestral primates than any of the present day anthropoids (monkeys, apes, and humans), and thus the distribution pattern of VGLUTs in galagos may more closely reflect the distribution pattern of early primates. Previous research on the visual systems of galagos showed that VGLUT2 is localized to the expected thalamocortical and subcortical pathways (Balaram et al., 2011b), so we predicted that VGLUT1 expression would be localized to intercortical and corticothalamic circuits. Our results show that, while VGLUT1 expression in primates is more widespread in subcortical and cortical areas than VGLUT1 expression in homologous areas of rodents, the expression patterns are largely confined to the expected pathways. These findings suggest that VGLUT1 expression patterns are

highly conserved across mammalian species and that VGLUT1 is widely utilized in glutamatergic transmission.

5.3 Materials and methods

Four adult galagos *(Otolemur garnetti)* were examined for VGLUT1 protein and mRNA expression. Experimental procedures were all approved by the Vanderbilt Institutional Animal Care and Use Committee and followed the guidelines published by the National Institutes of Health.

Tissue acquisition and histology

Animals were injected with a lethal overdose of sodium pentobarbital (80 mg/kg), and when areflexive, were perfused transcardially with sterile 0.1 M phosphate-buffered saline (PBS), followed by 4% paraformaldehyde (PFA) in sterile PBS. The brain was removed from the skull, postfixed for 2–4 hours in 4% PFA in sterile PBS and cryoprotected in 30% sucrose in sterile PBS. The whole brain was cut into 40 mm coronal sections on a sliding microtome, separated into six series, and stored at − 20°C in cryoprotectant solution (30% ethylene glycol, 30% glycerol, 10% phosphate buffer (pH 7.4), 1% 5 M NaCl, 29% sterile distilled deionized water) until further study. Two series from each animal were processed for cytochrome oxidase (CO) (Wong-Riley, 1979) and Nissl substance with thionin to determine the architectural and laminar boundaries of subcortical and cortical regions.

In situ hybridization

One series from each animal was labeled for VGLUT1 mRNA using in situ hybridization. Digoxigenin-labeled riboprobes for VGLUT1 were prepared using macaque cDNA libraries and labeled using a conventional DIG-dUTP labeling kit (Roche Diagnostics,

Indianapolis, IN). In situ hybridization was carried out as previously described (17). The forward and reverse primers for VGLUT1 were CCGCTACATTATCGCCATCA and CGATGGGCACGATGATGGTC, respectively, which targeted position 204–1093 of human VGLUT1 (AB032436). BLAST assessments of VGLUT1 homology across human, macaque, rat and mouse transcripts show 98%–100% homology, indicating that the VGLUT1 gene is highly conserved across species. However, sense and antisense probes for VGLUT1 were still used to evaluate the binding specificity and background reactivity of macaque VGLUT1 probes in galago tissue.

Immunohistochemistry

One series from each animal was labeled for VGLUT1 protein using commercial antibodies against VGLUT1 and previously described immunohistochemical techniques (Balaram et al., 2011b). Two antibodies against VGLUT1 were used in this study, a polyclonal antibody raised in rabbits (MAb Technologies, Atlanta GA) that recognized amino acids 543–560 of rat VGLUT1, and a polyclonal antibody raised in guinea pigs (Synaptic Systems, Goettingen, Germany) that recognized amino acids 456–560 of rat VGLUT1. Western blot analysis showed that both antibodies were highly specific for primate VGLUT1, but due to the profuse and indistinct distribution of VGLUT1 in cortex, it became necessary to corroborate our findings using more than one antibody. Slight differences in the intensity of labeling in brainstem nuclei were noted when the two antibodies were compared, but no differences were noted in the thalamus or cortex. Primary antibodies were subsequently labeled with biotinylated secondary antibodies (Vector Labs, Burlingame CA) amplified using an avidin/biotin conjugate kit (Vector Labs) and visualized using a diaminobenzidine reaction with nickel enhancement. Details of primary and secondary antibody concentrations are listed in Table 1.

Light microscopy

Digital photomicrographs of cortical and subcortical areas were captured using a Nikon DXM2200 camera (Nikon, Melville, NY) mounted on a Nikon E800 microscope. Images were adjusted for contrast using Adobe Photoshop (Adobe Systems, San Jose, CA), but were otherwise unaltered.

Analysis

Relative staining intensity for *VGLUT1* mRNA and VGLUT1 protein was analyzed using relative optical density; background relative optical density values were sampled in low magnification images of each area, from fiber tracts that did not show VGLUT1 expression, and subtracted out of relative optical density values from each area of interest. Relative density for both stains was analyzed using comparative cell counts of each area in high magnification images of serial Nissl and VGLUT1 sections. Analytical measures were only used to judge general differences in staining patterns for each area and were not intended to quantify levels of expression in any given region of interest.

5.4 Results

The regional distributions of *VGLUT1* mRNA and protein varied significantly between subcortical and cortical areas in the galago brain. *VGLUT1* mRNA was moderately expressed in the lateral geniculate nucleus (LGN), superior colliculus (SC), pulvinar, and middle temporal visual area (MT), but strongly expressed in V1 (area 17) and V2 (area 18). However, VGLUT1 protein was moderately expressed in MT and the SC, but strongly expressed in the LGN, pulvinar, V1, and V2. The detailed expression patterns of VGLUT1 are discussed below. Control staining using sense and antisense probes also confirmed that the engineered *VGLUT1* probe was

specific to *VGLUT1* mRNA in galago cortex. Additionally, Western blot analysis for both VGLUT1 antibodies confirmed specificity to VGLUT1 protein in primate tissue (data not shown).

5.4.1 VGLUT1 in the thalamus and midbrain

Lateral geniculate nucleus (LGN)

The dorsal LGN in galagos is classically divided into six layers with five interlaminar zones (Figure 1). As previously described (Kaas et al., 1978), terms for the layers reflect cell type (magnocellular [M], parvocellular [P], or koniocellular [k]) and relative location of (internal [I] or external [E]). Definitions for the interlaminar zones employ the neighboring dorsal and ventral LGN layer, such that the interlaminar zone between the internal M and P layers is termed Ipm. For the purposes of the present results, our identification of LGN layers and interlaminar zones follows previous descriptions.

Previous descriptions of CO expression in the galago LGN have shown that all layers and interlaminar zones have some level of cytochrome oxidase reactivity (McDonald et al., 1993; Casagrande and Kaas, 1994; Johnson and Casagrande, 1995). The M and P layers stain darkly for CO, while the K layers and interlaminar zones exhibit more moderate reactivity (fig. 1A). The LGN layers contain dense populations of darkly stained cells in Nissl preparations, while the interlaminar zones have sparse populations of more lightly stained cells (fig. 1B). We processed brain sections through the LGN for CO and Nissl substance in order to identify layers and relate *VGLUT1* mRNA and protein expression patterns to these layers (fig. 1). Our results were consistent with previous descriptions of CO and Nissl staining in the galago LGN.

In sections stained for *VGLUT1* mRNA, all layers of the LGN showed moderate levels of *VGLUT1* expression, while the interlaminar zones showed weaker levels of *VGLUT1* expression (figs. 1C, E). Comparisons of cell counts from Nissl and *VGLUT1* sections indicated that more than half the neurons in all layers express at least some *VGLUT1* mRNA. Neurons in the M layers most strongly expression *VGLUT1* mRNA were large in size but sparsely distributed within the layers, while neurons in the P layers positive for *VGLUT1* mRNA were smaller in size but densely packed (fig. 1E). These layers both project to layer IV of V1, which shows corresponding strong levels of VGLUT1 protein (discussed below). Neurons in the K layers positive for *VGLUT1* mRNA were smaller than both M and P cells, sparsely distributed within the layers and weakly stained overall. Cells within the interlaminar zones showed varying levels of *VGLUT1* expression, but in general, they were smaller and expressed less *VGLUT1* mRNA than cells within the K layers of the LGN. Both the K layers and relay cells in the interlaminar zones project to layers III and I of V1, which also showed weak levels of VGLUT1 protein.

In sections stained for VGLUT1 protein, dense immunoreactivity (ir) was visible in all the LGN layers and interlaminar zones (figs. 1D, F). VGLUT1 ir was largely confined to punctate terminals that seemed to surround unlabeled cell bodies (fig. 1F). The M, P, and K layers all showed strong, evenly distributed labeling of VGLUT1 terminals, indicating that retinogeniculate projections likely use VGLUT1 for glutamatergic transmission. Cell bodies positive for VGLUT1 were not found. The interlaminar zones of the LGN had somewhat stronger and denser labeling of VGLUT1 in comparison with the LGN layers, likely marking corticogeniculate terminations (Casagrande and Kaas, 1994) or, less likely, tectogeniculate projections from the upper superficial gray layer of the SC (May, 2006) to these zones.

Additionally, VGLUT1-positive terminals in the interlaminar zones seemed to be more clustered and appeared as darker puncta than those within the layers of the LGN (fig. 1F).

5.4.1.1 Figure 1. Coronal sections through the lateral geniculate nucleus stained for (A) CO, (B) Nissl, (C, E) *VGLUT1* mRNA, and (D, F) VGLUT1 protein. Scale bar is 500um for panels A-D, 250um for panels E-F. Thalamic midline is to the left.

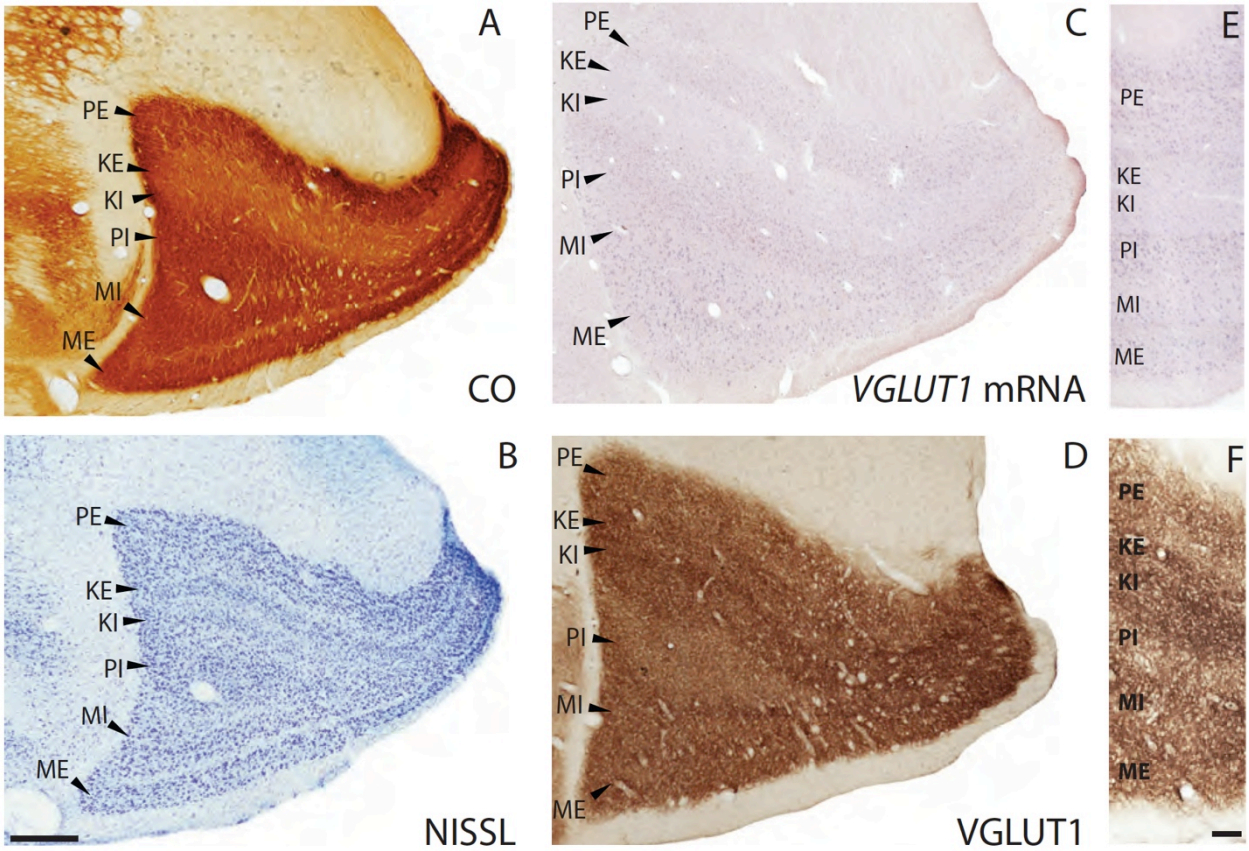

Pulvinar

The pulvinar of prosimian galagos is divided here into the three traditional divisions based on anatomic appearance and relative location, the medial, lateral, and inferior pulvinar (PM, PL, and PI, respectively) (Stepniewska, 2004). While it is almost certain that further subdivisions exist within these divisions, the anatomic identification of such partitions has

proven problematic due to the lack of markers that selectively label further subdivisions within the pulvinar complex of galagos. VGLUT1 expression in the galago pulvinar does give us some clues about its architectonic organization, but does not clearly differentiate any subdivisions within the major divisions.

All three major divisions of the pulvinar are easily identified by CO and Nissl preparations in galagos (Wong et al., 2009) (figs. 2A, B). PM is characterized by intense CO reactivity and dense populations of Nissl-stained cells, while PL is characterized by fiber tracts separating CO-rich regions with evenly dispersed Nissl populations. PI lies ventral to PM and PL, and is largely separated from PM and PL by the brachium of the SC, a large white matter tract that runs through this region of the thalamus (best seen in fig. 2D).

All three divisions of the pulvinar showed distinct distributions of positively labeled cells when stained for *VGLUT1* mRNA (figs. 2C, E-G). PM was densely populated by cells that showed moderate staining for *VGLUT1* mRNA, while PL was diffusely populated by cells that showed weak staining for *VGLUT1* mRNA. Although PM is reciprocally connected with multiple areas in frontal, temporal, and parietal cortex that are not predominantly visual (Wong et al., 2009), *VGLUT1* expression in this division indicates these projections likely use VGLUT1 for glutamatergic transmission as well. PL sends projections to V1 and V2, and weak *VGLUT1* expression here indicates that visual connections from PL to cortex may not utilize VGLUT1 to a great extent. PI showed both strong and weak labeling of *VGLUT1*-positie cells that varied in distribution across the division, likely indicating that multiple cell populations exist within this region. PI projects cortically to V1, V2, and MT, and weak VGLUT1 protein expression is seen in the recipient layers of those three areas, indicating that cell populations in PI that do project there may not rely heavily on VGLUT1.

5.4.1.2 Figure 2. Coronal sections through the pulvinar complex stained for (A) Nissl, (B), CO, (C) *VGLUT1* mRNA and (D) VGLUT1 protein. (E-J) High magnification images of subdivisions of the pulvinar complex stained for (E-G) *VGLUT1* mRNA and (H-J) VGLUT1 protein. Scale bar is 0.5mm. Thalamic midline is to the right.

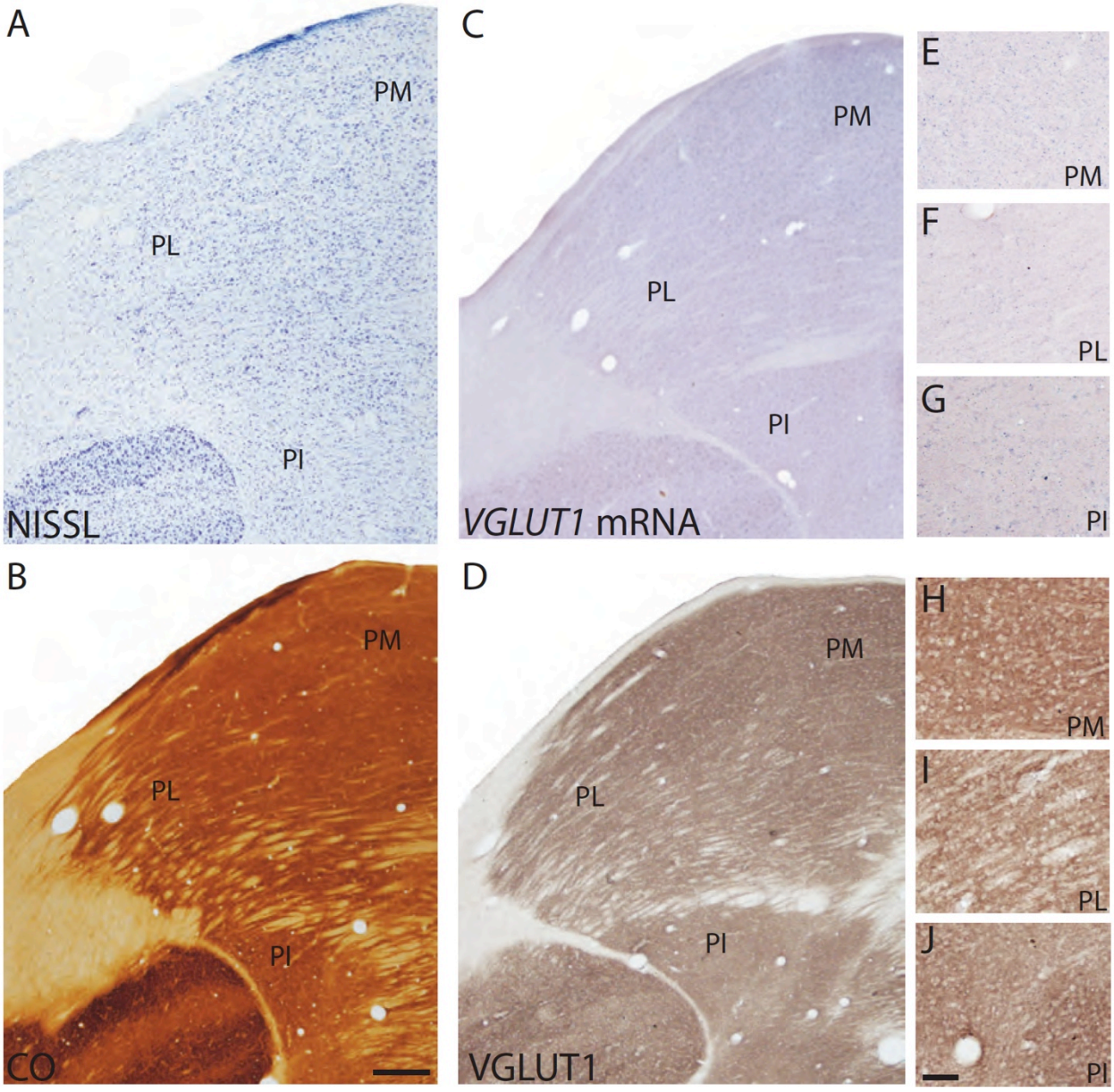

Similar distributions across the pulvinar were seen in sections stained for VGLUT1 protein (figs. 2D, H-J). PM showed dense, even labeling of VGLUT1 across the extent of the

pulvinar, while PL showed diffuse labeling of VGLUT1 that was confined to the regions around the fiber tracts and not within them. Frontal and parietal areas projecting to PM showed strong *VGLUT1* distributions, while visual connections to PL showed moderate *VGLUT1* distributions in comparison. These distributions correlated well with differential VGLUT1 ir in PM and PL, and again suggest that VGLUT1 is utilized to a lesser extent in visual projections to the pulvinar. PI showed regions of either strong or faint labeling of VGLUT1 across the nucleus, possibly reflecting subdivisions that differ in levels of glutamatergic input. PI in galagos is reciprocally connected with V1, V2, and MT in cortex (Wong et al., 2009) and receives subcortical visual input from the SC (Raczkowski and Diamond, 1978), all of which express *VGLUT1* mRNA at varying levels. These differential inputs could give rise to the varied distribution of VGLUT1 in PI.

Superior colliculus (SC)

The SC of galagos has been divided into seven layers based on histological and connectional differences (May, 2006). The superficial layers of the SC primarily process visual information, while the intermediate and deep layers regulate multisensory integration and brainstem motor functions. The laminar organization of the SC in CO and Nissl preparations in galagos (figs. 3A, B) has been characterized previously (Kaas et al., 1978; May, 2006). Low magnification images of the layers of the SC are shown in figure 3.

All layers of the SC only weakly expressed *VGLUT1* mRNA (figs. 3D, F), and comparative cell counts between Nissl and *VGLUT1* stained sections showed that *VGLUT1* was confined to a small percentage of cells in each layer. The zonal layer (SZ) showed weak expression of *VGLUT1* mRNA, with only a few stained cells scattered within the layer.

5.4.1.3 Figure 3. Coronal sections through the superior colliculus stained for (A) CO, (B) Nissl, (C, E) VGLUT1 protein, and (D,F) VGLUT1 mRNA. The stratum zonale or zonal layer (SZ) is a thin band that runs across the dorsal surface of the SC; immediately below is the stratum griseum super_ciale or super_cial gray layer (SGS) that is divided into upper and lower sublayers (uSGS and lSGS respectively); the stratum opticum or optic layer (SO) lies below the SGS and separates the super_cial layers from the intermediate layers; below the SGS lies the stratum griseum intermediale or intermediate gray layer (SGI), which is divided into three sublayers (SGIa, SGIb, and SGIc from dorsal to ventral); the stratum album intermediale or intermediate white layer (SAI) lies below the SGI and separates the intermediate layers from the deep layers; below the SAI lies the stratum griseum profundum or deep gray layer (SGP) and lastly; ventral to the SGP lies the stratum album profundum or deep white layer (SAP), which borders the periaqueductal gray. Scale bar is 0.5mm for panels A-D, 100um for panels E-F.

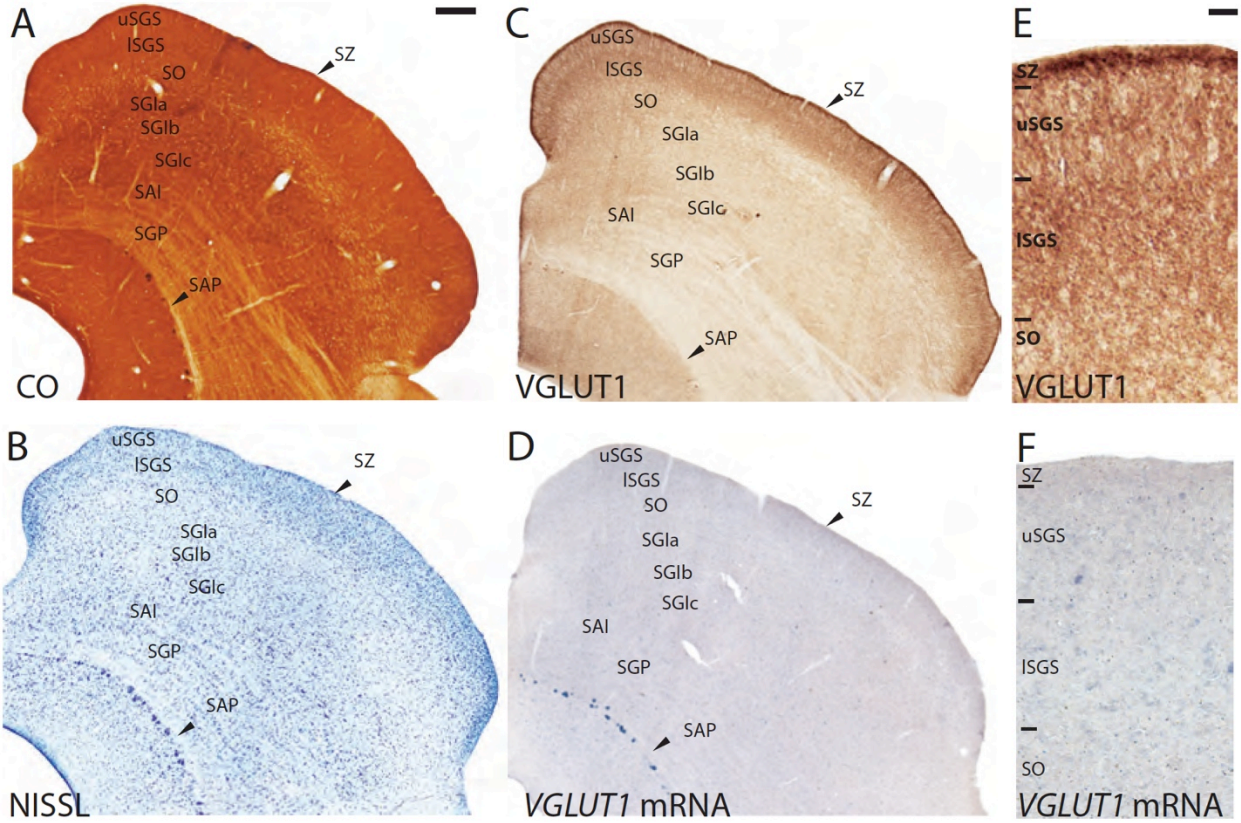

However, both layers of the superficial gray layer (SGS) showed dense distributions of small cells stained lightly for *VGLUT1* mRNA. The upper SGS (uSGS) projects to the interlaminar zones of the LGN, which showed dense labeling of VGLUT1 protein, while the lower SGS

(lSGS) projected to PI (Raczkowski and Diamond, 1978), which showed variable VGLUT1 distribution. The discrepancy in these expression patterns suggests that tectogeniculate and tectopulvinar projections likely use other glutamate transporters for glutamatergic transmission and *VGLUT1* expression in the SGS reflects intrinsic connections in this layer. The optic layer (SO) showed a sparse distribution of medium and large cells stained lightly for *VGLUT1* mRNA, also likely reflecting intrinsic connections because this layer is primarily a fiber tract through the SC. The deep layers of the SC had scattered distributions of medium and large cells stained weakly for *VGLUT1* mRNA that could represent relay projections or intrinsic connections in this multisensory area. Laminar boundaries within the SC were not readily apparent in sections stained for *VGLUT1* mRNA, but slight differences in cell size and density allowed us to differentiate the superficial layers (fig. 3F). However, the deep layers had largely homogeneous distributions of *VGLUT1*, preventing us from discerning anatomic boundaries. A few large cells along the edge of the deep white layer (SAP) stained darkly for *VGLUT1* mRNA but these cells are likely mesencephalic trigeminal neurons, and correspond to cells that stain strongly for Nissl and CO in this region. Overall, *VGLUT1* mRNA was widely distributed across the galago SC, but at weaker levels compared with expression in the LGN and pulvinar.

VGLUT1 protein was also widely distributed in the galago SC (fig. 3C, E). Overall, the superficial layers showed much stronger VGLUT1 ir than the deep layers of the colliculus. The SZ appeared as a thin, dark band of dense VGLUT1 ir across the dorsal surface of the SC. The SGS also showed strong VGLUT1 ir and could be anatomically segregated into sublayers based on VGLUT1 reactivity. The upper SGS could be subdivided into two layers of VGLUT1 reactivity; a dorsal band of moderate VGLUT1 ir followed by a thin ventral band of strong VGLUT1 ir. The lower SGS could be subdivided into three layers; a dorsal band of weaker

VGLUT1 ir, followed by a thin, middle band of strong VGLUT1 ir, and a ventral band of moderate VGLUT1 ir (figs. 3C, E). Retinotectal projections primarily terminate in the SGS and SZ (Casagrande and Kaas, 1994; May, 2006), and strong VGLUT1 ir in these layers indicate that retinal ganglion cells use VGLUT1 for glutamatergic transmission to the SC. Additionally, visual cortical inputs to the superior colliculus from layer V of V1 and MT terminate diffusely across the SGS and upper SO (Wall et al., 1982), and the strong *VGLUT1* expression seen in layer V of both those areas likely contributes to the dense VGLUT1 ir in the superficial SC. The SO below the SGS showed moderate levels of VGLUT1 reactivity, most of which was confined to areas around the white matter tracts. VGLUT1 ir in this layer could reflect inputs from association visual areas such as the medial, dorsomedial, and posterior parietal cortex projections seen in owl monkeys (Graham et al., 1979), although such connections have not yet been described in galagos. Lastly, the deep layers all showed weak, homogeneous VGLUT1 ir and could not be further differentiated based on staining intensity. Overall, visual inputs from the retina and cortex to the superficial SC use VGLUT1 for glutamatergic transmission, but this neurotransmitter is largely unused by projections in the deeper layers of the SC.

5.4.2 VGLUT1 in cortex

V1 (area 17)

V1 in galagos is easily distinguished from neighboring cortical areas by its distinct lamination, densely myelinated band of Gennari, and strong reactivity for CO and other immune markers (Wong and Kaas, 2010). In CO preparations, V1 is characterized by a dense CO band in layer IV that decreases markedly at the V1/V2 border, as well as moderate CO reactivity in layers I and VI and weak reactivity in layers III and V (figs. 4A, 5A). In Nissl preparations, V1 is characterized by dense populations of cells compared with other cortical areas, and distinct

lamination due to varying densities of cells in each layer (figs. 4B, 5B). The laminar subdivisions of V1 have been described previously (Weller and Kaas, 1982; Casagrande and Kaas, 1994) according to Nissl preparations, and are shown in figures 4 and 5.

When stained for *VGLUT1* mRNA, laminar boundaries in V1 were clearly visible due to differences in staining intensity between the layers (figs. 4C, 5C). Comparative cell counts between Nissl-stained sections and *VGLUT1*-stained sections indicated that most of the cells in V1 expressed some level of *VGLUT1* mRNA. Layer I lacked *VGLUT1*-positive cells and appeared as an unstained band across the surface of V1, consistent with its primary role as a recipient layer of pulvinar projections and feedback connections from other cortical areas (Weller and Kaas, 1982). Layer II appeared as a thin, dense band of medium and small cells that stained strongly for *VGLUT1* mRNA, which are likely projections to other layers in V1 and match the diffuse VGLUT1 ir across all the layers of V1. Layer III showed decreasing *VGLUT1* expression from dorsal to ventral sublayers; layer IIIa consisted of medium and large cells that showed strong *VGLUT1* expression, layer IIIb consisted of medium and small cells with moderate *VGLUT1* expression, and layer IIIc consisted of mostly small cells with weaker *VGLUT1* expression. Since layer III of V1 projects to MT and V2, varied *VGLUT1* expression in this layer likely contributes to the differential levels of VGLUT1 ir seen in those areas. Layer IV showed a minor distribution of small cells that stained weakly for *VGLUT1* mRNA scattered across the layer, consistent with its function as the primary recipient layer of thalamocortical projections. However, layer V showed significant *VGLUT1* expression and could be divided into upper and lower layers, defined as Va and Vb respectively. Layer Va consisted of a dense distribution of large cells that stained strongly for *VGLUT1* mRNA, while layer Vb was composed of small cells that stained moderately for *VGLUT1* mRNA. Known projections of

layer V in galagos include PL, PI, and the SGS of the SC, and all three areas showed varied VGLUT1 ir. Lastly, layer VI could also be subdivided into upper and lower layers based on staining intensity, termed Via and VIb, respectively. Layer Via primarily consistent of large cells stained strongly for *VGLUT1* mRNA while layer VIb was composed of medium cells and small cells with more moderate *VGLUT1* expression. Layer VI in galagos projects to the layers and interlaminar zones of the LGN, and *VGLUT1* expression here correlates well with the strong VGLUT1 ir in the LGN.

The distribution of VGLUT1 protein in cortex was robust across all areas, including V1 (figs. 4D, 5D). Although laminar organization in V1 was less visible in sections stained for VGLUT1, slight differences in reactivity between the layers were still evident. Layer I showed stronger VGLUT1 ir than the rest of the layers, and thus could be distinguished as a thin, dark band across the surface of V1. Because most feedback connections to V1 terminate in layer 1, strong VGLUT1 reactivity indicates that these projections heavily utilize VGLUT1 for glutamatergic transmission. Layers II, III, and V showed less staining for VGLUT1 and appeared as lighter bands through this region. Layer II does not receive dense projections from cortical or subcortical areas, layer III receives input from the K layers of the LGN, and layer V receives input from the pulvinar and V2. Weak VGLUT1 ir in these layers correlates with the weak *VGLUT1* expression seen in those areas. Layer IV appeared as a dark band of VGLUT1 ir that terminated at the V1/V2 border, similar to the layer IV band in CO sections and consistent with the *VGLUT1* expression in the LGN layers that project here. Layer VI, which receives some input from the LGN and MT, also showed stronger VGLUT1 ir than layers II, III and V and appeared as a thin, dark band along the internal edge of V1.

5.4.2.1 Figure 4. Low magnification images of coronal sections through V1 and V2. Dorsal surface of cortex is up, ventral surface is down, hemispheric midline is to the left. Scale bar is 2mm.

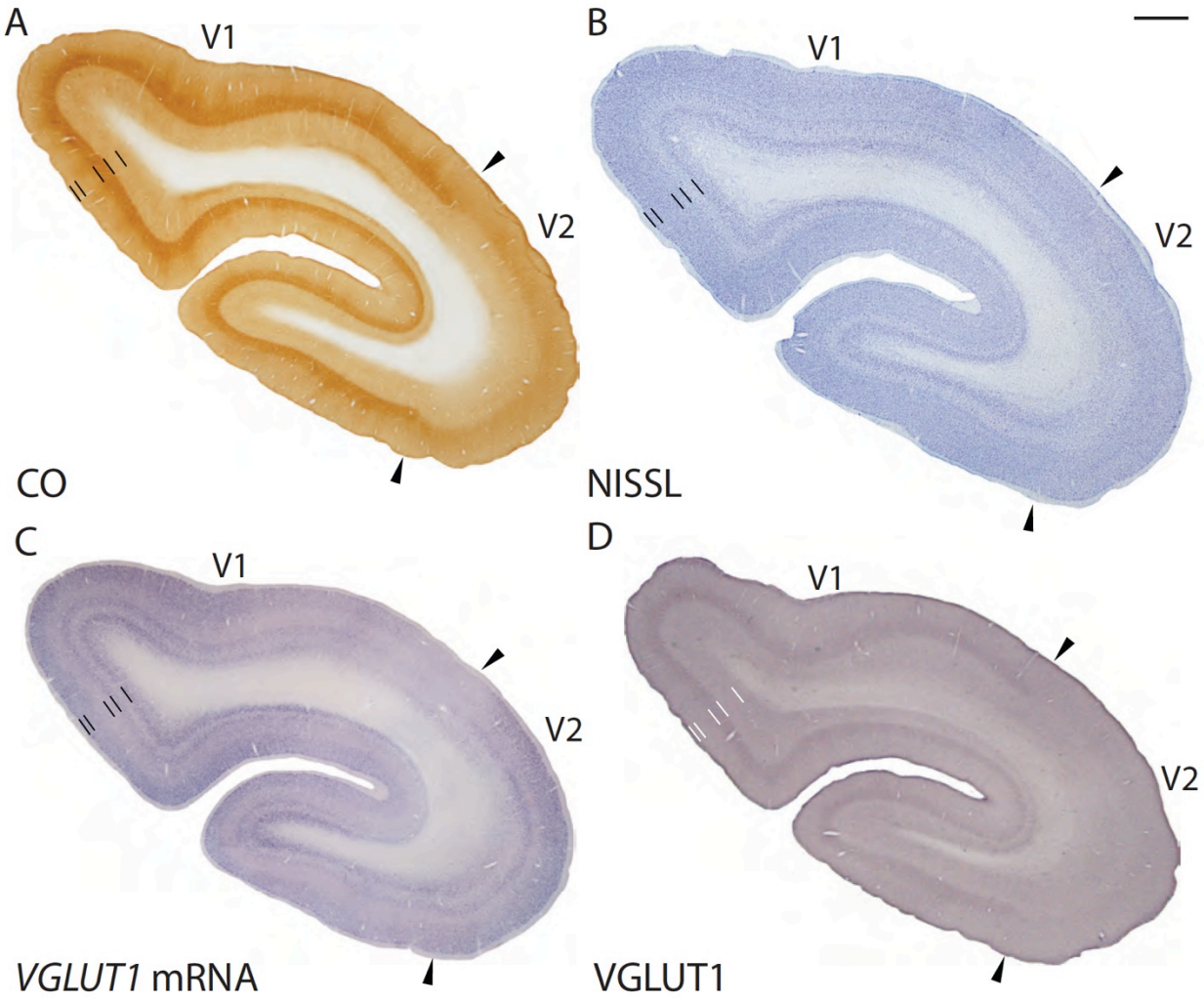

5.4.2.2 Figure 5. High magnification images of the laminar organization of V1 (Area 17). Scale bar is 250um.

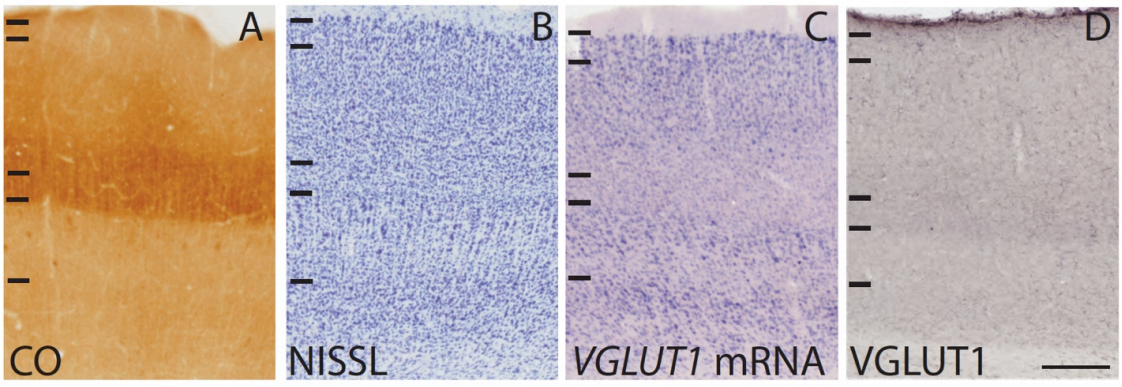

V2 (area 18)

V2 in galagos forms a long band along the length of the V1 border and extends about 3mm across the cortical surface rostral to V1 (Rosa et al., 1997). V2 is anatomically identified by its moderate level of myelination in comparison with V1. V2 is anatomically identified by its moderate level of myelination in comparison with V1. The CO stripes that characterize V2 of anthropoid primates are only weakly expressed in V2 of galagos (Lyon and Kaas, 2002). In coronal sections stained for CO, V2 showed moderate staining in lower parts of layer IIIc and upper parts of layer IV, but showed weak staining in the other layers (figs. 4A, 6A). In Nissl preparations, layer IV showed a denser cell distribution than the other layers (Wong and Kaas, 2010) and layers I-IV showed stronger Nissl reactivity while layers V and VI showed weaker Nissl reactivity (figs. 4B, 5B). Overall, the laminar organization of V2 was less well defined than that of V1, but slight differences in CO and Nissl reactivity allowed us to define laminar boundaries across the area.

5.4.2.3 Figure 6. High magnification images of the laminar organization of V2. Scale bar is 250um.

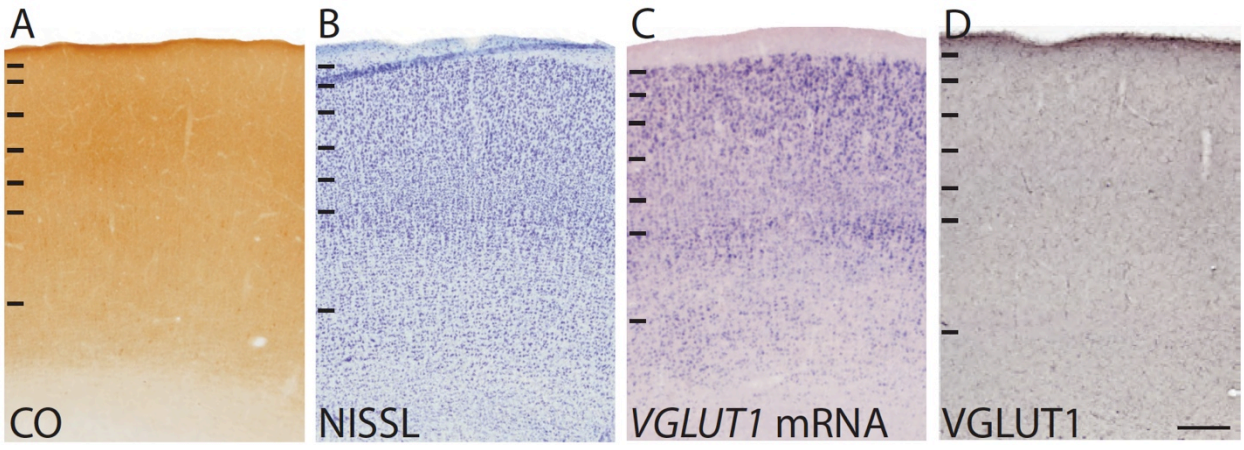

When stained for *VGLUT1* mRNA, V2 showed generally weaker levels of expression compared with V1. However, comparative cell counts between Nissl and *VGLUT1* stained sections still indicated that the majority of cells in V2 expressed some level of *VGLUT1* mRNA. Additionally, the laminar organization of V2 was far more evident in sections stained for *VGLUT1* mRNA than comparative CO and Nissl sections (fig. 6C). Layer I lacked *VGLUT1* expression entirely, while layer II showed an even distribution of medium and small cells that stained moderately for *VGLUT1* mRNA. Layer III showed differential *VGLUT1* expression in each sublayer. Layers IIIa and IIIc consisted of variably sized cells with weaker *VGLUT1* expression, while layer IIIb consisted of medium and small cells with slightly stronger *VGLUT1* expression. Layer IV showed a sparse distribution of small cells that stained weakly for *VGLUT1* mRNA. Layer V showed a dense distribution of medium and small cells that stained strongly for *VGLUT1* mRNA, although this is less apparent in figure 6. Finally, layer VI could be divided into two sublayers based on *VGLUT1* expression. The dorsal layer, VIa, consisted of scattered distributions of small cells that stained moderately for *VGLUT1* mRNA while the ventral layer, VIb, showed a dense distribution of medium cells with strong *VGLUT1* expression. Overall, the weak *VGLUT1* expression seen in layers I and IV correlates with their role as recipient layers of thalamocortical projections from the pulvinar and cortical projections from V1 and MT (Weller and Kaas, 1982). Similarly, the varied *VGLUT1* expression seen in layers II, III, V, and VI reflects the diverse projections of V2 to the pulvinar, V1, and MT, and correlates with VGLUT1 ir seen in these terminations.

VGLUT1 ir in V2 was strong but diffusely spread across the layers, and laminar patterns were less evident than those of V1 (fig. 6D). Layer I appeared as a thin, dark band across the surface of V2, fitting with its role as a recipient layer of pulvinar and MT projection. Layers IV

and VI also showed slightly stronger VGLUT1 ir, which likely arises from afferent projections from the pulvinar and higher order visual areas, such as V3 (Lyon and Kaas, 2002). Layers II, III, and V showed weaker VGLUT1 ir and appeared as lighter bands in between layers I, IV, and VI. In galagos, layers II and III only receive diffuse projections from MT, and layer V does not receive extrinsic visual input (Weller and Kaas, 1982), so weak VGLUT1 ir here accurately reflects the afferent projections that terminate in these layers of V2.

Middle temporal area (MT)

MT in galagos lies on the cortical surface just above the caudal end of the lateral sulcus, and occupies an oval-shaped region about 18mm^2 on the temporal lobe (Wall et al., 1982). MT is characterized by strong myelination, high CO reactivity in layers III and IV, weak CO reactivity in the other layers (figs. 7A, 8A), and a large, diffuse band of small cells across layer IV in Nissl preparations (figs. 7B, 8B). When stained for *VGLUT1* mRNA and compared with Nissl sections, almost all of the cells in MT showed robust expression of *VGLUT1* mRNA, but a distinct laminar pattern was still evident in this region (figs. 7C, 8C). Layer I did not show any *VGLUT1* expression. Layer II appeared as a thin, dense band of small cells with weak *VGLUT1* expression. Layers IIIa and IIIb showed even distributions of medium and large cells with moderate *VGLUT1* expression, while layer IIIc showed a denser distribution of medium and small cells with stronger *VGLUT1* expression. Layer IV showed a sparse distribution of small cells that stained weakly for *VGLUT1* mRNA. However, layer V could be split into two sublayers based on VGLUT1 expression; the dorsal sublayer, Va, showed a dense population of medium and large cells that stained strongly for *VGLUT1* mRNA while the ventral sublayer, Vb, showed a more diffuse population of medium and large cells that stained weakly for *VGLUT1* mRNA. Layer VI of MT appeared much thicker than layer VI of V1 and V2, consistent with its

appearance in CO and Nissl sections, and could be divided into sublayers based on *VGLUT1* expression. The dorsal third of layer VI showed a sparse distribution of medium cells with weaker *VGLUT1* expression, although a number of individual cells stained strongly for *VGLUT1* mRNA. The middle third of layer VI showed a dense distribution of medium and large cells that stained strongly for *VGLUT1* mRNA, and the ventral third of layer VI consisted of an even distribution of medium cells stained moderately for *VGLUT1* mRNA. Known projections of MT in galagos consist of efferent connections from layer III to PI, layer Vb to V2, and layer Via to V1, PL, and PI (Wall et al., 1982). *VGLUT1* expression in the projecting layers of MT reflects the VGLUT1 ir seen in these areas and confirms that VGLUT1 is widely utilized in transmitting visual information between cortical and subcortical areas.

When stained for VGLUT1 protein, MT again showed weaker reactivity compared with adjacent areas of cortex, making laminar divisions less apparent, but each layer had slight differences in reactivity (figs. 7D, 8D). Layer I appeared as a thin, dark band of strong VGLUT1 ir, while layer II appeared as a wider band of moderate VGLUT1 ir. Layer III showed a fairly homogeneous distribution of moderate VGLUT1 ir across all sublayers, only the lower half of layer IIIc had slightly weaker reactivity than the rest of layer III. Layer IV showed weak VGLUT1 ir and appeared as a lighter band between layers III and V Layer V showed a thin band of slightly stronger VGLUT1 ir in the ventral two thirds of the layer. Similarly, layer VI showed slightly stronger VGLUT1 ir in the dorsal half and weaker VGLUT1 ir in the ventral half of the layer. In galagos, known projections to MT from the pulvinar, V1, and V2, all terminate in layer IV (Weller and Kaas, 1982) and the weak VGLUT1 ir seen here reflects the weak *VGLUT1* expression seen in the projecting divisions of those areas. However, the strong VGLUT1 ir seen in layers I, II, and V likely reflects connections from higher order visual areas (Lyon and Kaas,

2002) and indicates that VGLUT1 is more utilized in higher order visual projections to MT and less utilized in primary visual input from the thalamus, V1, and V2.

5.5 Discussion

The primary aims of the present study were to characterize the distribution of VGLUT1 mRNA and protein across the visual system of galagos, identify novel anatomic features of visual structures revealed by VGLUT1 distributions, and compare VGLUT1 distributions in galagos with known VGLUT1 distributions in rodents. We find that VGLUT1 mRNA and protein expression varied distinctly between visual subcortical and cortical areas (table 2), but their expression patterns are largely consistent with the known projections between and within these regions (shown in figs. 9 and 10). *VGLUT1* mRNA expression revealed novel laminar characteristics of V1, V2, and MT, while VGLUT1 protein expression identified subdivisions within the superficial layers of the SC. Finally, we find that, contrary to most rodent studies of VGLUT1 distributions, VGLUT1 is widely expressed in both subcortical and cortical areas, and may be involved in subcortical and thalamocortical projections as well as intercortical and corticothalamic circuits.

Lateral geniculate nucleus (LGN)

The LGN is a central structure in the visual system of galagos because it is a primary recipient of visual input from the retina as well as the primary relay of visual information to cortex (Casagrande and DeBruyn, 1982; Weller and Kaas, 1982). Retinal input to the LGN layers is topographically organized and segregated; the external layers receive contralateral retinal input while the internal layers receive ipsilateral retinal input. When relaying information to cortex, the M layers project to layer IVa of V1 while the P layers project to layer IVb.

5.5.1.1 Figure 7. Low magnification images of coronal sections through the middle temporal area (MT). Scale bar is 1mm.

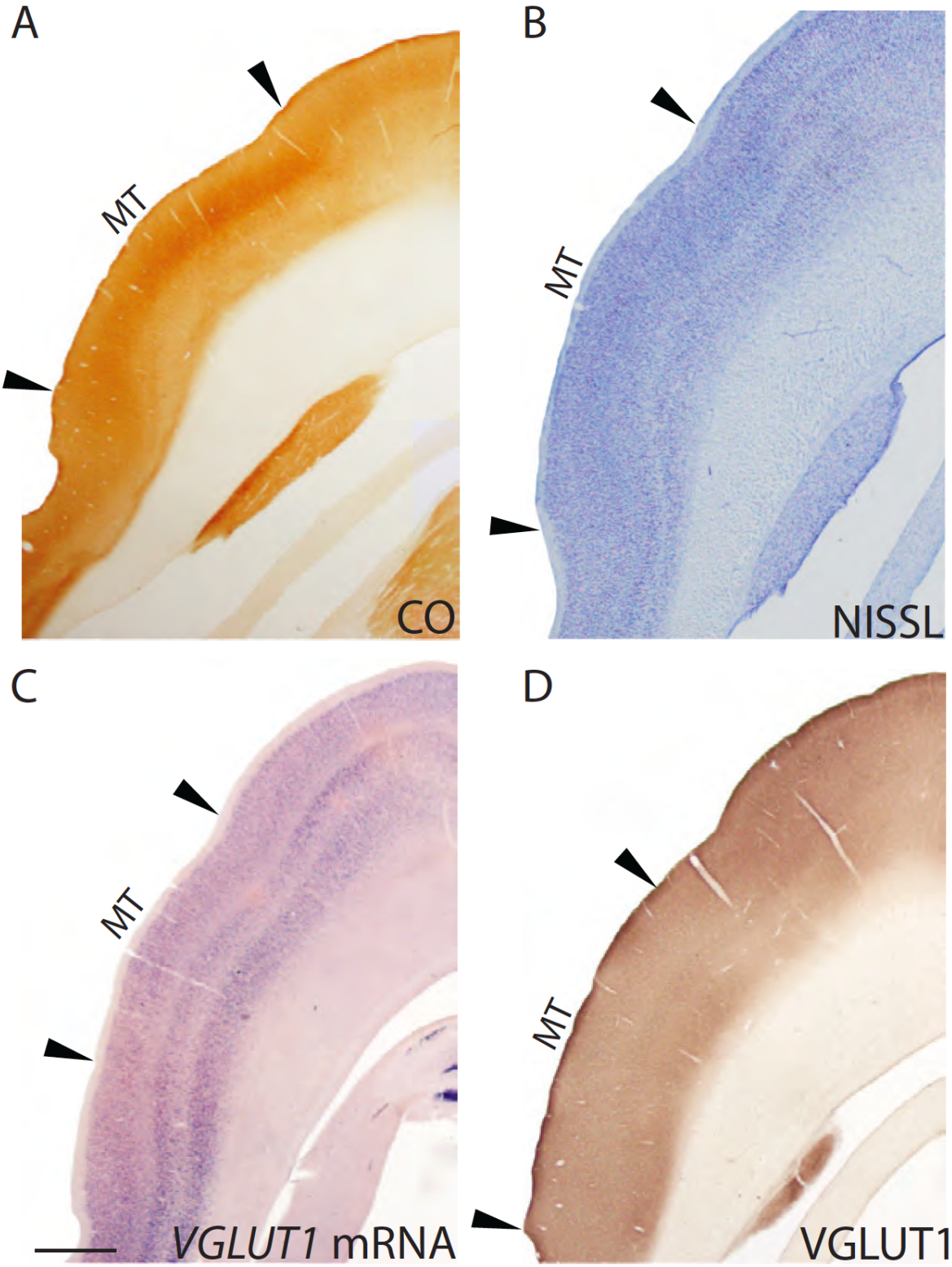

5.5.1.2 Figure 8. High magnification images of the laminar organization of MT. Scale bar is 250um.

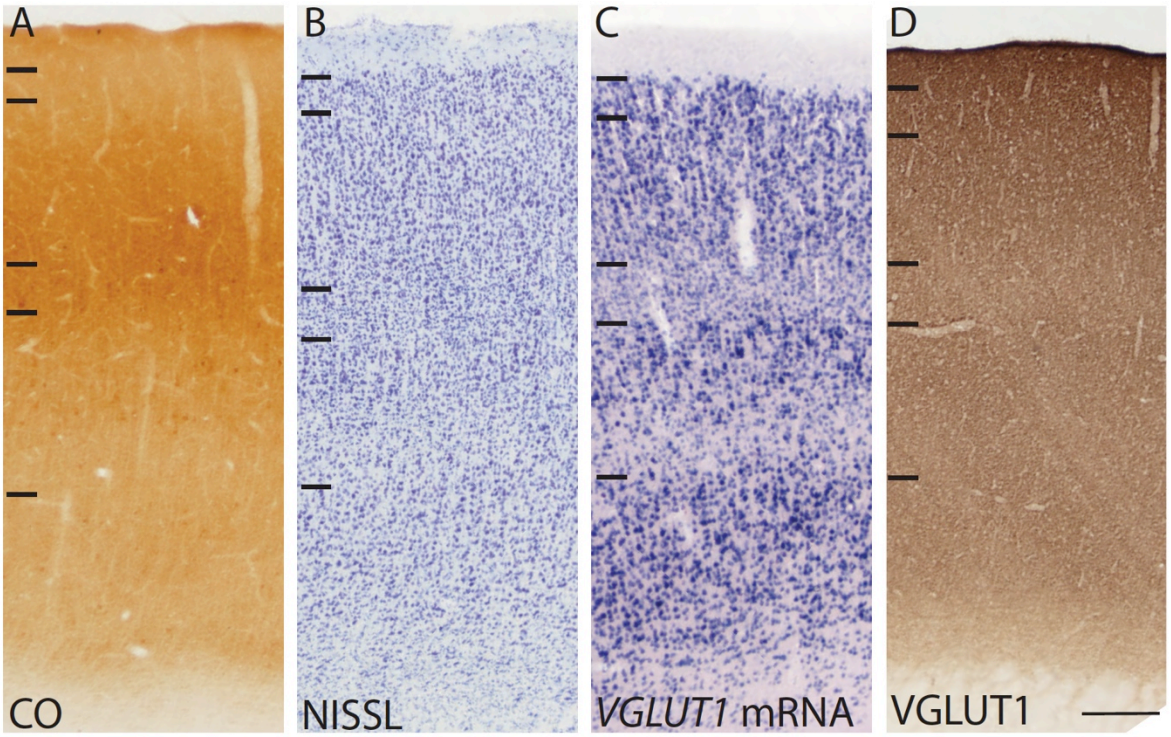

5.5.2 VGLUT1 distributions in the visual system of galagos

The K layers, as well as some cells in the interlaminar zones, project to all sublayers of layer III (centered on IIIb) and parts of layer I. Both the K layers and the interlaminar zones receive projections from the superficial gray layer of the SC (Raczkowski and Diamond, 1978), and all LGN layers and interlaminar zones receive feedback projections from layer IVa of V1 (Weller and Kaas, 1982; Casagrande and Kaas, 1994). Overall, VGLUT1 mRNA and protein distributions in the LGN correlate well with the known afferent and efferent projections of this nucleus. Previous work has shown that VGLUT2, another isoform in the VGLUT family, is strongly utilized in retinogeniculate and geniculocortical projections in galagos as well (Balaram et al., 2011b). Thus, both VGLUT1 and VGLUT2 appear to be involved in this circuit and likely

regulate different modes of glutamatergic transmission within these projections (Herzog et al., 2001; Fremeau et al., 2004b; Santos et al., 2009).

The galago pulvinar is a complex nucleus that is densely connected with a number of visual and nonvisual areas (Stepniewska, 2004) (fig. 9B). PM is reciprocally connected with multiple areas in fontal and parietal cortex that are not predominantly visual, so it is not examined in great detail in this discussion. PL and PI receive projections from layer Vb of V1 and send projections to layer I of V1, as well as layers III and IV of V2. PI sends an additional projection to layers III and IV of MT (Weller and Kaas, 1982; Wong et al., 2009). Subcortical connections of the pulvinar complex include projections from the parabigeminal nucleus to Pl (Diamond et al., 1992) and projections from the lower SGS of the SC to PI (Glendenning et al., 1975).

Moderate *VGLUT1* expression in afferent projections from V1, the SC, and the parabigeminal nucleus (not shown) to PL and PI confirm that VGLUT1 is utilized to a lesser extent in these subcortical and corticothalamic visual projections. Efferent projections with weak *VGLUT1* expression from PL and PI to V1, V2, and MT also illustrate the same finding. The faint *VGLUT1* expression in PL and PI could simply reflect intrinsic connections within these divisions, as opposed to projections outside of the pulvinar complex. Previous studies of VGLUT2 in the pulvinar of galagos showed that *VGLUT2* mRNA is strongly expressed in PL and PM, and correlates with strong VGLUT2 ir in the corresponding projection layers of cortex (Balaram et al., 2011b), suggesting that PL and PI preferentially use VGLUT2 over VGLUT1 in efferent projections to cortex. Tectopulvinar projections from the SC to PI have previously been shown to utilize VGLUT2 as well (Balaram et al., 2011b), suggesting that afferent subcortical projections to the pulvinar also use VGLUT1 to a limited extent.

5.5.2.1 Figure 9. Cortical and subcortical visual connections of the (A) lateral geniculate nucleus, (B) pulvinar complex, and (C) superior colliculus. Shading intensity reflects levels of expression for both VGLUT1 mRNA and protein. Summarized from the literature (16, 17, 30-31, 34-36, 41-43). Abbreviations: PI – inferior pulvinar, PL – lateral pulvinar, PM – medial pulvinar, MT – middle temporal area, LGN – lateral geniculate nucleus, lSGS – lower superficial gray layer, uSGS – upper superficial gray layer, C retina – contralateral retina, I retina – ipsilateral retina.

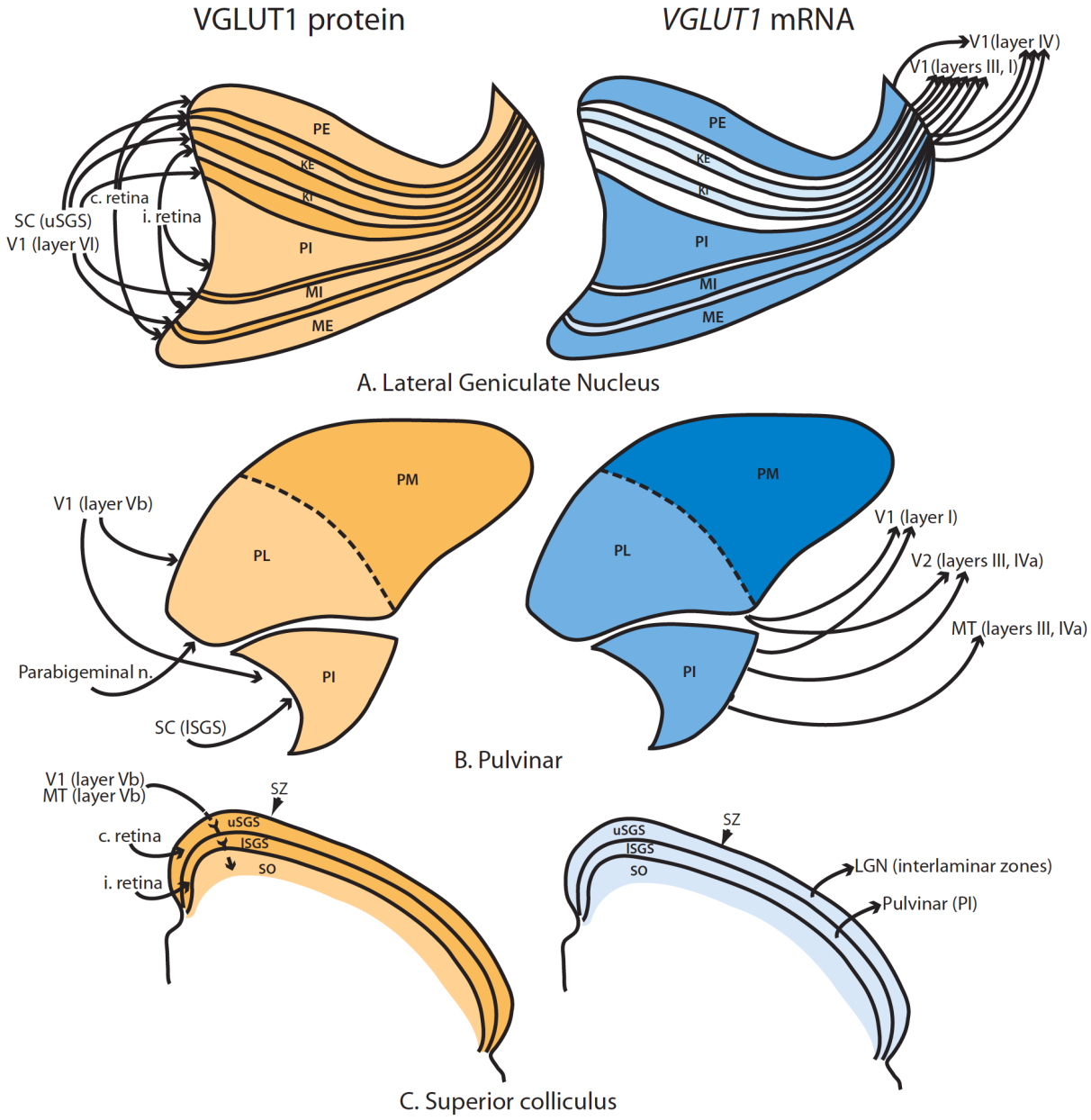

Pulvinar

In contrast with the lateral and inferior divisions, the strong *VGLUT1* expression and VGLUT1 ir seen in PM reflects its dense interconnectivity with frontal and parietal cortical areas, and suggests that VGLUT1 is preferentially used in circuits that process higher order information, as opposed to circuits that relay sensory input. However, examination of similar corticothalamic circuits in association areas would be necessary to justify this conclusion. Overall, PL and PI in galagos do not rely on VGLUT1 for thalamocortical or corticothalamic projections, while PM relies heavily on VGLUT1 for both thalamocortical and corticothalamic projections.

Superior colliculus

The SC in galagos is an intricate multisensory structure that integrates multiple modes of sensory input to influence motor behavior (May, 2006). Visual processing in the SC is largely restricted to the superficial layers (fig. 9C). The upper superficial gray receives contralateral retinal input while the lower superficial gray receives ipsilateral retinal input. The upper superficial gray then sends projections to the K layers and interlaminar zones of the LGN while the lower superficial gray sends projections to the inferior pulvinar. Feedback connections to the superior colliculus in galagos have not been studied in great detail, but previous work has shown that layer Vb of V1 and MT both project to the SGS and upper SO (Wall et al., 1982; Casagrande and Kaas, 1994). Studies in squirrel monkeys and owl monkeys (Graham et al., 1979) showed that V2, as well as the medial, dorsomedial, and posterior parietal visual areas, as project to the SC and terminate primarily in the SGS and SO, thus it is possible that galagos have similar feedback connections as well. Overall, we find that VGLUT1 in the SC is primarily confined to afferent cortical projections to the SC and less utilized in efferent projections from the SC to the pulvinar and LGN. Previous work in galagos showed that VGLUT2 is

predominantly used in tectogeniculate and tectopulvinar projections (Balaram et al., 2011b), which accounts for the weak expression of *VGLUT1* in the efferent visual connections of the SC.

The banded pattern of VGLUT1 ir seen in the superficial layers of the SC is a novel finding in galagos and could reflect differential inputs to the colliculus from retinal and cortical projections. The wide dorsal band of moderate VGLUT1 ir in the upper SGS likely reflects retinotectal projections from the contralateral retina, while the dorsal band of weaker VGLUT1 ir in the lower SGS likely reflects retinotectal projections from the ipsilateral retina. This is consistent with previous studies that show strong contralateral retinal projections to the upper SGS and more diffuse retinal projections to the lower SGS in galagos (Weller and Kaas, 1982). The wide ventral band of moderate VGLUT1 ir in the lower SGS likely arises from diffuse corticotectal projections that terminate across the SGS and SO. The thin, dark bands of VGLUT1 ir in the upper and lower superficial gray could reflect concentrations of corticotectal terminations or, less likely, retinotectal terminations in these layers; their relative depth from the surface of the SC places them closer to the average depth of corticotectal terminations from V1 and MT (Weller and Kaas, 1982). In owl monkeys, V1 projections to the SC terminate more dorsally in the SGS while MT projections terminate more ventrally (Graham et al., 1979). If similar patterns of terminations exist in galagos, the dorsal band of concentrated VGLUT1 ir could arise from strong *VGLUT1* expression in layer V of V1 while the ventral band of VGLUT1 ir could arise from similarly strong *VGLUT1* expression in layer V of MT. Alternatively, the banded pattern seen in VGLUT1 sections may reveal the presence of a third sublayer between the retinotectal projections in galagos, although a third superficial gray layer has not been described in other species.

V1 (Area 17)

V1 in galagos is a large area, approximately 200m^2, which occupies the caudal half of the occipital lobe (Rosa et al., 1997). It is the primary recipient of visual information from subcortical structures, and has a distinct pattern of lamination that corresponds to its afferent and efferent projections (figure 10). Thalamic inputs to V1 originate in the pulvinar and LGN; PL and PI both project to layer 1 of V1 (Casagrande and Kaas, 1994). From the LGN, the M layers project primarily to layer IVa of V1 with some collateral projections to the lower half of layer VI. The P layers project primarily to layer IVb with collateral projections to the upper half of layer V1, and the K layers project to the blob compartments in layer III with collateral projections to layer I (Casagrande and Kaas, 1994). V1 sends feedback projections to a number of subcortical regions in the thalamus, midbrain, and pons. Cells in the lower half of layer V in V1 project to the lower SGS and upper SO in the superior colliculus, as well as PL and PI. Cells in the upper half of layer Vi of V1 project primarily to the interlaminar zones of the LGN, and secondarily to the LGN layers themselves (Casagrande and Kaas, 1994; Rockland, 1994).

The major cortical projections of V1 in galagos are to V2 and MT. V1 projections to these areas arise through two major pathways (Casagrande and Kaas, 1994). First, neurons in layer IIIc of V1 project to layer IV of MT and to layer IV of V2. Second, neurons in the blob and interblob compartments of layer IIIa in V1 project differentially to compartments in layer IV of V2 that are likely homologous to the bands of V2 seen in other primate species. Feedback connections to V1 from V2 and MT terminate primarily in layer I with collateral projections to layers II, IVb, V, and VI. From V2, neurons originating in layer VI and (less significantly) layer IIIa terminate primarily in layer I, and secondarily in layer IIIa and Va.

5.5.2.2 Figure 10. Visual connections of V1, V2, and MT in prosimian galagos. Shading intensity reflects levels of expression for both VGLUT1 mRNA and protein. Brodmann's divisions listed in gray on the right side of each layer for V1. Summarized from the literature (16, 18-20, 22, 23, 25-34, 36, 37, 40-43.

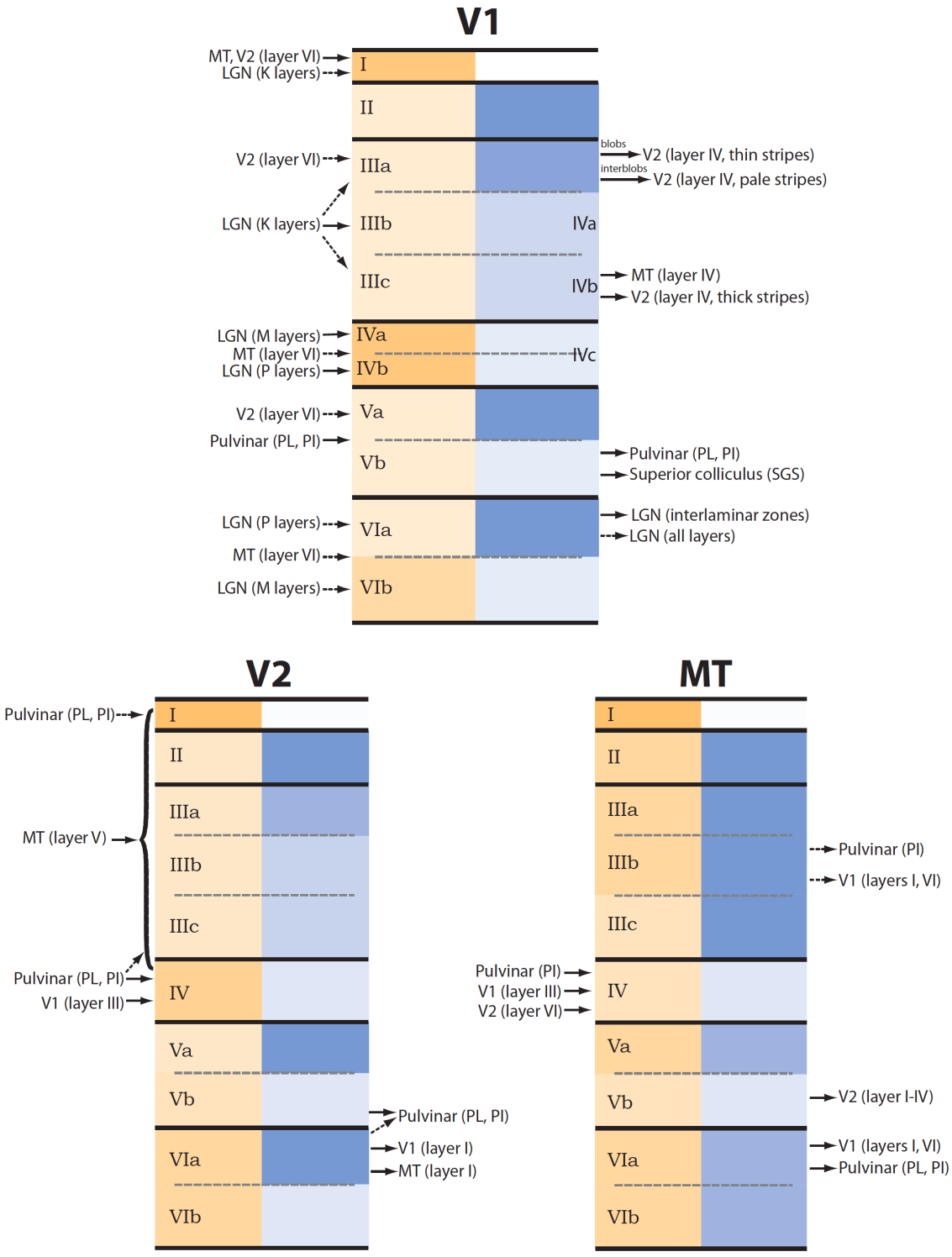

Similarly, neurons originating in layer VI and IIIa of MT terminate in layer I of V1 with collateral projections to layer IVb and V1 (Rockland, 1994). Patterns of VGLUT1 mRNA and protein expression in V1 correlate well with their known connections and complement previous studies of VGLUT2 distributions in V1 as well (16). Overall, VGLUT1 expression in the afferent and efferent projections of V1 indicates that this transport protein is heavily utilized in glutamatergic transmission of visual information.

The subdivision of layer V in V1 is a novel finding in galagos and has only been previously identified anatomically in tarsiers (38) and macaques (39). However, connectional studies in galagos have identified separate projections from upper and lower halves of layer V to other layers in V1 (40), and similar studies in macaques have identified separate divisions of layer V as well. In macaques, the upper half of layer V is defined as Va and the lower half is defined as Vb; layer Va primarily consists of interneurons that project to other layers in V1 while layer Vb consists of relay cells that project outside of V1 (39). Thus, differential levels of *VGLUT1* expression in layers Va and Vb of galagos could be an anatomic marker of the different projections that arise from these two divisions, and likely separates intrinsic and extrinsic connections of V1. Because connectional differences appear in both the strepsirrhine and haplorrhine suborders of primates, it is likely that these two sublayers of layer V are a common trait in primates that arose from a common ancestor. IT is expected that future studies on VGLUT1 expression in the other primates will identify similar divisions in layer V as well.

V2 (Area 18)

V2 in galagos shares many anatomic and connectional traits with V2 in simian primates, and appears to serve a similar functional role (31, 32, 41). V2 receives subcortical projections from PL and PI, which terminate primarily in layer IV and, to a lesser extent, in layer I (42) (Figure

10). V2 also projects back to both PL and PI, and efferent connections to both divisions arise from layers V and VI. In cortex, V2 is densely connected with V1 and MT, and also has reciprocal connections with other parts of visual cortex, such as the medial, dorsomedial, dorsolateral, and ventral posterior parietal areas (41). While the laminar organization of V2 connections has not been studied extensively in galagos, previous studies show that projections from V1 to V2 terminate primarily in layer IV (33), while MT projections to V2 are spread across layers I-IV (28). In return, layer VI of V2 projects back to layer I of V1 and MT (28, 30). VGLUT1 distributions in V2 appear consistent with the afferent and efferent projections of this area and indicate that VGLUT1 is well utilized in higher order processing of visual information. A similar subdivision of layer V into Va and Vb based on *VGLUT1* expression is apparent in V2. This division has not been noted in anatomic or functional studies of V2 in other primates but this is more likely due to the paucity of research on the laminar organization of V2 rather than the existence of a novel subdivision in galagos alone. Given the conclusions on layer V of V1, it is likely that subdivisions of layer V in V2 also reflect differential projections of layer V to intrinsic and extrinsic areas, as well as differential levels of glutamatergic transmission. Hopefully, further studies of *VGLUT1* expression in the visual system of primate species will identify similar subdivisions in other primates.

Middle temporal area (MT)

MT is a common visual area in all primate species (43), and is involved in the processing of motion information in visual stimuli. In galagos, MT receives subcortical projections from PI (26), which terminate primarily in layer III with some collaterals to layer IV, and send subcortical feedback to PL and PI, which likely arises in layer VI (29). Cortically, layer IV of

MT also receives dense projections from layer III of V1 and, based on studies in other primates (44), likely receives projections from layer III of V2. Feedback connections from MT to V1 arise primarily in layer VI and secondarily in layer III, and terminate in layers I and VI of V1 (28, 45). Similar connections from MT to V2 arise in layer V of MT and terminate diffusely across layers I-IV of V2 (28). Overall, VGLUT1 mRNA and protein expression in MT reflects these known projections to and from this area. Further laminar-specific connections of MT in galagos are unknown (30), but based on the diversity of VGLUT1 mRNA and protein expression patterns in this area, it is certain that laminar subdivisions identified by these techniques reveal additional afferent and efferent projections in MT, as well as differential levels of glutamatergic transmission in this area. Further anatomic and connectional studies will aid in understanding the exact nature of these projections.

5.5.3 Comparisons with rodents

Previous studies of VGLUT1 expression in the visual system of rodents have noted that *VGLUT1* mRNA is expressed at low levels in the dorsal LGN, and the lateral posterior complex (the rodent equivalent of the pulvinar complex), and not expressed in the SC (9, 11, 46). In the cortex, *VGLUT1* mRNA is strongly expressed in all areas. VGLUT1 protein is similarly strongly expressed across the cortex, but moderately expressed in the lateral posterior nucleus and weakly expressed in the SC and LGN. Following these patterns, it appears that VGLUT1 is primarily utilized in corticothalamic projections and intrinsic connections in the cortex. Our results showed that *VGLUT1* mRNA is moderately expressed in all visual subcortical nuclei, indicating that VGLUT1 is utilized to a greater extent in the subcortical projections of primates than those of rodents. Correspondingly, VGLUT1 immunoreactivity was also strong in the subcortical visual nuclei, indicating that efferent projections to these areas in primates also utilize VGLUT1 to a

greater extent than similar projections in rodents. While VGLUT1 expression does still appear to be employed more in intercortical and corticothalamic projections than subcortical or thalamocortical projections in galagos, which is consistent with rodent studies, the greater overall expression of VGLUT1 in the visual subcortical nuclei of galagos suggests a more widespread use of VGLUT1 for glutamatergic transmission in primates. While the significance of increased VGLUT1 expression in primates is still unclear, further studies on the comparative distributions of VGLUT1 and VGLUT2 may provide insight on the differential use of glutamate by these two transporters in excitatory transmission.

Acknowledgements

We thank Laura Trice for assistance with tissue processing and histology, Dr. Toru Takahata and the Yamamori laboratory (National Institute for Basic Biology, Japan) for supplying the VGLUT1 probe, Brett Begley and the Conti Core for assistance with Western blots, Dr. Lisa de la Mothe for assistance with image processing, and Mary Feurtado for assistance in animal care.

CHAPTER 6

Distributions of vesicular glutamate transporters 1 and 2 in the visual system of tree shrews *(Tupaia belangeri)*

The following chapter is submitted for publication in the Journal of Comparative Neurology by Pooja Balaram, Mir Isaamullah, Heywood Petry, Martha Bickford, Jon Kaas; September 2014.

6.1 Abstract

Vesicular glutamate transporter (VGLUT) proteins regulate the storage and release of glutamate from synapses of excitatory neurons. Two isoforms, VGLUT1 and VGLUT2, are found in most glutamatergic projections across the mammalian visual system. In general, VGLUT1 and VGLUT2 identify distinct modulatory and driving projections respectively (Sherman and Guillery, 1996). To expand current knowledge on the distribution of VGLUT isoforms in highly visual mammals, we examined the mRNA and protein expression patterns of VGLUT1 and VGLUT2 in the lateral geniculate nucleus (LGN), superior colliculus, pulvinar complex, and primary visual cortex (V1) in tree shrews (*Tupaia belangeri*), which are closely related to primates but classified as a separate order (Scandentia). We found that VGLUT1 was distributed in intrinsic and corticothalamic connections, which exhibit mostly modulatory features, whereas VGLUT2 was predominantly distributed in subcortical and thalamocortical connections, most of which exhibit features of driving glutamatergic projections. VGLUT1 and VGLUT2 were coexpressed in the LGN and in the pulvinar complex, as well as in restricted layers of V1, suggesting a greater heterogeneity in the range of efferent glutamatergic projections

from these structures. These findings provide further evidence that VGLUT1 and VGLUT2 identify distinct populations of excitatory neurons in visual brain structures across mammals. Observed variations in individual projections may highlight the evolution of these connections through the mammalian lineage.

6.2 Introduction

Vesicular glutamate transporters (VGLUTs) are a common feature of glutamatergic synaptic terminals in the mammalian central nervous system (CNS) (Ni et al., 1995; Bellocchio et al., 1998; Aihara et al., 2000; Bellocchio et al., 2000; Herzog et al., 2001; Fremeau et al., 2004b; Blakely and Edwards, 2012). Two isoforms, VGLUT1 and VGLUT2, are utilized in the majority of glutamatergic neurons in the CNS (Fremeau et al., 2001; Herzog et al., 2001; Kaneko et al., 2002), and may confer distinct functional properties to their host neurons (Bellocchio et al., 1998; Takamori et al., 2000; Herzog et al., 2001; Kaneko and Fujiyama, 2002; Boulland et al., 2004; Fremeau et al., 2004a; b; Ito et al., 2011; Weston et al., 2011; Rovó et al., 2012; Storace et al., 2012; Balaram et al., 2013). In sensory pathways, VGLUT1 and VGLUT2 are largely restricted to discrete subsets of glutamatergic projections that also appear to be functionally segregated (Takamori et al., 2000; Kaneko and Fujiyama, 2002; Li et al., 2003; Todd et al., 2003; Hur and Zaborszky, 2005; Persson et al., 2006; Scherrer et al., 2010; Hackett et al., 2011; Balaram et al., 2013). In general, VGLUT2 is present in the terminals of feedforward or driving projections (Herzog et al., 2001; Rovó et al., 2012), which significantly alter or 'drive' neural activity in their postsynaptic targets (Sherman and Guillery, 1996; 1998; Sherman, 2005). For example, retinal projections to the lateral geniculate nucleus (LGN) are commonly identified as driving projections (Sherman and Guillery, 1996) and predominantly

utilize VGLUT2 (Kaneko et al., 2002; Fujiyama et al., 2003; Nahmani and Erisir, 2005; Islam and Atoji, 2009; Balaram et al., 2011b). In contrast, VGLUT1 is often present in feedback or modulatory projections, which variably alter postsynaptic activity in their target cells. Projections from visual cortex to the LGN are commonly identified as modulatory projections (Sherman and Guillery, 1996) and primarily utilize VGLUT1 in their terminations within the LGN (Bellocchio et al., 1998; Kaneko et al., 2002; Fujiyama et al., 2003; Balaram et al., 2011a; 2013). Both proteins are occasionally found in nontraditional driving and modulatory synapses (Wei et al., 2011; Rovó et al., 2012; Marion et al., 2013), but in general, VGLUT1 and VGLUT2 appear to be restricted to functionally distinct glutamatergic projections in the CNS.

The use of a VGLUT isoform within a given projection is demonstrated by correlation of *VGLUT* mRNA labeling in neuronal cell bodies with VGLUT protein label in their respective terminals. This method appears to identify similar types of VGLUT1-positive and VGLUT2-positive projections between brain regions (Herzog et al., 2001; Kaneko and Fujiyama, 2002; Fremeau et al., 2004b; Graziano et al., 2008; Balaram et al., 2013), but the mRNA and protein distribution patterns of either VGLUT isoform may vary between species to some extent. For example, *VGLUT2* mRNA is only expressed in a subset of layers in primary visual cortex (V1) of rodents (Hisano et al., 2000; Fremeau et al., 2004b) but is found throughout the superficial layers of V1 in primates (Balaram et al., 2013). Species-specific variations in VGLUT1 and VGLUT2 distributions may simply reflect changes in the intracellular processes of glutamatergic neurons within a particular projection. Additionally, the driving or modulatory nature of individual sensory projections may vary between species and VGLUT1 and VGLUT2 are still correlated with the functional characteristics of those projections. In this case, differences in the relative distributions of VGLUT1 and VGLUT2 in a known sensory projection would reflect

alterations in the functional roles of that pathway within the larger sensory network. For the same example, the widespread distribution of *VGLUT2* mRNA in the superficial layers of V1 in primates may highlight driving projections from V1 to other visual areas, which could differ from similar projections in the superficial layers of V1 in rodents that lack *VGLUT2* mRNA.

In order to expand current knowledge on VGLUT distributions within driving and modulatory visual projections, we chose to examine the relative distributions of VGLUT1 and VGLUT2 mRNA and protein in the visual system of tree shrews. Tree shrews provide a model visual system that contains features found in both rodents and primates, as well as specialized features that differ from those in other mammalian species (see Lund et al, 1985 for review). They are grouped in the Euarchontoglire clade between rodents and primates, but are more closely related to primates (Huchon et al., 2002). Tree shrews are small, quadruped mammals, similar in size to rodents, but maintain a diurnal lifestyle, similar to most primates. Tree shrews possess many of the same visual structures found in rodents and primates – the superior colliculus, lateral geniculate nucleus, lateral posterior or pulvinar nucleus, and primary and secondary visual cortical areas for example – but each structure and its associated pathways is slightly different in tree shrews compared to other species (Clark, 1925; 1929; 1942; Chomsung et al., 2008; Wong and Kaas, 2009b; Chomsung et al., 2010). The tree shrew retina is cone-dominated (Samorajski et al., 1966), rather than rod-dominated as in rodents or primates (Glickstein, 1969; Wässle, 2004). The superior colliculus and lateral geniculate nucleus in tree shrews are both large and distinctly laminated, similar to primates, but both structures contain projections that differ from those found in rodent or primate species (Abplanalp, 1970; Harting et al., 1973b; Casagrande and Harting, 1975; Albano et al., 1979; Conway and Schiller, 1983; Conley et al., 1984). The pulvinar complex in tree shrews anatomically resembles the lateral

posterior nucleus of rodents (Diamond et al., 1970; Harting et al., 1973a), but contains similar subdivisions and connections as the pulvinar complex of primates (Lyon et al., 2003a; b). Additionally, visual cortical areas such as V1 and V2 in tree shrews are located at similar cortical positions as V1 and V2 in highly visual rodents such as squirrels (Wong and Kaas, 2008; 2009b), but their connections and lamination patterns more closely resemble those of V1 and V2 in primates (Clark, 1925; Snyder and Diamond, 1968; Lund et al., 1985). Lastly, V1 in tree shrews contains a unique pattern of segregation of geniculate inputs in layer 4 (Casagrande and Harting, 1975; Hubel, 1975; Humphrey et al., 1977; Norton et al., 1985), which relates to the larger segregation of parallel pathways across most projections in the tree shrew visual system (Lund et al., 1985). Thus, if VGLUT1 and VGLUT2 distinguish between driving and modulatory glutamatergic projections in visual circuits, regardless of the species in question, then their relative distributions across visual structures in the tree shrew should reflect the functional properties of their host projections. These distributions should also be comparable, to some extent, to known VGLUT distributions in the visual systems of both rodents and primates as well.

6.3 Materials and Methods

Four adult tree shrews were used to examine the distribution of VGLUT1 and VGLUT2 mRNA and protein across subcortical and cortical visual structures. Three animals were male, aged 8-9 months and weighing 120-135g, and one animal was female, aged 20 months and weighing 123g, but no age or sex-related differences were noted in this study. An additional three adult tree shrews were used to correlate the distributions of VGLUT2 protein across coronal, sagittal, and horizontal planes of section. All procedures were approved by the

Institutional Animal Care and Use Committee at the University of Louisville, and followed the guidelines published by the National Institutes of Health.

Tissue acquisition and histology

Each animal received a lethal intraperitoneal dose of sodium pentobarbital (250mg/kg; Beuthanasia-D, Merck Animal Health, Summit NJ) and placed in a dark enclosure for 3-5 minutes. When areflexive, the animal was transcardially perfused with sterile 0.1M phosphate-buffered saline (PBS; 0.9% NaCl) followed by sterile 4% paraformaldehyde (PFA) in 0.1M PBS. After fixation, the brains were removed from the skulls, rinsed briefly in sterile PBS, and postfixed overnight in 4% PFA. The following day, brains were blocked, bisected through the corpus callosum, placed in sterile cryoprotectant (30% sucrose in 0.1M phosphate buffer), and stored at 4°C prior to histology. Each block was cut into 40um coronal cryosections using a sliding microtome, and separated into 8 series for further study. One series from every block was processed for cytochrome oxidase (CO; Wong-Riley, 1979) to reveal boundaries of visual structures.

Immunohistochemistry (IHC)

Reagents and concentrations for all immunohistochemistry preparations are listed in Table 1. One series from every block was stained for neuronal cell bodies using a commercial antibody against neuronal nuclei (NeuN) to reveal areal and laminar divisions of cortical and subcortical visual structures. A second series was stained for VGLUT2 protein and a third series was stained for VGLUT1 protein, both using commercial antibodies, to identify the distribution of both proteins in synaptic terminals across visual structures. All IHC reactions were carried out as previously described (Balaram et al., 2013)

Antibody characterization

Both VGLUT antibodies have been extensively characterized in previous studies (VGLUT2: AB_262186, VGLUT1: AB_887876, in JCN antibody database) and were specifically tested against primate and rodent tissue for related projects (Balaram et al., 2013 and unpublished results). Rabbit anti- VGLUT1 from Synaptic Systems recognizes a large fragment of the VGLUT1 protein and labels a single band at 65kDa in western blot preparations (manufacturer's information and Balaram et al, 2013). Mouse anti- VGLUT2 from Millipore accurately recognizes VGLUT2 protein in primates (Balaram et al., 2011b; Rovó et al., 2012; Balaram et al., 2013; Garcia-Marin et al., 2013), as well as squirrels and tree shrews (Wong and Kaas, 2008; 2009b) and labels a single band at 56kDa in western blot preparations (manufacturer's information and Baldwin et al, 2012; Balaram et al, 2013).

In situ hybridization

Custom RNA probes against *VGLUT1* and *VGLUT2* were generated through cDNA libraries obtained from tree shrew liver and brain tissue using previously described techniques (Tochitani et al, 2001). Forward and reverse primers for *VGLUT1* were *cttctacctgctcctcatctct* and *acacttctcctcgctcatct* respectively, and targeted nucleotides 972-1545 of mouse *VGLUT1* (NM_182993). Forward and reverse primers for *VGLUT2* were *ggcaaggtcatcaaggagaa* and *gcacaagaatgccagctaaag* respectively, and targeted nucleotides 735-1125 of human *VGLUT2* (NM_020346). BLAST comparisons of each probe showed ~90-95% sequence homology with primate VGLUT1 and VGLUT2 and ~88-92% sequence homology with rodent VGLUT1 and VGLUT2. However, comparisons of both sequences to each other showed no overlap, confirming the specificity of each probe to its target sequence. One series from each block was labeled for *VGLUT1* mRNA and a second series from each block was labeled for *VGLUT2*

mRNA, to identify the cell bodies of neurons using each VGLUT isoform. ISH procedures were carried out as previously described (Balaram et al., 2013).

Image acquisition and analysis

Sections containing relevant visual structures were identified in CO or NeuN preparations and photographed using an MBF CX9000 camera mounted on an E80i microscope with Neurolucida software (RRID:nif-0000-10294). Adjacent sections stained for *VGLUT1* and *VGLUT2* mRNA and protein were then photographed at low magnification, and digitally montaged at high magnification to preserve details of cell bodies and processes. Boundaries of individual layers and nuclei within each structure were determined by superimposing images of VGLUT-labeled sections on images of adjacent CO- or NeuN-labeled sections and marking boundaries revealed by CO and NeuN staining on the VGLUT-labeled images. All images were cropped and equally adjusted for brightness and contrast, but were otherwise unaltered. Images were then qualitatively analyzed for labeling intensity and cell density of VGLUT1 and VGLUT2 positive neurons and terminals, and then correlated to known projections in the tree shrew visual system to identify VGLUT1- or VGLUT2-positive pathways between visual structures.

6.4 Results

6.4.1 Lateral geniculate nucleus

The lateral geniculate nucleus (LGN) in tree shrews consists of six distinct layers, numbered 1 through 6 from medial to lateral (Glickstein, 1967; Laemle, 1968; Harting et al., 1973a; Casagrande and Harting, 1975; Hubel, 1975; Conway and Schiller, 1983; Conley et al.,

1984; Lund et al., 1985) (Figures 1 and 2). CO and NeuN stained sections clearly revealed all six LGN layers (Fig. 1A, B). As previously described (Wong-Riley and Norton, 1988), LGN layers 1, 2, 4, and 5 showed dense CO reactivity, layers 3 and 6 showed moderate CO reactivity, and the interlaminar zones showed weaker reactivity compared to the surrounding LGN layers. In NeuN sections, NeuN-positive cell bodies were largely restricted to individual LGN layers, although fewer labeled cell bodies were present overall, compared to previous descriptions of Nissl-stained sections in the tree shrew LGN (Brunso-Bechtold and Casagrande, 1982; Conway and Schiller, 1983; Conley et al., 1984). However, other visual structures presented here showed nearly identical staining in NeuN or Nissl preparations (data not shown).

Diffuse labeling of VGLUT1 protein was present throughout the LGN (Figs. 1C, 2A), with only slightly denser labeling in layers 3 and 6 compared to layers 1, 2, 4 and 5. The interlaminar zones between LGN layers all labeled darkly for VGLUT1 protein, indicating greater densities of VGLUT1-positive terminals in these regions compared to the LGN layers. In contrast to VGLUT1, dense labeling of VGLUT2 protein was largely restricted to LGN layers 1 through 5, and far weaker VGLUT2 labeling was seen in layer 6, as well as the interlaminar zones (Fig. 1D, 2B). Layers 3 and 4 also appeared to merge at the dorsal and ventral LGN boundaries in all VGLUT2-labeled sections, but a clear difference in labeling density as well as a weakly labeled interlaminar zone separated these two layers in each case. Similarly, the ventral portion of layer 6 appeared continuous with the interlaminar zone between layers 4 and 5, and showed similarly diffuse VGLUT2 labeling as the remaining interlaminar zones. Laminar boundaries for layers 1, 2, and 5 were clearly visible in VGLUT2-labeled sections, but were less apparent for layers 3, 4, and 6.

6.4.1.1 Figure 1. Coronal sections through the tree shrew lateral geniculate nucleus (LGN) stained for (A) cytochrome oxidase (CO), (B) neuronal nuclear antigen (NeuN), (C) VGLUT1 protein, (D) VGLUT2 protein, (E) VGLUT1 mRNA, and (F) VGLUT2 mRNA. LGN layers are adapted from Glickstein, 1967. Midline is to the left, scale bar is 1mm.

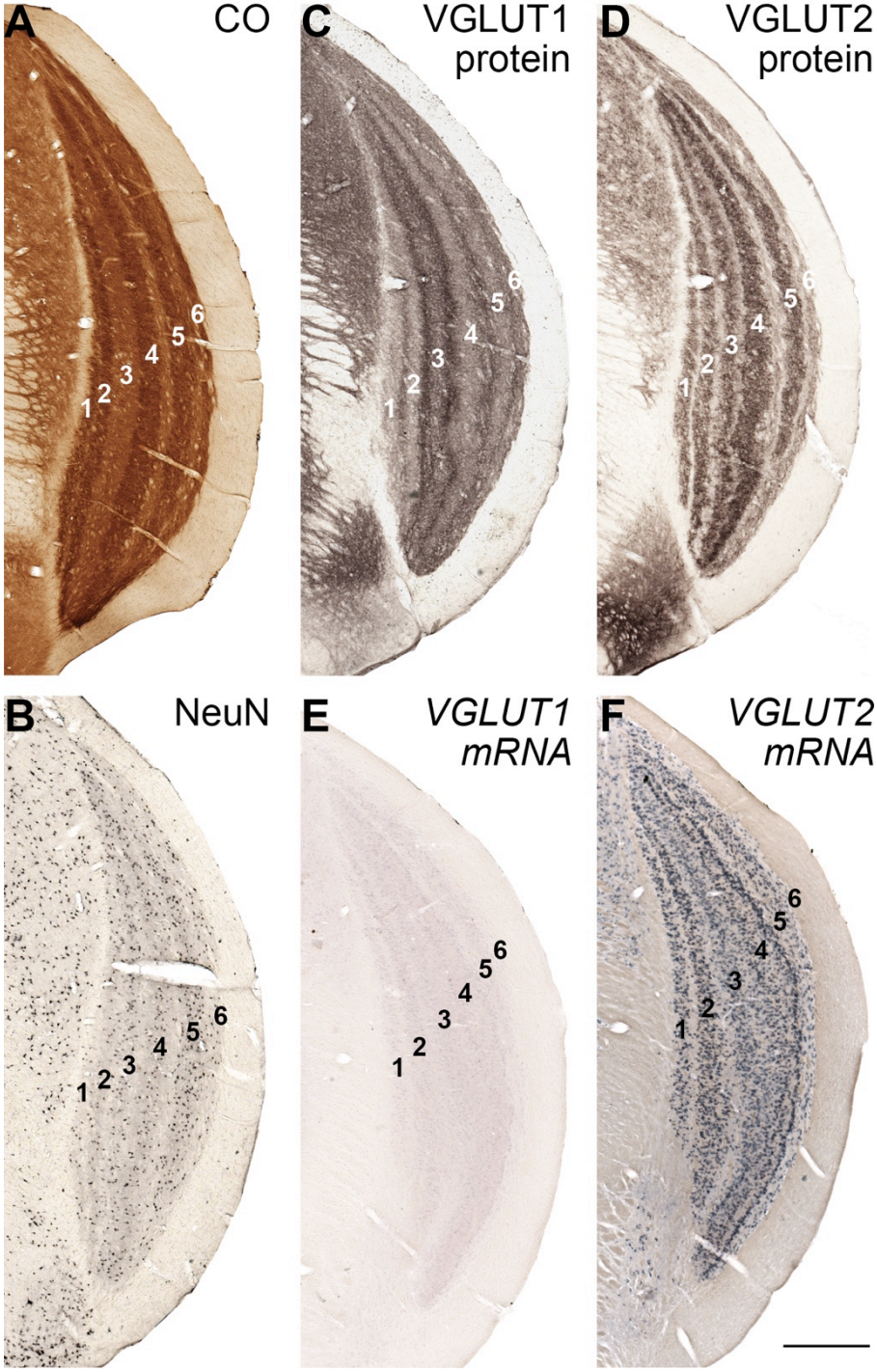

6.4.1.2 Figure 2: High magnification images of panels C-F in figure 1 highlight laminar differences in VGLUT1 and VGLUT2 protein (A, B) and mRNA (C, D) through the tree shrew LGN. Layer conventions as in figure 1. Midline is to the left, scale bar is 100µm.

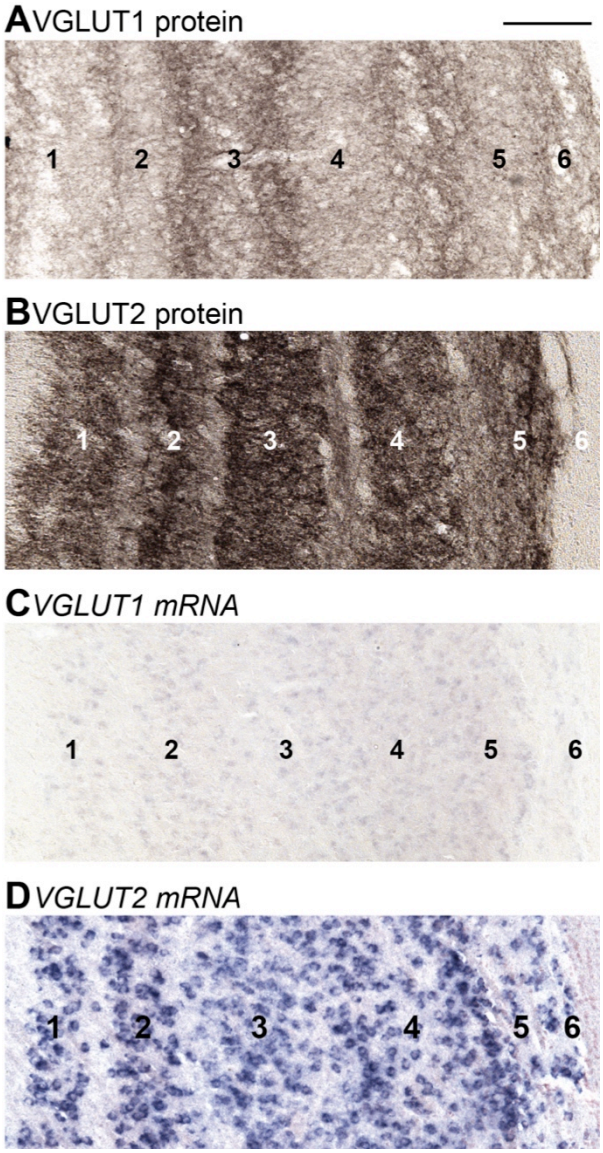

In sections hybridized for *VGLUT1* mRNA (Fig. 1E, 2C), scattered populations of weakly labeled cells were present throughout the LGN, but were concentrated in different locations depending on the layer. Layers 1 and 2 both showed even distributions of neurons that

weakly expressed *VGLUT1* mRNA, with no apparent intralaminar differences. Layer 3 contained weakly expressing *VGLUT1*-positive cells concentrated through the center of the layer. Layer 4, in contrast, contained two strips of cells along its dorsal borders that moderately expressed *VGLUT1* mRNA with hardly any *VGLUT1*-positive cells in between them. Towards the medial and ventral portions of layer 4, cells that expressed *VGLUT1* mRNA were more evenly distributed through the layer (Figs. 2C). Layer 5 contained similar distributions of cells as layers 1 and 2. Lastly, cells in layer 6 weakly expressed *VGLUT1* mRNA and were primarily located in the dorsal half of the layer, with far fewer cells in ventral locations throughout the LGN. Very few cells in the interlaminar zones expressed *VGLUT1* mRNA.

Sections hybridized for *VGLUT2* mRNA (Fig. 1F, 2D) showed dense distributions of *VGLUT2*-positive (*VGLUT2+)* neurons throughout the LGN. Layers 1 and 2 both contained even distributions of neurons that densely expressed *VGLUT2* mRNA. Neurons in layer 3 labeled more moderately for *VGLUT2* mRNA and were clustered together in the center of the layer compared to the medial and lateral edges. Layer 4 contained two narrow strips of neurons, which densely expressed *VGLUT2* mRNA and were packed in line with each other, along its lateral and medial boundaries, with more diffusely spread *VGLUT2+* cells between the two strips. The lateral strip of VGLUT2-positive cells contained the densest VGLUT2 expression of all geniculate cells and was easily visible at the border of layers 4 and 5 throughout the LGN (Fig. 2D). Layer 5 contained a similar distribution of neurons as the center of layer 4 that all densely expressed *VGLUT2* mRNA. Layer 6, in contrast, only contained a few scattered cells that were smaller and more moderately labeled for VGLUT2 mRNA compared to cells in the other LGN layers. Lastly, all the interlaminar zones of the tree shrew LGN contained mixed distributions of neurons that moderately labeled for *VGLUT2* mRNA.

6.4.2 Superior Colliculus

The superior colliculus (SC) in tree shrews is large and distinctly laminated (Campbell et al., 1967; Glickstein, 1967; Laemle, 1968), compared to that of similarly sized mammals (May, 2006), with segregated visual and visuomotor functions at different laminar depths. Retinal and cortical projections largely target the superficial layers of the SC (Figures 3 and 4). Retinal projections terminate primarily in the zonal layer (SZ) and upper and lower superficial gray layers (uSGS and lSGS, respectively), and secondarily in the optic layer (SO) (Campbell et al., 1967; Laemle, 1968). Striate cortex projections to the SC terminate densely along the boundary between the upper and lower superficial gray layers and more diffusely through the remaining superficial SC layers (Harting and Noback, 1971). CO stained sections through the SC (Fig. 3A) identified an additional separation within the upper SGS, where the ventral division (USGSv) labeled more densely for CO than the dorsal division (USGSd) in all cases. These divisions are visible, but not defined, in previous descriptions of CO (Wong-Riley and Norton, 1988) and Nissl (Snyder and Diamond, 1968; Albano et al., 1979) sections through the tree shrew SC. In comparison to the upper SGS, the lower SGS and SO both labeled moderately for CO. NeuN stained sections through the SC (Fig. 3B) clearly identified the SZ and SO as cell sparse layers flanking the SGS. A clear separation was not visible between the upper and lower sublayers within the SGS, but the upper SGS was differentiable from the lower SGS by smaller, more densely packed neurons. Cells in the upper SGS primarily project to the LGN, while cells in the lower SGS project to subdivisions of the pulvinar complex (Albano et al., 1979; Luppino et al., 1988; Chomsung et al., 2008).

6.4.2.1 Figure 3: Coronal sections through the tree shrew superior colliculus (SC) stained for (A) cytochrome oxidase, (B) neuronal nuclear antigen, (C) VGLUT1 protein, (D) VGLUT2 protein, (E) VGLUT1 mRNA, and (F) VGLUT2 mRNA. SC layers are adapted from May, 2006. Midline is to the right, scale bar is 500um. Abbreviations: SZ – zonal layer, uSGSd – dorsal division of the upper superficial gray layer, uSGSv – ventral division of the upper superficial gray layer, LSGS – lower superficial gray layer, SO – optic layer.

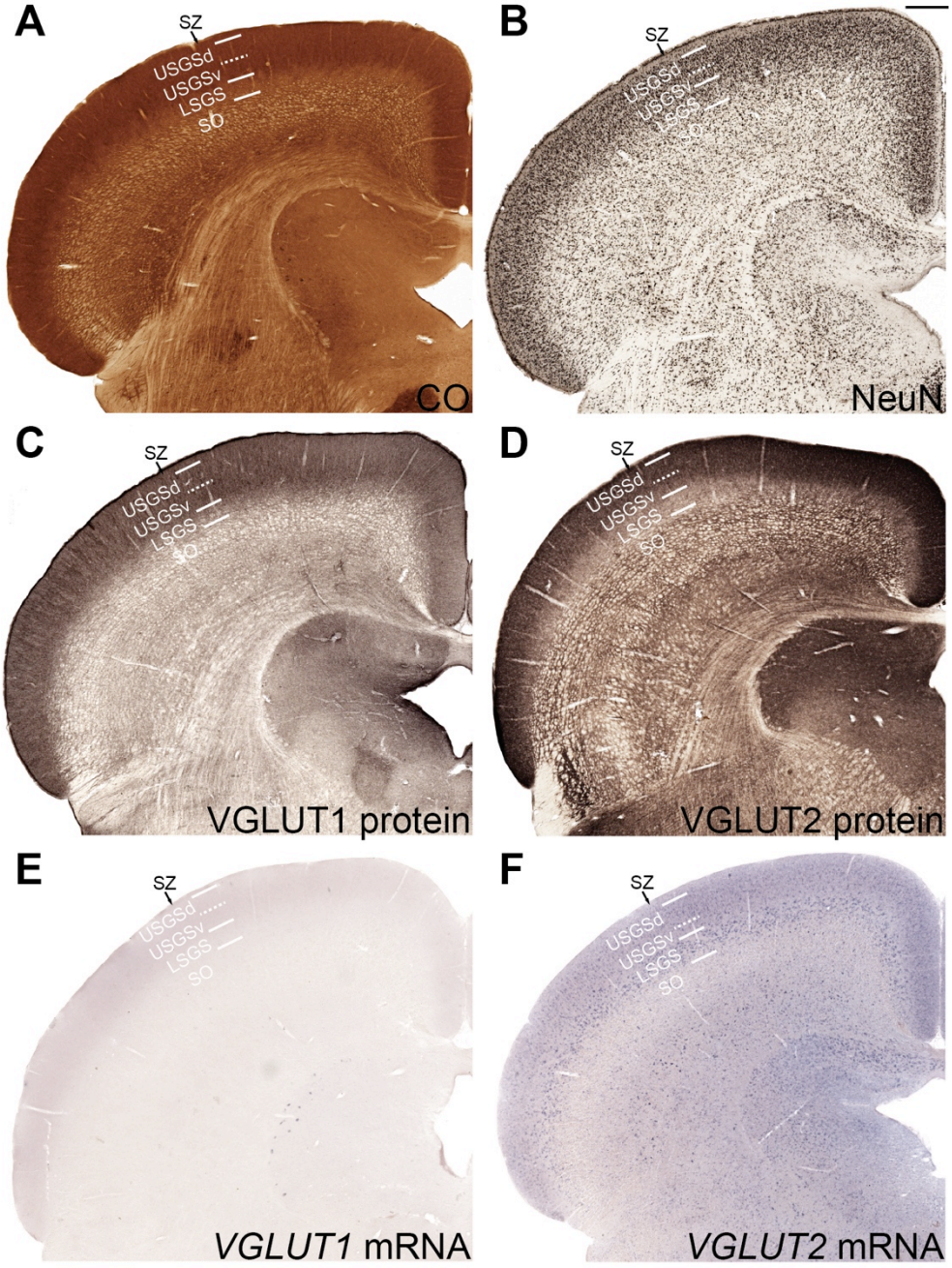

Both VGLUT1 and VGLUT2 protein (Fig. 3C-D, 4A-B) were differentially distributed in the five laminar divisions of the SC. The SZ labeled weakly for VGLUT1 and densely for VGLUT2. The upper SGS could be divided into dorsal and ventral divisions with complementary staining patterns; the dorsal division stained weakly for VGLUT1 but densely for VGLUT2, while the ventral division stained densely for VGLUT1 and weakly for VGLUT2 (best seen in Figs 3C, D). The lower SGS stained moderately for VGLUT1 and weakly for VGLUT2, and the SO showed even labeling of both VGLUTs surrounding the fiber pathways traversing this layer.

6.4.2.2 Figure 4: High magnification images of panels C-F in figure 3 show variations in VGLUT1 and VGLUT2 protein (A, B) and mRNA (C, D) distributions between layers of the SC. Layer conventions as in figure 3. Scale bar is 50um. Abbreviations: SZ – zonal layer, uSGSd – dorsal division of the upper superficial gray layer, uSGSv – ventral division of the upper superficial gray layer, LSGS – lower superficial gray layer, SO – optic layer.

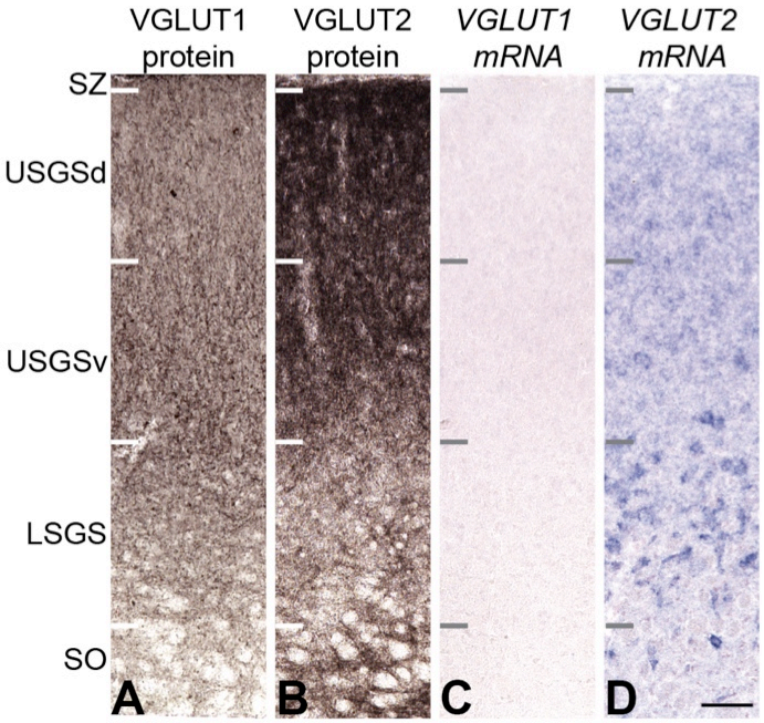

In mRNA preparations, no *VGLUT1* mRNA was visible anywhere in the SC (Fig. 3E, 4C). A few darkly labeled neurons were present along the boundary of the periaqueductal gray (Fig. 3E), but no neurons in the visually responsive SC layers expressed *VGLUT1* mRNA. *VGLUT2* mRNA however, was differentially expressed across the superficial SC (Fig. 3F, 4D). The SZ did not express *VGLUT2* since almost no cells are present in this layer of the SC. The upper SGS showed scattered populations of small neurons that weakly expressed *VGLUT2* mRNA, most of them concentrated in the dorsal division and far fewer present in the ventral division. The lower SGS contained dense populations of larger neurons that densely expressed *VGLUT2* mRNA, while the SO contained only a few scattered neurons that expressed *VGLUT2* mRNA. Thus, all VGLUT preparations identified the SZ, two tiers of the upper SGS, the lower SGS, and the SO in the tree shrew SC.

6.4.3 Pulvinar complex

The pulvinar complex in tree shrews can be divided into three distinct nuclei that differentially label for VGLUT1 and VGLUT2 mRNA and protein (Figs. 5 and 6) (Chomsung et al., 2008; Wei et al., 2011). All three pulvinar divisions have been identified previously, based on connectional and architectonic evidence (Lyon et al., 2003a; b; Chomsung et al., 2008; 2010). The dorsal pulvinar (Pd) lies dorsomedial to the central pulvinar (Pc), while the ventral pulvinar (Pv) lies ventral to Pc. Most of Pc and Pv lie lateral to the brachium of the superior colliculus, but parts of both nuclei are often seen medial to the brachium as well. All divisions of the pulvinar complex showed relatively even distributions of CO and NeuN (Fig 5A, B); a few patches of darker CO staining were scattered through the central nucleus, and neurons here appeared slightly more clustered than cells in Pd or Pv, but overall, both stains did not

conclusively differentiate pulvinar divisions in tree shrews. Similar results for CO and Nissl stained sections of the tree shrew pulvinar have been previously reported (Lyon et al., 2003a).

VGLUT1 and VGLUT2 protein distributions were less distinct in the pulvinar complex compared to the LGN or SC, but some differences between nuclei were still noticeable in both preparations (Figs 5C-D, 6A-B). First, although VGLUT1 immunoreactivity was evenly distributed across most of the pulvinar, the region between Pd and Pc showed irregular patches of slightly darker labeling for VGLUT1 (white asterisk, Fig 5C) and most of Pc showed uniformly denser VGLUT1 labeling compared to Pd and Pv (Figs 6A-C). Similar to previous descriptions (Chomsung et al., 2008; Wei et al., 2011), in VGLUT2 preparations, Pd showed dense, punctate labeling for VGLUT2 while Pv showed almost none, especially in the region of Pv medial to the brachium of the colliculus, which lacks SC input and receives dense input from striate cortex instead. Pc showed irregular distributions of moderately labeled VGLUT2 (Fig 5D, 6D-F). A small region between the dorsal borders of Pd and Pc (white asterisk, Fig. 5D) showed much sparser VGLUT2 terminal labeling, but the few VGLUT2-positive terminals present in this region were clustered together in tight groups compared to VGLUT2-positive terminals in the surrounding regions of Pd and Pc. This pattern of VGLUT2 labeling was remarkably similar to that seen in the medial inferior pulvinar of monkeys (Balaram et al., 2013) and the whole pale-stained region did not continue across the brachium of the SC.

6.4.3.1 Figure 5: Coronal sections through the tree shrew pulvinar complex stained for (A) cytochrome oxidase, (B) neuronal nuclear antigen, (C) VGLUT1 protein, (D) VGLUT2 protein, (E) VGLUT1 mRNA, and (F) VGLUT2 mRNA. Individual nuclei are demarcated after Lyon et al., 2003. Midline is to the right, scale bar is 500um. Abbreviations: Pd – dorsal pulvinar, Pc – central pulvinar, Pv- ventral pulvinar.

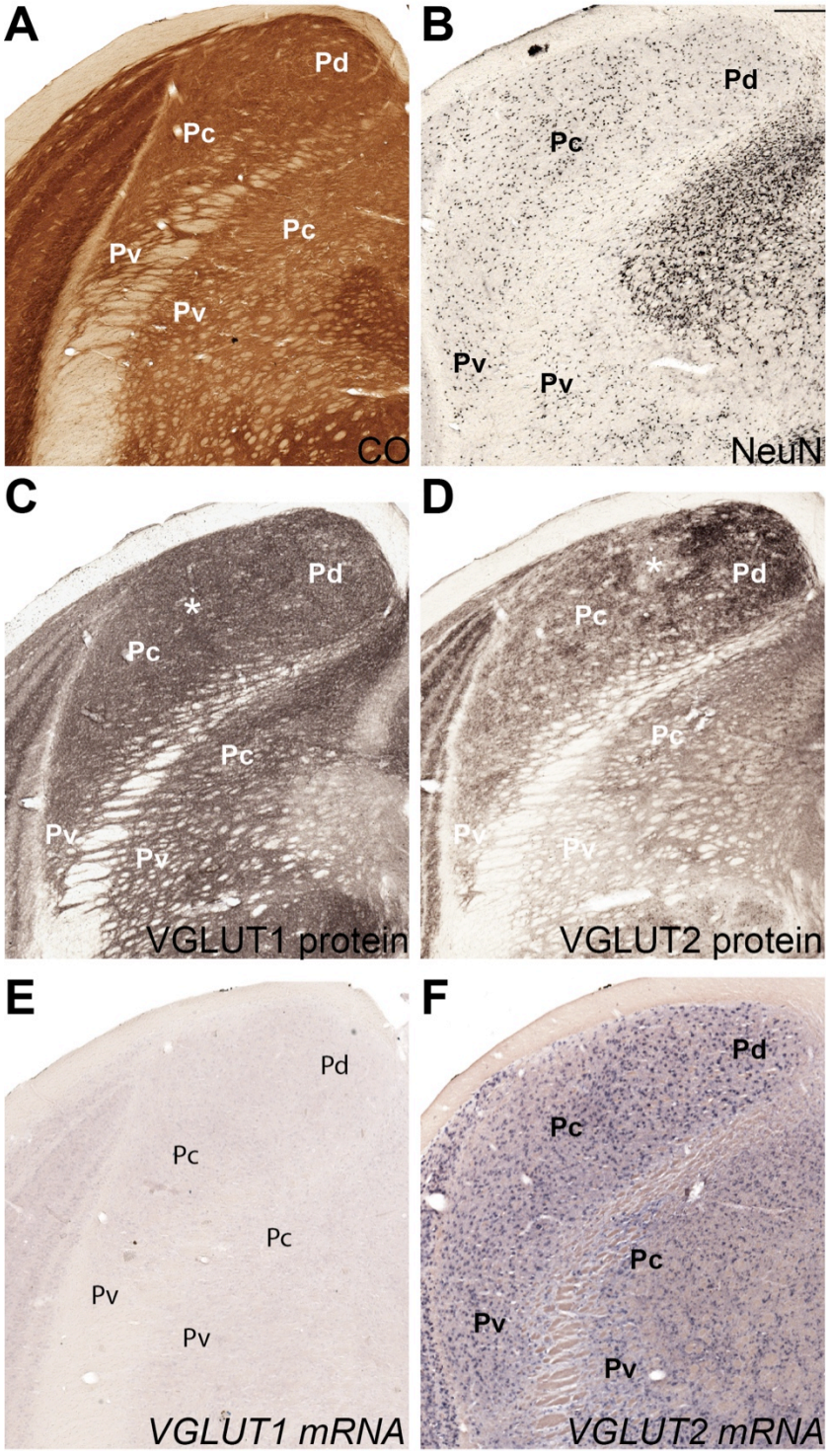

6.4.3.2 Figure 6: High magnification images of individual pulvinar divisions from panels C-F in figure 5 reveal differences in VGLUT1 and VGLUT2 protein (A, B) and mRNA (C, D) labeling across these nuclei. Scale bar is 50µm. Abbreviations: Pd – dorsal pulvinar, Pc – central pulvinar, Pv- ventral pulvinar.

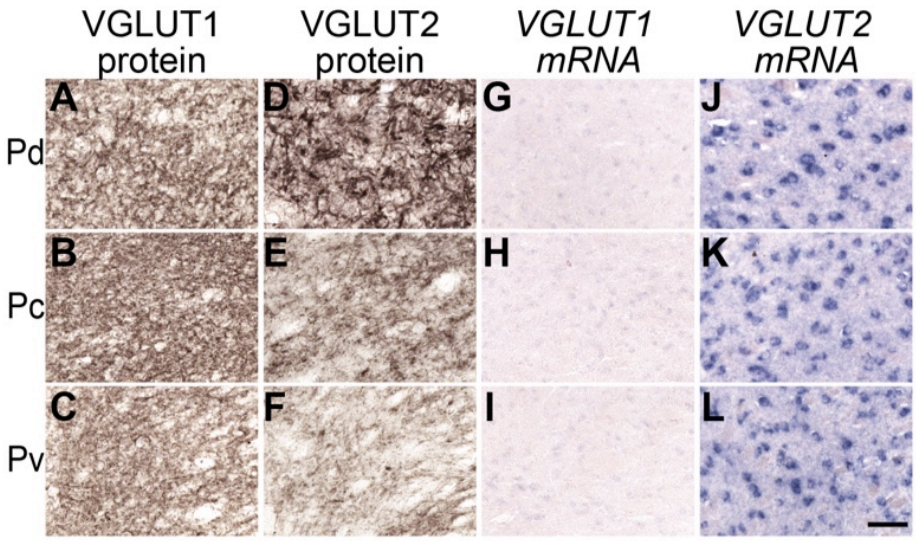

Cells in all three divisions of the pulvinar expressed both *VGLUT1* and *VGLUT2* mRNA (Figs 5E-F, 6C-D). *VGLUT1* mRNA was expressed at low levels in all three nuclei, with Pd and Pv containing slightly fewer *VGLUT1*-expressing neurons compared to Pc (Fig. 5E, 6G-I)). In contrast, *VGLUT2* mRNA was expressed at high levels in all three nuclei, and cells in Pd showed denser *VGLUT2* labeling compared to cells in Pc and Pv (Fig. 5F, 6J-L). Distinct boundaries between nuclei were not visible in *VGLUT* mRNA preparations, but both *VGLUT1* and *VGLUT2* mRNA distributions distinguished the dorsal pulvinar from the central and ventral pulvinar nuclei based on the density of *VGLUT* expression within positively stained cells.

6.4.4 Primary visual cortex (V1)

Primary visual cortex, or V1, occupies a large expanse of caudomedial neocortex and is easily identified by the distinct stratification of its neocortical layers, compared to those of other cortical areas, in the tree shrew brain (Figures 7 and 8) (Snyder and Diamond, 1968; Kaas et al., 1972; Lund et al., 1985; Wong and Kaas, 2009b). Layer 1, the dorsal most laminar division below the pial surface, largely consists of dense neuropil while layer 2, immediately ventral to layer 1, consists of small, densely packed neurons arranged in a thin band above layer 3. Layer 3 occupies most of the supragranular depth of V1, and can be divided into three distinct sublayers based on variations in neuronal size and density, termed 3A, 3B, and 3C, from dorsal to ventral in V1. Layer 4 of V1 is remarkably distinct in tree shrews, and consists of two densely populated granular layers, 4A and 4B, separated by a distinct cell-sparse cleft. Two thin rows of neurons immediately adjacent to either side of the cleft receive monocular input from the contralateral eye, while the remaining neurons throughout 4A and 4B receive binocular input instead (Fitzpatrick, 1996). Layer 5 is sparsely populated with medium and large cells, while layer 6 displays an upper tier of closely arranged large and medium cells and a lower tier of small cells that diffuse into the white matter below V1. These layer boundaries follow Hässler's (1967) scheme for laminar designations in V1 across mammals, rather than Brodmann's (1909) laminar scheme, since Hassler's scheme is more appropriate for comparisons of V1 functions across rodents, tree shrews, and primates (Brodmann, 1909; Hässler, 1967; Harting et al., 1973a; Hubel, 1975; Casagrande and Kaas, 1994). NeuN stained sections through V1 identified the same layers and sublayers described above (Fig. 7B), and revealed sharper interlaminar boundaries compared to those seen in Nissl stains of tree shrew V1 (see Lund et al, 1985 for example). A distinct subdivision of layer 5 was also visible, consisting of a thin band of weakly labeled cells below

the ventral boundary of layer 4 by and above the larger, more densely stained neurons in the ventral portion of layer 5, known as 5B. This superficial portion of layer 5, termed 5A in primates, appears to be a common feature of highly visual mammals (Balaram and Kaas, 2014). Layer 6 could also be differentiated into two divisions, a dorsal layer 6A and a ventral layer 6B, based on the size and packing density of neurons in this layer. CO stained sections of V1 also showed similar results to those previously described (Fig 7A) (Wong-Riley and Norton, 1988; Wong and Kaas, 2009b). Layer 4 showed the densest CO reactivity, with slightly denser reactivity at the dorsal and ventral boundaries compared to the middle of the layer, followed by moderate CO reactivity in 6A, 5A, and parts of 3C. The remaining layers showed evenly weak CO reactivity throughout V1.

Labeling for VGLUT1 and VGLUT2 protein in V1 of tree shrews revealed dense distributions of both proteins, with remarkably distinct laminar profiles for each isoform. (Figs 7C-D, 8A-B). VGLUT1 was abundantly expressed in all V1 layers, including layer 1, but each layer showed slight changes in staining density throughout the area (Fig. 7C, 8A). The superficial extent of V1, from layer 1 to layer 3C, displayed a gradual decrease in VGLUT1 label, which successively distinguished each layer at its dorsal and ventral boundaries. Both divisions of layer 4, 4A and 4B, showed significantly less VGLUT1 label than any other layer, clearly distinguishing them in the middle of V1. However, the cell-sparse cleft between 4A and 4B contained high levels of VGLUT1 (best seen in fig. 7C). Both subdivisions of layer 5 and layer 6A displayed moderate VGLUT1 reactivity, and appeared continuous through the ventral depth of V1. Layer 6B however, labeled weakly for VGLUT1 and appeared as a light band above the white matter below V1.

6.4.4.1 Figure 7: Coronal sections through primary visual cortex (V1) in tree shrews stained for (A) cytochrome oxidase, (B) neuronal nuclear antigen, (C) VGLUT1 protein, (D) VGLUT2 protein, (E) VGLUT1 mRNA, and (F) VGLUT2 mRNA. Individual V1 layers are named following the convention of Hässler (1967) and are shown on the left of each section. Solid lines are boundaries between V1 layers, dotted lines are sublaminar divisions. Hemispheric midline is to the right, scale bar is 500um.

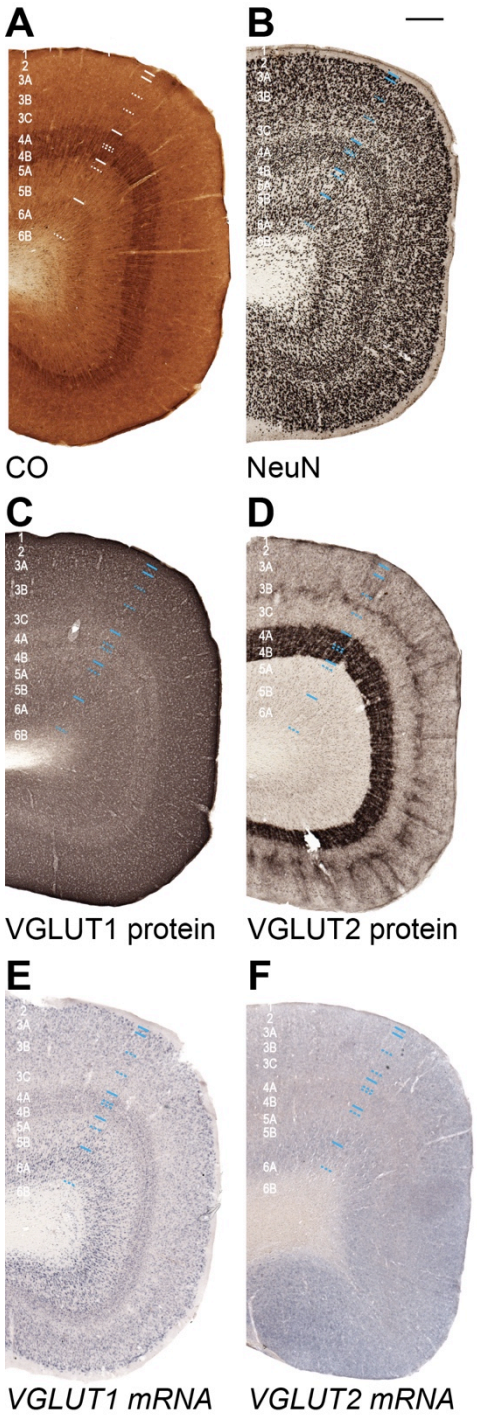

In contrast to the evenly dense VGLUT1 label, VGLUT2 labeling in V1 was highly restricted (Fig. 7D, 8B). The greatest density of VGLUT2 label in V1 was located in layer 4, which was clearly visible as a dark band throughout V1. Layers 4A and 4B, as well as the cell-sparse cleft, contained punctate distributions of densely labeled VGLUT2-positive terminals, with slightly denser labeling along the ventral boundary of 4B compared to the rest of layer 4. Similarly dense VGLUT2 label was seen in layer 3B, which contained a thin band of VGLUT2-labeled terminals that periodically clustered and extended up through the superficial layers to layer 1 (fig. 8B). These extended VGLUT2-positive terminations were more frequent in the monocular zone of V1 (best seen in fig. 7D). The remaining superficial V1 layers contained low levels of VGLUT2 protein in the neuropil as well. The deep layers of V1 contained sparse patches of VGLUT2-positive terminations in layer 5B, and an even band of moderately labeled VGLUT2 terminals in 6A, but little to no VGLUT2 label in layers 5A or 6B.

6.4.4.2 Figure 8: High magnification images of panels C-F in figure 7 identify sublaminar differences in VGLUT1 and VGLUT2 protein (A, B) and mRNA (C, D) distributions in V1. Laminar conventions as in figure 7. Scale bar is 100µm.

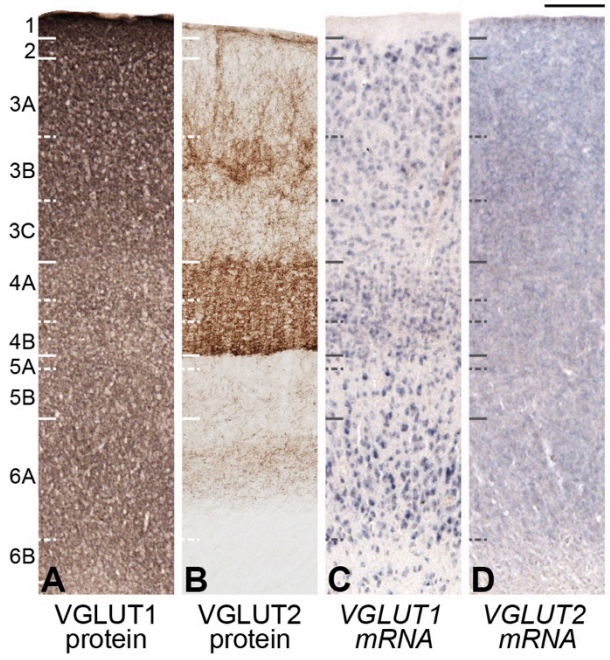

VGLUT1 mRNA distributions in V1 followed similar patterns compared to VGLUT1 protein distributions (Figs. 7E, 8C). *VGLUT1* mRNA was densely expressed in all V1 layers, excluding layer 1, but each layer showed slight variations in the density of *VGLUT1*-positive neurons. The superficial V1 layers showed a gradual decrease in *VGLUT1* mRNA expression from dorsal to ventral, such that layer 2 contained large cells that strongly expressed *VGLUT1* mRNA and layer 3C contained small cells with little or no *VGLUT1* mRNA expression. Most cells in layer 4 expressed moderate levels of *VGLUT1* mRNA as well. Interestingly, two thin bands of neurons with slightly elevated *VGLUT1* expression were clearly visible along either side of the cell sparse cleft in V1 (best seen in fig. 7E). Lastly, layers 5A and 6B contained small cells with moderate or weak *VGLUT1* mRNA expression while layers 5B and 6A contained much larger cells with denser *VGLUT1* mRNA expression. Cells in 6A were more condensed compared to cells in 5B, which identified the border between layers 5 and 6 in V1. *VGLUT2* mRNA was almost entirely absent in V1. A few weakly positive neurons were found scattered along the ventral border of 5B, and several more were present in layer 6B, but the vast majority of neurons in V1 did not express *VGLUT2* mRNA.

6.5 Discussion

The present study aimed to characterize the distribution of VGLUT1 and VGLUT2 in the visual system of tree shrews, in order to determine whether VGLUT isoforms are differentially restricted to functional classes of glutamatergic projections. A summary of these findings is presented in figure 9. The results demonstrate that VGLUT1 and VGLUT2 are separately utilized in most glutamatergic projections through visual structures in tree shrews, but the overlapping distribution of both VGLUTs in some structures suggests a more heterogeneous use

of VGLUT isoforms in the transmission of visual information. The distributions of each VGLUT isoform in the tree shrew visual system are largely consistent with VGLUT distributions in rodent (Bellocchio et al., 1998; Aihara et al., 2000; Hisano et al., 2000; Kaneko and Fujiyama, 2002; Kaneko et al., 2002) and primate (Wong and Kaas, 2010; Balaram et al., 2011a; b; 2013; Baldwin et al., 2013a) visual systems as well, indicating that VGLUT1 and VGLUT2 characterize distinct types of glutamatergic projections. When compared with the functional attributes of these projections, it becomes evident that VGLUT1 and VGLUT2 are generally characteristic of modulatory and driving glutamatergic neurons in most visual structures.

6.5.1 VGLUT1- and VGLUT2-positive projections in the tree shrew visual system

In every visual structure examined, VGLUT2 was restricted to a discrete subset of glutamatergic pathways (figure 9). The dense VGLUT2 labeling seen in retinorecipient layers of the LGN and SC (Campbell et al., 1967; Laemle, 1968) indicate that retinal ganglion cell projections to both structures utilize VGLUT2. LGN projections to layer 4 of V1 (Diamond et al., 1970; Harting et al., 1973a; Casagrande and Harting, 1975; Conley et al., 1984; Fitzpatrick, 1996) also predominantly use VGLUT2, as revealed by robust *VGLUT2* mRNA expression in all LGN layers, as well as dense VGLUT2 terminal labeling in layer 4 of V1. The band of VGLUT2-positive terminations in layer 3B, as well as the regular pattern of extended VGLUT2-positive terminations through layer 1, likely arises from LGN layers 3 and 6 (Hubel, 1975; Carey et al., 1979; Conley et al., 1984; Lund et al., 1985) and may alternate with modules of intrinsic connections in V1 (Rockland et al., 1982). Some of these superficial projections may arise from cells expressing *VGLUT2* mRNA in the ventral pulvinar as well (Carey et al., 1979; Lund et al., 1985; Lyon et al., 2003b).

6.5.1.1 Figure 9: Summary of VGLUT1-positive and VGLUT2-positive projections in the tree shrew visual system. VGLUT1 projections are shown in blue, VGLUT2 projections are shown in red, and dual VGLUT1/VGLUT2 projections are shown in alternating red and blue. Circles denote the origin of individual projections while arrowheads indicate the terminations of each projection. Abbreviations: LGN – lateral geniculate nucleus, SC – superior colliculus, SZ – zonal layer, uSGSd – dorsal division of the upper superficial gray layer, uSGSv – ventral division of the upper superficial gray layer, LSGS – lower superficial gray layer, SO – optic layer, Pd – dorsal pulvinar, Pc – central pulvinar, Pv- ventral pulvinar, V1 – primary visual cortex.

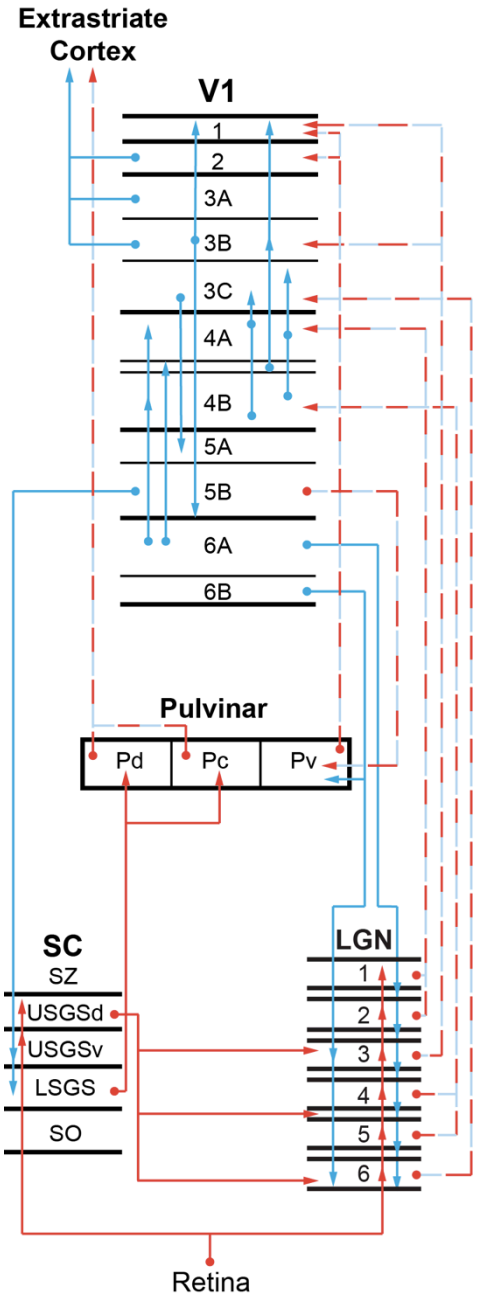

The relevance of sublaminar differences in *VGLUT2* expression in the LGN, particularly the densely labeled *VGLUT2*-positive neurons along the boundaries of LGN layer 4, is unclear since corresponding changes in VGLUT2 terminal labeling in layer 4 of V1 were not apparent. However, the dense band of *VGLUT2*-positive neurons along the lateral boundary of LGN layer 4 may also be associated with the interlaminar zone between LGN layers 4 and 5, which projects to layer 1 of V1 instead (Carey et al., 1979), and these cells could contribute to the periodic VGLUT2 terminal labeling seen in that layer of V1.

Tectal projections to the LGN and pulvinar in tree shrews predominantly utilize VGLUT2 as well. Projections from the upper SGS of the SC target layers 3 and 6 of the LGN as well as the interlaminar zone between LGN layers 4 and 5 (Harting et al., 1973b; Albano et al., 1979; Fitzpatrick et al., 1980; Diamond et al., 1991), and small, moderately labeled cells expressing *VGLUT2* mRNA in the upper SGS correspond to the moderately labeled VGLUT2-positive terminals distributed in these LGN regions. All three tectorecipient LGN layers target the superficial layers of V1 (Carey et al., 1979; Conley et al., 1984) and also predominantly use VGLUT2, as discussed above. Projections from the lower SGS of the SC target the dorsal and central divisions of the pulvinar (Harting et al., 1973b; Casagrande and Harting, 1975; Albano et al., 1979; Luppino et al., 1988; Chomsung et al., 2008), and the dense expression of *VGLUT2* mRNA by cells in this layer matches the dense VGLUT2 terminal labeling seen across the dorsal pulvinar and corresponding parts of the central pulvinar as well. Individual tectopulvinar terminals have been found to contain VGLUT2 (Wei et al., 2011), and the ultrastructure of VGLUT2-positive terminals in the tree shrew pulvinar nucleus is identical to that of tectopulvinar terminals (Chomsung et al., 2008). Tectopulvinar terminals in tree shrews do not exhibit classic driving or modulatory characteristics (Wei et al., 2011), and may release other

neurotransmitters in addition to glutamate (Stepniewska et al., 2000; Masterson et al., 2010), but the presence of VGLUT2 in this projection is consistent with VGLUT2-positive tectopulvinar projections in other visual mammals as well (Baldwin et al., 2011; Balaram et al., 2011b; Baldwin et al., 2013a).

Pulvinar projections to cortical visual areas are rather complex in tree shrews (Harting et al., 1972; 1973a; Carey et al., 1979). Retrograde tracing techniques suggest two major pathways (Luppino et al., 1988; Lyon et al., 2003b; Chomsung et al., 2008). One pathway from the Pc and Pv projects to occipital visual areas, and another pathway from the Pd and Pc projects to temporal visual areas (Luppino et al., 1988; Lyon et al., 2003b). More recent anterograde tracing techniques (Chomsung et al., 2010) have shown that Pd and Pc each project to two different regions of the temporal cortex. The dense *VGLUT2* mRNA seen in all divisions of the pulvinar implies that pathways to both the striate and temporal cortex predominantly utilize VGLUT2 in their synaptic terminations, but the weaker expression of *VGLUT1* mRNA in many pulvinar cells suggests that both VGLUT isoforms are utilized to different extents in individual pulvinar projections to cortical areas. Lastly, the scattered distributions of *VGLUT2* mRNA expressing neurons in the deep layers of V1 may project to the ventral pulvinar, as well as layers 3 and 6 of the LGN (Casseday et al., 1979; Usrey and Fitzpatrick, 1996), and contribute to more diffusely labeled VGLUT2 terminations in these locations.

VGLUT1 also appears to be restricted to a subset of glutamatergic projections in the tree shrew visual system. The dense expression of *VGLUT1* mRNA across all layers of V1 suggests that most intrinsic V1 projections exclusively utilize VGLUT1. The same is likely true for V1 projections to other cortical visual areas, given the exclusive *VGLUT1* mRNA expression in the superficial layers of V1. Feedback projections from V1 to the SC primarily arise in layer 5

(Casseday et al., 1979; Lund et al., 1985), and the strong expression of *VGLUT1* mRNA by neurons in this layer match the dense VGLUT1 terminal labeling in the corticorecipient layers of the SC (Huerta et al., 1985). Similarly, V1 projections to the LGN primarily arise from layer 6A, and neurons in this layer strongly expressed VGLUT1 mRNA while the corticorecipient interlaminar zones of the LGN contain dense distributions of VGLUT1-positive terminals. The ventral pulvinar also receives projections from layer 5 and 6B of V1 (Usrey and Fitzpatrick, 1996), both of which also express *VGLUT1* mRNA and likely contribute to the dark VGLUT1 terminal labeling across this pulvinar division. Although corticopulvinar terminals are larger than those of other corticothalamic projections, such as cortical terminations in the LGN, corticopulvinar projections in other species appear to utilize VGLUT1 in their terminations as well (Rovó et al., 2012).

Some projections in the tree shrew visual system appear to employ both VGLUT1 and VGLUT2. Weak *VGLUT1* mRNA expression alongside strong *VGLUT2* mRNA expression in neurons of the LGN and pulvinar complex implies that these projections utilize both isoforms in their target synapses. Individual neurons have been found to express both *VGLUT1* and *VGLUT2* mRNA (Barroso-Chinea et al., 2007; 2008), but both proteins do not colocalize to single synapses, suggesting that each transcript is differentially regulated within single neurons (Herzog et al., 2001; De Gois et al., 2005; Rovó et al., 2012). Thus, the LGN and pulvinar may contain overlapping or segregated distributions of VGLUT-positive projections. In the LGN for example, neurons expressing *VGLUT1* mRNA may contribute to the diffuse VGLUT1 terminal label in the geniculorecipient layers of V1, or they may project intrinsically (Hajdu et al., 1982)and contribute to the moderate VGLUT1 terminal labeling within each LGN layer. Similarly, given the variety of efferent projections from each division of the pulvinar nucleus (Lyon et al.,

2003b), weakly expressing *VGLUT1*-positive neurons in the pulvinar that project to the cortex, striatum, or amygdala, may be coincident with *VGLUT2*-positive projections, or they could represent distinct projections with different targets in cortical or subcortical areas. In cortex, layers 5B and 6B both contained neurons that weakly expressed *VGLUT2* mRNA alongside many more neurons that densely expressed *VGLUT1* mRNA, and both layers specifically target the ventral pulvinar and layers 3 and 6 of the LGN (Casseday et al., 1979; Usrey and Fitzpatrick, 1996). It is likely that neurons in these V1 layers are related to the fine VGLUT2-positive terminations seen in the recipient locations of both thalamic structures, but whether these terminations are distinct from VGLUT1-positive terminations in the same locations is unknown. The diffuse and even nature of VGLUT1 terminal labeling in every visual structure did not allow us to differentiate between individual VGLUT1-positive projections, but further studies involving colocalized labeling and tracing methods will shed light on the segregation of VGLUT1- and VGLUT2-positive projections from individual visual structures. Overall, VGLUT2 is predominantly found in ascending projections such as retinogeniculate, retinotectal, and tectopulvinar connections while VGLUT1 is predominantly distributed in descending projections such as corticopulvinar and corticogeniculate connections, as well as intrinsic connections in the thalamus and cortex. Both VGLUT1 and VGLUT2 appear to be dually expressed in thalamocortical projections and some corticothalamic projections as well, but further experiments are needed to fully demonstrate their colocalization and identify their respective contributions to synaptic transmission within a single glutamatergic projection.

6.5.2 Functional correlates of VGLUT1- or VGLUT2-positive projections in the tree shrew: comparisons with VGLUT distributions in other species

Recent studies on the distribution of VGLUT1 and VGLUT2 in the mammalian brain have converged on the hypothesis that VGLUT2 is primarily utilized by driving glutamatergic projections while VGLUT1 is utilized by projections that are more modulatory in nature (Herzog et al., 2001; Varoqui et al., 2002; Fremeau et al., 2004a; Weston et al., 2011; Rovó et al., 2012; Balaram et al., 2013). Although, modulatory and driving projections (Sherman and Guillery, 1996) have not been specifically documented in the tree shrew visual system, comparisons of VGLUT1- or VGLUT2-positive projections in the tree shrew with known VGLUT1/modulatory or VGLUT2/driving projections in other species gave us some insight on the functional attributes of these distributions in visual structures. In general, the distribution patterns of VGLUT1 and VGLUT2 in the tree shrew visual system closely resembled those seen in other species. The use of VGLUT2 in retinal projections to the SC and LGN in tree shrews is identical to retinal projections in other mammals (Fujiyama et al., 2003; Land et al., 2004; Gong et al., 2006; Islam and Atoji, 2009; Balaram et al., 2011b; 2013), and retinal projections are known to drive their postsynaptic targets (Sherman and Guillery, 1996; 1998; Sherman, 2005). VGLUT2- positive tectopulvinar projections have been previously identified in tree shrews (Chomsung et al., 2008; Wei et al., 2011) rodents (Hisano et al., 2000) and primates (Balaram et al., 2011b; Baldwin et al., 2013a). However, tectopulvinar projections appear to represent a separate category of terminations that have distinct features from classic driving (i.e. retinogeniculate) or modulatory (i.e. corticogeniculate) projections (Chomsung et al., 2008; Masterson et al., 2009; 2010; Wei et al., 2011). VGLUT2- positive tectogeniculate projections are not present in anthropoid primates (Balaram et al., 2013) but likely exist in prosimian primates (Balaram et al., 2011b), which

closely resemble early primate species (Kaas, 2013). Tectogeniculate projections in rodents likely utilize VGLUT2, since neurons expressing *VGLUT2* mRNA are found across the upper SGS in rats (Fremeau et al., 2001) and squirrels (unpublished results), and further experiments will determine if tectogeniculate terminations can be characterized as classic driving or modulatory projections (Sherman and Guillery, 1996; 1998; Sherman, 2005; Sherman and Guillery, 2006; 2011). LGN layers that do receive tectal projections in tree shrews primarily project to the superficial layers of V1 (Carey et al., 1979; Fitzpatrick et al., 1980)

All projections from the LGN to V1 across rodents, primates, and carnivores are VGLUT2-dominant, consistent with the driving nature of geniculostriate projections (Sherman and Guillery, 1996; Sherman, 2005). However, rodents and primates are known to exhibit low levels of VGLUT1 in geniculostriate projections as well (Fremeau et al., 2001; Fujiyama et al., 2001; Herzog et al., 2001; Balaram et al., 2011a; b; 2013). The same holds true for neurons in the pulvinar complex in primates and the homologous lateral posterior nucleus in rodents. In cortex, the presence of *VGLUT2* mRNA in small populations of V1 neurons has been described in primates (Balaram et al., 2013) but not rodents, although *VGLUT2* mRNA expressing neurons have been described in other rodent cortical areas (Hisano et al., 2000). In primates, neurons expressing *VGLUT2* mRNA in the deep layers of V1 likely target the pulvinar complex and constitute a driving projection within a larger corticothalamocortical framework (Sherman and Guillery, 2011), although corticopulvinar neurons appear to use VGLUT1 in their terminals as well (Rovó et al., 2012).

The predominant use of VGLUT1 in modulatory projections from V1 to the thalamus and midbrain is consistent across rodents and primates as well as tree shrews (Ni et al., 1995; Bellocchio et al., 1998; Fujiyama et al., 2001; Kaneko et al., 2002; Balaram et al., 2011a; 2013).

However, intrinsic V1 projections in primates appear to utilize both VGLUT isoforms, while intrinsic V1 projections in rodents almost exclusively express *VGLUT1* mRNA, placing tree shrews slightly closer to the rodent lineage in this regard. The dual expression of VGLUT1 and VGLUT2 in some projections may contribute to mechanisms of homeostatic plasticity within a glutamatergic circuit (De Gois et al., 2005; Nakamura et al., 2005; Anne and Gasnier, 2014), and since most neurons release more than one neurotransmitter from individual synapses (Hnasko and Edwards, 2012), the co-expression of VGLUT1 and VGLUT2 with other neurotransmitter transporters may contribute to a wide range of signal transmission, perhaps between distinct terminations from an individual projection (Herzog et al., 2001). The results presented here provide further evidence that VGLUT1 and VGLUT2 consistently identify classic driving and modulatory projections in the mammalian visual system, as well as other glutamatergic projections with distinct functional characteristics. Slight changes in the location and target regions of each projection demonstrate that these connections have evolved through the mammalian lineage, and further studies on functional changes within these projections will shed light on the role of VGLUT isoforms in regulating glutamatergic neurotransmission.

CHAPTER 7

Discussion

The primary goals of the preceding chapters were to (1) document the distribution of VGLUT1 and VGLUT2 in visual brain structures across a range of mammalian species, to (2) determine whether each VGLUT isoform is restricted to functionally distinct classes of glutamatergic projections between these structures. Collective results from Old World macaque monkeys, New World squirrel and owl monkeys, prosimian galagos, and tree shrews show that each VGLUT isoform is differentially expressed in subsets of glutamatergic visual projections, with limited overlap in individual connections between visual structures. When their distributions are compared to a range of classification systems for glutamatergic projections (Rockland and Pandya, 1979; Felleman and Van Essen, 1991; Callaway, 1998; Sherman, 2005), it is evident that VGLUT1 predominates in hierarchical feedback or modulatory glutamatergic projections while VGLUT2 predominates in hierarchical feedforward or driving projections in the mammalian visual system.

Definitions of driving and modulatory glutamatergic projections in the central nervous system are based on two components. First, the anatomical features of glutamatergic synapses formed by driving or modulatory projections are quite distinct from each other, and remain consistent across a wide range of glutamatergic connections in mammalian brains (Sherman and Guillery, 1996; 1998; Sherman, 2001; 2005; 2007; 2012). Second, the functional characteristics of action potentials and postsynaptic responses produced by driving or modulatory projections are also distinct, and the identification of these characteristics in the terminal zones of an individual projection can often indicate that projection is driving or modulatory in nature. A brief

review of the anatomical and functional characteristics of driving and modulatory projections, with respect to mammalian sensory systems, follows below. The distribution patterns of VGLUT1 and VGLUT2, when correlated with patterns of afferent terminations from individual visual projections, suggest that these two isoforms are segregated in driving and modulatory connections. However, consistent exceptions to these distinctions do exist, and are worth considering in relation to the larger construct of driving and modulatory projections in mammalian sensory systems.

7.1 Anatomical features of driving and modulatory glutamatergic projections in mammalian sensory systems: comparisons with the synaptic terminations of VGLUT1- and VGLUT2-positive projections

All glutamatergic terminations, whether driving or modulatory, have some anatomical features in common. First, glutamatergic projections across the CNS make asymmetric synapses on the dendrites of their postsynaptic cells, which differs from the symmetric synapses made by GABAergic projections as well as the variable synaptic contacts made by cholinergic and monoaminergic synapses (Webster, 2001). Second, glutamatergic terminals primarily make axo-somatic or axo-dendritic contacts with their postsynaptic targets, although some evidence of dendrodenritic synapses exist (Fremeau et al., 2002), which is similar to GABAergic terminals but distinct from most neuromodulatory terminations (Webster, 2001). Within these criteria, driving and modulatory synapses have some distinctions. Driving projections tend to make axosomatic contacts on the base of proximal dendrites or the cell soma of their postsynaptic targets, thus shortening the propagation time of individual excitatory postsynaptic potentials (EPSPs) and increasing the probability of a full action potential in their target neurons.

Modulatory projections tend to make axodendritic contacts on the distal dendrites of their postsynaptic targets, which produces variations in the propagation times of individual EPSPs depending on their distance from the cell soma, and allows for conduction interference from inhibitory or neuromodulatory synaptic contacts positioned closer to the cell body (Sherman and Guillery, 1996). In most visual structures, modulatory synapses significantly outnumber driving synapses (Sherman and Guillery, 2002; Sherman, 2005), but the effects of driving synapses still dominate the neural output of their target cells (discussed below). Individual driving and modulatory terminals also differ in size; driving terminals are consistently larger than modulatory terminals regardless of their origin of projection (Rockland, 1996; Crick and Koch, 1998; Sherman and Guillery, 1998). Driving terminals also tend to form clusters of boutons on the branched ends of an axon arbor while modulatory terminals tend to make individual contacts along the length of a primary axon (Crick and Koch, 1998; Sherman and Guillery, 1998; Sherman, 2005). Axons in driving projections are thicker and more arborized than axons in modulatory projections (Sherman, 2001), and are defined as class 1 (driving) and class 2 (modulatory) axons respectively (Guillery, 1966; Sherman, 2001).

The origins and terminations of glutamatergic projections within brain regions can be used to identify them as driving or modulatory in nature, particularly when functional data on these projections is limited. However, determining the locations of a single projection's origin and terminations is difficult and data on these types of connections is lacking for many brain structures (Sherman and Guillery, 1996; 2006). The limited data that does exist also reveals subcategories of driving and modulatory projections in many regions. In the thalamus for example, one class of driving projections originate in sensory relay nuclei and terminate in layer 4 of primary sensory cortical areas while modulatory projections arise in layer 6 of the target

cortical areas and project diffusely across their thalamic relay nuclei; these thalamic regions, with primary projections to cortex and reciprocal modulatory feedback projections, are designated as first-order nuclei (Sherman, 2001; 2005). Another class of driving projections originates in layer 5 of cortical areas and projects subcortically to another group of thalamic structures known as higher-order nuclei, which subsequently send modulatory projections to multiple layers of other cortical areas. Anatomical and functional characteristics of driving terminals in first-order and higher-order nuclei are similar in some cases (Sherman and Guillery, 2002), but subtle differences in their distribution and neural output (Van Horn and Sherman, 2007; Sherman and Guillery, 2011; Sherman, 2012) suggest that these two subcategories have distinct functions in excitatory neurotransmission.

Many of the anatomical features of VGLUT1- and VGLUT2-positive terminations align well with features of modulatory and driving terminations. Both VGLUT1 and VGLUT2 terminals make asymmetric synapses on their target neurons (Bellocchio et al., 1998; Aihara et al., 2000; Takamori et al., 2000; Fremeau et al., 2001), but VGLUT2-positive terminals tend to contact the proximal dendrites or soma of their target cells while VGLUT1-positive terminals make contacts along distal dendrites (Altschuler et al., 2008), similar to driving and modulatory projections. In visual structures (chapters 2-6), dense distributions of VGLUT1-positive terminals appear to outnumber VGLUT2-positive terminals in the same location (chapters 2-6) (Masterson et al., 2009), much like modulatory projections that outnumber driving projections, but further quantification of this difference is required. Although relative axon sizes of VGLUT1- and VGLUT2- positive projections have not been measured, VGLUT2-positive terminations are consistently larger than VGLUT1-positive terminations (Kaneko and Fujiyama, 2002; Todd et al., 2003; Persson et al., 2006; Graziano et al., 2008; Rovó et al., 2012), and

VGLUT2-positive projections tend to form clusters of terminals on branched axon arbors while VGLUT1-positive projections tend to make diffuse contacts over wide regions of neuropil in their target structures (Kaneko and Fujiyama, 2002; Li et al., 2003; but see Persson et al., 2006; Altschuler et al., 2008). Thus, many features of VGLUT1- and VGLUT2-positive synapses correlate well with features of modulatory and driving terminations in the central nervous system.

7.2 Functional characteristics of driving and modulatory glutamatergic projections in mammalian sensory systems: correlations with neural activity in VGLUT1- and VGLUT2-positive projections

Driving and modulatory glutamatergic projections are tautologically defined by their functional characteristics. Driving projections significantly alter the postsynaptic responses of their target cells; they "carry the message, defining essential patterns of activity" (Sherman and Guillery, 1998), "by themselves, can make the relevant neurons fire strongly" (Crick and Koch, 1998), "bring the main information to a cell or cell group" and "dominate the receptive field properties of their target cells" (Sherman and Guillery, 2002). Modulatory projections only slightly alter the postsynaptic responses of their target cells; they "alter the effectiveness of the drive without contributing significantly to the general pattern of message" (Sherman and Guillery, 1998), and "by themselves, cannot make the relevant neurons fire strongly, but can modify the firing produced by the driving inputs" (Crick and Koch, 1998). The functional identification of a driving or modulatory projection is based on how well correlated the spiking activity of a given neuron is to its target cell. For example, in the visual system, a single action potential from a retinal ganglion cell gives rise to a single action potential with a fixed latency in

its target LGN cell; when plotted in the form of a cross-correlogram (Sherman and Guillery, 1998), this driving projection produces a sharp, narrow peak over a relatively smooth baseline of activity. Conversely, a single action potential from a layer 6 neuron in V1 does not usually generate a single action potential in its target LGN neuron. Instead, the summed potentials from many modulatory inputs on a single LGN neuron will gradually produce a single EPSP. When plotted in the form of a cross-correlogram, modulatory projections produce a small peak with a broad base over a relatively high level of baseline activity (Sherman and Guillery, 1998). Thus, the level of correlated activity between projection neurons and their targets within a glutamatergic projection may identify it as driving or modulatory in nature, particularly in brain structures where anatomical data on projection terminals is scant.

Another contributing factor to functional differences in the neural output of driving and modulatory projections is the complement of glutamate receptors present on the postsynaptic surface of target neurons. The postsynaptic contacts of driving projections contain ionotropic glutamate receptors (iGluRs), which are rapidly activated following an EPSP and generate immediate action potentials by opening ion channels along the postsynaptic membrane. The rapid activation and deactivation of these channels allows for the precise coding of high frequency information during sustained periods of neural activity. The postsynaptic contacts of modulatory projections contain both ionotropic and metabotropic glutamate receptors (mGluRs), which indirectly open ion channels via molecular signaling cascades within the neuron. The slower and more variable effects of mGluRs compared to iGluRs allows modulatory terminals to generate a wide range of EPSPs that subsequently modify the neural output of their target neurons without necessarily generating a full action potential at any time (Sherman and Guillery, 1996; Sherman, 2001; 2005). Under conditions of repetitive stimulation, driving projections

exhibit paired-pulse depression over time, where the size of the postsynaptic response decreases due to the reduction in available synaptic vesicles for neurotransmitter release. Modulatory projections exhibit paired-pulse facilitation instead, where the size of the postsynaptic response increases due to presynaptic fluctuations in calcium conductance (Kandel et al., 2000). In general, synapses with a low probability of initial vesicle release exhibit paired-pulse facilitation while synapses with a high probability of initial vesicle release exhibit paired-pulse depression.

Although functional distinctions between VGLUT1- and VGLUT2-positive projections have not been extensively studied, some characteristics have been determined and these traits correlate well with functional differences between driving and modulatory projections. VGLUT1-positive synapses tend to have lower release probabilities while VGLUT2-positive synapses tend to have higher release probabilities (Fremeau et al., 2001; Herzog et al., 2001; Fremeau et al., 2004a), and VGLUT1-positive synapses exhibit paired-pulse facilitation while VGLUT2-positive synapses exhibit paired-pulse depression instead (Varoqui et al., 2002; Fremeau et al., 2004a; Weston et al., 2011). Sensory projections from the retina to the lateral geniculate nucleus and superior colliculus, from the inferior colliculus to the medial geniculate nucleus, and from the brainstem and spinal cord to the ventroposterior nucleus are all considered as driving projections based on correlated patterns of activity (Sherman and Guillery, 1996; 1998; 2002; Sherman, 2005; 2007; 2012) and all of them utilize VGLUT2 (chapters 2-6)(Fujiyama et al., 2003; Land et al., 2004; Graziano et al., 2008; Hackett et al., 2011; Ito et al., 2011). Conversely, layer 6 projections from primary visual cortex to the lateral geniculate nucleus, from primary auditory cortex to the medial geniculate nucleus, and from primary somatosensory cortex to the ventroposterior nucleus are all considered modulatory projections(Sherman and Guillery, 1996; 1998; 2002; Sherman, 2005; 2007; 2012), and these

projections utilize VGLUT1 (chapters 2-6) (Kaneko and Fujiyama, 2002; Graziano et al., 2008). Direct evidence for the apposition of VGLUT1- or VGLUT2-positive synapses to specific complements of ionotropic or metabotropic glutamate receptors does not exist to date, but given the segregated distribution of VGLUT1 and VGLUT2 in the projections discussed above, it is likely that VGLUT2-positive synapses act on iGluRs while VGLUT1-positive synapses act on mGluRs as well as iGluRs to produce excitatory postsynaptic potentials. Thus, driving projections may preferentially utilize VGLUT2 while modulatory projections utilize VGLUT1 to produce distinct patterns of neural activity in their target cells.

7.3 Other glutamatergic projections in mammalian sensory systems: the many exceptions to the rule

While some glutamatergic projections can be classically defined as driving or modulatory in nature, the vast majority of glutamatergic connections between sensory brain structures have features of both driving and modulatory projections or have separate anatomical and functional qualities altogether, and in these instances, the segregation of VGLUT1 and VGLUT2 within individual projections is less distinct. First-order thalamic nuclei such as the lateral geniculate nucleus, medial geniculate nucleus, and ventroposterior nucleus all have driving inputs from the sensory periphery that contain VGLUT2 and modulatory inputs from cortex that contain VGLUT1. However, higher-order thalamic nuclei such as parts of the pulvinar or medial dorsal nucleus receive driving projections from layer 5 of one cortical area and send driving projections to other cortical areas that usually terminate in layer 4, as well as modulatory projections back to the first cortical area that terminate diffusely across the superficial and deep layers (Sherman, 2005; 2007; Sherman and Guillery, 2011). Projections from layer 5 of most cortical areas

primarily utilize VGLUT1 instead of VGLUT2, and neurons in higher-order nuclei such as parts of the pulvinar express both VGLUT1 and VGLUT2 (chapters 2-6)(Rovó et al., 2012). Putative driving projections from the pulvinar to V2 are known to utilize VGLUT2 while similar projections from V1 to V2 utilize VGLUT1 instead (Marion et al., 2013), but both isoforms may also be coexpressed in the same pulvinar neurons, further complicating the segregation of VGLUT1 and VGLUT2 to modulatory and driving projections. In fact, most first-order thalamic relay nuclei also coexpress VGLUT1 and VGLUT2 (Herzog et al., 2001; Fremeau et al., 2004b; Ito et al., 2011; Rovó et al., 2012), and it is unclear whether both isoforms are consistently used in the same driving terminations, or each isoform is separately utilized in a driving projection to cortex or modulatory projection to another subcortical structure such as the thalamic reticular nucleus (Sherman and Guillery, 1998; Sherman, 2007). Colocalization of the two VGLUT proteins in terminals from first order relay nuclei has been demonstrated in primary somatosensory cortex (Graziano et al., 2008), but similar evidence in the auditory or visual systems does not exist. Thalamic relay nuclei also exhibit two modes of firing activity, burst and tonic (Sherman and Guillery, 1996; 1998; Sherman, 2005; 2012), which could be mediated by vesicle pools with distinct release properties such as those exhibited by VGLUT1 and VGLUT2, but this requires demonstration of their colocalization within the same synapses in layer 4 of sensory cortex.

Glutamatergic projections outside of the thalamus also blur the boundaries between traditional driving and modulatory projections. Most neurons from the superior colliculus that project to the lateral posterior nucleus or pulvinar complex solely utilize VGLUT2 across a range of species (chapters 2-6), but these projections have features of both driving and modulatory projections (Masterson et al., 2009; Wei et al., 2011), and some tectopulvinar projections don't

appear to utilize VGLUT2 (Baldwin and Kaas, 2012). Projections through auditory brainstem structures also contain variable populations of neurons that express either VGLUT1 or VGLUT2, or VGLUT1 and VGLUT2 (Ito and Oliver, 2010; Ito et al., 2011; Storace et al., 2012), and the driving or modulatory nature of these projections is not well-defined. In the somatosensory system, parallel pathways through the cuneate, gracile, and principal trigeminal nuclei express multiple populations of VGLUT1- and VGLUT2-positive synapses, but outside of the ventroposterior nucleus (Graziano et al., 2008), their role in driving or modulating neural activity is less defined. The driving or modulatory nature of corticocortical projections is also difficult to determine given the extensive interconnectivity of cortical areas (Crick and Koch, 1998), particularly in primate brains (Casagrande and Kaas, 1994). The dense and abundant expression of *VGLUT1* mRNA by most cortical neurons suggest that these projections mainly utilize only one VGLUT isoform in their terminations, regardless of whether the projection is driving or modulatory in nature. However, a subset of cortical neurons do express *VGLUT2* mRNA (Hisano et al., 2000; Kaneko and Fujiyama, 2002) (chapters 2-6) and their role in driving or modulatory transmission is unknown as well. Further investigations that characterize the functional contributions of individual glutamatergic projections to larger sensory networks, as well as the distributions of VGLUT1 and VGLUT2 within each projection will elucidate whether VGLUT1 and VGLUT2 truly differentiate between these two projection types.

REFERENCES

Abplanalp P. 1970. Some subcortical connections of the visual system in tree shrews and squirrels. Brain Behav Evol 3:155–168.

Adams MM, Hof PR, Gattass R, Webster MJ, Ungerleider LG. 2000. Visual cortical projections and chemoarchitecture of macaque monkey pulvinar. J Comp Neurol 419:377–393.

Aihara Y, Mashima H, Onda H, Hisano S, Kasuya H, Hori T, Yamada S, Tomura H, Yamada Y, Inoue I. 2000. Molecular Cloning of a Novel Brain□Type Na+□Dependent Inorganic Phosphate Cotransporter. J Neurochem 74:2622–2625.

Albano JE, Norton TT, Hall WC. 1979. Laminar origin of projections from the superficial layers of the superior colliculus in the tree shrew, Tupaia glis. Brain Res 173:1–11.

Allman J, McGuinness E. 1988. Visual cortex in primates. In: Neurosciences: Comparative Primate Biology. Vol. 4. Alan R Liss Inc. p 279–326.

Allman JM, Kaas JH. 1971. Representation of the visual field in striate and adjoining cortex of the owl monkey(Aotus trivirgatus). Brain Res 35:89–106.

Altschuler RA, Tong L, Holt AG, Oliver DL. 2008. Immunolocalization of vesicular glutamate transporters 1 and 2 in the rat inferior colliculus. NSC 154:226–232.

Amilhon B, Lepicard E, Renoir T, Mongeau R, Popa D, Poirel O, Miot S, Gras C, Gardier AM, Gallego J, Hamon M, Lanfumey L, Gasnier B, Giros B, Mestikawy El S. 2010. VGLUT3 (Vesicular Glutamate Transporter Type 3) Contribution to the Regulation of Serotonergic Transmission and Anxiety. Journal of Neuroscience 30:2198–2210.

Anderson JC, Martin KAC. 2009. The synaptic connections between cortical areas V1 and V2 in macaque monkey. Journal of Neuroscience 29:11283–11293.

Anne C, Gasnier B. 2014. Vesicular neurotransmitter transporters: mechanistic aspects. Curr Top Membr 73:149–174.

Bai L, Xu H, Collins JF, Ghishan FK. 2001. Molecular and Functional Analysis of a Novel Neuronal Vesicular Glutamate Transporter. J Biol Chem 276:36764–36769.

Balaram P, Hackett TA, Kaas JH. 2011a. VGLUT1 mRNA and protein expression in the visual system of prosimian galagos (Otolemur garnetti). Eye Brain 2011:81–98.

Balaram P, Hackett TA, Kaas JH. 2013. Differential expression of vesicular glutamate transporters 1 and 2 may identify distinct modes of glutamatergic transmission in the macaque visual system. Journal of Chemical Neuroanatomy 50-51:21–38.

Balaram P, Kaas JH. 2014. Towards a unified scheme of cortical lamination for primary visual

cortex across primates: insights from NeuN and VGLUT2 immunoreactivity. Front Neuroanat 8.

Balaram P, Takahata T, Kaas JH. 2011b. VGLUT2 mRNA and protein expression in the visual thalamus and midbrain of prosimian galagos (Otolemur garnetti). Eye Brain 2011:5–15.

Baldwin MKL, Balaram P, Kaas JH. 2013a. Projections of the superior colliculus to the pulvinar in prosimian galagos (Otolemur garnettii) and VGLUT2 staining of the visual pulvinar. J Comp Neurol 521:1664–1682.

Baldwin MKL, Kaas JH. 2012. Cortical projections to the superior colliculus in prosimian galagos (Otolemur garnetti). J Comp Neurol 520:2002–2020.

Baldwin MKL, Wei H, Reed JL, Bickford ME, Petry HM, Kaas JH. 2013b. Cortical projections to the superior colliculus in tree shrews (Tupaia belangeri). J Comp Neurol 521:1614–1632.

Baldwin MKL, Wong P, Reed JL, Kaas JH. 2011. Superior colliculus connections with visual thalamus in gray squirrels (Sciurus carolinensis): evidence for four subdivisions within the pulvinar complex. J Comp Neurol 519:1071–1094.

Barroso-Chinea P, Castle M, Aymerich MS, Lanciego JL. 2008. Expression of vesicular glutamate transporters 1 and 2 in the cells of origin of the rat thalamostriatal pathway. Journal of Chemical Neuroanatomy 35:101–107.

Barroso-Chinea P, Castle M, Aymerich MS, Pérez-Manso M, Erro E, Tuñon T, Lanciego JL. 2007. Expression of the mRNAs encoding for the vesicular glutamate transporters 1 and 2 in the rat thalamus. J Comp Neurol 501:703–715.

Bellocchio EE, Hu H, Pohorille A, Chan J, Pickel VM, Edwards RH. 1998. The localization of the brain-specific inorganic phosphate transporter suggests a specific presynaptic role in glutamatergic transmission. J Neurosci 18:8648–8659.

Bellocchio EE, Reimer RJ, Fremeau RT, Edwards RH. 2000. Uptake of glutamate into synaptic vesicles by an inorganic phosphate transporter. Science 289:957–960.

Bender DB. 1983. Visual activation of neurons in the primate pulvinar depends on cortex but not colliculus. Brain Res 279:258–261.

Benevento LA, Fallon JH. 1975. The ascending projections of the superior colliculus in the rhesus monkey (Macaca mulatta). J Comp Neurol 160:339–361.

Benevento LA, Standage GP. 1983. The organization of projections of the retinorecipient and nonretinorecipient nuclei of the pretectal complex and layers of the superior colliculus to the lateral pulvinar and medial pulvinar in the macaque monkey. J Comp Neurol 217:307–336.

Benevento LA, Yoshida K. 1981. The afferent and efferent organization of the lateral geniculo-prestriate pathways in the macaque monkey. J Comp Neurol 203:455–474.

Berman RA, Wurtz RH. 2010. Functional identification of a pulvinar path from superior colliculus to cortical area MT. Journal of Neuroscience 30:6342–6354.

Bernard A, Lubbers LS, Tanis KQ, Luo R, Podtelezhnikov AA, Finney EM, McWhorter MME, Serikawa K, Lemon T, Morgan R, Copeland C, Smith K, Cullen V, Davis-Turak J, Lee C-K, Sunkin SM, Loboda AP, Levine DM, Stone DJ, Hawrylycz MJ, Roberts CJ, Jones AR, Geschwind DH, Lein ES. 2012. Transcriptional architecture of the primate neocortex. Neuron 73:1083–1099.

Bickford ME, Ramcharan E, Godwin DW, Erişir A, Gnadt J, Sherman SM. 2000. Neurotransmitters contained in the subcortical extraretinal inputs to the monkey lateral geniculate nucleus. J Comp Neurol 424:701–717.

Billings-Gagliardi S, Chan-Palay V, Palay SL. 1974. A review of lamination in Area 17 of the visual cortex of Macaca mulatta. J Neurocytol 3:619–629.

Blakely RD, Edwards RH. 2012. Vesicular and plasma membrane transporters for neurotransmitters. Cold Spring Harb Perspect Biol 4.

Blasdel GG, Lund JS. 1983. Termination of afferent axons in macaque striate cortex. J Neurosci 3:1389–1413.

Boulland J-L, Qureshi T, Seal RP, Rafiki A, Gundersen V, Bergersen LH, Fremeau RT, Edwards RH, Storm-Mathisen J, Chaudhry FA. 2004. Expression of the vesicular glutamate transporters during development indicates the widespread corelease of multiple neurotransmitters. J Comp Neurol 480:264–280.

Brodmann K. 1909. Vergleichende Lokalisationslehre der Gro hirnrinde. Leipzig: Verlag von Johann Ambrosius Barth.

Brunso-Bechtold JK, Casagrande VA. 1982. Early postnatal development of laminar characteristics in the dorsal lateral geniculate nucleus of the tree shrew. J Neurosci 2:589–597.

Bryant KL, Suwyn C, Reding KM, Smiley JF, Hackett TA, Preuss TM. 2012. Evidence for ape and human specializations in geniculostriate projections from VGLUT2 immunohistochemistry. Brain Behav Evol 80:210–221.

Bullier J, Kennedy H. 1983. Projection of the lateral geniculate nucleus onto cortical area V2 in the macaque monkey. Exp Brain Res 53:168–172.

Bullier J. 2004. Communications between cortical areas of the visual system. The visual neurosciences 2:522–540.

Callaway EM. 1998. Local circuits in primary visual cortex of the macaque monkey. Annu Rev Neurosci 21:47–74.

Campbell CBG, Jane JA, Yashon D. 1967. The retinal projections of the tree shrew and

hedgehog. Brain Res 5:406–418.

Campos-Ortega JA, Hayhow WR. 1972. On the organisation of the visual cortical projection to the pulvinar in Macaca mulatta. Brain Behav Evol 6:394–423.

Carey RG, Fitzpatrick D, Diamond IT. 1979. Layer I of striate cortex of Tupaia glis and Galago senegalensis: projections from thalamus and claustrum revealed by retrograde transport of horseradish peroxidase. J Comp Neurol 186:393–437.

Casagrande VA, DeBruyn EJ. 1982. The galago visual system: aspects of normal organization and developmental plasticity. In: The lesser bushbaby (Galago) as an animal model: selected topics. CRC Press, Boca Raton, Fla. p 138–168.

Casagrande VA, Harting JK. 1975. Transneuronal transport of tritiated fucose and proline in the visual pathways of tree shrew Tupaia glis. Brain Res 96:367–372.

Casagrande VA, Joseph R. 1980. Morphological effects of monocular deprivation and recovery on the dorsal lateral geniculate nucleus in galago. J Comp Neurol 194:413–426.

Casagrande VA, Kaas JH. 1994. The afferent, intrinsic, and efferent connections of primary visual cortex in primates. In: Peters A, Rockland KS, editors. Cerebral Cortex: Primary Visual Cortex of Primates. Vol. 10. New York: Plenum Press. p 201–259.

Casagrande VA, Khaytin I, Boyd JD. 2006. The evolution of parallel visual pathways in primates. In: Preuss TM, Kaas JH, editors. Evolution of the nervous system. London: Elsevier.

Casagrande VA, Norton TT. 1991. The neural basis of vision function: vision and visual dysfunction. In: The Neural Basis of Vision Function: Vision and Visual Dysfunction. Vol. 4. p 41–84.

Casagrande VA, Yazar F, Jones KD, Ding Y. 2007. The morphology of the koniocellular axon pathway in the macaque monkey. Cereb Cortex 17:2334–2345.

Casagrande VA. 1994. A third parallel visual pathway to primate area V1. Trends in Neurosciences 17:305–310.

Casseday JH, Jones DR, Diamond IT. 1979. Projections from cortex to tectum in the tree shrew,Tupaia glis. J Comp Neurol 185:253–291.

Cheng G, Kaminski HJ, Gong B, Zhou L, Hatala D, Howell SJ, Zhou X, Mustari MJ. 2008. Monocular visual deprivation in macaque monkeys: a profile in the gene expression of lateral geniculate nucleus by laser capture microdissection. Mol Vis 14:1401–1413.

Chomsung RD, Petry HM, Bickford ME. 2008. Ultrastructural examination of diffuse and specific tectopulvinar projections in the tree shrew. J Comp Neurol 510:24–46.

Chomsung RD, Wei H, Day-Brown JD, Petry HM, Bickford ME. 2010. Synaptic organization of

connections between the temporal cortex and pulvinar nucleus of the tree shrew. Cerebral Cortex 20:997–1011.

Clark WELG. 1925. The Visual Cortex of Primates. Journal of Anatomy 59:350.

Clark WELG. 1929. The thalamus of Tupaia minor. Journal of Anatomy.

Clark WELG. 1942. The visual centres of the brain and their connexions. Physiol Rev 22:205–232.

Conley M, Fitzpatrick D, Diamond IT. 1984. The laminar organization of the lateral geniculate body and the striate cortex in the tree shrew (Tupaia glis). J Neurosci 4:171–197.

Conley M, Fitzpatrick D. 1989. Morphology of retinogeniculate axons in the macaque. Vis Neurosci 2:287–296.

Conway JL, Schiller PH. 1983. Laminar organization of tree shrew dorsal lateral geniculate nucleus. Journal of Neurophysiology 50:1330–1342.

Covic EN, Sherman SM. 2011. Synaptic properties of connections between the primary and secondary auditory cortices in mice. Cerebral Cortex 21:2425–2441.

Crick F, Koch C. 1998. Constraints on cortical and thalamic projections: the no-strong-loops hypothesis. Nature 391:245–250.

Cusick CG, Scripter JL, Darensbourg JG, Weber JT. 1993. Chemoarchitectonic subdivisions of the visual pulvinar in monkeys and their connectional relations with the middle temporal and rostral dorsolateral visual areas, MT and DLr. J Comp Neurol 336:1–30.

Dai Y, Sun X. 2005. Expression of Immediate Early Genes and Calbindin D-28k in the Lateral Geniculate Nucleus and the Retina of Rats With Optic Nerve Crush. Investigative Ophtalmology and Visual Science.

Danbolt NC, Storm-Mathisen J, Ottersen OP. 1994. Sodium/potassium-coupled glutamate transporters, a "new" family of eukaryotic proteins: do they have “new” physiological roles and could they be new targets for pharmacological intervention? Prog Brain Res 100:53–60.

Daniels RW, Collins CA, Gelfand MV, Dant J, Brooks ES, Krantz DE, DiAntonio A. 2004. Increased expression of the Drosophila vesicular glutamate transporter leads to excess glutamate release and a compensatory decrease in quantal content. Journal of Neuroscience 24:10466–10474.

Davanger S, Manahan-Vaughan D, Mulle C, Storm-Mathisen J, Ottersen OP. 2009. Protein trafficking, targeting, and interaction at the glutamate synapse. NSC 158:1–3.

De Gois S, Schäfer MK-H, Defamie N, Chen C, Ricci A, Weihe E, Varoqui H, Erickson JD. 2005. Homeostatic scaling of vesicular glutamate and GABA transporter expression in rat neocortical circuits. Journal of Neuroscience 25:7121–7133.

DeYoe EA, Van Essen DC. 1985. Segregation of efferent connections and receptive field properties in visual area V2 of the macaque. Nature 317:58–61.

Diamond IT, Conley M, Fitzpatrick D, Raczkowski D. 1991. Evidence for separate pathways within the tecto-geniculate projection in the tree shrew. Proc Natl Acad Sci USA 88:1315–1319.

Diamond IT, Conley M, Itoh K, Fitzpatrick D. 1985. Laminar organization of geniculocortical projections in Galago senegalensis and Aotus trivirgatus. J Comp Neurol 242:584–610.

Diamond IT, Fitzpatrick D, Conley M. 1992. A projection from the parabigeminal nucleus to the pulvinar nucleus in Galago. J Comp Neurol 316:375–382.

Diamond IT, Snyder M, Killackey H, Jane J, Hall WC. 1970. Thalamo-cortical projections in the tree shrew (Tupaia glis). J Comp Neurol 139:273–306.

Disbrow JK, Gershten MJ, Ruth JA. 1982. Uptake of L-[3H] glutamic acid by crude and purified synaptic vesicles from rat brain. Biochem Biophys Res Commun 108:1221–1227.

Djamgoz MBA, Stell WK. 1984. Tetrodotoxin does not block the axonal transmission of S-potentials in goldfish retina. Neuroscience Letters 49:233–238.

Doty RW, Glickstein M, Calvin WH. 1966. Lamination of the lateral geniculate nucleus in the squirrel monkey, Saimiri sciureus. J Comp Neurol 127:335–340.

Edwards RH. 2007. The Neurotransmitter Cycle and Quantal Size. Neuron 55:835–858.

Erickson JD, De Gois S, Varoqui H, Schäfer MK-H, Weihe E. 2006. Activity-dependent regulation of vesicular glutamate and GABA transporters: a means to scale quantal size. Neurochem Int 48:643–649.

Felleman DJ, Van Essen DC. 1991. Distributed hierarchical processing in the primate cerebral cortex. Cereb Cortex 1:1–47.

Fitzpatrick D, Carey RG, Diamond IT. 1980. The projection of the superior colliculus upon the lateral geniculate body in Tupaia glis and Galago senegalensis. Brain Res 194:494–499.

Fitzpatrick D, Itoh K, Diamond IT. 1983. The laminar organization of the lateral geniculate body and the striate cortex in the squirrel monkey (Saimiri sciureus). J Neurosci 3:673–702.

Fitzpatrick D, Usrey WM, Schofield BR, Einstein G. 1994. The sublaminar organization of corticogeniculate neurons in layer 6 of macaque striate cortex. Vis Neurosci 11:307–315.

Fitzpatrick D. 1996. The functional organization of local circuits in visual cortex: insights from the study of tree shrew striate cortex. Cereb Cortex 6:329–341.

Florence SL, Casagrande VA. 1987. Organization of individual afferent axons in layer IV of striate cortex in a primate. J Neurosci 7:3850–3868.

Florence SL, Sesma MA, casagrande VA. 1983. Morphology of geniculo-striate afferents in a prosimian primate. Brain Res 270:127–130.

Foss SM, Li H, Santos MS, Edwards RH, Voglmaier SM. 2013. Multiple dileucine-like motifs direct VGLUT1 trafficking. Journal of Neuroscience 33:10647–10660.

Fremeau RT, Burman J, Qureshi T, Tran CH, Proctor J, Johnson J, Zhang H, Sulzer D, Copenhagen DR, Storm-Mathisen J, Reimer RJ, Chaudhry FA, Edwards RH. 2002. The identification of vesicular glutamate transporter 3 suggests novel modes of signaling by glutamate. Proc Natl Acad Sci USA 99:14488–14493.

Fremeau RT, Kam K, Qureshi T, Johnson J, Copenhagen DR, Storm-Mathisen J, Chaudhry FA, Nicoll RA, Edwards RH. 2004a. Vesicular glutamate transporters 1 and 2 target to functionally distinct synaptic release sites. Science 304:1815–1819.

Fremeau RT, Troyer MD, Pahner I, Nygaard GO, Tran CH, Reimer RJ, Bellocchio EE, Fortin D, Storm-Mathisen J, Edwards RH. 2001. The expression of vesicular glutamate transporters defines two classes of excitatory synapse. Neuron 31:247–260.

Fremeau RT, Voglmaier S, Seal RP, Edwards RH. 2004b. VGLUTs define subsets of excitatory neurons and suggest novel roles for glutamate. Trends in Neurosciences 27:98–103.

Fries W. 1984. Cortical projections to the superior colliculus in the macaque monkey: a retrograde study using horseradish peroxidase. J Comp Neurol 230:55–76.

Fujiyama F, Furuta T, Kaneko T. 2001. Immunocytochemical localization of candidates for vesicular glutamate transporters in the rat cerebral cortex. J Comp Neurol 435:379–387.

Fujiyama F, Hioki H, Tomioka R, Taki K, Tamamaki N, Nomura S, Okamoto K, Kaneko T. 2003. Changes of immunocytochemical localization of vesicular glutamate transporters in the rat visual system after the retinofugal denervation. J Comp Neurol 465:234–249.

Fyk-Kolodziej B, Dzhagaryan A, Qin P, Pourcho RG. 2004. Immunocytochemical localization of three vesicular glutamate transporters in the cat retina. J Comp Neurol 475:518–530.

Gamlin PDR, McDougal DH, Pokorny J, Smith VC, Yau K-W, Dacey DM. 2007. Human and macaque pupil responses driven by melanopsin-containing retinal ganglion cells. Vision Res 47:946–954.

Garcia-Marin V, Ahmed TH, Afzal YC, Hawken MJ. 2013. Distribution of vesicular glutamate transporter 2 (VGluT2) in the primary visual cortex of the macaque and human. J Comp Neurol 521:130–151.

Garey LJ. 2006. Brodmann's ‘Localisation in the cerebral cortex’. 3rd ed. New York: Springer Science+Business Media.

Glendenning KK, Hall JA, Diamond IT, Hall WC. 1975. The pulvinar nucleus of Galago senegalensis. J Comp Neurol 161:419–458.

Glendenning KK, Kofron EA, Diamond IT. 1976. Laminar organization of projections of the lateral geniculate nucleus to the striate cortex in Galago. Brain Res 105:538–546.

Glickstein M. 1967. Laminar structure of the dorsal lateral geniculate nucleus in the tree shrew (Tupaia glis). J Comp Neurol 131:93–102.

Glickstein M. 1969. Organization of the visual pathways. Science 164:917–926.

Gong J, Jellali A, Mutterer J, Sahel JA, Rendon A, Picaud S. 2006. Distribution of vesicular glutamate transporters in rat and human retina. Brain Res 1082:73–85.

Graham J, Lin CS, kaas JH. 1979. Subcortical projections of six visual cortical areas in the owl monkey, Aotus trivirgatus. J Comp Neurol 187:557–580.

Graham J. 1982. Some topographical connections of the striate cortex with subcortical structures in Macaca fascicularis. Exp Brain Res 47:1–14.

Gras C, Herzog E, Bellenchi GC, Bernard V, Ravassard P, Pohl M, Gasnier B, Giros B, Mestikawy El S. 2002. A third vesicular glutamate transporter expressed by cholinergic and serotoninergic neurons. Journal of Neuroscience 22:5442–5451.

Graziano A, Liu X-B, Murray KD, Jones EG. 2008. Vesicular glutamate transporters define two sets of glutamatergic afferents to the somatosensory thalamus and two thalamocortical projections in the mouse. J Comp Neurol 507:1258–1276.

Guillery RW. 1966. A study of Golgi preparations from the dorsal lateral geniculate nucleus of the adult cat. J Comp Neurol 128:21–50.

Gutierrez C, Yaun A, Cusick CG. 1995. Neurochemical subdivisions of the inferior pulvinar in macaque monkeys. J Comp Neurol 363:545–562.

Hackett TA, la Mothe de LA. 2009. Regional and laminar distribution of the vesicular glutamate transporter, VGluT2, in the macaque monkey auditory cortex. Journal of Chemical Neuroanatomy 38:106–116.

Hackett TA, Takahata T, Balaram P. 2011. VGLUT1 and VGLUT2 mRNA expression in the primate auditory pathway. Hear Res 274:129–141.

Hackett TA. 2011. Information flow in the auditory cortical network. Hear Res 271:133–146.

Hajdu F, Hässler R, Somogyi G. 1982. Neuronal and synaptic organization of the lateral geniculate nucleus of the tree shrew, Tupaia glis. Cell Tissue Res 224:207–223.

Harting JK, Casagrande VA, Weber JT. 1978. The projection of the primate superior colliculus upon the dorsal lateral geniculate nucleus: autoradiographic demonstration of interlaminar distribution of tectogeniculate axons. Brain Res 150:593–599.

Harting JK, Diamond IT, Hall WC. 1973a. Anterograde degeneration study of the cortical

projections of the lateral geniculate and pulvinar nuclei in the tree shrew (Tupaia glis). J Comp Neurol 150:393–440.

Harting JK, Hall WC, Diamond IT, Martin GF. 1973b. Anterograde degeneration study of the superior colliculus in Tupaia glis: evidence for a subdivision between superficial and deep layers. J Comp Neurol 148:361–386.

Harting JK, Hall WC, Diamond IT. 1972. Evolution of the pulvinar. Brain Behav Evol 6:424–452.

Harting JK, Huerta MF, Frankfurter AJ, Strominger NL, Royce GJ. 1980. Ascending pathways from the monkey superior colliculus: An autoradiographic analysis. J Comp Neurol 192:853–882.

Harting JK, Huerta MF, Hashikawa T, van Lieshout DP. 1991. Projection of the mammalian superior colliculus upon the dorsal lateral geniculate nucleus: organization of tectogeniculate pathways in nineteen species. J Comp Neurol 304:275–306.

Harting JK, Noback CR. 1971. Subcortical projections from the visual cortex in the tree shrew (Tupaia glis). Brain Res 25:21–33.

Hartinger J, Jahn R. 1993. An anion binding site that regulates the glutamate transporter of synaptic vesicles. Journal of Biological Chemistry 268:23122–23127.

Hayashi M, Otsuka M, Morimoto R, Hirota S, Yatsushiro S, Takeda J, Yamamoto A, Moriyama Y. 2001. Differentiation-associated Na+-dependent inorganic phosphate cotransporter (DNPI) is a vesicular glutamate transporter in endocrine glutamatergic systems. Journal of Biological Chemistry 276:43400–43406.

Hässler R. 1967. Comparative anatomy of the central visual system in day- and night-active primates. (Hässler R, Stephen S, editors.). Thieme, Stuttgart: Evolution of the forebrain.

Helms MC, Ozen G, Hall WC. 2004. Organization of the intermediate gray layer of the superior colliculus. I. Intrinsic vertical connections. Journal of Neurophysiology 91:1706–1715.

Hendrickson AE, Wilson JR, Ogren MP. 1978. The neuroanatomical organization of pathways between the dorsal lateral geniculate nucleus and visual cortex in Old World and New World primates. J Comp Neurol 182:123–136.

Hendry SH, Reid RC. 2000. The koniocellular pathway in primate vision. Annu Rev Neurosci 23:127–153.

Herzog E, Bellenchi GC, Gras C, Bernard V, Ravassard P, Bedet C, Gasnier B, Giros B, Mestikawy El S. 2001. The existence of a second vesicular glutamate transporter specifies subpopulations of glutamatergic neurons. J Neurosci 21:1–6.

Herzog E, Gilchrist J, Gras C, Muzerelle A, Ravassard P, Giros B, Gaspar P, Mestikawy El S. 2004. Localization of VGLUT3, the vesicular glutamate transporter type 3, in the rat brain.

NSC 123:983–1002.

Hevner RF, Daza RAM, Rubenstein JLR, Stunnenberg H, Olavarria JF, Englund C. 2003. Beyond laminar fate: toward a molecular classification of cortical projection/pyramidal neurons. Dev Neurosci 25:139–151.

Hevner RF. 2007. Layer-specific markers as probes for neuron type identity in human neocortex and malformations of cortical development. J Neuropathol Exp Neurol 66:101–109.

Hisano S, Hoshi K, Ikeda Y, Maruyama D, Kanemoto M, Ichijo H, Kojima I, Takeda J, Nogami H. 2000. Regional expression of a gene encoding a neuron-specific Na(+)-dependent inorganic phosphate cotransporter (DNPI) in the rat forebrain. Brain Res Mol Brain Res 83:34–43.

Hnasko TS, Edwards RH. 2012. Neurotransmitter corelease: mechanism and physiological role. Annu Rev Physiol 74:225–243.

Horton JC. 1984. Cytochrome oxidase patches: a new cytoarchitectonic feature of monkey visual cortex. Philos Trans R Soc Lond, B, Biol Sci 304:199–253.

Hubel DH, LeVay S, Wiesel TN. 1975. Mode of termination of retinotectal fibers in macaque monkey: an autoradiographic study. Brain Res 96:25–40.

Hubel DH. 1975. An autoradiographic study of the retino-cortical projections in the tree shrew (Tupaia glis). Brain Res 96:41–50.

Huchon D, Madsen O, Sibbald MJJB, Ament K, Stanhope MJ, Catzeflis F, de Jong WW, Douzery EJP. 2002. Rodent Phylogeny and a Timescale for the Evolution of Glires: Evidence from an Extensive Taxon Sampling Using Three Nuclear Genes. Molecular Biology and Evolution 19:1053–1065.

Huerta MF, Harting JK. 1983. Sublamination within the superficial gray layer of the squirrel monkey: an analysis of the tectopulvinar projection using anterograde and retrograde transport methods. Brain Res 261:119–126.

Huerta MF, Weber JT, Rothstein LR, Harting JK. 1985. Subcortical connections of area 17 in the tree shrew: an autoradiographic analysis. Brain Res 340:163–170.

Humphrey AL, Albano JE, Norton TT. 1977. Organization of ocular dominance in tree shrew striate cortex. Brain Res 134:225–236.

Hur EE, Zaborszky L. 2005. Vglut2 afferents to the medial prefrontal and primary somatosensory cortices: a combined retrograde tracing in situ hybridization study. J Comp Neurol 483:351–373.

Islam MR, Atoji Y. 2009. Distribution of vesicular glutamate transporter 2 and glutamate receptor 1 and 2 mRNA in the pigeon retina. Experimental Eye Research 89:439–443.

Ito T, Bishop DC, Oliver DL. 2011. Expression of glutamate and inhibitory amino acid vesicular transporters in the rodent auditory brainstem. J Comp Neurol 519:316–340.

Ito T, Oliver DL. 2010. Origins of Glutamatergic Terminals in the Inferior Colliculus Identified by Retrograde Transport and Expression of VGLUT1 and VGLUT2 Genes. Front Neuroanat 4:135.

Johnson JK, Casagrande VA. 1995. Distribution of calcium-binding proteins within the parallel visual pathways of a primate (Galago crassicaudatus). J Comp Neurol 356:238–260.

Kaas JH, Hall WC, Killackey H, Diamond IT. 1972. Visual cortex of the tree shrew (Tupaia glis): Architectonic subdivisions and representations of the visual field. Brain Res 42:491–496.

Kaas JH, Huerta MF, Weber JT, Harting JK. 1978. Patterns of retinal terminations and laminar organization of the lateral geniculate nucleus of primates. J Comp Neurol 182:517–553.

Kaas JH, Huerta MF. 1988. The subcortical visual system of primates. In: Comparative Primate Biology. Vol. 4. Alan R Liss Inc. p 327–391.

Kaas JH, Lin CS, Casagrande VA. 1976. The relay of ipsilateral and contralateral retinal input from the lateral geniculate nucleus to striate cortex in the owl monkey: a transneuronal transport study. Brain Res 106:371–378.

Kaas JH, Lyon DC. 2007. Pulvinar contributions to the dorsal and ventral streams of visual processing in primates. Brain Res Rev 55:285–296.

Kaas JH. 2005. The future of mapping sensory cortex in primates: three of many remaining issues. Philos Trans R Soc Lond, B, Biol Sci 360:653–664.

Kaas JH. 2006. Evolution of the neocortex. Current Biology 16:R910–R914.

Kaas JH. 2012. The evolution of neocortex in primates. Prog Brain Res 195:91–102.

Kaas JH. 2013. The Evolution of Brains from Early Mammals to Humans. Wiley Interdiscip Rev Cogn Sci 4:33–45.

Kandel ER, Schwartz JH, Jessell TM. 2000. Principles of neural science. 2nd ed. New York: McGraw-Hill.

Kaneko T, Fujiyama F, Hioki H. 2002. Immunohistochemical localization of candidates for vesicular glutamate transporters in the rat brain. J Comp Neurol 444:39–62.

Kaneko T, Fujiyama F. 2002. Complementary distribution of vesicular glutamate transporters in the central nervous system. Neurosci Res 42:243–250.

Krubitzer LA, Kaas JH. 1989. Cortical integration of parallel pathways in the visual system of primates. Brain Res 478:161–165.

Kubota Y, Kawaguchi Y. 1994. Three classes of GABAergic interneurons in neocortex and neostriatum. Jpn J Physiol 44 Suppl 2:S145–8.

Lachica EA, Casagrande VA. 1992. Direct W-like geniculate projections to the cytochrome oxidase (CO) blobs in primate visual cortex: axon morphology. J Comp Neurol 319:141–158.

Laemle LK. 1968. Retinal Projections of *Tupaia Glis*. Brain Behav Evol 1:473–499.

Land PW, Kyonka E, Shamalla-Hannah L. 2004. Vesicular glutamate transporters in the lateral geniculate nucleus: expression of VGLUT2 by retinal terminals. Brain Res 996:251–254.

Lein ES, Hawrylycz MJ, Ao N, Ayres M, Bensinger A, Bernard A, Boe AF, Boguski MS, Brockway KS, Byrnes EJ, Chen L, Chen L, Chen T-M, Chi Chin M, Chong J, Crook BE, Czaplinska A, Dang CN, Datta S, Dee NR, Desaki AL, Desta T, Diep E, Dolbeare TA, Donelan MJ, Dong H-W, Dougherty JG, Duncan BJ, Ebbert AJ, Eichele G, Estin LK, Faber C, Facer BA, Fields R, Fischer SR, Fliss TP, Frensley C, Gates SN, Glattfelder KJ, Halverson KR, Hart MR, Hohmann JG, Howell MP, Jeung DP, Johnson RA, Karr PT, Kawal R, Kidney JM, Knapik RH, Kuan CL, Lake JH, Laramee AR, Larsen KD, Lau C, Lemon TA, Liang AJ, Liu Y, Luong LT, Michaels J, Morgan JJ, Morgan RJ, Mortrud MT, Mosqueda NF, Ng LL, Ng R, Orta GJ, Overly CC, Pak TH, Parry SE, Pathak SD, Pearson OC, Puchalski RB, Riley ZL, Rockett HR, Rowland SA, Royall JJ, Ruiz MJ, Sarno NR, Schaffnit K, Shapovalova NV, Sivisay T, Slaughterbeck CR, Smith SC, Smith KA, Smith BI, Sodt AJ, Stewart NN, Stumpf K-R, Sunkin SM, Sutram M, Tam A, Teemer CD, Thaller C, Thompson CL, Varnam LR, Visel A, Whitlock RM, Wohnoutka PE, et al. 2006. Genome-wide atlas of gene expression in the adult mouse brain. Nature 445:168–176.

Levitt JB, Lund JS, Yoshioka T. 1996. Anatomical substrates for early stages in cortical processing of visual information in the macaque monkey. Behav Brain Res 76:5–19.

Levitt JB, Yoshioka T, Lund JS. 1995. Connections between the pulvinar complex and cytochrome oxidase-defined compartments in visual area V2 of macaque monkey. Exp Brain Res 104:419–430.

Li J-L, Fujiyama F, Kaneko T, Mizuno N. 2003. Expression of vesicular glutamate transporters, VGluT1 and VGluT2, in axon terminals of nociceptive primary afferent fibers in the superficial layers of the medullary and spinal dorsal horns of the rat. J Comp Neurol 457:236–249.

Liguz-Lecznar M, Skangiel-Kramska J. 2007. Vesicular glutamate transporters VGLUT1 and VGLUT2 in the developing mouse barrel cortex. International Journal of Developmental Neuroscience 25:107–114.

Lin CS, kaas JH. 1977. Projections from cortical visual areas 17, 18, and MT onto the dorsal lateral geniculate nucleus in owl monkeys. J Comp Neurol 173:457–474.

Lin CS, kaas JH. 1979. The inferior pulvinar complex in owl monkeys: architectonic subdivisions and patterns of input from the superior colliculus and subdivisions of visual

cortex. J Comp Neurol 187:655–678.

Livingstone MS, Hubel DH. 1983. Specificity of cortico-cortical connections in monkey visual system. Nature 304:531–534.

Lock TM, Baizer JS, Bender DB. 2003. Distribution of corticotectal cells in macaque. Exp Brain Res 151:455–470.

Lund JS, Boothe RG. 1975. Interlaminar connections and pyramidal neuron organisation in the visual cortex, area 17, of the Macaque monkey. J Comp Neurol 159:305–334.

Lund JS, Fitzpatrick D, Humphrey AL. 1985. The striate cortex of the tree shrew. Plenum Press 3:157–205.

Lund JS, Hawken MJ, Parker AJ. 1988. Local circuit neurons of macaque monkey striate cortex: II. Neurons of laminae 5B and 6. J Comp Neurol 276:1–29.

Lund JS, Lund RD, Hendrickson AE, Bunt AH, Fuchs AF. 1975. The origin of efferent pathways from the primary visual cortex, area 17, of the macaque monkey as shown by retrograde transport of horseradish peroxidase. J Comp Neurol 164:287–303.

Lund JS. 1988. Anatomical organization of macaque monkey striate visual cortex. Annu Rev Neurosci 11:253–288.

Lund RD. 1972. Synaptic patterns in the superficial layers of the superior colliculus of the monkey, Macaca mulatta. Exp Brain Res 15:194–211.

Luppino G, Matelli M, Carey RG, Fitzpatrick D, Diamond IT. 1988. New view of the organization of the pulvinar nucleus in Tupaia as revealed by tectopulvinar and pulvinar-cortical projections. J Comp Neurol 273:67–86.

Lyon DC, Jain N, Kaas JH. 2003a. The visual pulvinar in tree shrews I. Multiple subdivisions revealed through acetylcholinesterase and Cat-301 chemoarchitecture. J Comp Neurol 467:593–606.

Lyon DC, Jain N, Kaas JH. 2003b. The visual pulvinar in tree shrews II. Projections of four nuclei to areas of visual cortex. J Comp Neurol 467:607–627.

Lyon DC, Kaas JH. 2002. Connectional evidence for dorsal and ventral V3, and other extrastriate areas in the prosimian primate, Galago garnetti. Brain Behav Evol 59:114–129.

Lyon DC, Nassi JJ, Callaway EM. 2010. A Disynaptic Relay from Superior Colliculus to Dorsal Stream Visual Cortex in Macaque Monkey. Neuron 65:270–279.

Marion R, Li K, Purushothaman G, Jiang Y, Casagrande VA. 2013. Morphological and neurochemical comparisons between pulvinar and V1 projections to V2. J Comp Neurol 521:813–832.

Marrocco RT, McClurkin JW, Young RA. 1981. Spatial properties of superior colliculus cells projecting to the inferior pulvinar and parabigeminal nucleus of the monkey. Brain Res 222:150–154.

Martin RD. 2003. Palaeontology: Combing the primate record. Nature 422:388–391.

Masterson SP, Li J, Bickford ME. 2009. Synaptic organization of the tectorecipient zone of the rat lateral posterior nucleus. J Comp Neurol 515:647–663.

Masterson SP, Li J, Bickford ME. 2010. Frequency-dependent release of substance P mediates heterosynaptic potentiation of glutamatergic synaptic responses in the rat visual thalamus. Journal of Neurophysiology 104:1758–1767.

Maunsell JH, Van Essen DC. 1983. The connections of the middle temporal visual area (MT) and their relationship to a cortical hierarchy in the macaque monkey. J Neurosci 3:2563–2586.

May PJ. 2006. The mammalian superior colliculus: laminar structure and connections. Prog Brain Res 151:321–378.

McDonald CT, McGuinness ER, Allman JM. 1993. Laminar organization of acetylcholinesterase and cytochrome oxidase in the lateral geniculate nucleus of prosimians. NSC 54:1091–1101.

Miyazaki T, Fukaya M, Shimizu H, Watanabe M. 2003. Subtype switching of vesicular glutamate transporters at parallel fibre-Purkinje cell synapses in developing mouse cerebellum. European Journal of Neuroscience 17:2563–2572.

Nahmani M, Erisir A. 2005. VGluT2 immunochemistry identifies thalamocortical terminals in layer 4 of adult and developing visual cortex. J Comp Neurol 484:458–473.

Naito S, Ueda T. 1983. Adenosine triphosphate-dependent uptake of glutamate into protein I-associated synaptic vesicles. Journal of Biological Chemistry 258:696–699.

Nakadate K, Imamura K, Watanabe Y. 2012. Effects of monocular deprivation on the spatial pattern of visually induced expression of c-Fos protein. Neuroscience 202:17–28.

Nakamura K, Hioki H, Fujiyama F, Kaneko T. 2005. Postnatal changes of vesicular glutamate transporter (VGluT)1 and VGluT2 immunoreactivities and their colocalization in the mouse forebrain. J Comp Neurol 492:263–288.

Nakamura K, Watakabe A, Hioki H, Fujiyama F, Tanaka Y, Yamamori T, Kaneko T. 2007. Transiently increased colocalization of vesicular glutamate transporters 1 and 2 at single axon terminals during postnatal development of mouse neocortex: a quantitative analysis with correlation coefficient. European Journal of Neuroscience 26:3054–3067.

Ni B, Wu X, Yan GM, Wang J, Paul SM. 1995. Regional expression and cellular localization of the Na(+)-dependent inorganic phosphate cotransporter of rat brain. J Neurosci 15:5789–5799.

Norden JJ, Kaas JH. 1978. The identification of relay neurons in the dorsal lateral geniculate nucleus of monkeys using horseradish peroxidase. J Comp Neurol 182:707–725.

Norton TT, Rager G, Kretz R. 1985. ON and OFF regions in layer IV of striate cortex. Brain Res 327:319–323.

O'Brien BJ, Caldwell JH, Ehring GR, Bumsted O'Brien KM, Luo S, Levinson SR. 2008. Tetrodotoxin-resistant voltage-gated sodium channels Nav1.8 and Nav1.9 are expressed in the retina. J Comp Neurol 508:940–951.

Ogren MP, Hendrickson AE. 1977. The distribution of pulvinar terminals in visual areas 17 and 18 of the monkey. Brain Res 137:343–350.

Ogren MP, Hendrickson AE. 1979. The morphology and distribution of striate cortex terminals in the inferior and lateral subdivisions of the Macaca monkey pulvinar. J Comp Neurol 188:179–199.

Olszewski J. 1952. The thalamus of Macaca mulatta. Basel, Switzerland: Karger Publishers.

Ortega F, Hennequet L, Sarría R, Streit P, Grandes P. 1995. Changes in the pattern of glutamate-like immunoreactivity in rat superior colliculus following retinal and visual cortical lesions. NSC 67:125–134.

Partlow GD, Colonnier M, Szabo J. 1977. Thalamic projections of the superior colliculus in the rhesus monkey, Macaca mulatta. A light and electron microscopic study. J Comp Neurol 171:285–317.

Persson S, Boulland J-L, Aspling M, Larsson M, Fremeau RT, Edwards RH, Storm-Mathisen J, Chaudhry FA, Broman J. 2006. Distribution of vesicular glutamate transporters 1 and 2 in the rat spinal cord, with a note on the spinocervical tract. J Comp Neurol 497:683–701.

Pollack JG, Hickey TL. 1979. The distribution of retino-collicular axon terminals in rhesus monkey. J Comp Neurol 185:587–602.

Poppel E, Held R, Frost DO. 1973. Residual Visual Function after Brain Wounds involving the Central Visual Pathways in Man. Nature 243:295–296.

Raczkowski D, Diamond IT. 1978. Cells of origin of several efferent pathways from the superior colliculus in Galago senegalensis. Brain Res 146:351–357.

Reimer RJ, Edwards RH. 2004. Organic anion transport is the primary function of the SLC17/type I phosphate transporter family. Pfl[illegible]gers Archiv European Journal of Physiology 447:629–635.

Reimer RJ, Fremeau RT, Bellocchio EE, Edwards RH. 2001. The essence of excitation. current opinion in cell biology 13:417–421.

Rockland KS, Lund JS, Humphrey AL. 1982. Anatomical banding of intrinsic connections in

striate cortex of tree shrews (Tupaia glis). J Comp Neurol 209:41–58.

Rockland KS, Pandya DN. 1979. Laminar origins and terminations of cortical connections of the occipital lobe in the rhesus monkey. Brain Res 179:3–20.

Rockland KS. 1994. The organization of feedback connections from area V2 (18) to V1 (17). In: Peters A, Jones EG, editors. Primary Visual Cortex in Primates. New York: Plenum Press.

Rockland KS. 1996. Two types of corticopulvinar terminations: round (type 2) and elongate (type 1). J Comp Neurol 368:57–87.

Rosa MG, Casagrande VA, Preuss T, Kaas JH. 1997. Visual field representation in striate and prestriate cortices of a prosimian primate (Galago garnetti). Journal of Neurophysiology 77:3193–3217.

Rovó Z, Ulbert I, Acsády L. 2012. Drivers of the primate thalamus. J Neurosci 32:17894–17908.

Salin PA, Bullier J. 1995. Corticocortical connections in the visual system: structure and function. Physiol Rev 75:107–154.

Samorajski T, Ordy JM, Keefe JR. 1966. Structural organization of the retina in the tree shrew (Tupaia glis). J Cell Biol 28:489–504.

Santos MS, Li H, Voglmaier SM. 2009. Synaptic vesicle protein trafficking at the glutamate synapse. NSC 158:189–203.

Schäfer MK-H, Varoqui H, Defamie N, Weihe E, Erickson JD. 2002. Molecular cloning and functional identification of mouse vesicular glutamate transporter 3 and its expression in subsets of novel excitatory neurons. Journal of Biological Chemistry 277:50734–50748.

Scherrer G, Low SA, Wang X, Zhang J, Yamanaka H, Urban R, Solorzano C, Harper B, Hnasko TS, Edwards RH, Basbaum AI, Jan LY. 2010. VGLUT2 expression in primary afferent neurons is essential for normal acute pain and injury-induced heat hypersensitivity. Proc Natl Acad Sci USA 107:22296–22301.

Schmidt TM, Chen SK, Hattar S. 2011. Intrinsically photosensitive retinal ganglion cells: many subtypes, diverse functions. Trends in Neurosciences.

Schönitzer K, Holländer H. 1984. Retinotectal terminals in the superior colliculus of the rabbit: a light and electron microscopic analysis. J Comp Neurol 223:153–162.

Seal RP, Edwards RH. 2006. Functional implications of neurotransmitter co-release: glutamate and GABA share the load. Curr Opin Pharmacol 6:114–119.

Sherman SM, Guillery RW. 1996. Functional organization of thalamocortical relays. Journal of Neurophysiology 76:1367–1395.

Sherman SM, Guillery RW. 1998. On the actions that one nerve cell can have on another:

distinguishing "drivers" from "modulators". Proc Natl Acad Sci USA 95:7121–7126.

Sherman SM, Guillery RW. 2002. The Role of the Thalamus in the Flow of Information to the Cortex. Philosophical Transactions: Biological Sciences 357:1695–1708.

Sherman SM, Guillery RW. 2006. Exploring the role of the thalamus and its role in cortical function. MIT Press, Cambridge MA.

Sherman SM, Guillery RW. 2011. Distinct functions for direct and transthalamic corticocortical connections. Journal of Neurophysiology 106:1068–1077.

Sherman SM. 2001. Thalamic relay functions. In: Casanova C, Ptito M, editors. Progress in brain research. Vol. 134. Progress in Brain Research. Elsevier. p 51–69.

Sherman SM. 2005. Thalamic relays and cortical functioning. Prog Brain Res Volume 149:107–126.

Sherman SM. 2007. The thalamus is more than just a relay. Curr Opin Neurobiol 17:417–422.

Sherman SM. 2012. Thalamocortical interactions. current opinion in cell biology 22:575–579.

Shipp S. 2001. Corticopulvinar connections of areas V5, V4, and V3 in the macaque monkey: a dual model of retinal and cortical topographies. J Comp Neurol 439:469–490.

Sincich LC, Horton JC. 2002. Divided by cytochrome oxidase: a map of the projections from V1 to V2 in macaques. Science 295:1734–1737.

Sincich LC, Horton JC. 2003. Independent projection streams from macaque striate cortex to the second visual area and middle temporal area. Journal of Neuroscience 23:5684–5692.

Sincich LC, Jocson CM, Horton JC. 2010. V1 Interpatch Projections to V2 Thick Stripes and Pale Stripes. J Neurosci 30:6963–6974.

Sincich LC, Park KF, Wohlgemuth MJ, Horton JC. 2004. Bypassing V1: a direct geniculate input to area MT. Nature Neuroscience 7:1123–1128.

Snyder M, Diamond IT. 1968. The Organization and Function of the Visual Cortex in the Tree Shrew. Brain Behav Evol 1:264–288.

Soares JGM, Pereira ACCN, Botelho EP, Pereira SS, Fiorani M, Gattass R. 2005. Differential expression of Zif268 and c-Fos in the primary visual cortex and lateral geniculate nucleus of normal Cebus monkeys and after monocular lesions. J Comp Neurol 482:166–175.

Spatz WB, Tigges J, Tigges M. 1970. Subcortical projections, cortical associations, and some intrinsic interlaminar connections of the striate cortex in the squirrel monkey (Saimiri). J Comp Neurol 140:155–174.

Spitzer NC, Root CM, Borodinsky LN. 2004. Orchestrating neuronal differentiation: patterns of Ca2+ spikes specify transmitter choice. Trends in Neurosciences 27:415–421.

Stepniewska I, Kaas JH. 1997. Architectonic subdivisions of the inferior pulvinar in New World and Old World monkeys. Vis Neurosci 14:1043–1060.

Stepniewska I, Qi HX, kaas JH. 1999. Do superior colliculus projection zones in the inferior pulvinar project to MT in primates? Eur J Neurosci 11:469–480.

Stepniewska I, Ql HX, kaas JH. 2000. Projections of the superior colliculus to subdivisions of the inferior pulvinar in New World and Old World monkeys. Vis Neurosci 17:529–549.

Stepniewska I. 2004. The pulvinar complex. In: Kaas JH, Collins CE, editors. The primate visual system. Boca Raton: CRC Press.

Stoerig P, Cowey A. 2007. Blindsight. Current Biology 17:R822–4.

Storace DA, Higgins NC, Chikar JA, Oliver DL, Read HL. 2012. Gene expression identifies distinct ascending glutamatergic pathways to frequency-organized auditory cortex in the rat brain. Journal of Neuroscience 32:15759–15768.

Symonds LL, Kaas JH. 1978. Connections of striate cortex in the prosimian, Galago senegalensis. J Comp Neurol 181:477–511.

Takahata T, Hashikawa T, Higo N, Tochitani S, Yamamori T. 2008. Difference in sensory dependence of occ1/Follistatin-related protein expression between macaques and mice. Journal of Chemical Neuroanatomy 35:146–157.

Takahata T, Miyashita M, Tanaka S, Kaas JH. 2014. Identification of ocular dominance domains in New World owl monkeys by immediate-early gene expression. Proc Natl Acad Sci USA 111:4297–4302.

Takahata T, Shukla R, Yamamori T, Kaas JH. 2012. Differential Expression Patterns of Striate Cortex-Enriched Genes among Old World, New World, and Prosimian Primates. Cerebral Cortex 22:2313–2321.

Takamori S, Rhee JS, Rosenmund C, Jahn R. 2000. Identification of a vesicular glutamate transporter that defines a glutamatergic phenotype in neurons. Nature 407:189–194.

Takamori S. 2006. VGLUTs: “Exciting” times for glutamatergic research? Neurosci Res 55:343–351.

Tamietto M, Cauda F, Corazzini LL, Savazzi S, Marzi CA, Goebel R, Weiskrantz L, de Gelder B. 2010. Collicular vision guides nonconscious behavior. J Cogn Neurosci 22:888–902.

Tate S, Benn S, Hick C, Trezise D, John V. 1998. Two sodium channels contribute to the TTX-R sodium current in primary sensory neurons. Nature.

Thompson L, Holt C. 1989. Effects of intraocular tetrodotoxin on the development of the retinocollicular pathway in the syrian hamster. J Comp Neurol 282:371–388.

Tigges J, Tigges M. 1981. Distribution of retinofugal and corticofugal axon terminals in the superior colliculus of squirrel monkey. Investigative ophthalmology & visual science 20:149–158.

Tigges M, Tigges J. 1970. The retinofugal fibers and their terminal nuclei in Galago crassicaudatus (primates). J Comp Neurol 138:87–101.

Tochitani S, Liang F, Watakabe A, Hashikawa T, Yamamori T. 2001. The occ1 gene is preferentially expressed in the primary visual cortex in an activity-dependent manner: a pattern of gene expression related to the cytoarchitectonic area in adult macaque neocortex. Eur J Neurosci 13:297–307.

Todd AJ, Hughes DI, Polgar E, Nagy GG, Mackie M, Ottersen OP, Maxwell DJ. 2003. The expression of vesicular glutamate transporters VGLUT1 and VGLUT2 in neurochemically defined axonal populations in the rat spinal cord with emphasis on the dorsal horn. Eur J Neurosci 17:13–27.

Trojanowski JO, Jacobson S. 1975. Peroxidase labeled subcortical afferents to pulvinar in rhesus monkey. Brain Res 97:144–150.

Trusk TC, Kaboord WS, Wong-Riley MTT. 2009. Effects of monocular enucleation, tetrodotoxin, and lid suture on cytochrome-oxidase reactivity in supragranular puffs of adult macaque striate cortex. Vis Neurosci 4:185–204.

Usrey WM, Fitzpatrick D. 1996. Specificity in the axonal connections of layer VI neurons in tree shrew striate cortex: evidence for distinct granular and supragranular systems. J Neurosci 16:1203–1218.

Valverde F. 1985. The organizing principles of the primary visual cortex in the monkey. In: Peters A, Jones EG, editors. Cerebral Cortex: Visual Cortex. Vol. 3. New York: Plenum Press. p 207–252.

Van Essen DC. 1985. Functional organization of primate visual cortex. In: Peters A, Jones EG, editors. Cerebral Cortex: Visual Cortex. Vol. 3. New York: Plenum Press. p 259–320.

Van Essen DC. 2005. A Population-Average, Landmark- and Surface-based (PALS) atlas of human cerebral cortex. Neuroimage 28:635–662.

Van Horn SC, Sherman SM. 2004. Differences in projection patterns between large and small corticothalamic terminals. J Comp Neurol 475:406–415.

Van Horn SC, Sherman SM. 2007. Fewer driver synapses in higher order than in first order thalamic relays. NSC 146:463–470.

Varoqui H, Schäfer MK-H, Zhu H, Weihe E, Erickson JD. 2002. Identification of the differentiation-associated Na+/PI transporter as a novel vesicular glutamate transporter expressed in a distinct set of glutamatergic synapses. Journal of Neuroscience 22:142–155.

Viaene AN, Petrof I, Sherman SM. 2011a. Synaptic properties of thalamic input to the subgranular layers of primary somatosensory and auditory cortices in the mouse. Journal of Neuroscience 31:12738–12747.

Viaene AN, Petrof I, Sherman SM. 2011b. Properties of the thalamic projection from the posterior medial nucleus to primary and secondary somatosensory cortices in the mouse. Proc Natl Acad Sci USA 108:18156–18161.

Voglmaier SM, Kam K, Yang H, Fortin DL, Hua Z, Nicoll RA, Edwards RH. 2006. Distinct Endocytic Pathways Control the Rate and Extent of Synaptic Vesicle Protein Recycling. Neuron 51:71–84.

Wall JT, Symonds LL, Kaas JH. 1982. Cortical and subcortical projections of the middle temporal area (MT) and adjacent cortex in galagos. J Comp Neurol 211:193–214.

Wang MM, Frishman LJ, Sherry DM. 2002. Distribution and Expression of Vesicular Glutamate Transporters in Developing Mouse Retina. ARVO Meeting Abstracts 43:2706.

Wässle H. 2004. Parallel processing in the mammalian retina. Nat Rev Neurosci 5:747–757.

Webster R. 2001. Neurotransmitter systems and function: overview. In: Webster R, editor. Neurotransmitters, Drugs and Brain Function. Chichester, West Sussex: John Wiley & Sons, Inc.

Wei H, Masterson SP, Petry HM, Bickford ME. 2011. Diffuse and specific tectopulvinar terminals in the tree shrew: synapses, synapsins, and synaptic potentials. PLoS ONE 6:e23781.

Weller RE, Kaas JH. 1982. The organization of the visual system in galago. Comparisons with monkeys. In: Haines DE, editor. The Lesser Bushbaby (Galago) as an Animal Model: Selected Topics. Boca Raton, FL: CRC Press.

Weston MC, Nehring RB, Wojcik SM, Rosenmund C. 2011. Interplay between VGLUT isoforms and endophilin A1 regulates neurotransmitter release and short-term plasticity. Neuron 69:1147–1159.

Wilson ME, Toyne MJ. 1970. Retino-tectal and cortico-tectal projections in Macaca mulatta. Brain Res 24:395–406.

Wilson NR, Kang J, Hueske EV, Leung T, Varoqui H, Murnick JG, Erickson JD, Liu G. 2005. Presynaptic regulation of quantal size by the vesicular glutamate transporter VGLUT1. Journal of Neuroscience 25:6221–6234.

Wojcik SM, Rhee JS, Herzog E, Sigler A, Jahn R, Takamori S, Brose N, Rosenmund C, Südhof TC. 2004. An Essential Role for Vesicular Glutamate Transporter 1 (VGLUT1) in Postnatal Development and Control of Quantal Size. Proc Natl Acad Sci USA 101:7158–7163.

Wong P, Collins CE, Baldwin MKL, Kaas JH. 2009. Cortical connections of the visual pulvinar

complex in prosimian galagos (Otolemur garnetti). J Comp Neurol 517:493–511.

Wong P, Kaas JH. 2008. Architectonic Subdivisions of Neocortex in the Gray Squirrel (Sciurus carolinensis). Anat Rec 291:1301–1333.

Wong P, Kaas JH. 2009a. An Architectonic Study of the Neocortex of the Short-Tailed Opossum *(Monodelphis domestica)*. Brain Behav Evol 73:206–228.

Wong P, Kaas JH. 2009b. Architectonic Subdivisions of Neocortex in the Tree Shrew (Tupaia belangeri). Anat Rec 292:994–1027.

Wong P, Kaas JH. 2010. Architectonic subdivisions of neocortex in the Galago (Otolemur garnetti). Anat Rec 293:1033–1069.

Wong-Riley M, Carroll EW. 1984. Effect of impulse blockage on cytochrome oxidase activity in monkey visual system. Nature 307:262–264.

Wong-Riley M. 1979. Changes in the visual system of monocularly sutured or enucleated cats demonstrable with cytochrome oxidase histochemistry. Brain Res 171:11–28.

Wong-Riley MT, Huang Z, Liebl W, Nie F, Xu H, Zhang C. 1998. Neurochemical organization of the macaque retina: effect of TTX on levels and gene expression of cytochrome oxidase and nitric oxide synthase and on the immunoreactivity of Na+ K+ ATPase and NMDA receptor subunit I. Vision Res 38:1455–1477.

Wong-Riley MTT, Norton TT. 1988. Histochemical localization of cytochrome oxidase activity in the visual system of the tree shrew: Normal patterns and the effect of retinal impulse blockage. J Comp Neurol 272:562–578.

Wong-Riley MTT. 1972a. Changes in the dorsal lateral geniculate nucleus of the squirrel monkey after unilateral ablation of the visual cortex. J Comp Neurol 146:519–547.

Wong-Riley MTT. 1972b. Neuronal and synaptic organization of the normal dorsal lateral geniculate nucleus of the squirrel monkey,Saimiri sciureus. J Comp Neurol 144:25–59.

Yamamori T. 2011. Selective gene expression in regions of primate neocortex: implications for cortical specialization. Prog Neurobiol 94:201–222.

Yamashita T, Ishikawa T, Takahashi T. 2003. Developmental Increase in Vesicular Glutamate Content Does Not Cause Saturation of AMPA Receptors at the Calyx of Held Synapse. The Journal of ….

Yukie M, Iwai E. 1981. Direct projection from the dorsal lateral geniculate nucleus to the prestriate cortex in macaque monkeys. J Comp Neurol 201:81–97.

Zeng C, Shroff H, Shore SE. 2011. Cuneate and spinal trigeminal nucleus projections to the cochlear nucleus are differentially associated with vesicular glutamate transporter-2. Neuroscience 176:142–151.